University of
Southern
Queensland

ZINC BIOFORTIFICATION OF RICE USING CARBON NANODOTS

A Thesis submitted by

Peella Kankanamage Chamika Buddhinie Wijerathna
MPhil (USJ, Sri Lanka), BSc (Hons) (UoC, Sri Lanka)

For the award of

Doctor of Philosophy

2023

ABSTRACT

Increasing Zn content of cereals, particularly rice, is an approach for combating global Zn malnutrition. This project aimed to investigate the use of CNPs as a Zn carrier to increase rice Zn content. CDs bound with Zn were used as a foliar spray in the study to determine their effectiveness in delivering Zn to rice plants. The CNPs utilized in the study neither had detrimental effect on the growth nor showed deleterious effect on physiology of the rice plants tested. The possible physiological and molecular mechanism of a Zn efficient rice variety (IR36) and a Zn inefficient variety (IR26) were also studied under CNP. ZnCD application significantly increased shoot and seed Zn content of the IR36 variety, and this response was not seen in the IR26 variety. In contrast, the Fe content of IR 36 seeds increased significantly compared to the bulk Zn application. This validates prior research that found a positive relationship between Zn and Fe uptake in rice. Nonetheless, the responses of the two rice varieties revealed differences in Zn uptake and grain loading demonstrating varying Zn utilization efficiency. Comparative transcriptome and proteome analysis were used to determine the molecular mechanism by which rice responds to CNP-under contrast Zn utilization genetics. RNA-Seq-based transcriptomic analysis found 251 upregulated genes in IR36 in response to ZnCDs that were not upregulated in IR26. These set of activated IR36-specific genes implicated in Zn uptake, grain filling, auxin signalling, and abiotic stress signalling pathways. Our finding clearly demonstrates that the genetics of Zn use efficiency is further amplified by ZnCDs. The comparative proteomics analysis showed ZnCD application to IR36 upregulated 38 proteins, while IR26 upregulated 210 proteins, with just 2 similarities between the two groups. These IR36-specific proteins were heavily implicated in pathways like glucose metabolism, and photosynthesis. Findings of this study could be successfully used in formulation of a CNP based nano-fertilizer which could be used to address the global Zn malnutrition. In addition, greater understanding of the genetic mechanism of Zn utilization efficiency will open up new avenues for breeding and engineering cereals to increase their grain Zn content.

CERTIFICATION OF THESIS

I Peella Kankanamage Chamika Buddhinie Wijerathna declare that the PhD Thesis entitled *Zinc biofortification of rice using carbon nanodots* is not more than 100,000 words in length including quotes and exclusive of tables, figures, appendices, bibliography, references, and footnotes. The thesis contains no material that has been submitted previously, in whole or in part, for the award of any other academic degree or diploma. Except where otherwise indicated, this thesis is my own work.
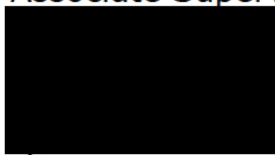
Date: 27 – 03 - 2023

Endorsed by:

Professor Saman Seneweera
Principal Supervisor

Professor Stephen Neate
Associate Supervisor

Professor Qin Li
Associate Supervisor

Student and supervisors' signatures of endorsement are held at the University.

ACKNOWLEDGEMENTS

DEDICATION

This thesis is dedicated to my beloved husband;

Najith Wijerathna

for always loving me, believing in me, and supporting

me whenever I'm in need.

TABLE OF CONTENTS

LIST OF TABLES

LIST OF FIGURES

ABBREVIATIONS

AAS	Atomic absorption spectroscopy
AFM	Atomic force microscopy
Ag NPs	Silver nanoparticles
Al	Aluminium
ANOVA	Analysis of variance
ATP	Adenosine triphosphate
Au NPs	Gold nanoparticles
BP	Biological process
CC	Cellular component
cDNA	Complementary DNA
CDs	Carbon dots
CeO2 NPs	Cerium Oxide nanoparticles
Ci	Intercellular CO_2 concentration
CNPs	Carbon nanoparticles
CNTs	Carbon nanotubes
CPM	Counts per Million
CuO NPs	Copper oxide nanoparticles
DEGs	Differentially expressed genes
DFA	Discriminant Function Analysis
DLS	Dynamic light scattering
DNA	Deoxyribonucleic acid
ENPs	Engineered nanoparticles
FDR	False discovery rate
Fe	Iron
Fe-EDTA	Ethylenediaminetetraacetic acid iron(III)
FTIR	Fourier-transform infrared spectroscopy
GLM	General linear model
GO	Gene ontology
Gs	Stomatal conductance

KEGG	Kyoto Encyclopaedia of Genes and Genomes
LEEP	Lipid exchange envelope and penetration
MF	Molecular function
MNPs	Metal nanoparticles
MWCNTs	Multiwalled carbon nanotubes
NA	Nicotianamine
NMR	Nuclear Magnetic Resonance
NPs	Nanoparticles
PAR	Photosynthetically Active Radiation
PCA	Principal component analysis
PL	Photoluminescence
Pn	Photosynthesis rate
ppm	Parts per million
PS	Phytosiderophores
PS II	Photosystem II
RCBD	Randomized Complete Block Design
RNA	Ribonucleic acid
RNA-Seq	RNA-sequencing
RO	Reverse osmosis
ROS	Reactive oxygen species
RPKM	Reads per kilobase of transcript per million reads mapped
RuBisCo	Ribulose 1,5-bisphosphate carboxylase-oxygenase
SE	Standard error
SEM	Scanning electron microscope
SWCNHs	Single walled carbon nano horns
SWCNTs	Single walled carbon nanotubes
TALENs	Transcription activator-like effector nucleases
TEM	Transmission electron microscopy
TiO_2 NPs	Titanium dioxide nanoparticles
Tr	Transpiration rate
UV	Ultraviolet

UV-Vis	Ultraviolet–visible spectrophotometry
XPS	X-ray photoelectron spectroscopy
ZIP	zinc-regulated, iron-regulated transporter-like proteins
ZnAc	Zinc Acetate
ZnCDs	Zinc bound carbon dots
ZnO	Zinc oxide

CHAPTER 1: INTRODUCTION

1.1. Zinc biofortification of rice

Enrichment of rice grains with zinc (Zn) is a current global need to resolve problems arising from consuming food with low mineral nutrients. Nearly two billion people in the developing world suffer from Zn deficiency, leading to serious health issues (Corbo et al., 2013, Deshpande et al., 2013, Myers et al., 2014). Consumption of cereal-based, diets especially wheat and rice that are particularly low in Zn are the main cause of Zn deficiency (Singh et al., 2005). Enhancing the Zn content of cereals, especially wheat and rice, is a strategy to increase Zn uptake.

Agronomic biofortification achieved through the application of Zn-enriched fertilisers and the genetic biofortification attained through plant breeding strategies are widespread methods of Zn biofortification (Cakmak, 2008). Narrow genetic variation for Zn content in plants makes breeding for new varieties rich in Zn a difficult task (Cakmak, 2008). Further, since many soil types (calcareous, sandy, saline etc.) in agricultural lands are zinc deficient and soil factors such as pH, organic and clay content control the amount of Zn in the soil solution (Alloway, 2008), simply adding fertiliser to soil will not universally increase grain Zn content. Foliar application of Zn at an appropriate plant growth stage and to the correct plant organ brings about more positive results (Habib, 2009, Boonchuay et al., 2013, Zhao et al., 2014), but foliar application may cause scorching of leaves (Deshpande et al., 2017) and there is a financial cost for the chemical and application. Further, these traditional approaches take much time and are less efficient too. Thus, the necessity of introducing new techniques for biofortification is of significance.

1.2. Use of Carbon nanoparticles in rice biofortification

In the recent past, researchers have focussed on novel techniques such as nanotechnology to deliver products to both plant and animal cells. Carbon nanoparticles (CNPs) such as single-walled carbon nanotubes (SWCNTs), multiwalled carbon nanotubes (MWCNTs), Fullerene C_{60}, carbon nanodots (CDs) and others have been successful in chloroplast-selective gene delivery, drug delivery, biological imaging, and many other applications in biology (Kim et al., 2015, Tripathi et al., 2015, Kwak et al., 2019). Importantly, CNPs including CDs have been successful in agriculture, enhancing seed germination, promoting growth, water absorption of cereals (Tripathi et al., 2011, Nair et al., 2012, Anita et al., 2014, Tiwari et al., 2014, Lahiani et al., 2015, Joshi et al., 2018, Wang et al., 2018).

Therefore, CNPs could be successfully used in tissue-selective micronutrient delivery in cereal crops. This project aims to investigate using CDs as a Zn carrier material to increase Zn content in rice plants. CDs bound with Zn (ZnCDs) will be used as a foliar spray in the study to deliver Zn ions to rice plants and then to improve grain Zn level.

1.2.1. Effect of CDs on physiology of rice plants

The introduction of CDs to a plant system may change routine plant physiological processes. Any possible changes in photosynthesis, gaseous exchange, plant growth and grain development may cause significant impacts on plant productivity. It is therefore necessary to measure common physiological processes like photosynthesis and nutrient uptake in order to assess the effectiveness of CD application to plants and investigate any potential adverse effects. The effect of CNPs and many other metal-based Nanoparticles (MNPs) and engineered nanoparticles (ENPs) on plant physiology has been widely studied (Mondal et al., 2011, Giraldo et al., 2014, Tiwari et al., 2014, Jalali et al., 2017, Zhang et al., 2017, Hussain et

al., 2021, Sahoo et al., 2021). Few studies have been conducted to study the responses of food plants such as wheat and mung bean on CD application (Wang et al., 2018, Xiao et al., 2019, Swift et al., 2021) but such experimental information on rice is limited (Li et al., 2018). Thus, we decided to investigate the physiological responses of rice plants towards the application of different concentrations of ZnCDs.

In subsequent experiments, the dose-dependent response of ZnCDs and CDs (without the Zn component) on physiological, agronomical responses, Zn uptake and Zn accumulation in the grains were investigated.

1.2.2. Effect of CDs on rice transcriptome and proteome

The transcriptome, proteome, and gene expression of plants treated with nanomaterials have not been extensively studied. Most research has been restricted to studying the effect of MNPs such as silver nanoparticles (Ag NPs), Zinc oxide nanoparticles (ZnO NPs) or Titanium dioxide nanoparticles (TiO$_2$ NPs) on the transcriptome and the proteome of the model plant *Arabidopsis thaliana* (Landa et al., 2012, Kaveh et al., 2013, Qian et al., 2013, Syu et al., 2014). Xun et al. (2017) have reported the results of transcriptome profile analysis of maize exposed to ZnO NPs but information on gene expression, transcriptomics, and proteomics studies of CNP application on cereals is rare.

Therefore, this study will examine the effect of ZnCD application on the expression of a small number of Zn uptake and translocation-related genes, the entire transcriptome, and the proteome of rice. A comparative and integrative analysis of rice transcriptomics and proteomics data will provide critical information for the use of CNP bound with Zn in for one of the world's most economically important plants.

1.3. Objectives of the study

Carbon nanodots are potential nanocarriers which could be used in agronomic nutrient biofortification of plants. Zinc complexed chitosan nanoparticles have been successfully used as a Zn nanocarrier (Deshpande et al., 2017). However, there is no evidence of the use of CNPs as micronutrient nanocarriers. Although a few studies have been conducted on the effects of CDs on the physiology of rice, a more comprehensive set of molecular-level data is lacking. Thus, this study focuses on establishing a novel method of micronutrient delivery into plants using CDs. In particular, Zn is used as delivery material to facilitate Zn biofortification. This research was divided into four studies with four specific objectives.

1. Effects of carbon nanoparticles on physiological process and zinc uptake of rice (Chapter 3)

It has been established that CNPs and metal NPs treated rice exhibit dose-dependent responses (Ghasemi et al., 2017, Zhang et al., 2017, Itroutwar et al., 2020). The effective dose of applied NP depends on the physico-chemical properties of the NP, method of application, uptake process of the plant, and presence of other nutrients in the growing medium, (Lin et al., 2009, Koelmel et al., 2013, Li et al., 2016, Akmal et al., 2022). Consequently, the primary objective of this study was to establish the optimal concentration of ZnCDs to be applied to rice plants. A subsequent study was designed to assess the physiological responses and Zn uptake efficiency of rice plants treated with ZnCD (using the effective dose). This second experiment examines the impact of applied CNPs on growth and physiology of rice plants during a selected growth period.

2. ZnCD's effect on the physiology and micronutrient content of two different rice varieties having contrasting Zn use efficiency (Chapter 4)

Several studies have demonstrated the impact of MNPs on the physiology, agronomy, and Zn uptake of rice (Ghasemi et al., 2017, Itroutwar et al., 2020, Akmal et al., 2022). However, there is little information available on the effects of CNP application on physiology of rice plants. Therefore, the second goal of the research is to investigate how ZnCDs moderate the Zn utilization efficiency of rice using two cultivars that differ significantly in their Zn utilization efficiency.

3. Comparative transcriptomic analysis of zinc efficient rice variety IR36 against zinc inefficient variety IR26 (Chapter 5)

Lettuce treated by TiO_2 NPs and ZnO NPs (Wang et al., 2017) and *Arabidopsis thaliana* treated with Ag NPs expressed hundreds of differentially expressed genes (DEGs) (Landa et al., 2012, Zhang et al., 2019). However, little is known about variations in the transcriptomics of CNP-treated cereals. Xun et al. (2017) reported that genes (DEGs) expression in Maize after treating with ZnO NPs was altered. Another study carried out with rice treated with CDs (Li et al., 2018) reported increase in the thionine gene expression, but data on transcriptomics are absent. Thus, the third objective of the research project is to determine the transcriptome response to CDs in two cultivars that differ significantly in their Zn utilization efficiency.

4. Comparative proteomics analysis of Zinc efficient rice variety IR36 against zinc inefficient variety IR26 (Chapter 6)

Sawati et al. (2022) reported significant alterations in the proteomics profile with respect to the proteins associated with photosynthesis, transport, glycolysis, and stress response in *Brassica* plants exposed to Zn NPs. Application of CDs may also have a significant effect on the proteome of rice. This objective was to obtain knowledge of the molecular level effect of CD application on rice by comparing the proteomic profile of the ZnCD treated rice to an untreated control.

CHAPTER 2: LITERATURE REVIEW

2.1. Rice, Zinc, and human health

Cereal grains play a major role in the diet of humans around the world. Rice in particular is the staple food for Asians and Africans and is the most important cereal crop for more than 3.5 billion people and provides more than 20% of the daily calorie intake for primary rice consumers (Seck et al., 2012, Muthayya et al., 2014). Though rice is a good source of carbohydrates, it does not provide adequate levels of proteins and micronutrients such as Fe and Zn, compared to other cereals; wheat, corn, barley, millet, and sorghum (Muthayya et al., 2014).

Out of all micronutrients, Zn is vital for eukaryotes. Thus far, around 300 Zn enzymes have been identified having Zn as co- factor (Coleman, 1992). In plants Zn only exist as Zn (II) and involved in many key metabolic processes as a cofactor. The ability of Zn to act as a cofactor is due to its non-redox property (Bashir et al., 2012). Metabolism of biomolecules such as proteins, lipids, carbohydrates and nucleic acids, DNA transcription are some of the key pathways where Zn is critical as a cofactor (Coleman, 1992, Bashir et al., 2012). Additionally, Zn is crucial to the 'Zinc-fingers' such as TFIIIA and GATA type, LIM and RING finger type which are involved in gene transcription, and in protein-protein interaction (Takatsuji, 1998, Bashir et al., 2012). In addition to most of the Zinc-fingers found in eukaryotes, few new motifs such as 'WRKY' and 'Dof' motifs have been identified in plants recently (Takatsuji, 1998). Apart from these, Zn metalloenzymes such as RNA polymerase, reverse transcriptase, and transcription factors play an essential role in DNA and RNA synthesis (Bashir et al., 2012).

In a human body Zn is the second most abundant micronutrient and approximately 2.3 g of Zn is detected in an average adult male body

(Coleman, 1992). Micronutrient deficiency in humans is well documented in rice-based diets.   This causes severe health problems including impaired immunity, brain functionality and physical development (Cakmak, 2008, Cakmak et al., 2010). The RDI for Zn is 8 and 11mg/day for women and for men respectively (National Institutes of Health, 2019) while 100g of rice provides only around 1.7 mg of Zn (The International Rice Commission, 2002). Concentration of Zn in brown rice varies widely; the germplasm collection at International Rice Research Institute (IRRI) reports between 13.5 – 58.4 mgkg^{-1}, with an average of 25.4 mg Zn kg^{-1} (Welch et al., 2002, Boonchuay et al., 2013, Nakandalage et al., 2016). Zn content in rice grain decreases in the order of bran > hulls > whole grain > brown rice > polished rice (Lu et al., 2013). Due to its large mass, endosperm contains nearly 75% of the grain Zn content but Zn concentration in the bran is much higher than in the hull and endosperm. Dehulling and polishing removes Zn from grains and finally only 20% of the daily Zn requirement is provided by the polished rice (Nakandalage et al., 2016). For these reasons, increasing micronutrient concentration in grains, especially Zn is priority research.

2.2. Approaches to increase Zinc content in rice

Zn bio-fortification of crops can be achieved through either an "agronomic approach" or "genetic approach". Out of these, agronomic biofortification is carried out through Zn fertilization and genetic biofortification is carried out through plant breeding strategies and transgenic approaches (Cakmak, 2008). To support genetic biofortification of plants, new breeding techniques such as gene silencing, genome editing (using systems like TALENs, ZFNs, CRISPER-Cas), overexpression, gene transfer from other species has been introduced recently (Shahzad et al., 2021). Hussain et al. (2018) reported a successful attempt of a field study to enhance Fe/Zn nutritional targets in rice using transgenic events and Vasconcelos et al. (2003) reported manipulation of soybean ferritin gene expression could be

used in enhancing Fe and Zn levels in transgenic rice variety. However, use of other new genetic breeding techniques is rare in Zn biofortification of cereals.

Alternatively, the interaction between environmental (E) and genetic factors (G) on Zn homeostasis is largely unknown thus, understanding of E×G interaction is essential for Zn biofortification. Very limited amount of research has been carried out with rice in this aspect which is important as most of rice plants grown anaerobically where the nutrient assimilatory process is different to their aerobic counterparts (Nakandalage et al., 2016).

2.2.1. Agronomic approaches to increase Zn content in rice

Many studies have been carried out to improve growth, yield and Zn content of rice grain using different agronomic strategies. The success of the strategy depends on the form of application, type and the condition of the soil and the type of fertiliser used (Cakmak, 2008). Soil application of Zn fertiliser is very convenient method and deliver positive results as well. Ghoneim (2016) details the success of the soil Zn application with compared to foliar and root soaking methods. Zn fertilization is recommended as a rapid solution to mitigate the Zn deficiency in plants (Cakmak, 2008).

Synchronization of N and Zn fertilization could deliver better results than individual application and soil P application may slow down the uptake of Zn by increasing Zn adsorption to soil particles (Alloway, 2008). $ZnSO_4$, is the most common Zn fertiliser, but its efficiency is not as high as ZnO, $ZnCO_3$, $Zn(NO_3)_2$ or $ZnC_4H_6O_4$ forms (Nakandalage et al., 2016).

Besides, soil application of Zn fertiliser has many drawbacks. Dissolved humic substances can complex with Zn in soil solution, and either make Zn less available to plants (in aerobic soils) or more available (in anaerobic soils) (Nakandalage et al., 2016). Additionally, only a small portion of

applied fertiliser is absorbed by the plant and the excess causes serious environmental hazards like micronutrient leaching and ground water contamination. Further, applied nutrients could be lost due to runoff, evaporation, phytolysis and microbial action (Gogos et al., 2012). Thus, soil fertiliser application should be practiced with care and thorough knowledge of the soil conditions in the field.

Boonchuay et al. (2013) and Mabesa et al. (2013) reported, foliar application of Zn fertilisers at early grain filling increased grain Zn content. Compared to soil fertilization of micronutrients, foliar application has many benefits. Foliar application at the right plant growth stage and to the correct plant organ brings about more positive results (Habib, 2009, Boonchuay et al., 2013, Zhao et al., 2014). However, foliar application may cause scorching of leaves (Deshpande et al., 2017). If these issues can be resolved, foliar intervention is the ideal strategy for micronutrient management in plants. Recently, there has been interest in novel techniques such as nanotechnology to deliver micronutrients to plants avoiding the above disadvantages.

2.2.2. *Uptake, translocation and grain loading of Zinc*

Rice genetically controls Zn uptake from the root, transportation through Zn transporters, Zn ligands and phytosiderophores. These factors regulate the total Zn content of plant and its grains (Nakandalage et al., 2016). Zn uptake from rhizosphere and transportation of absorbed Zn is mainly governed by members of The zinc-regulated, iron-regulated transporter-like proteins (ZIP) family genes such as OsZIP1 and OsZIP3 (Grotz et al., 2006, Ishimaru et al., 2011).

Besides, low molecular weight phytosiderophores (PS) with high affinity to Zn^{2+} such as malate, mugineic acid family too play a critical role in enhancing Zn uptake from the soil (Ishimaru et al., 2011, Nakandalage et

al., 2016). Genes such as OsNAS1, OsNAS2, OsNAS3, OsDMAS1, and OsHMA2 are involved in genetic control of Zn transportation from root to shoot (Suzuki et al., 2008, Satoh-Nagasawa et al., 2011, Takahashi et al., 2012).

In rice, Zn is directly transported through the xylem into the rachis and grain vascular bundles from the stem (Jiang et al., 2008, Nakandalage et al., 2016). The apoplastic pathway plays a key role in transporting Zn from the nucellar epidermis and aleurone cells to the endosperm of the rice grain (Jiang et al., 2008). Further, a higher proportion of grain Zn is deposited on the outer aleurone layer (Jiang et al., 2008). Two key genes involved in grain Zn loading are OsZIP4 and OsZIP8 (Nakandalage et al., 2016). As exposure to NPs may generate unexpected changes in the gene expression and the transcriptome of the plants, a detailed transcriptomic analysis would reveal such changes in the rice transcriptome.

Zinc speciation plays an important role in Zn homeostasis. Zn makes ligands in the cytosol with low molecular weight compounds such as nicotianamine (NA), histidine, malate, citric acid etc. and these compounds help in Zn solubility and mobility (Ishimaru et al., 2011, Sinclair et al., 2012). NA act as the dominant Zn ligand in the cytosol, xylem and phloem (Clemens et al., 2013). In grains, phytic acid act as the major chelating molecule to bind with Zn and this produces an insoluble compound called phytate (Cakmak, 2008, Sperotto, 2013). Zn content in rice grains is largely depends on Zn allocation between different organs of the plant. Nutrient status and the physiological growth stage of the rice plant governs this allocation. During the vegetative phase, Zn is primarily supplied to the leaves and during the reproductive phase it is supplied to the grains (Nakandalage et al., 2016).

2.3. NPs in agriculture

2.3.1. *Use of NPs in enhancing crop productivity*

Use of NPs in plant research is an emergent field of natural science dealing with nano-scale materials. Incorporation of nanotechnology to plant biology has given rise to a new fields of science called "Plant Nanobionics" and "Phyto-nanotechnology" which aims to employ nanotechnology to improve plant growth, development and productivity (Khatri et al., 2018, Li et al., 2020a). As a result, NPs have been successfully used in the areas of nano-fertilisers, nanoparticulate plant growth enhancers, crop protection (herbicide, pesticide delivery), chemical compound detection (especially for heavy metals) in biological and environmental entities, gene transfer, bio labelling, development of nanobionic light emitting plants (Torney et al., 2007, Liu et al., 2014, Kashyap et al., 2015, Liu et al., 2015, Kwak et al., 2017, Tuerhong et al., 2017). In many of these applications NPs act as carriers to transport a gene, molecule, or an ion to the biological material. In the plant cell model, *Nicotiana tabacum* "bright yellow cells (BY-2)" exhibited the ability of CNTs to penetrate cell walls and membranes to deliver molecular cargoes (Liu et al., 2009). Use of NPs as transporters has advantages over the gene gun, electroporation, and microinjection methods, due to its high efficiency and the capacity to deliver molecules other than nucleic acids (Liu et al., 2009). Kwak et al. (2019) demonstrated that NPs can be used to deliver molecules not only to the cell interior but also to the interior of the subcellular organelles such as chloroplasts.

Several studies have reported successful attempts at using NPs as micronutrient carriers (chitosan, zeolite, carbon NPs) (Kashyap et al., 2015, Liu et al., 2015, Ashfaq et al., 2017) as well as micronutrient NPs (such as Fe, Mn, Zn, Cu, Mo) themselves to supply micronutrients to plants (Liu et al., 2015, Hong et al., 2016). Zn bound chitosan NPs have been used successfully to deliver Zn to wheat plants and to increase grain Zn content (Deshpande et al., 2017, Deshpande et al., 2018) and water-soluble CDs enhanced growth of both root and shoot of wheat plants (Tripathi et al.,

2015). Foliar applications of CeO_2 and CuO NPs to cucumber negatively affected photosynthesis and uptake of Zn of immature leaves but not on mature leaves (Hong et al., 2016). Nanoparticulate ZnO foliar applications on maize plants reported significant increases in plant height, leaf area, dry weight, chlorophyll index, and grain yield (Subbaiah et al., 2016).

Many researchers reported enhancements in agronomical traits, agro-morphological characteristics, and stress tolerance of rice due to the application of NPs such as ZnO, CNPs etc., (Ghasemi et al., 2017, Panda, 2017, Zhang et al., 2017, Itroutwar et al., 2020, Singh et al., 2022). However, studies on the use of NPs to increase the Zn uptake and grain Zn content of rice is limited. Study done by Yang et al. (2021) confirmed the efficiency of ZnO NPs with compared to the inorganic Zn salts and recorded significant increase in grain yield, NPK uptake, and grain Zn content resulted due to the NP application at panicle stage. Bala et al. (2019) and Akmal et al. (2022) also have confirmed the effectiveness of foliar applied ZnO NPs as a method of Zn fortification compared to soil and bulk applications.

Other than being micronutrient suppliers, NPs exhibit many roles in rice. Application of nano chelated iron fertiliser has increased yield by 1/4th, and protein content by 1/8th of the total (Itroutwar et al., 2020), whereas Ag NP application displayed nearly 15 – 30% increase in rice yield (Ikhajiagbe et al., 2021). Applications of CNPs such as SWCNTs, MWCNTs, C_{60}, Graphene, SWCNHs confirmed that they could enhance plant growth, seed germination, root and shoot growth in rice plants effectively (Nair et al., 2012, Lahiani et al., 2015, Yan et al., 2016).

2.3.2. Uptake and translocation of NPs in plants

Nanomaterial uptake, translocation and final fate depends on the plant and the properties of the NP. Carbon based NPs such as fullerene C_{70} and fullerols (functionalized fullerenes) and most of the metal-based NPs

accumulate inside the plant cells (Rico et al., 2011). The primary use of NPs in agriculture is to reduce the concentration of phytochemicals, optimise fertiliser applications and increase yield and quality of the plant products through maximum usage of nutrients (Gogos et al., 2012). High surface area to volume ratio and appropriate sorption properties of NPs help to reduce runoff and minimize losses due to release kinetics (Gogos et al., 2012). Smaller NPs can pass through the pores on the cell wall and membrane while others enter via carrier proteins (transmembrane proteins which allow transportation of molecules), aquaporins (specialized channel proteins for water molecules), and ion channels (transmembrane proteins with pores specialized for ion transportation) or by endocytosis (cellular uptake via engulfing and fusing with cell membrane) (Rico et al., 2011, Tripathi et al., 2017). However, Kwak et al. (2019) report that traversing subcellular organelles' double lipid bilayers (in chloroplast) is governed by NP size and surface charge (ζ potential) employing a specific method called lipid exchange envelope penetration (LEEP) model (Wong et al., 2016, Kwak et al., 2019). Studies utilized water-soluble SWCTs have revealed, larger NPs mainly enter plant cells through endocytosis (Rico et al., 2011). However, information on uptake of CDs by plant cells and their fate inside the cells is limited.

Concentration of the NP also plays a critical role in uptake. In soybean, maize, and wheat NP solutions such as water-soluble CDs, ZnO of moderate concentrations i.e., 200 – 500 ppm were more effective in absorption (Rico et al., 2011, Tripathi et al., 2015, Subbaiah et al., 2016). Higher concentrations of NPs (more than 1000 ppm) tend to agglomerate which increases their size and makes it harder to traverse the membrane via pores (Rico et al., 2011). Once NPs are absorbed by the cells, they either follow a symplastic or apoplastic mechanism. Also, NPs can be transported from one cell to another through plasmodesmata. Following integration with the apoplast of the endodermis, the vascular system serves as the main pathway for translocating NPs to primary sinks in the leaves or grains.

Detection of carbon-based NPs in plant material has been done using many techniques. Lin et al. (2009) used bright field microscopy to detect MWNT and fullerene 70 in seeds, roots and leaves of rice plants. Fluorescence and confocal 3D mapping have also been used with fluorescent SWCTs in spinach chloroplasts (Giraldo et al., 2014). Fluorescence has also been used in determining root uptake of water-soluble CDs in wheat seedlings (Tripathi et al., 2015). Uptake and translocation of fluorescent CDs in mung seedlings has been successfully studied using laser scanning confocal microscopy images (Li et al., 2016a, Wang et al., 2018). In addition, TEM and SEM have been utilized in studies of carbon-based NPs applied to plant cells (Chen et al., 2010, Tripathi et al., 2015, Li et al., 2016a, Wang et al., 2018).

2.3.3. NP toxicity to crops

The use of NPs including CNPs, and metal-based NPs have been documented as depicted above. However, studies done with some NPs exhibit toxicity towards rice plant growth. Tan et al. (2009), Begum et al. (2014), Zhang et al. (2020), Guo et al. (2022) provided information on toxicity of CNPs such as MWCNTs and graphene oxide. Rice plants at seedling stage showed phytotoxicity at higher concentration levels of MWCNTs such as 1000, 2000 ppm (Begum et al., 2014), but decreased cell viability of rice cell lines (Oryza sativa C5928) was observed at low concentration of MWCNTs (20 ppm) as well (Tan et al., 2009). However, application of MWCNTs at 100 ppm level at the atmospheric pressure has not affected physiological factors and growth of rice seedlings but the same application has affected the growth factors of rice seedlings highly under low pressure conditions (Guo et al., 2022). Rice protoplast treated with SWCNTs of 5 – 100 ppm levels exhibited dose dependent survival and oxidative stress (Shen et al., 2010). Moreover, application of Graphene oxide at 100 and 250 ppm levels showed oxidative damage in the 3 weeks old rice seedlings due to enhancement of iron (Fe) translocation and

accumulation in shoots. Nevertheless, application of reduced graphene oxide at same concentrations did not result any toxicity, proving that the reduced forms of graphene-based nanomaterials are less toxic (Zhang et al., 2020).

In addition to the toxicity of Carbon-based NPs, MNPs have displayed toxicity towards rice plant growth. Boonyanitipong et al. (2011) reported application of ZnO NPs at early seedling growth of rice caused detrimental effects. Yet, application of TiO_2 NPs of same concentration did not result same outcome. A similar study carried out by, Wu et al. (2017) reported decrease in biomass, disturbances in antioxidant defence system and in carbohydrate metabolism whereas, increase in crop quality related metabolites such as fatty acids, amino acids and secondary metabolites demonstrating a mixed effect of TiO_2 NPs application.

CDs have been reported as relatively less toxic nanoparticle (Li et al., 2018a). Studies carried out with *Petunia axillaris* seedlings and mung bean plants treated with different levels of CDs reported less or no phytotoxicity (Li et al., 2016b, Kim et al., 2018). Plants treated with higher doses (such as 2000 ppm and 1000 ppm) of other CNPs; namely MWCNTs, graphene oxide showed phytotoxicity (Lin et al., 2007, Chen et al., 2017). Additionally, higher doses of Zn NPs also reported to have genotoxic effects on soybean germination (López-Moreno et al., 2010a). Nevertheless, Du et al. (2019) reported that, toxicity of higher concentrations of Zn NPs are comparatively less toxic than that caused by the bulk Zn source. Toxicity of CeO_2 NPs application at 2000 ppm was reported in studies carried out with plants including corn and soy (López-Moreno et al., 2010a, López-Moreno et al., 2010b). Toxicity of the widely used ENP, Ag has been studied in many instances. (Qian et al., 2013, Song et al., 2013, Vannini et al., 2014, Wang et al., 2017a) reported Ag NP toxicity of plants at varying concentrations from 10 to 5000 ppm.

Outcome of these toxicity studies proves that the toxicity of NPs gets varied significantly. The effect is totally dependent on the type of NP, concentration of the application, size of the material and the species/variety and the growth stage of the plant used for the study.

2.4. Carbon nanodots (CDs)

2.4.1. CDs: Properties, and characterization

Besides popular members of the carbon nanomaterial family such as graphene, SWCTs and MWCTs used in agriculture, CDs have recently gained much attention. CDs are nano sized 0D, luminescent, surface passivated carbon based NPs with a size range of 1 – 10 nm in diameter (Kim, 2015). Inexpensive production methods, ease of bio-conjugation, luminescence emission and low toxicity make CDs appropriate for use with biological material (Baker et al., 2010). Due to the presence of oxidized moieties such as carboxyl on the surface of the dot, CDs display exceptional water solubility and possibility of making new bonds for further functionalization with desired molecules (Baker et al., 2010, Kim, 2015). These properties of CDs are principally governed by the synthetic approaches and the materials used. Arc discharge, laser ablation, electrochemical oxidation, pyrolysis, plasma treatment and hydrothermal or microwave pyrolysis can be used to synthesize CDs (Kim, 2015).

It is vital to determine the CDs physio-chemical properties since bioactivity of an NP depends on its size, shape, aggregation state, surface charge and functionality. UV-Vis and fluorescent spectroscopy are used to determine the fluorescence of CDs. Functionality, purity, and structure can be determined by NMR and FTIR. TEM can be used to define particle size distribution and shape. AFM provides information on topography of the materials and particle size. Optical spectroscopy is used to detect emission, reflection, and absorption of the photoluminescence of CDs. Zeta (ζ)

potential analysis determines the surface charge which provides a good estimate of the CD's ability to traverse biological membranes (Kim, 2015).

2.4.2. Use of CDs in crop improvement

CDs are widely studied for its capabilities in the fields of bioimaging, drug delivery and fluorescence; while limited research has been carried out on CDs in plants. A nearly 15% increase in yield and resistance to diseases have been resulted following application of CDs of 200 ppm to rice plants (Li et al., 2018a). A study done by Tripathi et al. (2015) reported water soluble CDs (150 ppm) enhanced productivity of wheat plants but did not speculate on the mechanisms involved. Another study done by Li et al. (2016b) showed positive trend in root and shoot growth with the application of 400 ppm of CDs in mung bean seedlings. Further, mung bean sprouts grown with CDs showed dose-dependent response in terms of root, stem elongation and increase in biomass. Further this application reported nearly 20% increase in plant carbohydrate content. Capability of CDs to enhance the electron transfer rate could improve the photosynthesis rate of the plant and thereby raise the carbohydrate level (Wang et al., 2018). Application of glucose-functionalized carbon dots to wheat plants displayed nearly 20% increase in yield, photoprotection and pigment production (Swift et al., 2021) but no evidence was found on the application of CDs bound with micronutrient such as Zn. Magnesium-nitrogen co-doped CDs were capable of improving the photosynthesis capacity of the rice plants considerably resulting a substantial increase in height and fresh biomass of rice plants (Li et al., 2021b).

Being a benign molecule, CDs can easily be loaded with bioactive molecules or trace elements. A compound like Zn acetate could be bound to CDs via its carboxylic functional group. Zn acetate is widely used in obtaining ZnO nanoparticles via thermal decomposition (Yang et al., 2004). CDs bound

with Zn acetate will be used in the proposed study to increase the Zn content in rice plants. Bonding pattern and the exact structure of the developing NP (CD with Zn acetate) can be elucidated with the NP characterization methods described above.

Information on the effects of Zn acetate on plant growth and development is limited. However, a number of commercial products based on Zn acetate (e.g.: CultivAce Zinc, MicroSolutions® MicroMark™ RGS®, Zn-Ac at Custom Agronomics etc.) are available in the agrochemical market (Cultivacegrowth.com, 2019, Custom Agronomics, 2019, The Andersons, 2019). The effect of CDs alone and Zn acetate bound CDs on plant growth processes are not well understood. Therefore, characterisation of CD along with its impact on plant physiological processes should be further studied to determine the physiological mechanisms that drive the Zn transport via CDs. Findings of these experiments will be important for Zn biofortification programs in rice in future. Further, these techniques can be adapted to other trace nutrients for nutrient biofortification for other crops.

2.4.3. Effect of CD application on plant physiology

CDs effect on plant growth has been studied in many instances but their specific effect on plant physiological aspects such as photosynthesis is rare to be reported. Wang et al. (2018) and Hu et al. (2022) showed that the application of CDs 20 ppm and 30 ppm respectively enhanced the photosynthesis rate considerably and there by increased the fresh biomass of mung beans and lettuce plants. CDs are excellent electron donors and acceptors thus it fosters electron transfer of photosystems. Further, supplement of CDs enhanced the chloroplast activity, Rubisco and other enzyme activities, light absorption, and energy conversion efficiency of the plant (Chandra et al., 2014, Li et al., 2018b, Wang et al., 2018, Li et al., 2020b). All these amendments boost the photosynthesis rate of the plants

and thereby increase the carbohydrate content and the growth of the plant. A similar pattern of observation was made with rice plants seedlings treated with Mg-N co-doped CDs at 300 ppm concentration (Li et al., 2021b). Additionally, application of nontoxic orange CDs (o-CDs) at 1 ppm and 5 ppm levels in maize seedlings showed increased in gas exchange parameters such as photosynthetic rate and transpiration rate and also increased the photosynthetic pigments concentration such as chlorophyl *a*, *b,* and carotenoids (Milenković et al., 2021). The same application has also enhanced the plant antioxidant as well as the total phenolics (Milenković et al., 2021).

Incubation of isolated chloroplast from lettuce plants with 300 ppm CDs exhibited quantum yield effect of CDs. Chloroplasts supplemented with CD converted UV radiation to photosynthetically active radiation (PAR). This light conversion of CDs were evidenced by the reduction of ferricyanide in photosynthesis under pure UV radiation (Li et al., 2021a). Therefore, the detrimental effect of UV radiation in the sunlight to the plant photosynthesis (due to the production of reactive Oxygen species (ROS)) could be resolved by the application of CDs. Further, this study confirmed substantial increase of the photosynthetic activity of chloroplasts due to the conversion of toxic UV radiation (300 – 370 nm) to PAR (370 nm – 500 nm) (Li et al., 2021a). Additionally, foliar applied CDs (300 ppm) to rice plants recorded increased electron transport rate, photosynthetic efficiency of PS II and enhanced RuBisCO carboxylase activity in the same study. As a result, rice seedlings reported significant increase in growth (Li et al., 2021a). In addition to the improvement of photosynthetic rate, CDs report adjustments of rhizospheric properties and drought tolerance in plants as well. Foliar applied CDs (5 ppm) to 25 days old maize seedlings under drought stress increased the contents of root exudates such as succinic acid, pyruvic acid etc, and the relative abundance of soil microbiota such as *Pseudomonas, Sphingomonas, Nitrospira* etc. These changes improved plant water uptake and improved soil available N and P allowing the plant to increase the

biomass (Yang et al., 2022). Thus, it is proved that CDs have positive approach in terms of augmenting the plant physiological processes specially the photosynthesis.

2.4.4.   Effect of CDs on transcriptome and gene expression

Much research carried out all over the world have proved that the application of NPs in agriculture could bring about many positive impacts. However, the molecular and transcriptional changes behind these impacts were hardly understood. Particularly, limited research has been carried out to discover the changes in the transcriptome and proteome level response to NP application. Several studies have been conducted on rice to reveal expressional changes in the genes of interest in response to NP treatments, but this is the first comprehensive study on how the whole genome and proteome respond to NP in any species.

Chen et al. (2018) reported the molecular level changes of the rice seedlings following ZnO NP application with respect to the gene expression of three antioxidant enzymes. Another study done by Song et al. (2021) revealed that foliar application of ZnO NPs upregulated chilling induced gene expression of the antioxidant genes as well as the chilling response transcription factors of rice seedlings under chilling stress. Further, a study carried out by Nair et al. (2014), reported rice seedlings treated with Ag NPs had significantly reduced root elongation, shoot and root fresh weights, total chlorophyll contents and demonstrated differential transcription of genes related to oxidative stress tolerance of rice seedlings. Rice seedlings treated with CuO NPs as well exhibit shifts in the gene expression. Weedy rice grown for several months with CuO NPs at 150 ppm level upregulated the auxin associated genes substantially (Deng et al., 2022). Rice seedling roots treated with 5 ppm CuO NPs suspension upregulated the expression level of two genes associated the root growth (Wang et al., 2015).

A very few recent studies reported transcriptomics analysis of rice due to treatments other than NPs. Studies of Bao et al. (2021) revealed changes in the rice transcriptome with respect to upregulation of pyrroline related genes and transcriptional factors following foliar Zn applications. Further, Baldoni et al. (2021) described comparative transcriptomic changes between drought tolerant and susceptible genotypes of rice, barley, maize and *Brachypodium*. The results exposed 69 conserved drought tolerant-related genes in all species tested and specific transcriptional factors that regulate photosynthesis and senescence.

Nevertheless, hardly any research reported effect of transcriptomics following application of NPs plants other rice. Effect Ag NPs in transcriptome of model dicot plant *Arabidopsis* was reported (Zhang et al., 2019). This study revealed that nearly 60% of genes were alters in their expression and 302 genes out of those were particularly regulated due to the Ag NP application. Use of TiO_2 and ZnO on lettuce plants exposed significant changes in the transcriptomics. More than 3500 differentially expressed genes (DEGs) were identified in shoots of plant including genes related to photosynthesis, carbohydrate and nitrogen metabolism, and antioxidant pathway (Wang et al., 2017b). A study carried out by García-Sánchez et al. (2015) reported transcriptomic changes in *Arabidopsis thaliana* treated with different NPs such as TiO_2, Ag and MWCNTs. This study revealed, NP exposure repressed transcriptional responses to microbial pathogen infections and exhibited transcriptional patterns characteristic of phosphate starvation. A transcriptomic profile analysis of ZnO NP treated maize plants exhibited differences in DEGs and enrichment of gene ontology (GO) terms in roots and shoots. Out of all, genes involved in nitrogen compound metabolism and cellular component were highly up regulated in roots treated with ZnO NPs (Xun et al., 2017).

Additionally, few more studies have been carried to unravel the transcriptomic changes of the plants due to different treatment types other than NP application (Mohammadi-Dehcheshmeh et al., 2018, Shiri et al.,

2018, Nezamivand-Chegini et al., 2023). Several studies have been carried out to explore the changes on expression level of genes of interest following metal-based NP applications in various plants. The model dicot plant *Arabidopsis* has been used widely in these investigations. In *Arabidopsis* treated with TiO_2 and CeO_2 NPs altered the regulation of 204 and 142 genes, respectively (Tumburu et al., 2015). Other research with *Arabidopsis* treated with to AgNPs found upregulation of 286 genes and downregulation of 81 genes including genes involved in plant defence (Kaveh et al., 2013). Burklew et al. (2012) reported, tobacco plants treated with Al_2O_3 NPs show increased expression of some microRNAs resulting in reduced growth and development of the seedlings. Wheat seedlings treated with zinc loaded chitosan NPs also demonstrated changes in the gene expression level including ZIP family genes, phloem transporters, genes involved in metal homeostasis and leaf senescence (Deshpande et al., 2018).

Outcome of all these experiments demonstrate that the possible changes in the molecular level and in the transcriptome of the plants is highly subjective to the physiological state, type of treatment application of plant. Thus, use of CDs and Zn bound CDs on rice plants as well would result in unique changes in the transcriptome.

2.4.5. Effect of CDs on proteome

Much attention has received on the field of proteomics recently. However, information on effect of NP application on plant proteomics is limited. Li et al. (2018c) reported alteration in the proteomic profile due to the application of graphene oxide NPs into the rice seedlings. Proteins such as ascorbate peroxidase, aquaporins, proteins involved in ATP synthesis, oxidative stress and transmembrane transport were detected with altered synthesis. Another quantitative proteomics experiment carried out with rice

seedlings treated with CuO NPs showed substantial increase in differentially expressed proteins compared to the control treatments (Peng et al., 2022). Few recent studies reported the results of quantitative proteomics analysis of rice plants subjected to various stress conditions including salinity, cold and defence response (Cui et al., 2005, Neilson et al., 2011, Feng et al., 2022, Nguyen et al., 2022). These results suggest that stress condition triggered due to abiotic or biotic factors could lead to changes in the protein profile of rice plants. Thus, application of NPs (which may be a possible reason for an induced abiotic stress condition of rice plants) could also prompt changes in the proteomic profile.

In addition to rice, several other plants also have expressed proteome changes due to the application of MNPs. *Brassica napus* treated with Zn NPs exhibited a significant increase in photosynthesis, transport, glycolysis, and stress response proteins (Sawati et al., 2022). Similar type of results was showed in a proteomic study done with tobacco plants treated with Ag NPs. Ag NP treatment has affected the photosynthesis, by up regulating the proteins involved in primary metabolism including photosynthesis and energy production (Štefanić et al., 2018). Soybean roots treated with Al_2O_3 NPs also showed changes in the abundance of 211 common proteins including proteins related to stress conditions, cell wall synthesis, and cell signalling (Yasmeen et al., 2016).

Consequently, it is evident that NP application would alter the rice plant proteome. The combination of proteomics and transcriptomics data will provide a comprehensive understanding of the molecular regulation of a plant system in response to NP application.

CHAPTER 3: EFFECTS OF CARBON NANOPARTICLES ON PHYSIOLOGICAL PROCESS AND ZINC UPTAKE OF RICE

3.1. Introduction

Several studies have investigated the effect of MNPs, ENPs, and CNPs on rice biology. Application of ZnO NPs, Fe NPs, SWCNTs, MWCNTs, C_{60} graphene were successful in promoting growth, rate of seed germination, Zn/Fe uptake, grain yield, water uptake and improving many more agronomic traits (Nair et al., 2012, Ghasemi et al., 2017, Zhang et al., 2017, Li et al., 2018, Bala et al., 2019, Itroutwar et al., 2020, Yang et al., 2021, Akmal et al., 2022). Nevertheless, most plant responses towards applied NPs are dose dependent (Ghasemi et al., 2017, Panda, 2017, Itroutwar et al., 2020). On contrary, applications of CNPs of higher doses and MNPs such as Ag NPs depicted negative effects on plant biology (Begum et al., 2012, Begum et al., 2014, Thuesombat et al., 2014, Hao et al., 2018).

The presence of ligands, complexed molecules and functionalization of NPs determine the uptake and effect of NPs. Glucose bound CDs, Zn complexed chitosan CNPs exhibit improved NP uptake and Zn uptake in cereals respectively (Deshpande et al., 2017, Swift et al., 2021) and gold NPs (Au NPs) functionalized with short ligands of cysteine, cysteamine and thioglycolic and AuNPs charged as positively, negatively, and neutrally showed differences in their amount and rate of uptake in rice plants (Koelmel et al., 2013, Li et al., 2016). NP application to plants has been accomplished in a number of ways, including soil application, foliar treatment, root dip technique, and so on. Out of all, Hussain et al. (2018),

Hussain et al. (2019), Akmal et al. (2022) confirmed that the foliar application is much effective than the soil application of NPs.

Out of the NPs used in crop improvement of cereals, CDs become popular recently due to their unique chemical, physical properties such as tuneable photoluminescence, low to none toxicity, water solubility, low production cost etc., (Hao et al., 2016, Li et al., 2018). Application of CDs of 20- 120 ppm showed dose-response on the root/shoot elongation and positive output on photosynthesis of Mung bean sprouts (Wang et al., 2018). Li et al. (2018) reported nearly 14.8 % enhancement in rice yield and increased rice plant resistance to diseases. Additionally, Swift et al. (2021) proves improved NP uptake, photoprotection and pigment production due to the application of glucose complexed CDs to Wheat plants. However, studies on Zn bound CDs have not been carried out yet, and their most effective dose has not been investigated. Therefore, this experiment was designed to determine the most effective dose of Zn bound CDs in terms of their responses to the rice plant physiology and agronomic traits and Zn uptake at early rice plant growth stages.

A Zn efficient, salt tolerant, late maturing rice variety 'Pokkali' was used in this experiment to accurately determine Zn uptake. The two medium maturing varieties selected for the whole study; IR 26 (Zn inefficient) and IR 36 (Zn efficient) those are close relatives of each other according to their pedigree (Khush, 2005). Those varieties could not be cultivated in a Zn-free media, indicating that Zn dependency is genetically inherited. Thus, a Zn efficient rice genotype 'Pokkali' which was confirmed by the studies of Naher et al. (2014), Begum et al. (2016), Kabir et al. (2017) for absence of significant difference in morpho-physiological parameters due to Zn deficiency in the growing medium selected for the study.

Zn, an essential micronutrient, regulates many metabolic processes in plants, including DNA – RNA synthesis, protein, carbohydrate, lipid metabolism, and Auxin metabolism (Alloway, 2008). Thus, Zn uptake and

use efficiency was measured during different physiological ages to evaluate the Zn use efficiency. Agronomic traits such as plant height, total number of tillers, leaf area of total plant, leaf area of flag leaf, dry weight and nutritional measurements like Zn content were also measured (Ghasemi et al., 2017).

3.1.1. *Goal of the study*

The goal of the study is to test the following hypotheses: 1; ZnCD increase grain Zn concentration 2; ZnCD promotes plant growth and development by modifying physiological and agronomic characteristics; 3; Zn utilization efficiency is critical to grain Zn accumulation.

3.2. Materials and methods

3.2.1. Experimental site and design

The experiment was conducted at the Centre for Crop Health, University of Southern Queensland, Toowoomba, Australia from September 2019 – January 2020. The 'Pokkali' rice variety, which can withstand a Zn-free growing medium for up to three months, was chosen for this dose determination experiment. The nine treatments included four different concentrations of CDs (50 ppm, 100 ppm, 250 ppm, 500 ppm), four different concentrations of ZnCDs (50 ppm, 100 ppm, 250 ppm, 500 ppm) and Control (without NP addition).

The experiment was carried out in a glasshouse using a randomized complete block design at 5 replicates level. The experimental 'unit' will be a pot with single rice plant, where as 'block' will be a tank set up for the sand culture.

The temperature of the glasshouse was maintained at 25°C (day) and 22 °C (night) and relative humidity was maintained at 60 – 75% throughout the experiment.

3.2.2. CNPs: characterization and preparation for treatments

The carbon nanomaterials used for the study 'carbon dots' (CD), and 'Zn bound carbon dots' (ZnCD) are proprietary material obtained from Queensland Micro- and Nanotechnology Centre & Environmental Engineering, Griffith University, Brisbane, Australia. Characterization of CNPs has been done using Analytical X-ray Photoelectron Spectroscopy (XPS), UV-Vis Spectroscopy and Dynamic Light Scattering (DLS). Working concentrations of 50, 100, 250 and 500 ppm CD and ZnCD were prepared by dispersing known amounts of NPs in deionized water (w/v). Tween 20

(0.2% V/V) was added to each solution to facilitate effective spraying of CNPs.

3.2.3. *Plant material and growing conditions*

A highly tolerant rice variety to Zn deficiency 'Pokkali' (Naher et al., 2014, Begum et al., 2016, Kabir et al., 2017) selected for the study as they need to be grown in a zero Zn medium. Seedlings were cultured using sand culture technique described in (Mae et al., 1981).

Coarse double washed river sand from Downs Sand Gravel & Landscape Supplies, Drayton, Australia was initially washed several times with tap water to remove clay particles and impurities. Next, sand was acid washed using 5% HNO_3 (v/v) and washed again for five times with reverse osmosis (RO) water. Air dried acid washed sand was filled into plastic pots (50 mm Black square tube pot).

Nutrient media was prepared as per the method described in (Mae et al., 1981). Separate macro-nutrient stock solutions KNO_3, NH_4NO_3, $NaH_2PO_4.2H_2O$, K_2SO_4, $CaCl_2.2H_2O$, $MgCl_2.6H_2O$, Fe-EDTA were prepared with deionized water as mentioned in Table 3.1. Micro-nutrient stock solution was prepared by dissolving all micronutrients H_3BO_3, $MnSO_4.5H_2O$, $CuSO_4.5H_2O$, $NaMoO_4.2H_2O$ in deionized water (Table 3.1). To ensure precise determination of Zn absorption from CNPs, a Zn free nutrient medium was used in the study. Thus, $ZnSO_4.7H_2O$ was not added to the micro-nutrient stock solution. One ml of each macro and 0.1 ml of micro-nutrient stock solution were diluted with 1 L of deionized water to prepare growing solutions. Growing solution pH was maintained at 5.5 ±1.

The method described in Nair et al. (2012) was slightly changed to surface disinfect the Rice seeds. First RO water was used to wash seeds three times. The seeds were then sterilised double by soaking in 70% ethanol for

2 minutes with gentle agitation and then in 1% Sodium hypochlorite for 5 minutes with gentle shaking. In the end, the seeds were rinsed with RO water for four times and air dried on a sterile tissue paper.

Rice seeds were dispersed on a clean saran net and the net was allowed to float on RO water until the seeds were germinated. Seedlings with 2 – 3 leaves were used to transplant in pots in sand culture.

Table 3.1: Micro and micro-nutrient composition of growing solution

		Macro-nutrient solutions		
Macro-nutrient	Chemical formula used	Concentration in stock solution (M)	Concentration in growing solution (M)	stock solution Volume needed to prepare 1L of growing solution (ml)
N, K	KNO_3	2.0	2.0×10^{-3}	1
N	NH_4NO_3	1.0	1.0×10^{-3}	1
P	$NaH_2PO_4.2H_2O$	0.6	0.6×10^{-3}	1
K, S	K_2SO_4	0.3	0.3×10^{-3}	1
Ca	$CaCl_2.2H_2O$	0.3	0.3×10^{-3}	1
Mg	$MgCl_2.6H_2O$	0.6	0.6×10^{-3}	1
Fe	Fe-EDTA	45×10^{-2}	45×10^{-5}	1

		Micro-nutrient solution		
Micro-nutrient	Chemical formula used	Concentration in stock solution (M)	Concentration in growing solution (M)	stock solution Volume needed to prepare 1L of growing solution (ml)
B	H_3BO_3	4.87×10^{-1}	5.0×10^{-5}	
Mn	$MnSO_4.5H_2O$	9.0×10^{-2}	9.0×10^{-6}	0.1
Cu	$CuSO_4.5H_2O$	3×10^{-3}	3×10^{-7}	
Mo	$NaMoO_4.2H_2O$	1×10^{-3}	1×10^{-7}	

3.2.4. Crop growth and maintenance

Acid washed sand were filled into square tube pots (up to 1cm below the pot surface) and nine pots were kept inside a black plastic container (volume 06 L). To accommodate all 5 replicates according to the RCBD model 5 tanks were prepared and pots inside the tanks were randomized to minimize the spatial effect. Five litres of $1/8^{th}$ strength of growing solution were added to each container as the solution level was 1 cm above the pot surface. Rice seedlings with 2 – 3 leaves were transplanted in sand-filled pots as each pot has one rice plant.

To avoid algal growth inside the tanks, surface of the tank was covered with black polythene keeping sufficient space for rice plants growth. The growing solution's strength was doubled every week (1st week - $1/8^{th}$ strength; 2nd week - $1/4^{th}$ strength; 3rd week -half strength; 4th week – full strength) until the concentration is in its full strength. While waiting for plants to grow for 6 weeks, the growth solution was renewed in every 4 days to supply nutrients in consistent manner.

3.2.5. Treatment application

Six weeks old rice plants were subjected to nine different treatments, which included CD concentrations of 50, 100, 250, and 500 ppm, ZnCD concentrations of 50, 100, 250, and 500 ppm, and a control. Each treatment was applied for all 5 replicates.

A Paasche® VL 0908 sprayer coupled with Dynavac® pump was used to spray NPs. Each plant was removed from the growing solution tank and kept inside a front open cardboard box to prevent contamination while spraying. Plants were sprayed with designated treatment solution for 3 times in 4 hrs intervals. In each round, 7 ml of solution was sprayed onto leaves of each replicate. The pot's surface and the stem's base were covered with Al foil to

avoid mixing treatment solution with the wet soil. Plants were treated as all leaves are evenly wet without dripping. Once all the droplets have been dried, the plants were returned to the growing solution tank. Plants were grown further one month period after the application of treatments and used to collect data.

3.2.6. *Growth, Physiological and Zn uptake parameters of rice*

Following one month of the treatment, plant growth, physiology, and Zn uptake data were collected. Plant height, Number of tillers, Number of leaves were also recorded at each sampling stage. Leaves of a plant was detached at their leaf blade base. Total area of all leaves of a plant was measured using a LI-3100 Area Meter.

Whole plants were uprooted and washed with tap water and finally with RO water to remove adhering sand particles. Samples were then dried at 65°C to constant weight. Dry weights were measures and recorded.

Photosynthesis and gas exchange measurements such as Photosynthesis rate (Pn), Stomatal conductance (Gs), Intercellular CO2 concentration (Ci), and Transpiration rate (Tr) were measured using a portable photosynthesis system (LI-6400xt, LI-COR, USA) coupled with a LI-COR transparent conifer chamber to determine the physiological response of rice plants to CNPs (LI-COR, Lincoln, NE, USA 6400-05). Photosynthesis and gas exchange measurements of the last fully expanded leaf were carried out as Evans et al. (2014) described between 9.00 am and 2.00 pm. The LI-COR system's leaf chamber temperature and air flow rate were maintained at 25°C and 500 µmol S^{-1} respectively. Leaf chamber [CO_2] was controlled by the [CO_2] mixer and reference [CO_2] in the chamber was maintained at either 400 µmol mol-1 under ambient [CO_2] and elevated [CO_2], respectively. Relative humidity of the leaf chamber was maintained between 50–70%. Prior to starting gas exchange measurements, the leaf was allowed to reach a

steady state of photosynthesis. The steady state of photosynthesis was achieved between 10–15 min and then spot measurements of the Pn, Gs, Ci and Tr were recorded for each treatment.

All plants were sampled, and their leaves and stems were separated before grinding them for biochemical examination. Dried harvested plant parts were finely ground using a Foss CT193 Cyclotec (Midland scientific, USA) and a Tissue Lyser (Qiagen, USA) grinder. The concentrations of Zn were measured on plant samples using AAS (Shimadzu Atomic absorption Spectrophotometer – AA 7000 series) as described by Elmer (1996). One (01) g of each ground samples were ashed at 500°C in a muffle furnace. The ash was dissolved in 2.5 ml of 20 % (w/w) HCl, and filter through acid washed filter papers into 25 ml volumetric flask. The filtrate was diluted up to 50 ml using RO water. Known Zn standards (1000 µg mL^{-1} were included in each assay to determine the Zn concentrations.

3.2.7. Determining the effect of selected CNP doses on growth, Photosynthesis, gas exchange and Zn uptake of rice plants for a duration of one month following their application

Dose of ZnCD which was exhibiting the highest positive significant impact on the rice plant growth parameters, Photosynthesis and gas exchange parameters and Zn uptake was determined using the results of the first set of experiments. The selected ZnCD dose together with its nano counterpart (CD), bulk counterpart (ZnAc – used as a starting material in producing ZnCD) and the control (without any application) was used in this experiment to determine how these treatments would change the above measured parameters throughout a period of one month. Following application of treatments, the growth, Photosynthesis and gas exchange and Zn is developmentally regulated. Therefore, data for all the parameters were

collected on weekly intervals throughout a period of one months. Together 5 different set of data were collected as follows:

1. One day after treatment application (S + 1D)

2. One week after treatment application (S + 1W)

3. Two weeks after treatment application (S + 2W)

4. Three weeks after treatment application (S + 3W)

5. Four weeks after treatment application (S + 4W)

Same Zn free nutrient sand culture technique (Table 3.1) was used to raise Pokkali rice plants. Experiment was conducted in RCBD model with three (03) replicates. Each tank with growing medium contained all four treatments (CD, ZnCD, ZnAc and Control) and 15 tanks (three tanks per each sampling time) were maintained throughout the period. Plants were re-randomized within tanks to minimize the spatial effects, and weekly between tanks to minimize confounded tank effect.

3.2.8. Statistical analysis

The statistical differences between the variables (Plant height, Total leaf area, Dry weight, Photosynthesis and Gas exchange measurements, and Zn content) were determined by using the Minitab statistical analysis system (Minitab 17) in conjunction with analysis of variance (ANOVA). Significant differences were assessed at $P \leq 0.05$ and standard error was calculated. Non-parametric parameters (Number of tillers) were assessed using Kruskal Wallis and Friedman non-parametric tests accordingly and significant difference in average were calculated.

3.3. Results

3.3.1. Characterization of CNPs used for treatment

Successfully prepared the ZnCD for this study using (NP prep method). Changes in the UV-Vis absorption was measured for both CDs and ZnCDs as presented in Figure 3.1 (a) which show two strong absorption peaks at 288 and 294 nm in the UV-Vis absorption spectra. ZnCD sample exhibited an extra obvious absorption peak at 355 nm. Kim et al. (2015) has reported a similar pattern of absorption peak at 310 nm for amine-rich carbon nanodots. They have reported another slight shoulder peak at 350 nm, similar to the peak observed for ZnCD at 355 nm. These absorption peaks could arise due to the n-π* and π-π* transition corresponding to C=O band and sp^2 respectively. Photoluminescence (PL) emission spectra in Figure 3.1 (b) presents two strong emission peaks at 445 and 488 nm for both CDs and ZnCDs. The emission peaks may result due to the much narrow size of the CNPs as well as due to purer chemical composition (Kim et al., 2015).

The chemical nature of CNPs was examined using XPS as depicted in Figure 3.1 (C) and (d). The following XPS spectra were obtained for Zn 2p3/2, O 1s and C 1s and binding energy of 1021 eV, 533 eV, and 288 eV respectively. Interpretation of the XPS analysis suggested that the Zn(II) is incorporated in the nano-formulation; and the Zn(II) appears to be bound with O, rather than directly with C. The elemental percentage (by weight) obtained from XPS is Zn: 5.49%, O: 61.19%, and C: 33.34%. The low carbon content in the nano-formulation suggests that the formed nanoparticles are likely to a kind of Zn-complexed Carbon dots.

The narrow size range of the two synthesize CNPs are confirmed by DLS characterization as depicted in Figure 3.1 (e) and (f). As per the DLS spectrum for CDs, in Figure 3.1 (e) the mean particle size of CD sample is 140 nm. Figure 3.1 (f) confirms the mean particle size of synthesized ZnCD is 142 nm.
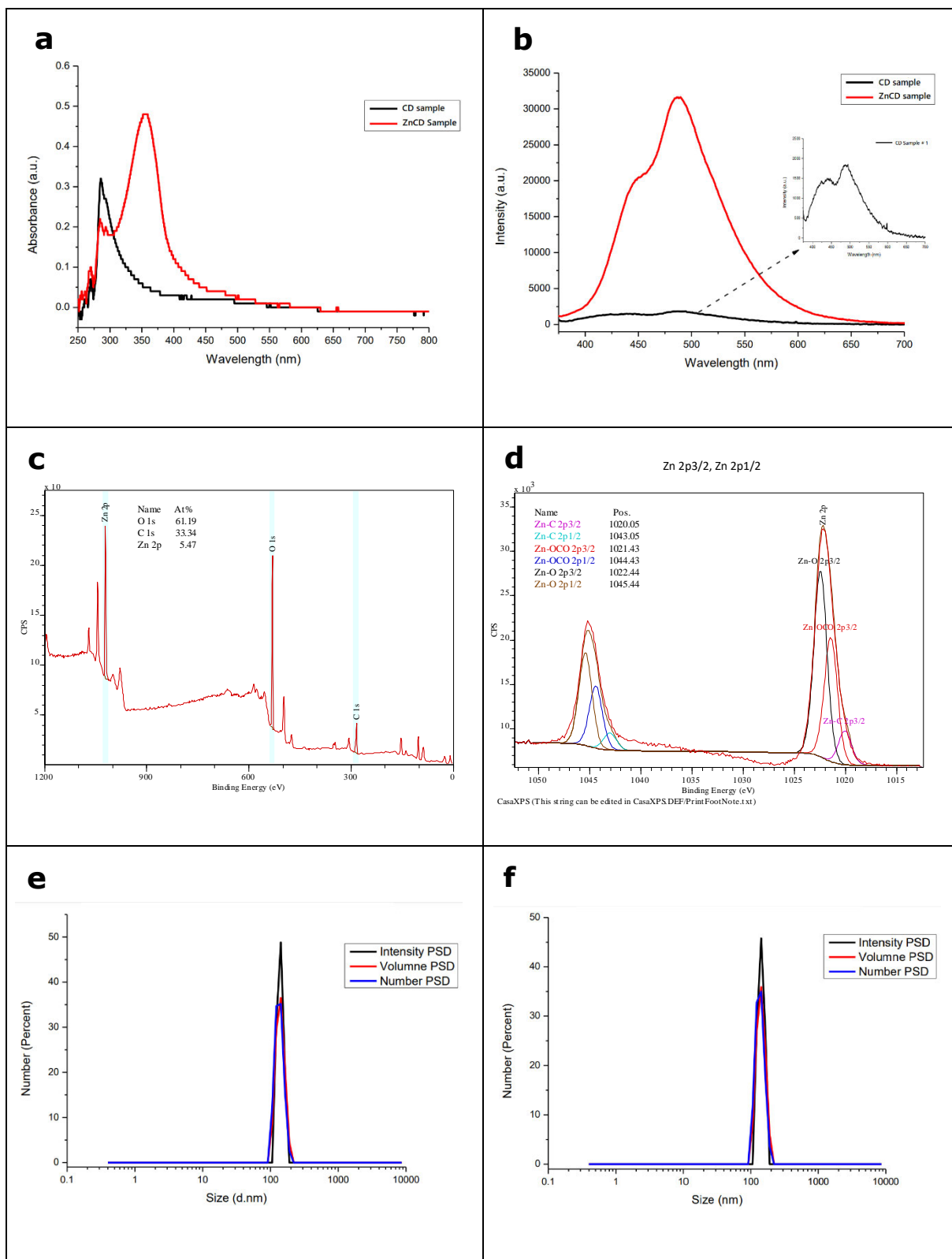
Figure 3.1: (a) UV-Vis absorption spectra for synthesized CDs and Zn incorporated CDs (ZnCDs), (b)Photoluminescence emission spectra of prepared CDs and ZnCDs, (c) XPS full survey spectra of ZnCDs, and (d) Zn 2p3/2, Zn 2p1/2 spectra of ZnCDs, (e) DLS spectra of prepared CDs and (f) ZnCD sample showing relevant particle size of the CNPs.

3.3.2. CNPs on plant growth and Zn concentration

All four growth parameters used to determine the effect of different concentrations of CD s and ZnCDs do not show any significant difference in pairwise mean comparisons of treatments. However, the highest response was recorded with the control treatment for all four parameters tested: plant growth, total leaf area of plant, number of tillers in plants, and dry weight of plants (Figure 3.2).

Pokkali rice plants treated with different doses of CDs have reported 3% to 9.6% reduction in their height compared to control, where CD 500 ppm dose exhibit the lowest % reduction in height (3.1%) among them (Table 3.2). ZnCD treatments show more height reduction, ranging from 8.4% to 15.5%. ZnCD 500 ppm depicts the highest decrease in height compared to control which is 15.5% (Table 3.2). Among all CNP treatments, the highest difference in height was recorded with CD 500ppm and ZnCD 500 ppm doses. However, the variation for plant height for all treatments only ranged between 3.2% to 18.3% (Table 3.2).

Similar patterns of variation in the mean values of treatments have also been observed for total leaf area of plants. Though the mean differences are not significant, the set of plants did not treat with CNPs (control), showing the highest value in mean leaf area compared to other treatments (Figure 3.2 C). The second highest response was marked for CD 500ppm dose (mean of 387.47 cm^2) and the lowest response for total mean leaf was recorded for ZnCD 500ppm treatment (154.57 cm^2). All the CD treatments show higher total leaf area with compared to ZnCD treatments except for ZnCD 100ppm (Table 3.2).

The pattern of variation retained same with the growth parameter dry weight as well (Figure 3.2 d). Control set of plants exhibit the highest dry weight of 5.7 g compared to all other CNP treatments (Table 3.2). However, this increase is not statistically significant. The second highest and the

lowest dry weight was observed with CD 500 ppm and ZnCD 500 ppm treatments respectively. The percentage decline recorded for treatments from the highest to the lowest dry weight ranged from 7.5% to 69.1%.

In addition, the control group of plants were found to have the highest average tillers number, which was 5.4 tiller per plant (Table 3.2). Second and third highest tillers number per plant were observed for CD 250 ppm and CD 500 ppm treatments, respectively (Figure 3.2 b). ZnCD 500 ppm showed the lowest number of tillers per plant (2.8 average tillers). Average number of tillers recorded for CD treatments exhibit higher average number compared to ZnCD treated plants. However, these variations are not statistically significant.

The total Zn content showed large variation between treatments (Figure 3.3). Plants treated with ZnCD 500 ppm had higher Zn content than all other treatments in the study. Compared to other growth parameters, mean Zn content of all treatment's reverses (Figure 3.3). Plants treated with CD 500, CD 100 ppm and control treatments record significantly lower mean Zn content (Table 3.2). For example, the difference between treatments — ZnCD 500 ppm, CD 500 ppm, control, and CD100 ppm—ranged from 48.3 percent to 65.5 percent. All the ZnCD treated plants showed higher Mean Zn content than CD treated plants except CD 250 ppm.

Overall, there is a clear distinction between Control, CD 500 ppm, and ZnCD ppm treatments in all growth and Zn uptake parameters. However, only the Zn content of rice plants makes this demarcation statistically significant.

Table 3.2: Mean comparison of growth parameters and Zn content of Pokkali rice plants treated with different concentrations of foliar applied CDs, ZnCDs and control (without CNP).

Treatment	Plant Height (cm)	Total leaf area (cm^2)	Number of tillers	Dry weight (g)	Zn content (mgKg^{-1})
Control	102.2 ± 3.06[a]	424.6 ± 75.2[a]	5.4 ± 0.75[a]	5.7 ± 1.34[a]	48.5 ± 3.68[b]
CD 50	92.4 ± 3.32[a]	234.0 ± 46.3[a]	4 ± 0.55[a]	3.1 ± 0.77[a]	52.3 ± 2.85[ab]
CD 100	95.5 ± 3.73[a]	291.5 ± 56.4[a]	3.8 ± 0.8[a]	4.1 ± 1.16[a]	45.3 ± 2.12[b]
CD 250	98.9 ± 6.64[a]	321.4 ± 95.2[a]	5.0 ± 0.97[a]	4.4 ± 1.31[a]	68.2 ± 8.27[ab]
CD 500	99.0 ± 5.75[a]	387.5 ± 78.2[a]	4.4 ± 0.75[a]	5.3 ± 1.11[a]	50.6 ± 4.42[b]
ZnCD 50	89.1 ± 7.70[a]	212.5 ± 65.0[a]	3.0 ± 0.6[a]	3.0 ± 0.99[a]	62.6 ± 4.39[ab]
ZnCD 100	93.6 ± 8.25[a]	345.0 ± 128.0[a]	3.4 ± 0.93[a]	4.3 ± 1.72[a]	63.4 ± 7.45[ab]
ZnCD 250	86.4 ± 6.45[a]	219.3 ± 52.9[a]	3.2 ± 0.49[a]	2.6 ± 0.76[a]	59.9 ± 6.56[ab]
ZnCD 500	86.4 ± 3.76[a]	154.6 ± 21.4[a]	2.8 ± 0.37[a]	1.8 ± 0.28[a]	75.0 ± 2.38[a]

Data are the mean of three replicates ± 1SE and the means followed by different letters indicate a significant difference between the treatments at $P \leq 0.05$ based on Tukey's multiple comparisons. Whereas data on number of tillers column show the comparison between the average value of three replicates ± 1SE and the significant difference of average among the treatments at $P \leq 0.05$ based on Kruskal Wallis test.
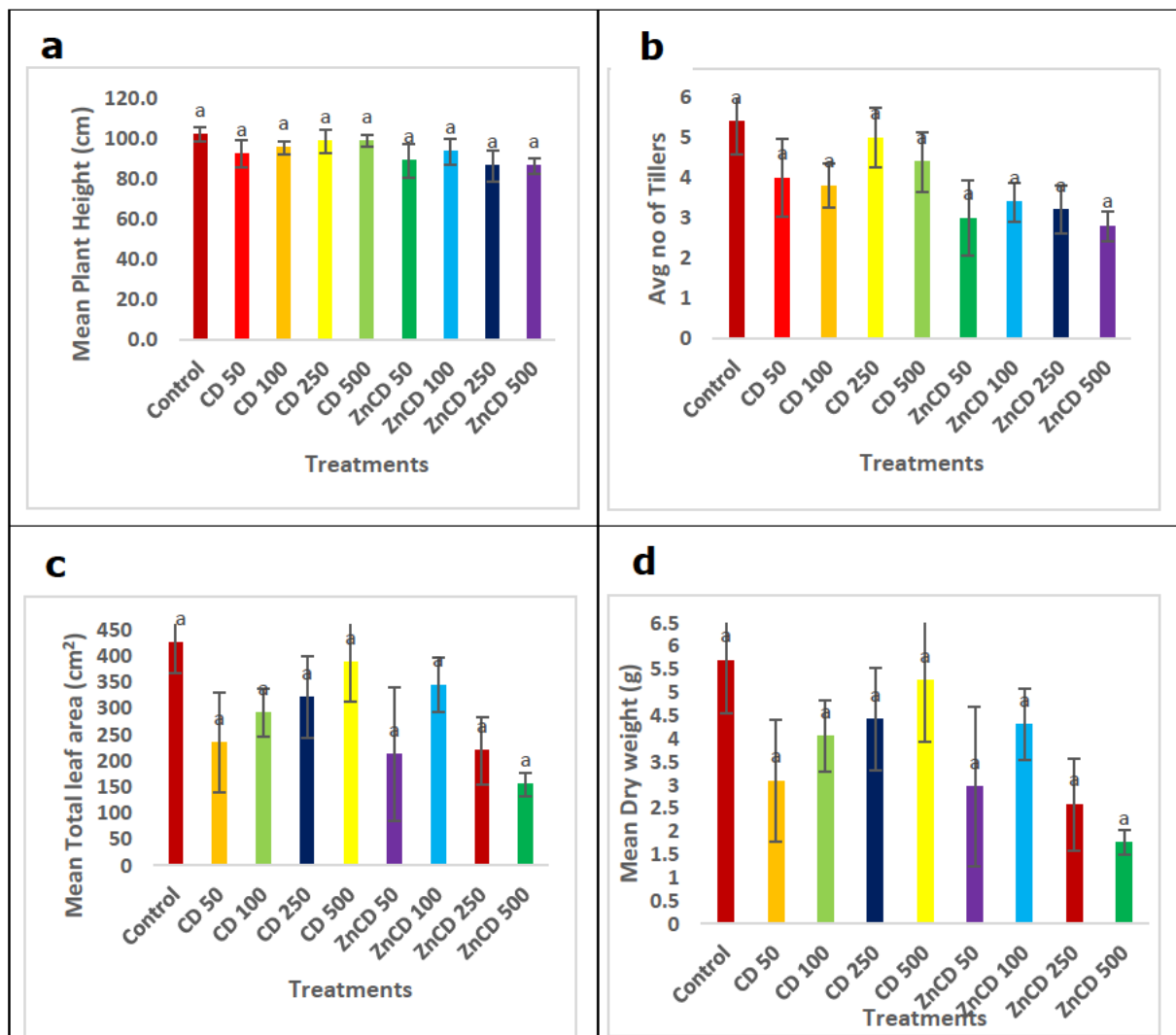
Figure 3.2: Effect of different concentrations of foliar applied CDs, ZnCDs and control (without CNP) on (a) mean plant height(cm), (b) average number of tillers, (c) mean total leaf area (cm^2), (d) mean dry weight (g) of 10 weeks old 'Pokkali' rice plants. Columns show the mean values of three replicates and the bars show the standard error at P ≤ 0.05. Mean sharing the similar letters are not significant with each other.
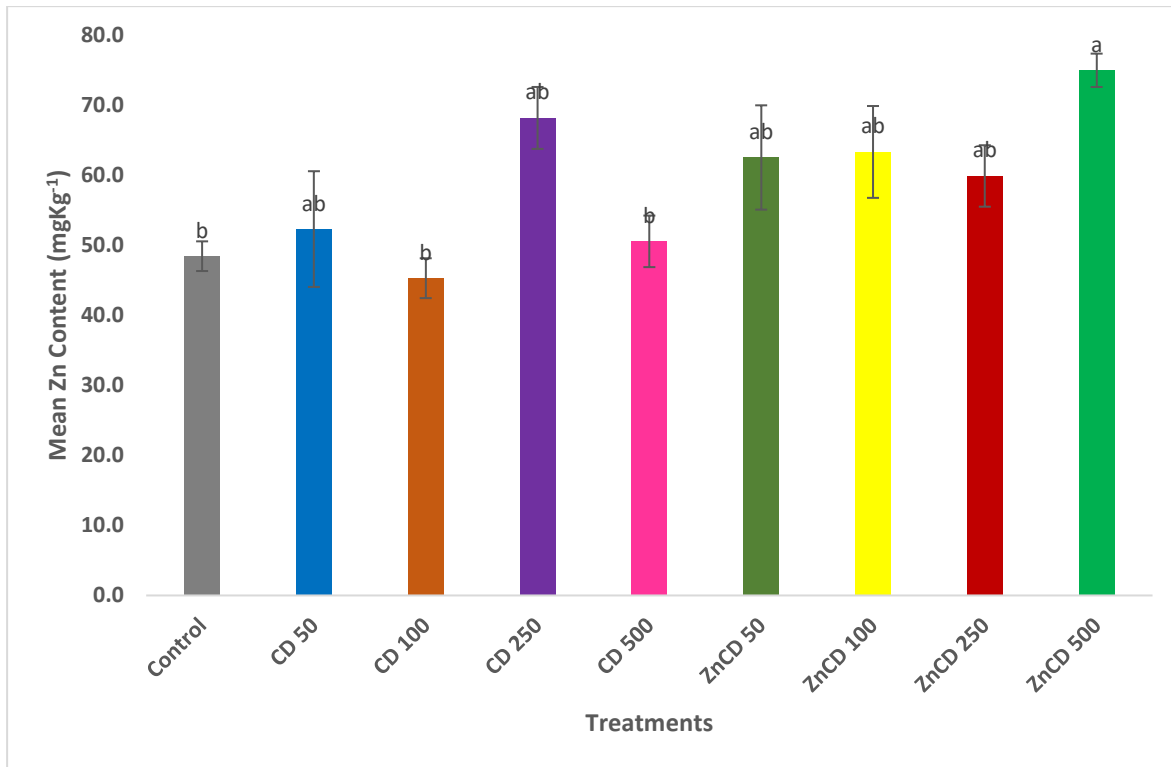
Figure 3.3: Effect of different concentrations of foliar applied CDs, ZnCDs and control (without CNP) on Mean Zn content (mgKg^{-1}) of whole 'Pokkali' rice plants (10 weeks old). Columns show the mean values of three replicates and the bars show the standard error at P ≤ 0.05. Mean sharing the similar letters are not significant with each other.

3.3.3. *Variation in photosynthesis and gas exchange parameters of rice plants treated with different concentrations of CNPs*

Pn, Gs and Ci do not exhibit any significant change due to the application of CNPs (Table 3.3). However, highest Pn and Gs were recorded for CD 500 ppm treatment followed by the blank treatment (control). The ZnCD 500 ppm treatment had the second- and third-lowest rates for Pn and Gs, respectively, while the lowest Pn and Gs were recorded with the CD 50 ppm treatment (Figure 3.4). Again, the control treatment showed the highest Ci value (285.2 µmol CO_2 mol^{-1}). ZnCD 500 ppm treatment reported the second highest value for the Ci which is only a 0.3% decrease from the

control treatment (Figure 3.4). The difference between mean Pn for all the treatments range between 0 – 30% where this range lies between 0 – 45% for Gs. However, Ci's mean difference only ranges from 0 to 6%. CD500ppm, Control, CD 50ppm, CD 250 ppm and ZnCD 500 ppm treatments for Pn and Gs showed highly positive relationship, but the rest do not. Ci does not exhibit any kind of a noticeable relationship together with responses of Pn and Gs.

The CNP application had a considerable impact on the mean Tr, which differed significantly from the mean Pn, Gs, and Ci. CD 500 ppm recorded the highest Tr, where the CD 50 ppm recorded the lowest significant Tr. The ZnCD 500ppm treatment exhibited the second highest Tr. Both CD 500 and ZnCD 500 ppm treatments have marked more than 50% increase in Tr with compared to the lowest recorded. Tr for the Control treatment was recorded as 3.04, nearly a 28% reduction compared to the highest Tr. Though Gs and Tr of a plant has a positive relationship, there is no evident relationship expressed between Tr and the other factors of gas exchange in the results of our experiment.

Table 3.3: Mean comparison of gas exchange parameters of Pokkali rice variety treated with different concentrations of foliar applied CDs, ZnCDs and control (without NP).

Treatments	Photosynthesis rate (µmol CO_2 m^{-2} S^{-1})	Stomatal conductance to H_2O (mol H_2O m^{-2} S^{-1})	Intercellular CO_2 concentration (µmol CO_2 mol^{-1})	Transpiration rate (mmol H_2O m^{-2} S^{-1})
Control	14.7 ± 0.69[a]	0.3 ± 0.01[a]	285.2 ± 4.14[a]	3.0 ± 0.17[ab]
CD 50	11.5 ± 1.40[a]	0.2 ± 0.01[a]	270.8 ± 9.41[a]	2.5 ± 0.26[b]
CD 100	13.2 ± 1.67[a]	0.2 ± 0.05[a]	277.0 ± 8.92[a]	2.7 ± 0.43[ab]
CD 250	12.5 ± 1.86[a]	0.2 ± 0.03[a]	275.4 ± 7.63[a]	3.6 ± 0.36[ab]
CD 500	16.5 ± 1.55[a]	0.3 ± 0.04[a]	277.2 ± 5.03[a]	4.2 ± 0.39[a]
ZnCD 50	12.6 ± 0.62[a]	0.2 ± 0.02[a]	280.4 ± 6.62[a]	3.4 ± 0.30[ab]
ZnCD 100	14.1 ± 1.11[a]	0.2 ± 0.01[a]	271.6 ± 7.35[a]	3.3 ± 0.26[ab]
ZnCD 250	13.4 ± 1.31[a]	0.2 ± 0.03[a]	268.0 ± 5.52[a]	3.4 ± 0.43[ab]
ZnCD 500	11.7 ± 1.34[a]	0.2 ± 0.03[a]	284.4 ± 1.72[a]	3.8 ± 0.45[ab]

Data are the mean of three replicates ± 1SE and the means followed by different letters indicate a significant difference between the treatments at $P \leq 0.05$ based on Tukey's multiple comparisons.
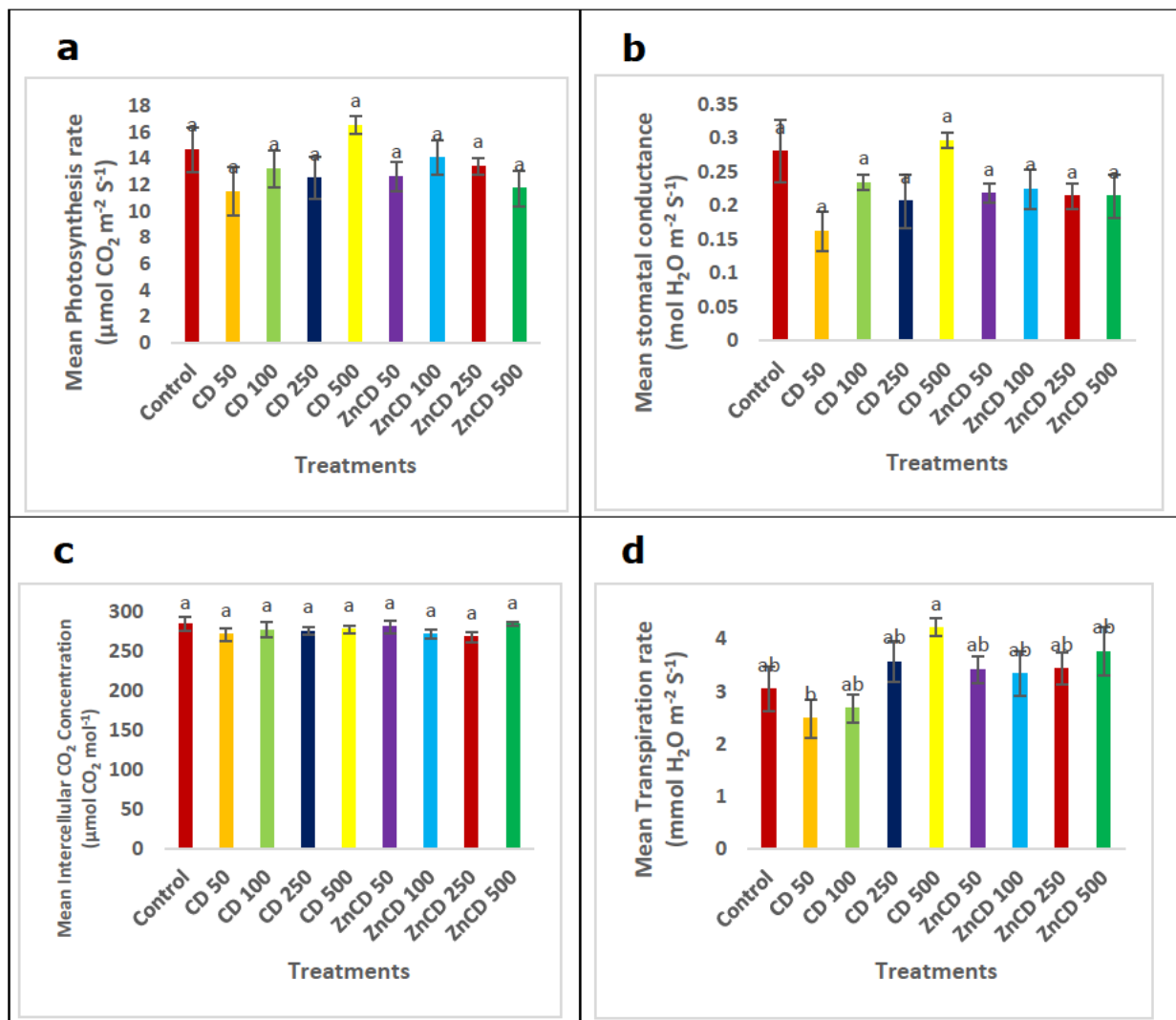
Figure 3.4: Effect of different concentrations of foliar applied CDs, ZnCDs and control (without NP) on (a) Mean Photosynthesis rate (μmol CO_2 m^{-2} S^{-1}), (b) Mean stomatal conductance (mol H_2O m^{-2} S^{-1}), (c) Mean Intercellular CO_2 Concentration (μmol CO_2 mol^{-1}), (d) Mean Transpiration rate (mmol H_2O m^{-2} S^{-1}) of 10 weeks old 'Pokkali' rice plants. Column shows the mean value of three replicates and the bars show the standard error at P $\leq$ 0.05. Mean sharing the similar letters are not significant with each other.

Overall, the data on growth, Zn uptake, photosynthesis, and gas exchange indicated that there was a noticeable difference between the effects of control, CD 500ppm, and ZnCD 500ppm when compared to one another. In the subsequent stage of the experiment, which was created to ascertain the impact of these doses on the same growth, Zn uptake, photosynthesis, and

gas exchange parameters over a month, 500ppm doses of both CD and ZnCD were chosen to be used.

3.3.4. CNPs on early growth and Zn uptake

This experiment was carried out to determine the effect of selected doses of CNPs on the growth, Zn uptake, photosynthesis, and gas exchange parameters over one month period. The selected 500 ppm doses of CD and ZnCD were applied together with control treatment and inorganic bulk Zn source (ZnAc) to determine the effectiveness of CNP application precisely.

All plant growth related parameters (plant height, total number of tillers, total leaf area and dry weight) showed significant difference over the sampling time and a positive relationship with the sampling time (Table 3.4). Except plant height other parameters did not show any significance difference for the four treatments (CD, ZnCD, ZnAc and control) used (Figure 3.4).

Plant height of the ZnAc treated plants were significantly higher than the control set of plants. Further, ZnAc and ZnCD treatments recorded higher plant height than CD and untreated plants. The total leaf area and dry weight showed a similar pattern of response, though there was no statistically significant difference between treatment. There were similar numbers of tillers overall for all four treatments, with no detectable patterns of distribution (Table 3.5).

Zn content of rice plants show significant difference in mean values for sampling times as well as for treatment types (Table 3.4). Zn contents of the plants gradually decreased with the progress of plant development. Zn content of S+1D is significantly higher than all sampling times. Sampling times S+1W and S+2W show significant decrease of 26% and 39% Zn content compared to S+1D respectively. Further, variables S+3W and

S+4W do not show significant difference between each other, whereas they show significantly lower Zn content compared to all other sampling times (Table 3.5).

All four growth parameters and the Zn content show significant interaction effect between sampling time and treatment at $P \leq 0.05$ level (Table 3.4). Pairwise mean comparisons show significantly high Zn content for ZnAc and ZnCD treatments at S+1D, S+1W and S+2W sampling times (Table 3.5). However, these Zn contents drastically decreased over the course of the growth period, resulting in a total drop of 27% and 23% for ZnAc and ZnCD treatments, respectively (Figure 3.5). Zn content of CD and Control treatments gradually decreases over the course of the five sampling times. However, the reduction in ZnAC and ZnCD treatments were steep during last two weeks than the first two weeks of growing. From S+1D to S+2W, Zn content was reduced for nearly 25% for both ZnAc and ZnCD. But this reduction has been increased up to 78% and 66% for ZnAC and ZnCD respectively during the last two weeks from S+2W to S+4W (Figure 3.5).

Plant height, number of tillers, total leaf area and dry weight were increased throughout the growth period from S+1D to S+4W (Figure 3.6 a-d). As per the Pairwise mean comparisons, responses for all the treatments at S+4W and S+3W level show significant increase than the responses for S+1D and S+1W sampling levels. All treatments exhibit positive relationship throughout the tested period (Figure 3.6 a-d).

Table 3.4: Summarizing analysis of variance results for plant growth parameters of Pokkali rice plants throughout one month duration following foliar application of CDs, ZnCDs, ZnAc 500 ppm and control (without NP).

	Plant Height (cm)	Total leaf area (cm^2)	Average number of tillers	Dry weight (g)	Zn content (mgKg^{-1})
Sampling time	*	*	*	*	*
Treatment	*	ns	ns	ns	*
Sampling time * Treatment	*	*	*	*	*

Abbreviations: ns – not significant, * P ≤ 0.05

Table 3.5: Mean comparison of growth parameters and Zn content of Pokkali rice plants throughout one month duration following foliar application of different concentrations of CNPs and control (without NP).

	Plant Height (cm)	Total leaf area (cm^2)	Median number of tillers	Dry weight (g)	Zn content (mgKg^{-1})
Sampling time					
S + 1D	79.4 ± 1.67[d]	176.3 ± 9.0[d]	3.0 ± 0.11[d]	1.9 ± 0.1[c]	62.5 ± 7.11[a]
S + 1W	83.8 ± 1.16[d]	250.3 ± 17.0[cd]	4.0 ± 0.11[c]	3.7 ± 0.23[b]	45.4 ± 6.37[b]
S + 2W	90.1 ± 1.01[c]	316.8 ± 17.1[bc]	5.0 ± 0.13[b]	5.1 ± 0.33[b]	38.3 ± 7.41[b]
S + 3W	97.2 ± 1.09[b]	392.5 ± 27.1[ab]	5.0 ± 0.11[ab]	8.2 ± 0.61[a]	12.6 ± 3.09[c]
S + 4W	103.6 ± 1.39[a]	482.2 ± 24.2[a]	5.50 ± .015[a]	9.9 ± 0.59[a]	11.0 ± 2.57[c]
Treatment					
Control	88.3 ± 2.80[b]	311.8 ± 32.5[a]	5.0 ± 0.27[a]	5.6 ± 0.76[a]	19.2 ± 4.70[b]
CD	89.4 ± 2.88a[b]	308.9 ± 32.5[a]	5.0 ± 0.27[a]	5.5 ± 0.83[a]	18.4 ± 3.96[b]
Zn Ac	93.4 ± 2.41[a]	356.7 ± 34.8[a]	5.0 ± 0.24[a]	6.3 ± 0.93[a]	48.3 ± 7.95[a]
ZnCD	92.2 ± 2.01[ab]	317.2 ± 32.9[a]	5.0 ± 0.24[a]	5.6 ± 0.91[a]	50.0 ± 6.80[a]
Sampling time * Treatment					
S + 1 D * Ctrl	74.7 ± 4.69[h]	146.0 ± 14.9[f]	3.0 ± 0.0[e]	1.6 ± 0.09[g]	46.0 ± 11.00[bc]
S + 1 D * CD	76.4 ± 2.79[gh]	162.1 ± 16.1[f]	3.0 ± 0.0[e]	1.8 ± 0.25[fg]	39.3 ± 9.48[bcd]
S + 1 D * ZnAc	83.1 ± 0.33[fgh]	201.8 ± 14.2[def]	3.0 ± 0.33[de]	2.2 ± 0.13[fg]	82.9 ± 2.80[a]
S + 1 D * ZnCD	83.5 ± 0.87[efgh]	195.2 ± 5.2[ef]	3.0 ± 0.33[de]	2.1 ± 0.06[fg]	81.9 ± 9.42[a]

	Plant Height (cm)	Total leaf area (cm^2)	Median number of tillers	Dry weight (g)	Zn content (mgKg^{-1})
S + 1 W * Ctrl	80.9 ± 1.7[fgh]	224.2 ± 23.8[def]	4.0 ± 0.33[cde]	3.5 ± 0.45[fg]	24.1 ± 2.16[cde]
S + 1 W * CD	81.5 ± 2.7[fgh]	228.2 ± 42.4[def]	4.0 ± 0.00[bcde]	3.3 ± 0.60[fg]	26.4 ± 3.01[cde]
S + 1 W * ZnAc	86.1 ± 2.4[defgh]	284.0 ± 49.6[bcdef]	4.0 ± 0.00[bcde]	4.0 ± 0.63[defg]	66.6 ± 6.54[ab]
S + 1 W * ZnCD	86.5 ± 0.5[defgh]	264.8 ± 16.6[cdef]	4.0 ± 0.33[cde]	3.7 ± 0.23[efg]	64.9 ± 4.21[ab]
S + 2 W * Ctrl	89.1 ± 1.0[cdefg]	330.6 ± 28.1[abcdef]	5.0 ± 0.00[abc]	5.4 ± 0.55[bcdefg]	17.7 ± 5.22[cde]
S + 2 W * CD	88.7 ± 3.3[defg]	347.5 ± 17.7[abcdef]	5.0 ± 0.33[abcd]	5.5 ± 0.58[bcdefg]	13.0 ± 2.35[de]
S + 2 W * ZnAc	92.3 ± 1.9[abcdef]	330.4 ± 48.3[abcdef]	5.0 ± 0.33[abcd]	5.2 ± 1.02[cdefg]	63.0 ± 10.30[ab]
S + 2 W * ZnCD	90.3 ± 1.7[bcdef]	258.9 ± 26.2[cdef]	5.0 ± 0.33[abcd]	4.1 ± 0.25[defg]	59.3 ± 3.54[ab]
S + 3 W * Ctrl	94.3 ± 1.5[abcdef]	397.1 ± 31.1[abcde]	5.0 ± 0.33[ab]	8.6 ± 0.58[abcd]	4.9 ± 2.49[e]
S + 3 W * CD	97.0 ± 3.11[abcde]	309.8 ± 21.4[abcdef]	5.0 ± 0.33[ab]	6.3 ± 0.58[abcdef]	5.7 ± 2.01[e]
S + 3 W * ZnAc	99.6 ± 0.46[abcd]	452.0 ± 63.2[abc]	5.0 ± 0.00[abc]	9.7 ± 1.71[abc]	15.2 ± 5.18[cde]
S + 3 W * ZnCD	98.0 ± 2.51[abcd]	411.3 ± 73.1[abcd]	5.0 ± 0.00[abc]	8.3 ± 1.21[abcde]	24.6 ± 6.63[cde]
S + 4 W * Ctrl	102.5 ± 2.94[abc]	460.9 ± 43.8[abc]	5.0 ± 0.33[ab]	8.7 ± 0.28[abcd]	3.3 ± 3.71[e]
S + 4 W * CD	103.6 ± 3.15[ab]	496.8 ± 40.1[ab]	6.0 ± 0.33[a]	10.4 ± 1.23[a]	7.5 ± 6.06[e]
S + 4 W * ZnAc	105.6 ± 4.40[a]	515.2 ± 35.8[a]	6.0 ± 0.33[a]	10.4 ± 0.16[a]	13.7 ± 2.81[de]
S + 4 W * ZnCD	102.8 ± 1.30[ab]	456.0 ± 82.8[abc]	5.0 ± 0.33[ab]	10.0 ± 2.24[ab]	19.6 ± 3.19[cde]

Data are the mean of three replicates ± 1SE and the means followed by different letters indicate a significant difference between the treatments at P ≤ 0.05 based on Tukey's multiple comparisons. Whereas data on number of tillers column shows the comparison between the average value of three replicates ± 1SE and the significant difference of average among the treatments at P ≤ 0.05 based on Kruskal Wallis test.
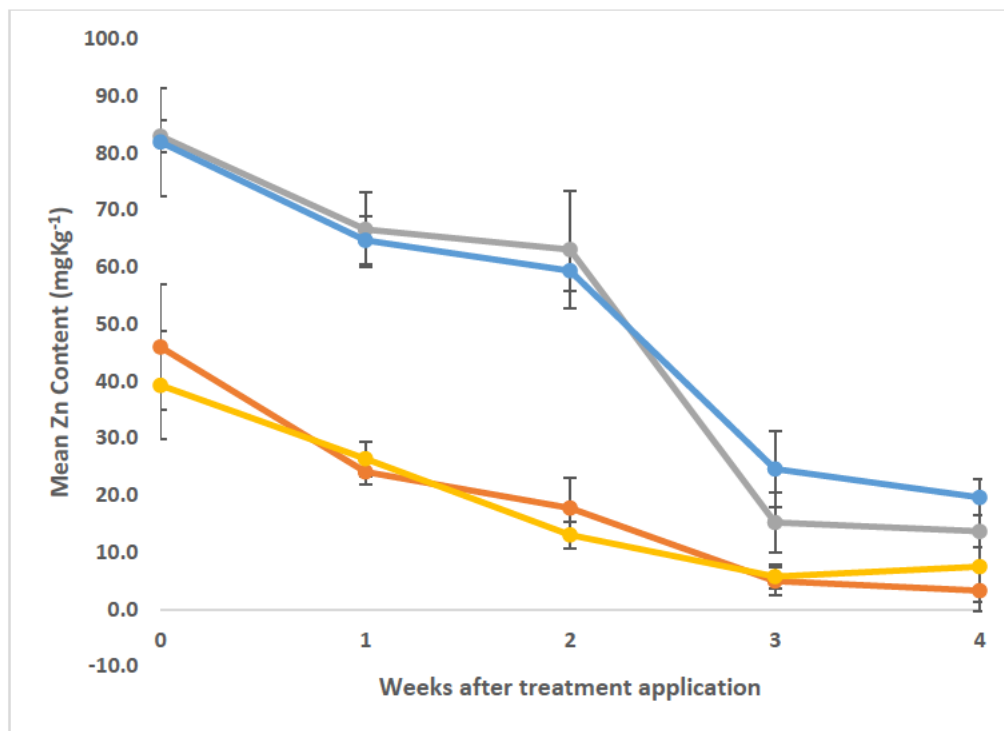
Figure 3.5: Effect of foliar application of CDs, ZnCDs, ZnAc 500 ppm and control (without NP) over one month period on Mean Zn content (mgKg^{-1}) of 10 weeks old 'Pokkali' rice plants. Each data point shows the mean value of three replicates and the bars show the standard error at P ≤ 0.05.
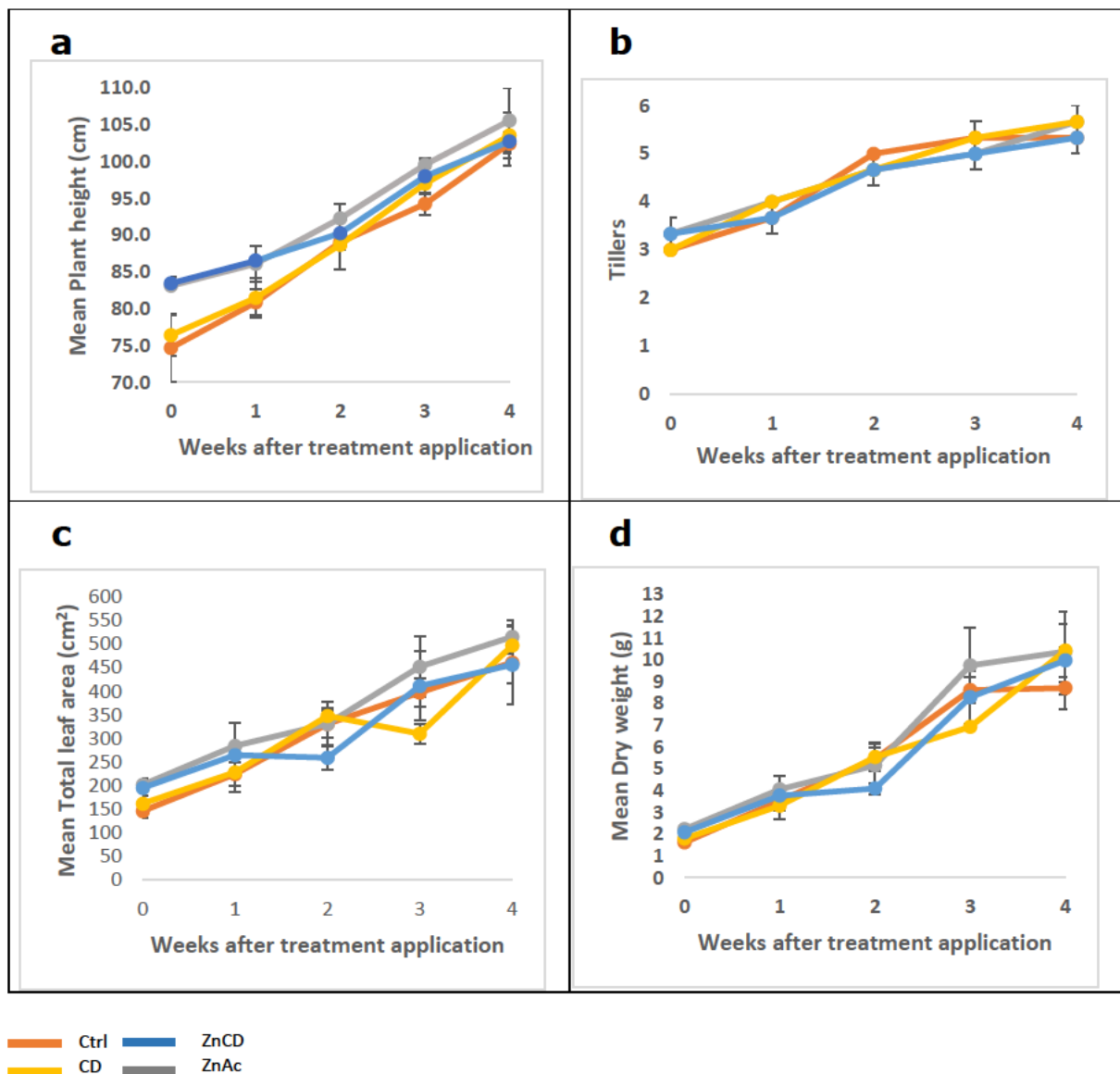
Figure 3.6: Effect of foliar application of CDs, ZnCDs, ZnAc 500 ppm and control (without NP) over one month period on (a) mean plant height(cm), (b) average number of tillers, (c) mean total leaf area (cm^2), (d) mean dry weight (g) of 10 weeks old 'Pokkali' rice plants. Each data point shows the mean value of three replicates and the bars show the standard error at P ≤ 0.05.

3.3.5. Influence of CNPs plant gas exchange parameters

Gas exchange parameters demonstrated no significant differences between treatments, whereas sampling time varies significantly between levels of sampling (Table 3.6). Pn and Gs show similar type of pairwise mean comparison grouping for different sampling times where S+1D is significantly higher than S+4W (Table 3.7). both Pn and Gs do not have significantly different pairs of means for interactions. Further the data distribution pattern is much similar in both parameters of Pn and Gs (Table 3.7).

The distribution pattern of Ci data does not resemble that of other parameters, but the value of Ci for S+1D was significantly greater than that of S+3W and S+4W. Compared to ZnAc treatment at S+4W level, Ci of control plants at S+1D level is significantly higher. All the other treatments do not show any significant difference between means (Table 3.7). Total decrease for Ci throughout the studying period (from S+1D to S+4W) has marked (Figure 3.7 c) 5.8%, 6%, 8.9% and 5.7% for Control, CD, ZnAc and ZnCD respectively. Treatments of Pn and Gs have, in most cases, shown declines of more than 20%, despite the fact that all treatments of Ci have reduced by percentages less than 10%. (Figure 3.7 a,d,c). As a result, the Pn and Gs parameters have experienced greater reductions than the Ci.

Variation of the Tr is not similar to any of Pn, Gs or Ci. Tr of S+1W and S+1W are significantly higher than S+1D. While all the other parameters Pn, Gs, and Ci decrease over time, Tr of the plants increases gradually throughout the 4 weeks period (Figure 3.7 d). This has recorded 57%, 31%, 27% and 23% increase in Tr from the treatment application time (S+1D) to end of the reporting period (S+4W) for Control, CD, ZnAc and ZnCD respectively.

Table 3.6: Summarizing analysis of variance results for gas exchange parameters of Pokkali rice varieties treated with different treatments of nanoparticles.

	Photosynthesis rate (μmol CO_2 m^{-2} S^{-1})	Stomatal conductance to H_2O (mol H_2O m^{-2} S^{-1})	Intercellular CO_2 concentration (μmol CO_2 mol^{-1})	Transpiration rate Seeds (mmol H_2O m^{-2} S^{-1})
Sampling time	*	*	*	*
Treatment	ns	ns	ns	ns
Sampling time * Treatment	ns	ns	*	ns

Abbreviations: ns – not significant, * P ≤ 0.05

Table 3.7: Summarizing analysis of variance results for gas exchange parameters of Pokkali rice plants throughout one month duration following foliar application of CDs, ZnCDs, ZnAc 500 ppm and control (without NP).

	Photosynthesis rate (µmol CO_2 m^{-2} S^{-1})	Stomatal conductance to H_2O (mol H_2O m^{-2} S^{-1})	Intercellular CO_2 concentration (µmol CO_2 mol^{-1})	Transpiration rate Seeds (mmol H_2O m^{-2} S^{-1})
Sampling time				
S + 1D	15.6 ± 0.55^a	0.3 ± 0.017^a	293.1 ± 2.44^a	4.0 ± 0.17^b
S + 1W	14.0 ± 0.50^{ab}	0.3 ± 0.016^{ab}	279.5 ± 3.88^{ab}	5.8 ± 0.25^a
S + 2W	14.9 ± 0.69^{ab}	0.3 ± 0.015^{ab}	278.9 ± 2.73^{ab}	6.3 ± 0.25^a
S + 3W	12.8 ± 0.88^{ab}	0.2 ± 0.019^b	269.1 ± 4.18^b	5.3 ± 0.45^{ab}
S + 4W	12.7 ± 0.69^b	0.2 ± 0.019^b	273.7 ± 3.64^b	5.4 ± 0.44^{ab}
Treatment				
Control	14.4 ± 0.64^a	0.3 ± 0.021^a	282.8 ± 3.94^a	5.7 ± 0.41^a
CD	13.7 ± 0.75^a	0.3 ± 0.017^a	279.0 ± 3.52^a	5.3 ± 0.37^a
Zn Ac	13.7 ± 0.59^a	0.2 ± 0.016^a	273.6 ± 3.98^a	5.0 ± 0.31^a
ZnCD	14.2 ± 0.68^a	0.3 ± 0.018^a	280.0 ± 2.96^a	5.4 ± 0.31^a
Sampling time * Treatment				
S + 1 D * Ctrl	15.8 ± 1.31^a	0.4 ± 0.05^a	299.0 ± 4.51^a	4.2 ± 0.56^a
S + 1 D * CD	14.1 ± 0.46^a	0.3 ± 0.02^a	293.0 ± 5.51^{ab}	3.8 ± 0.28^a
S + 1 D * ZnAc	16.1 ± 0.65^a	0.3 ± 0.02^a	286.3 ± 2.60^{ab}	3.8 ± 0.21^a
S + 1 D * ZnCD	16.5 ± 1.67^a	0.3 ± 0.05^a	294.0 ± 5.69^{ab}	4.3 ± 0.30^a

	Photosynthesis rate (μmol CO_2 m^{-2} S^{-1})	Stomatal conductance to H_2O (mol H_2O m^{-2} S^{-1})	Intercellular CO_2 concentration (μmol CO_2 mol^{-1})	Transpiration rate Seeds (mmol H_2O m^{-2} S^{-1})
S + 1 W * Ctrl	12.9 ± 0.59[a]	0.2 ± 0.03[a]	280.3 ± 8.97[ab]	5.5 ± 0.50[a]
S + 1 W * CD	15.8 ± 1.14[a]	0.3 ± 0.02[a]	284.3 ± 4.18[ab]	6.5 ± 0.43[a]
S + 1 W * ZnAc	13.3 ± 1.10[a]	0.2 ± 0.04[a]	269.7 ± 12.21[ab]	5.2 ± 0.70[a]
S + 1 W * ZnCD	14.2 ± 0.41[a]	0.3 ± 0.01[a]	283.7 ± 4.10[ab]	5.8 ± 0.09[a]
S + 2 W * Ctrl	17.0 ± 0.95[a]	0.3 ± 0.02[a]	285.7 ± 1.76[ab]	7.2 ± 0.38[a]
S + 2 W * CD	14.8 ± 2.34[a]	0.3 ± 0.03[a]	275.7 ± 6.57[ab]	6.2 ± 0.62[a]
S + 2 W * ZnAc	14.1 ± 0.52[a]	0.3 ± 0.01[a]	281.7 ± 3.53[ab]	6.2 ± 0.01[a]
S + 2 W * ZnCD	13.7 ± 0.59[a]	0.2 ± 0.03[a]	272.7 ± 7.31[ab]	5.8 ± 0.56[a]
S + 3 W * Ctrl	12.3 ± 0.97[a]	0.2 ± 0.05[a]	267.3 ± 12.70[ab]	5.2 ± 1.00[a]
S + 3 W * CD	12.3 ± 1.54[a]	0.2 ± 0.03[a]	267.0 ± 7.00[ab]	4.7 ± 0.73[a]
S + 3 W * ZnAc	12.7 ± 2.02[a]	0.2 ± 0.24[a]	269.7 ± 12.80[ab]	5.2 ± 0.87[a]
S + 3 W * ZnCD	13.9 ± 2.93[a]	2.2 ± 0.06[a]	272.3 ± 1.45[ab]	5.9 ± 1.34[a]
S + 4 W * Ctrl	14.1 ± 1.56[a]	0.3 ± 0.05[a]	281.7 ± 4.63[ab]	6.6 ± 1.18[a]
S + 4 W * CD	11.4 ± 1.98[a]	0.2 ± 0.05[a]	275.0 ± 9.85[ab]	5.0 ± 1.07[a]
S + 4 W * ZnAc	12.4 ± 1.28[a]	0.2 ± 0.03[a]	260.7 ± 3.18[b]	4.8 ± 0.71[a]
S + 4 W * ZnCD	12.7 ± 0.75[a]	0.2 ± 0.02[a]	277.3 ± 6.17a[b]	5.2 ± 0.34[a]

Data are the mean of three replicates ± 1SE and the means followed by different letters indicate a significant difference between the treatments at $P \leq 0.05$ based on Tukey's multiple comparisons.
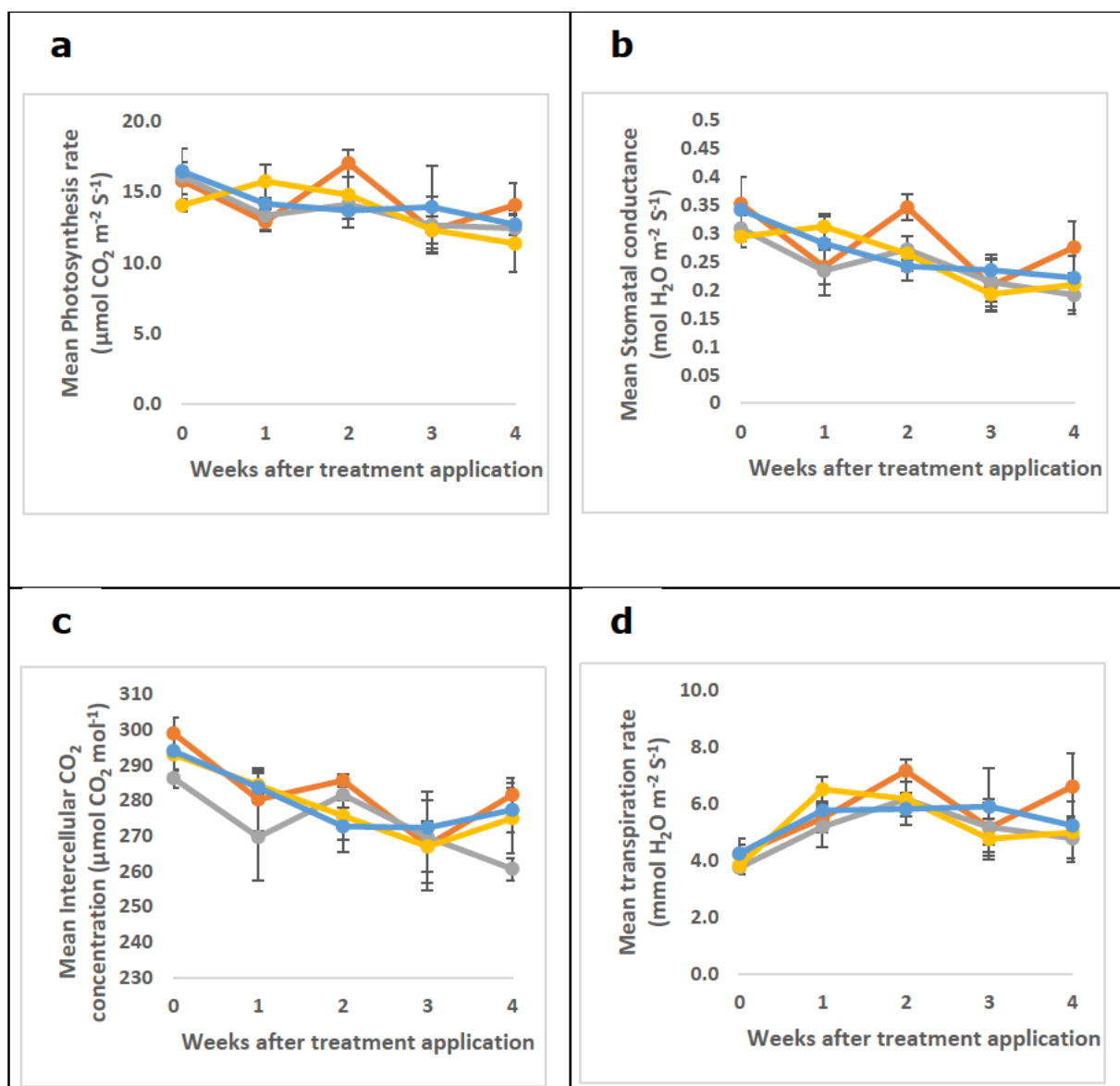
Figure 3.7: Effect of foliar application of CDs, ZnCDs, ZnAc 500 ppm and control (without NP) over one month period on (a) Mean Photosynthesis rate (µmol CO_2 m^{-2} S^{-1}), (b) Mean stomatal conductance (mol H_2O m^{-2} S^{-1}), (c) Mean Intercellular CO_2 Concentration (µmol CO_2 mol^{-1}), (d) Mean Transpiration rate (mmol H_2O m^{-2} S^{-1}) of 10 weeks old 'Pokkali' rice plants. Each data point shows the mean value of three replicates and the bars show the standard error at $P \leq 0.05$.

3.4. Discussion

3.4.1. CNDs application promote plant growth and shoot Zn content

There were no significant differences in plant growth and physiological traits between rice plants treated with various doses of CDs and ZnCDs. However, control plants exhibited better growth particularly in plant height, total leaf area, number of tillers and dry weight. Yet, these parameters did not exhibit dose-dependent response whereas responses for treatments of CD doses were higher compared to those of ZnCDs most of the time. Many studies have reported positive impact of carbon dots on plant growth parameters. Tripathi et al. (2015) reported increased shoot and root growth of wheat plant after exposing seeds to water soluble CDs. Application of ZnO NPs has increased rice yield and nutrient uptake significantly (Yang et al., 2021), while application of Zn NPS on germinating rice reported an increase in radicle and plumule length (Panda, 2017). Similar type of observation of Zn NPs applied rice plants were made in the studies of Panda (2017), Ghasemi et al. (2017) and Singh et al. (2022). CNTs and CDs applied rice plants too reported positive impact of CNPs on plant growth parameters (Zhang et al., 2017, Li et al., 2018).

Nevertheless, some studies have reported the negative effects of NPs specially CNPs on rice plants and other cereal crops. Studies carried out by Begum et al. (2012) and Hao et al. (2018) reported negative effects of MWCNTs, C60 fullerene, and graphene oxide on rice plant growth and development. Not only CNPs, but MNPs too have exhibited their negative effect on rice plant growth (Nair et al., 2014, Thuesombat et al., 2014). Therefore, the highest recorded growth parameters for control treatment of our study may be due to either suppression of cell division or inhibition of cell expansion by CDs and ZnCDs applied. Further, these results suggest that effect of NPs on plant growth and physiology is totally dependent on the type and the characteristics of the NMs and also on the species. Our

findings, however, don't indicate either a noticeably positive or negative impact. This may be due to close range of doses selected, which should be more elaborated in order to obtain positive/negative results. Furthermore, the timing of the application could have been a factor. However, Cd500 ppm application resulted comparatively higher responses for all the growth parameters, while ZnCD 500ppm illustrated comparatively lower response. It makes sense to choose both CD and ZnCD 500 for the subsequent studies in light of the growth parameters. By using these two, the application of CDs with and without Zn was distinguished for subsequent experiments.

The majority of the research findings are in agreement with the Zn uptake reported in Pokkali, the rice variety use in this study. ZnCD 500 which provides Zn and the CDs to rice plants have significantly increased the Zn concentration in the plants. Significantly lower Zn content was reported in Control, CD 100and CD 500 treatments. Application of ZnO NPs on rice and other cereals have reported increase in Zn content of plants/grains on many occasions. A study carried out by Yang et al. (2021) reported nearly 20% increase in Zn content of rice plants with Zn NP application at their tillering stage. These findings are very consistent with our findings, which showed that most ZnCD doses increased Zn content by between 15 and 25% when compared to the control. The choice of these parameters for the ensuing experiment is justified by the fact that ZnCD 500 is the highest and CD 500 and the control are the second and third treatments with the lowest Zn content.

3.4.2. CNPs influence gas exchange of rice plants

To determine the effect of CNPs on gas exchange, the dose dependent experiment was carried out and measured the Pn, Gs, Ci, and Tr. Gs which estimates the rate of gas exchange through stomata and Tr which quantifies the leaf water balance have direct linear relationship with the Pn (Ding et

al., 2020). Ci determines the flux of CO_2 into the chloroplast via stomata apertures and increase the activity of photosynthesis enzymes Rubisco and thereby increase the Pn (Moss et al., 1963). Higher the Ci, always promote the photosynthesis of the plant. On other hand, Gs, Tr and Ci become limiting factors of the Pn. Accumulation of photosynthetic products inside the chloroplast also inhibits the photosynthesis (Luo et al., 2019, Liu et al., 2020).

Our study clearly demonstrated a direct relationship between Pn and Gs for various CNP doses. However, Ci and Tr does not show such similarity in the variation of data. These finding suggest that the variation in the Pn observed in this study is due to the non-stomatal factors (Ding et al., 2020). In addition, there was a strong correlation between Pn and the dry weight of the plant, which suggests that the products of photosynthesis are directly contributing to the growth and development of the plant. Furthermore, the total leaf area of rice plants, which is directly proportional to the area of the plant that is available for photosynthesis, agrees with the findings of Pn. Similar trend has been reported in a study with different upland rice varieties in China in which effect of Se application on photosynthesis has been evaluated (Ding et al., 2020). Control set of plants have the better gas exchange characteristics including Pn, Gs and Ci while ZnCD 500 show lowest. Further highest Pn and Gs were recorded for CD 500 ppm suggest that perhaps CDs would improve the stomatal conductance and thereby increase the photosynthesis rate of the plant. And this indicates the positive use of NPs on plant physiology as well.

The Tr data, on the other hand, have completely invalidated the above-mentioned pattern. Tr shows a dose dependent response for the NP concentration where control set of plants have lower Tr. Li et al. (2018) has explained the presence of hydrophilic groups (OH and COOH) on the surface of the CD combines with the water molecules and support the transportation of wate molecules throughout the plant. Further, they report that the increased O_2% which is higher than 29% would accelerate this process. XPS

full survey data of ZnCD synthesizes for our study revealed that the O% is nearly 60% which would help in absorbing more H_2O to the plant. This has been proved in a study carried out by Tripathi et al. (2015). The results of the CD 500 and ZnCD 500 treatments were clearly different when the photosynthetic and gas exchange parameters were measured. Results thus supported the choice of CD500 and ZnCD500 for the subsequent experiments.

3.4.3. CNPs influences the growth and Zn uptake at latter part of plant development

The experiment with selected CNP doses (CD 500 ppm and ZnCD 500 ppm) in conjunction with a bulk Zn source (ZnAc) and a control yielded some interesting results. Though Hao et al. (2018) and Begum et al. (2012) have reported negative effects of applying CNPs on rice plants, our study reveals that applying CDs and ZnCDs at 500 ppm concentration does so not signify any negative effect. Instead, all the four treatments have resulted a % increase ranged from 23% to 37% for plant height, from 60% to 89% for total number of tillers after the whole one-month growing period. Additionally, there is a nearly two-fold increase in the total leaf area and three-to-four-fold increase in the dry weight of the plants at the end of the one month growing period. Highest recorded plant growth parameters such as height, total leaf area and dry weight for ZnAc treatment explains the positive impact of Zn treatment on cell division and expansion. Many studies have reported positive effect of CNP and MNP application on rice and other cereal growth (Tripathi et al., 2011, Saxena et al., 2014, Tripathi et al., 2015, Ghasemi et al., 2017, Panda, 2017, Lee et al., 2018, Li et al., 2018, Itroutwar et al., 2020, Yang et al., 2021) However, data on sequential analysis is hard to come by. This study is the first to present data on a weekly basis for up to one month to describe the behaviour of growth parameters following NP application.

Zn content of the rice plants treated with ZnCD, CD, ZnAc and control show a decline over the time of four weeks. Since plants were grown on a Zn free medium, only seed Zn is available for rice seedlings for their growth and development. Zn is an indispensable micronutrient for plants which affects many metabolic process including carbohydrate, protein, auxin and many enzyme synthesis pathways at its deficiency (Castillo-González et al., 2018). The total available Zn (seeds + Zn from ZnCD and ZnAc) will be used in subsequent weeks for the growth and development of the plants. In general, all four treatments show a decline in their Zn content throughout the reporting period. ZnCD and ZnAc treatments of S+1D, S+1W, S+2W show significantly higher Zn contents than their counter treatments (CD and Control). Subsequently, reduction in Zn content gets more steeper from 2nd week to 3rd week. This is more prominent with the ZnCD and ZnAc treatments which records reduction of 34.8 mg/Kg and 47.8 mg/Kg respectively. Yet, CD and control treatments reports decrease in 7.3 mg/kg and 12.8 mg/Kg respectively from S+2W to S+3W. However, at the end of the reported time, both set of plants treated with ZnCD and ZnAc contain nearly 5 times of Zn than the control and nearly 2 times of Zn content compared to CD treatment. This enhancement is totally due to the supply of Zn externally as bulk, and nano incorporated. It's interesting to note that plants treated with ZnCD have a Zn content that is almost 1.5 times higher at the end of the reporting period than plants treated with bulk Zn. This gives an insight that the supplements of nutrients through nanomaterials would be more beneficial than through bulk material. This was supported by many studies including Deshpande et al. (2017), Dimkpa et al. (2017), Sahoo et al. (2021) and Subbaiah et al. (2016). Deshpande et al. (2017)further explain the possibility of NPs like chitosan in using as nanocarriers to translocate Zn through plants.

3.4.4. CNPs affect during plant development

Throughout the reporting period, the behaviour of Pn, Gs, Ci, and Tr in plants treated with ZnCD, ZnAc, CD, and control is not comparable. All Pn, Gs, and Ci parameters have decreased over the reporting period with the exception of Tr. Multiple pairwise comparisons show that there are no significant differences between the interaction groups, indicating that the parameters have not decreased significantly despite a pattern of declining. However, this visible reduction is also not steady for all treatments. Interestingly, the two treatments without NPs, show relatively similar pattern throughout the period for parameters Pn, Gs and Ci. On contrary, ZnCD and ZnAc treated plants demonstrate a random pattern for Pn, Gs and Ci implying a novel physiological role of NPs in plants. Li et al. (2018) explains with the help of experiment that carried out with rice in which plants treated with CDs showed that these molecules could enter cells at the subcellular level and even alter metabolism at the level of plant gene expression. However, no study has been conducted to demonstrate the effect of NPs on plant gas exchange over selected period. Zhang et al. (2017) reports the exposure time of CNT to rice plants will exhibit a significant change in the photosynthetic rate but the effect through a period has not been found.

Similar data distribution patterns for CD and Control treatments for Pn, Gs, Ci, and Tr has been observed with positive linear relationship with parameters (Ma et al., 2012, Ding et al., 2020). The pattern of data distribution for ZnCD and ZnAc is random, however suggesting the impact of NPs on key plant physiological process. These results suggest that the different chemical and physical properties of CNPs would cause a alters the physiological process that could be used in a positive way.

3.5. Conclusion

The effective dose determination experiment revealed that CD500 ppm and ZnCD 500 ppm had mutually distinct effects on plant growth, Zn uptake parameters, and gas exchange parameters compared to the other combinations of treatments. Thus, these two doses were selected for the subsequent experiments with CNPs. Further, results revealed that the CNPs have a marked effect on Zn uptake and transpiration rate. ZnCD 500 supports the highest uptake of Zn, while higher concentrations of CNPs also significantly increase Tr.

The evaluation of plant growth, Zn uptake, and gas exchange characteristics indicates that Zn supplied via CNPs is a promising way Zn biofortification of cereal. Alternatively, both CDs and ZnCDs do not have any negative effect on plant growth, and gas exchange. Consequently, the results of these two experiments indicate that CNPs could be used effectively with plant systems to deliver micronutrients such as zinc in an effort to address global zinc malnutrition.

CHAPTER 4: ZnCD'S EFFECT ON THE PHYSIOLOGY AND MICRONUTRIENT CONTENT OF TWO DIFFERENT RICE VARIETIES HAVING CONTRASTING Zn USE EFFICIENCY

4.1. Introduction

The international rice research institute (IRRI) has identified a vast difference in rice genotypes for Zn efficiency. Genotypes that can grow well in Zn deficient soil and yield better than a standard genotype are identified as a zinc-efficient genotype (Hajiboland et al., 2005). Genotypes that do not grow well in a Zn deficient soil are labelled as zinc-inefficient genotypes. IR36 is a Zn efficient and IR26 is a Zn inefficient rice genotype which were widely used in Zn use efficiency related studies (Navarro et al., 1980, Welfare et al., 1996, Hajiboland et al., 2001, Hajiboland et al., 2003, Hajiboland et al., 2005, Hajiboland et al., 2006, Meng et al., 2014, Nakandalage et al., 2023). These two popular genotypes were selected for our study, to determine the effect of ZnCD NP application on rice plant growth, physiology and micronutrient uptake.

The effects of Zn and carbon-based NPs as plant growth promoters are well known. Enhanced growth, seed germination, increase in biomass and yield are common outcome of Zn and carbon based NPs (including CDs) application to rice plants (Nair et al., 2012, Yan et al., 2016, Ghasemi et al., 2017, Li et al., 2018, Bala et al., 2019, Yang et al., 2021, Akmal et al., 2022). CNMs such as graphene oxide and MWCNTs successfully delivered micronutrients, agrochemicals and pesticides to the plant systems (Ghasemi et al., 2017). However, although CDs are well known for their carrier properties (Wang et al., 2013, Wang et al., 2014, Ding et al., 2015) no studies were found for CDs used as micronutrient delivery carriers for

plants. This experiment was undertaken to find out the efficiency of a zinc bound CD (ZnCDs) in enhancing rice plant growth, physiology and micronutrient uptake. Using two genotypes with different Zn use efficiency further demonstrates the mechanistic insight into Zn delivery into the plant. Many studies have compared the effect between nano and bulk particle application in rice and other cereals. Previous studies have shown that the impacts of NP and bulk material on cereals are determined by the chemical nature of the NP and the bulk material utilised as well as the size and concentration of the material (Dimkpa et al., 2012, Subbaiah et al., 2016, Bala et al., 2019, Yang et al., 2021, Akmal et al., 2022). Our experiment was included zinc acetate (ZnAc) the bulk inorganic source of Zn which is used as the source of Zn when preparing ZnCDs.

4.1.1 Goal of the study

The goal of the experiment was to compare the effects of ZnCDs (zinc bound NP), CDs (NP without zinc), ZnAc (inorganic bulk source of zinc) and control (absence of NP and zinc) on the growth, physiology and micronutrient uptake of two rice genotypes of different Zn use efficiency.

4.2. Materials and methods

4.2.1. Experimental site and design

The experiment was carried out at the same location described in chapter 3 from January to August 2020. A Zn efficient variety IR36 and Zn inefficient variety IR26 were used for the study. Four treatments namely - CD 500 ppm, ZnCDs 500 ppm, ZnAc (Zinc Acetate) 500 ppm and control was utilised in the experiment. Sand culture nutrient medium with low Zn content was used for plant growing inside a glasshouse.

The glasshouse temperature was maintained between 25°C (day) and 22 °C (night) and relative humidity was retained at 60 – 75% throughout the experimental period. The experiment was conducted using a randomised complete block design with 3 replicates. The experimental 'unit' was a pot with a single rice plant, whereas 'block' was a tank set up for the sand culture.

4.2.2. Treatments for the experiment

The CD and ZnCDs NPs wereprovided by the Queensland Micro- and Nanotechnology Centre & Environmental Engineering, Griffith University, Brisbane, Australia. The results drawn from the experiment described in chapter 3 revealed that the most effective dose of ZnCDs and CD NP in terms of their impact on growth and physiology of rice plants is 500 ppm. Therefore, the four treatments used for the study are CD 500 ppm, ZnCDs 500 ppm, ZnAc 500 ppm (as the bulk Zn source) and control (without any treatment). The solutions of above treatments were made by dispersing/dissolving a known amount of NPs and bulk ZnAc in deionised water (w/v). To facilitate effective spraying, Tween 20 (0.2% v/v) was added to each solution.

4.2.3. Plant material and growing conditions

The study used two medium maturing varieties IR36 and IR26 with high and low Zn use efficiency, respectively (Khush, 2005). Germinated rice seedlings of both varieties were grown using the sand culture technique described in (Mae et al., 1981). However, since both varieties cannot grow in a Zn free medium, the culture medium was modified to include a low Zn (0.1×10^{-3} mM) concentration. Seed germination and the establishment of the sand culture with nutrient medium was similar to the method described in Chapter 3.

4.2.4. Crop growth and maintenance

Four acid washed sand filled pots (up to 1cm below the pot surface) were kept inside a black plastic container (volume: 54 L) and 20 L of growing solution was filled into each container. Three tanks were prepared according to the CRBD experimental design to accommodate all 3 replicates. Pots were randomised weekly to minimise the spatial effect.

At the establishment of the sand culture, 20 L of 1/8th strength of growing solution was added to each container with the solution level 1 cm above the soil surface. A single rice seedling was transplanted into each pot. The growing solution's strength was doubled every week (1st week - 1/8th strength; 2nd week - 1/4th strength; 3rd week -half strength; 4th week – full strength) until the concentration reached its full strength. The growing solution was renewed every 4 days to supply nutrients in constant manner.

As described in the chapter 3 containers were covered using black polythene (while keeping sufficient space for rice plant growth) to avoid algal growth inside the tanks. Plants were grown until maturity.

4.2.5. Treatment application

Rice plants at the stage of 'heading' were sprayed with the relevant treatment using a Paasche® VL 0908 sprayer coupled with Dynavac® pump as described in Chapter 3. All 3 replicates were sprayed with the appropriate procedures, with minimal contamination between treatments. Following the treatments, plants were grown until maturity and harvested to collect data.

4.2.6. Measurement of growth, physiological and nutritional parameters

The physiological maturity stage of the rice plants was used to collect data for their growth, physiology, and nutritional uptake. Plant height, number of tillers, total number of panicles, panicle lengths, number of spikelets per panicle was recorded before harvesting. Average panicle length and average number of spikelets per panicle were also calculated.

Seeds, shoots and roots were harvested manually at physiological maturity of the plant. Seeds, shoots and roots were oven dried separately at 60 °C for 72 h. Dry weight of seeds, straw and roots were recorded and dry weight of total plant (summation of dry weight of seeds + shoots + roots) were calculated. Above ground biomass was calculated using dry weight of seeds and shoots and recorded. Thousand grain weight (at 13% moisture content) was calculated by randomly selecting and weighing 3 samples of 100 seeds from each plant (Amini et al., 2016, Ghasemi et al., 2017). Brown rice was obtained by manually threshing seeds, and the total harvest was recorded by weighing threshed brown rice with a computerised balance (Rehmani et al., 2014). Harvest index was calculated by dividing the total harvest weight from the total above ground biomass.

Gas exchange parameters namely, Photosynthesis rate (Pn), Stomatal conductance (Gs), Intercellular CO_2 concentration (Ci) and Transpiration

rate (Tr) of IR36 and IR26 plants subjected to different treatments were made using a portable photosynthesis system (LI-6400xt, LI-COR, USA) coupled with LI-COR transparent conifer chamber (LI-COR, Lincoln, NE, USA 6400-05) as described in chapter 03. To obtain measurements, flag leaves were selected as they are the most efficient functional leaf at grain filling stage, contributing to yield related traits (Wang et al., 2011, Zhang et al., 2015). Dried, harvested plant parts: shoots, roots and de-husked grains were finely ground using a Foss CT193 Cyclotec (Midland scientific, USA) and a Tissue Lyser (Qiagen, USA) grinder. The concentrations of Zn, Fe, Mn and Cu were measured on plant samples using AAS (Shimadzu Atomic absorption Spectrophotometer – AA 7000 series) as described in chapter 3.

4.2.7. Statistical analysis

Multivariate analysis of data was performed using Mintab version 20 (www.minitab.com), including Principle Component Analysis (PCA) and Multivariate analysis of variance (MANOVA) (O'Brien et al., 1985). MANOVA was performed using the following models: Wilks', Lawley-Hotelling, and Pillai's. MANOVA performed the analysis of variance for multiple dependent variables by the employed Zn treatment groups. For physiological features of flag leaf and agronomical features, the data was Z-standardised before running MANOVA. Absolute values of coefficients derived from PCA (multivariate analysis) were used as a criterion of feature importance (feature selection), as described previously (Malhi et al., 2004, Song et al., 2010, Ebrahimie et al., 2018).

Univariate analysis was performed using Minitab version 20 to compare the Zn treatments (ZnCDs: Zn carbon dots, ZnAc: Zn acetate, CDs: carbon dots, and control) inside each variety: IR36 (Zn efficient variety) or IR26 (Zn inefficient variety) by Analysis of Variance (ANOVA). Normality of data was tested based on Ryan-Joiner approach (also called Shapiro-Wilk)

method. When the data were not normally distributed, the data was transformed, or the non-parametric Mann-Whitney test was applied. The figures were created using Minitab version 20 and GraphPad Prism Version 9.

4.3. Results

4.3.1. Nutritional analysis in grain and shoot

Multivariate analysis was performed on 12 features of nutritional contents, including: Zn content of shoots, Zn content of roots, Zn content of grains, Fe content of shoots, Fe content of roots, Fe content of grains, Mn content of shoots, Mn content of roots, Mn content of grains, Cu content of shoots, Cu content of roots, and Cu content of grains. The MANOVA results are presented in Table 4.1, comparing the effects of ZnCDs, ZnAc, CDs, and control on 12 nutritional features (n=12) in shoots, roots, and grain two studied varieties of IR36 (Zn efficient variety) and IR26 (Zn inefficient variety). As it can be inferred from Table 4.1, the treatments are significantly different (p=0.01) between the employed Zn treatments.

Table 4.1: Multivariate results of the effects of Zn carbon dots (ZnCDs), Zn acetate (ZnAc), carbon dots (CDs), and control on a range of nutritional features (n=12) in IR36 (Zn efficient variety) and IR26 (Zn inefficient variety).

Criterion	Approx F	P
Wilks'	4.706	0.000
Lawley-Hotelling	7.373	0.000
Pillai's	2.152	0.000

Figure 4.1 presents the results of PCA analysis on nutritional features and (A) Visualising groups. PCA 1 and PCA 2 together represent 55.9% of variation in data. IR36 control samples group together and are separate from the other treatments, including IR36 CDs. It can be concluded that the effects on control and CDs on nutritional features in IR36 are not similar as they locate far from each other. The largest distance was the IR36 group from IR36 ZnCDs group. It can be inferred from Figure 4.1 that PCA1 discriminates IR36 ZnCDs from both IR36 Control and IR36 CDs. In contrast, PCA2 separates IR36 variety from IR26 variety.

Absolute values of coefficients in PCA1 and PCA2, as index of importance in PCA analysis is presented in Table 4.2. As ranked in Table 4.2, the important features in PCA 1 are: Mn Grains, Cu Grains, Mn Shoots, Mn Roots, Zn Grains, Fe Shoots, Fe Roots, Zn Shoots, Cu Shoots, Zn Roots, and Cu Roots. In contrast, the ranked important features in PCA2, distinguishing IR36 from IR26, were; Fe Grains, Zn Roots, Cu Roots, Cu Shoots, Mn Shoots, Zn Grains, Mn Roots, Cu Grains, Zn Shoots, and Fe Roots.

Table 4.3. compares the effect of Zn treatments on important nutritional features derived from PCA1 coefficients, in IR26 and IR36 varieties. In the IR36 variety, there were remarkable increases in the contents of Mn in grains, Cu in grains, and Zn in grains in response to ZnCDs and ZnAc treatments. Also, Mn in roots showed a noticeable increase in response to ZnCDs in IR36 compared to the other treatments (ZnAc, CDs, and control). The effect of Zn treatment on the Zn content of shoots (p=0.0001), Zn content of roots (p=0.0001), Zn content of grains (p=0.001), Mn content of shoots (p=0.008), Mn content of grains (p=0.0001), and Cu content of grains (p=0.0001) was significant in the IR36 variety. However, it was not significant for Fe content of shoots (p=0.058), Fe content of roots (p=0.094), Fe content of grains (p=0.054), Mn content of roots (p=0.123), Cu content of shoots (p=0.256), and Cu content of roots (p=0.15). Mean comparison using Tukey test is presented in Table 4.3 where ZnCDs outperformed the other Zn treatments. In particular, ZnCDs significantly

(p=0.05) increased the contents of Mn in grains, Cu in grains, Mn in shoots, and Zn in grains compared to the control.

As demonstrated by the PCA2 coefficient in Table 4.2. and visualised by the boxplot in Figure 4.3., IR26 has a higher content of grain Fe in all treatments compared to IR36.

Table 4.2: PCA-based selection of nutritional features responding to Zn treatments (Zn carbon dots, Zn acetate, carbon dots, and Control)

PCA1			PCA2		
Nutritional variable	Coefficient	Absolute value of coefficient	**Nutritional variable**	Coefficient	Absolute value of coefficient
Mn Grains	0.428	0.428	Fe Grains	-0.467	0.467
Cu Grains	0.391	0.391	Zn Roots	-0.405	0.405
Mn Shoots	0.361	0.361	Cu Roots	-0.387	0.387
Mn Roots	0.36	0.36	Cu Shoots	0.366	0.366
Zn Grains	0.277	0.277	Mn Shoots	0.29	0.29
Fe Shoots	0.267	0.267	Zn Grains	-0.257	0.257
Fe Roots	0.245	0.245	Mn Roots	0.234	0.234
Zn Shoots	0.242	0.242	Cu Grains	0.222	0.222
Cu Shoots	0.215	0.215	Zn Shoots	-0.211	0.211
Zn Roots	0.214	0.214	Fe Roots	-0.187	0.187
Cu Roots	0.213	0.213	Mn Grains	-0.024	0.024
Fe Grains	0.018	0.018	Fe Shoots	0.005	0.005
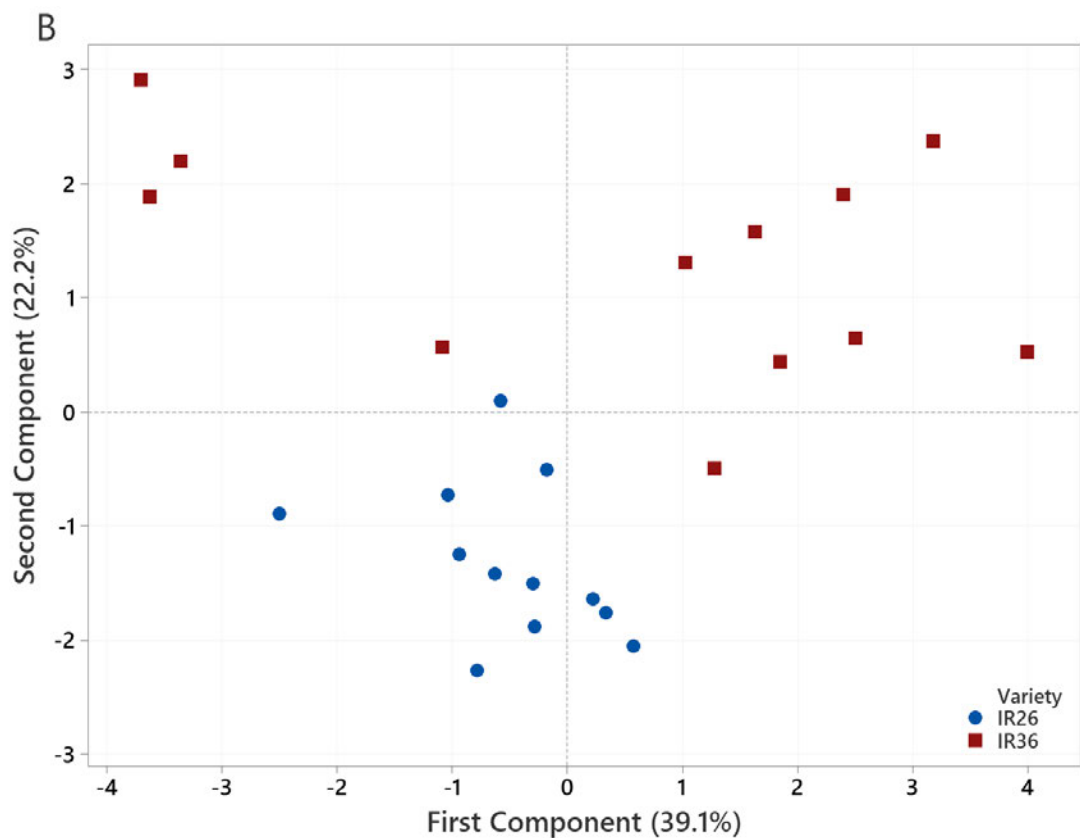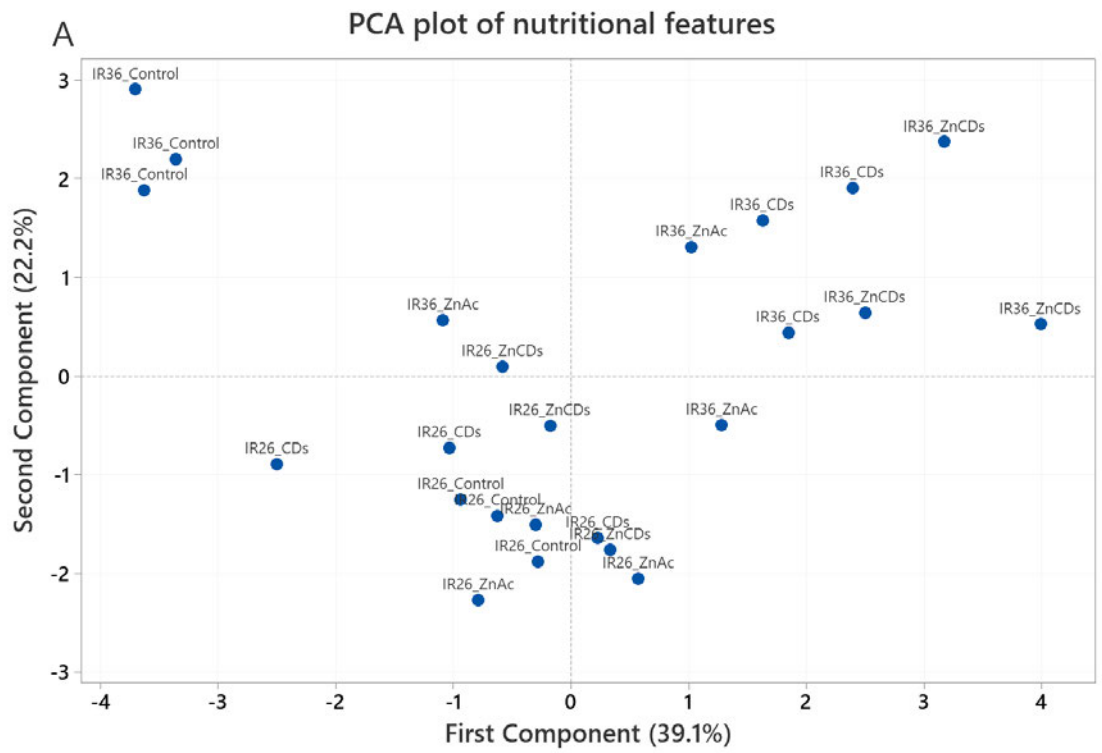
Figure 4.1: PCA plots of nutritional features. (A) Visualising groups. (B) Visualising varieties. ZnCDs: Zn carbon dots, ZnAc: Zn acetate, CDs: carbon dots, IR36 (Zn efficient variety), IR26 (Zn inefficient variety).
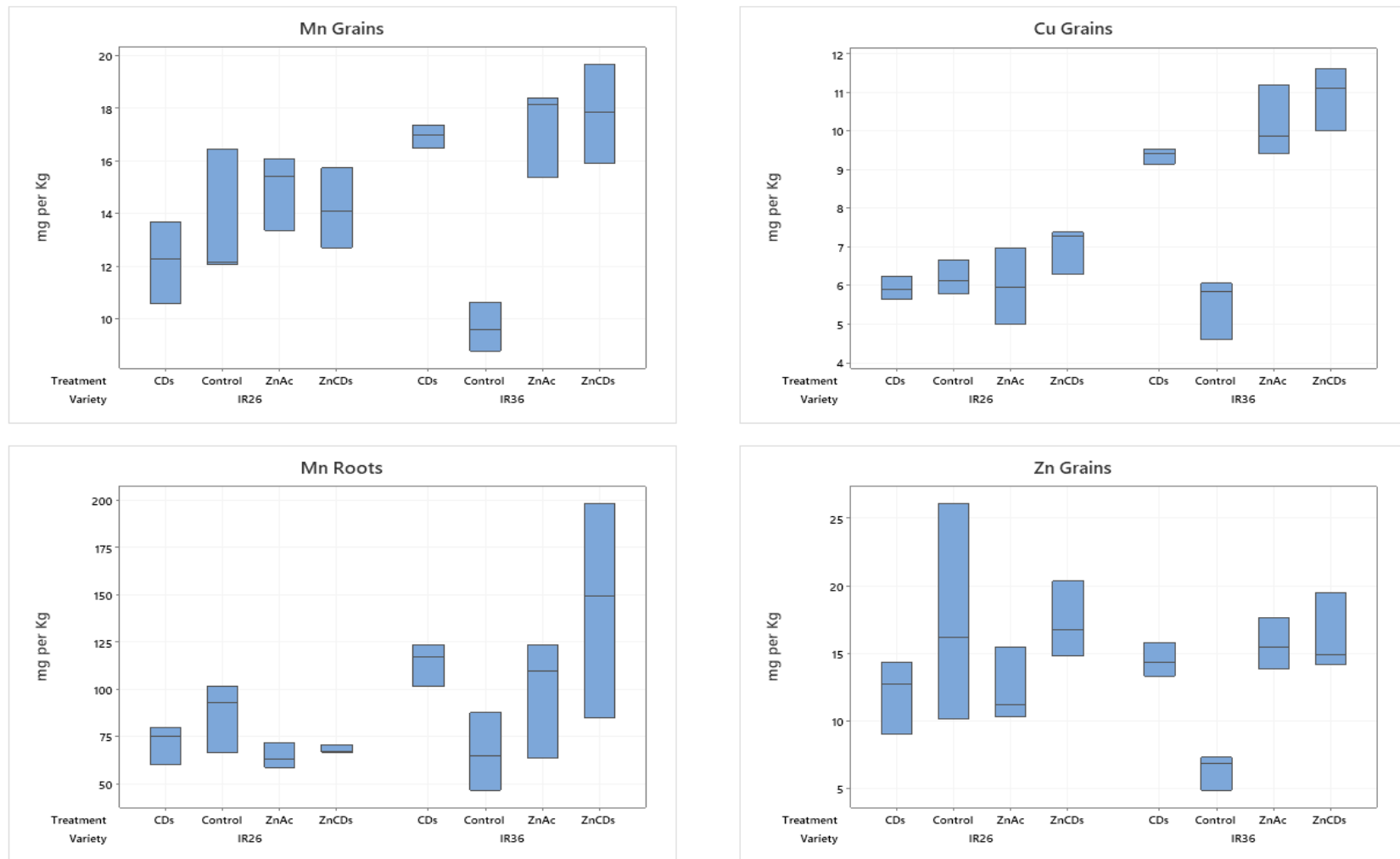
Figure 4.2: Comparison of the effect of Zn treatments on nutritional features in IR26 and IR36 varieties. ZnCDs: Zn carbon dots, ZnAc: Zn acetate, CDs: carbon dots, IR36: Zn efficient variety, and IR26: Zn inefficient variety.

Table 4.3: Comparison of some nutritional features (selected based on PCA analysis) between Zn treatments in IR36 variety (ZnCDs: Zn carbon dots, ZnAc: Zn acetate, CDs: carbon dots, and control) using Tukey pairwise method at 95% Confidence. Means that do not share a letter are significantly different. Mean values are based on mgKg^{-1}.

Zn treatment	Mn Grains		Cu Grains		Mn Shoots		Zn Grains	
	Mean	Grouping	Mean	Grouping	Mean	Grouping	Mean	Grouping
IR36_ZnCDs	17.8	A	10.9	A	423.7	A	16.2	A
IR36_ZnAc	17.3	A	10.2	A	236.4	B	15.7	B
IR36_CDs	16.9	A	9.4	A	401.6	A	14.5	A
IR36_Control	9.7	B	5.5	B	232.1	B	6.4	B
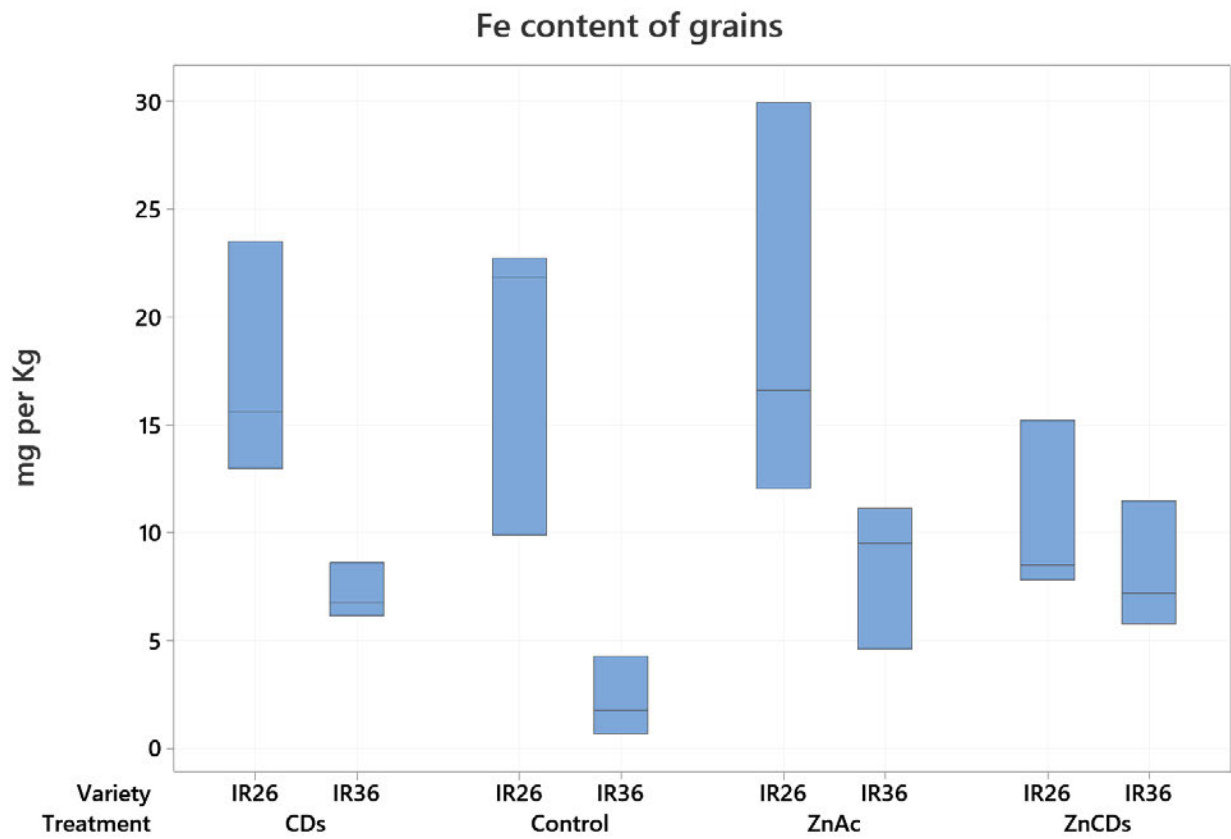
Figure 4.3: Comparison of the Fe content of grains between IR36 and IR26 variety in different Zn treatments (ZnCDs: Zn carbon dots, ZnAc: Zn acetate, CDs: carbon dots, and control).

4.3.2. Physiological features of flag leaf in response to ZnCDs

Multivariate MANOVA analysis was conducted on 4 physiological features, including photosynthetic rate ($\mu molCO_2m^{-2}S^{-1}$), stomatal conductance to H_2O ($molH_2Om^{-2}S^{-1}$), intercellular CO_2 concentration ($\mu molCO_2mol\ air^{-1}$), and transpiration rate ($mmolH_2Om^{-2}S^{-1}$) (Table 4.4). MANOVA showed that there is no significant effect on the physiological features of the flag leaf among the applied Zn treatments (ZNCDs, ZnAc, CDs, and control). The means of each comparison in IR36 and IR26 are presented in Table 4.5 and Table 4.6.

PCA analysis also confirmed the MANOVA result where PCA was not able to discriminate Zn groups using physiological traits of flag leaf (data not shown).

Table 4.4: Multivariate analysis of the effects of Zn carbon dots (ZnCDs), Zn acetate (ZnAc), carbon dots (CDs), and control on four physiological features in IR36 (Zn efficient variety) and IR26 (Zn inefficient variety).

Criterion	Approx F	P
Wilks'	0.731	0.000
Lawley-Hotelling	0.664	0.000
Pillai's	0.789	0.000

Table 4.5: Comparison of physiological features of flag leaf in IR36 variety. ZnCDs: Zn carbon dots, ZnAc: Zn acetate, CDs: carbon dots, and control.

Physiology Data- IR36					
Flag Leaf (After treatment application)	**P-value and mean**				
	CDs vs Control	**ZnAc vs Control**	**ZnCDs vs Control**	**ZnCDs vs CDs**	**ZnCDs vs ZnAc**
Photosynthetic rate ($\mu mol CO_2 m^{-2}S^{-1}$)	NS (10.8 vs 7.9)	NS (6.7 vs 7.9)	NS (8.1 vs 7.9)	NS (8.1 vs 10.8)	NS (8.1 vs 6.7)
Stomatal Conductance to H2O ($mol H_2O m^{-2}S^{-1}$)	p= 0.08 (0.18 vs 0.3)	NS (0.09 vs 0.3)	NS (0.39 vs 0.31)	NS (0.39 vs 0.17)	NS (0.39 vs 0.43)
Intercellular CO2 concentration ($\mu mol CO_2 mol air^{-1}$)	NS (268.7 vs 263.3)	NS (256.7 vs 263.3)	NS (259.6 vs 263.3)	NS (259.6 vs 268.7)	NS (259.6 vs 256.7)
Transpiration rate ($mmol H_2O m^{-2}S^{-1}$)	NS (5.7 vs 4.1)	NS (3.4 vs 4.1)	NS (4.14 vs 4.17)	NS (4.14 vs 5.75)	NS 4.14 vs 3.46)

Table 4.6: Comparison of physiological features of flag leaf in IR26 variety. ZnCDs: Zn carbon dots, ZnAc: Zn acetate, CDs: carbon dots, and control.

Physiology Data- IR26					
Flag Leaf (After treatment application)	**P-value and mean**				
	CDs vs Control	**ZnAc vs Control**	**ZnCDs vs Control**	**ZnCDs vs CDs**	**ZnCDs vs ZnAc**
Photosynthetic rate ($\mu mol CO_2 m^{-2} S^{-1}$)	NS	NS	NS	NS	NS
	(12.2 vs 9.03)	(11.4 vs 9.0)	(10.1 vs 9.0)	(10.1 vs 12.2)	(10.1 vs 11.4)
Stomatal Conductance to H_2O ($mol H_2O m^{-2} S^{-1}$)	NS	p= 0.08	NS	p= 0.08	p= 0.08
	(0.17 vs 0.13)	(0.18 vs 0.13)	(0.13 vs 0.13)	(0.13 vs 0.17)	(0.13 vs 0.18)
Intercellular CO_2 concentration ($\mu mol CO_2 mol air^{-1}$)	NS	NS	NS	NS	NS
	(251.3 vs 256)	(261 vs 256)	(241 vs 256)	(241.3 vs 251.3)	(241.3 vs 261)
Transpiration rate ($mmol H_2O m^{-2} S^{-1}$)	NS	p= 0.08	NS	p= 0.08	p= 0.08
	(5.6 vs 4.5)	(5.6 vs 4.5)	(4.4 vs 4.5)	(4.4 vs 5.6)	(4.4 vs 5.6)

4.3.3. Agronomical important trait response to CDs

Thirteen agronomic features including dry weight of seeds, straws, roots, and total plant, as well as harvest index and 1000 grain weight were subjected to multivariate analysis by PCA (Figure 4.4). Figure 4.4 shows the PCA1 and PCA2, which explain 54.8 percent and 22.3 percent of the variation in data, respectively. PCA successfully distinguished control samples in IR26 from the rest of groups using agronomic traits. Dry weight of the total plant, above ground biomass, dry weight of straw, dry weight of seed, and total harvest had the higher importance in PCA1 (Table 4.7).

As shown in Figure 4.5, the IR26 control samples had significantly higher dry weights of seed, straw, root, and total plant than the Zn treatments. In IR36, however, there was no substantial difference between the mentioned traits.

Figure 4.4: PCA plot based on agronomical features. ZnCDs: Zn carbon dots, ZnAc: Zn acetate, CDs: carbon dots, IR36: Zn efficient variety, IR26: Zn inefficient variety.
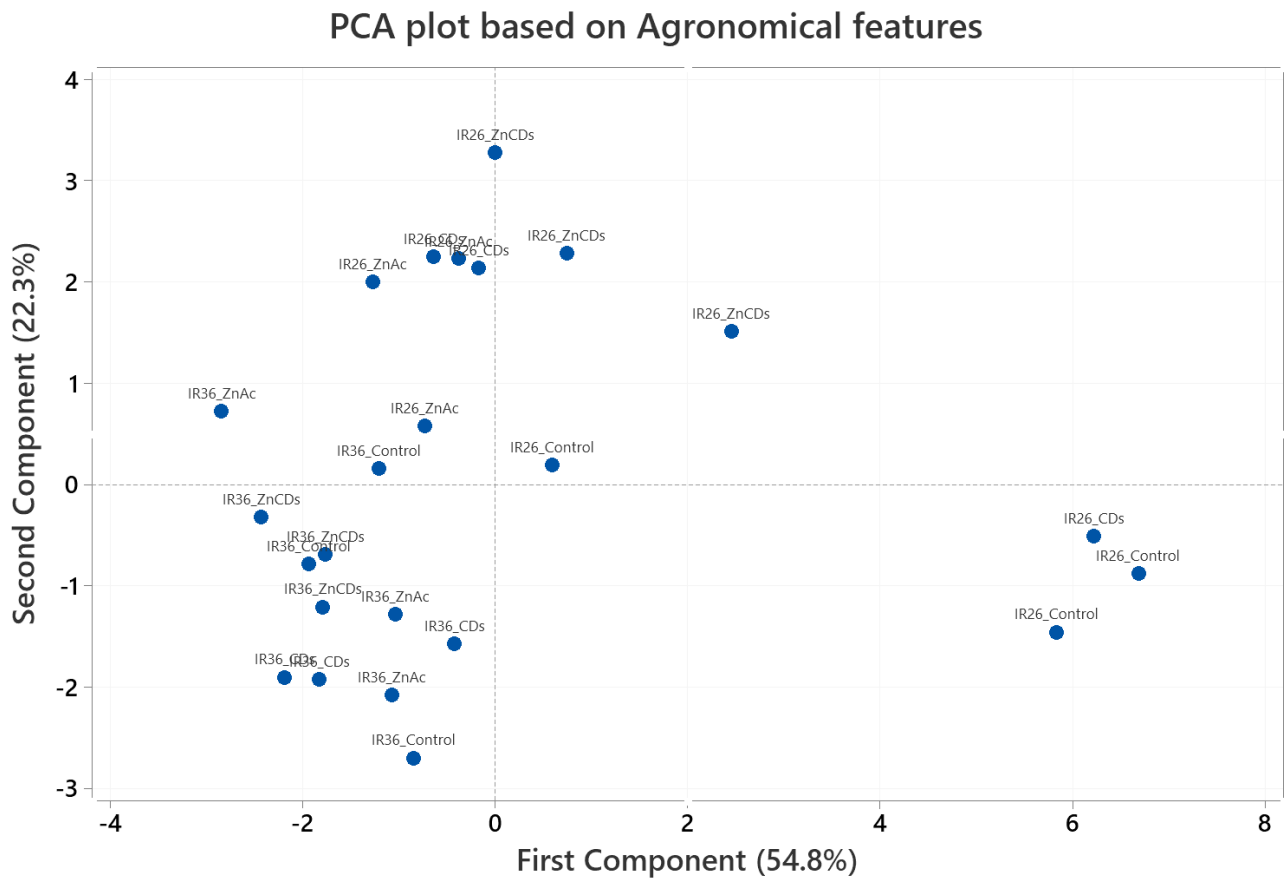
Table 4.7: Coefficients of PCA1 of Agronomical features. The higher weight demonstrated the higher importance in PCA1.

Agronomical features	PC1 coefficient	Absolute PCA weight
Dry weight Total plant	0.372	0.372
Above ground biomass	0.371	0.371
Dry weight - Straw	0.366	0.366
Dry weight - Root	0.351	0.351
Dry weight - Seed	0.348	0.348
Total harvest	0.333	0.333
Average number of branches per panicle	0.238	0.238
Total number of tillers	0.235	0.235
Plant Height	0.211	0.211
Number of panicles	0.208	0.208
Harvest index	-0.142	0.142
1000 grain weight	-0.125	0.125
Average Panicle length	0.005	0.005
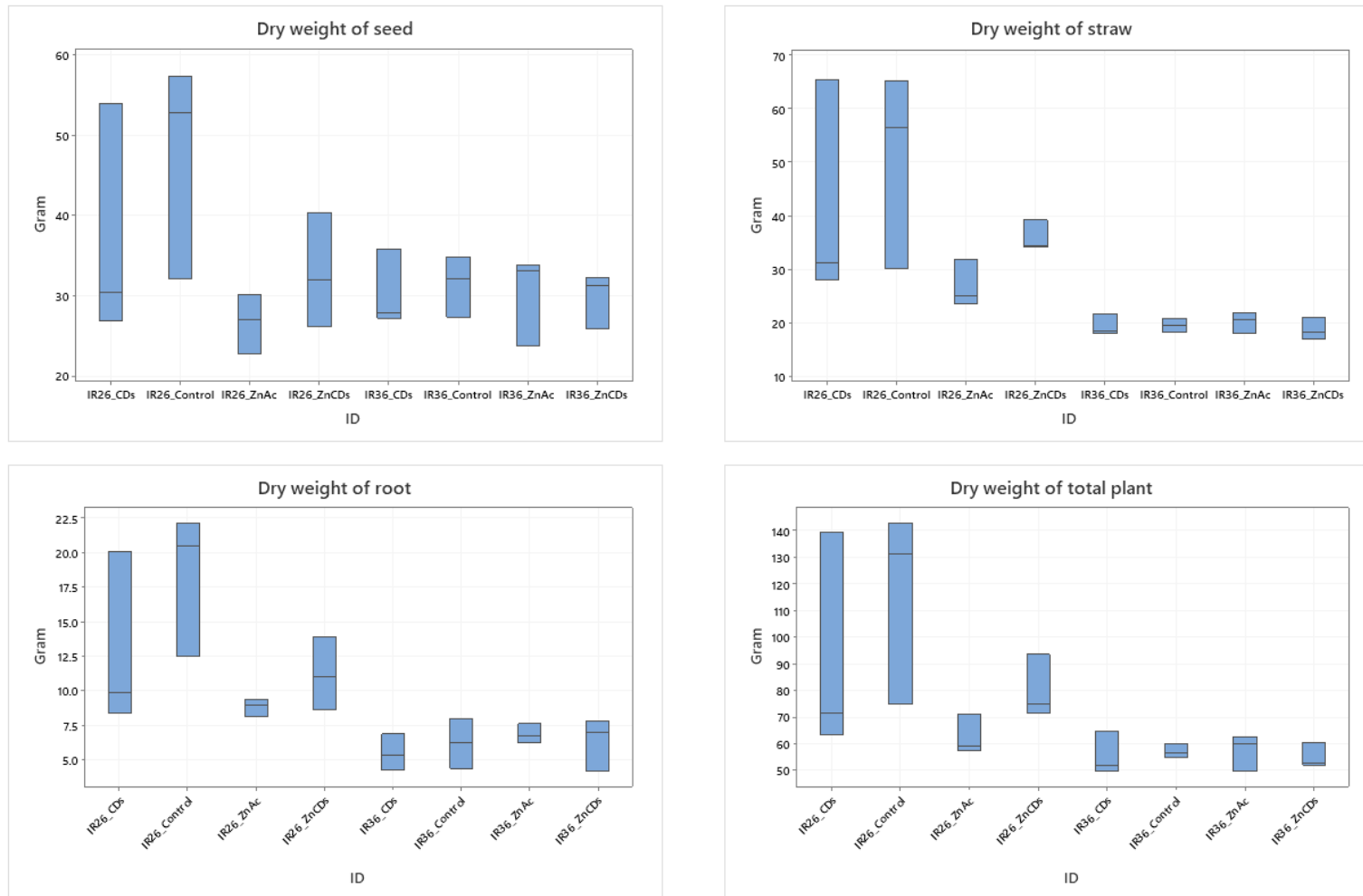
Figure 4.5: Comparison of dry weight of seed, dry weight of straw, dry weight of root, and dry weight of total plant between Zn treatments in two varieties. ZnCDs: Zn carbon dots, ZnAc: Zn acetate, CDs: carbon dots, IR36: Zn efficient variety, IR26: Zn inefficient variety.

4.4. Discussion

Conducting multivariate analysis on 30 measurements in three categories of 12 nutritional traits, four physiological traits, and 14 agronomical traits provided a comprehensive view on the effect of foliar application of Zn nanoparticles (NPs). Furthermore, comparing the response of Zn efficient (IR36) and Zn inefficient (IR26) offered the chance of evaluating the effect of variety (genotype) with a distinguished level of Zn processing to ZnCDs.

Nano particles (NPs) have opened a new opportunity to increase the quality and yield of grains. However, previous results are contrasting. A reduction in the quality of rice grains was observed after the treatment of soil with cerium oxide nanoparticles (CeO_2 NPs) (Rico et al., 2013). In contrast, treatment of soil with CeO_2 NPs improved the plant growth, shoot biomass, and grain yield of wheat by 9.0%, 12.7%, and 36.6%, respectively, demonstrating the high potential of NPs to influence crop physiology and food quality (Rico et al., 2014). In a recent study, soil-amended copper oxide (CuO) NPs increased the Fe content in cultivar rice, highlighting the potential application of CuO NPs as nano fertiliser (Deng et al., 2022). In another study, adding silver NPs to soil was beneficial for rice and bacteria in soil microbiota (Yan et al., 2022). Species-dependent manner is reported in response to CeO_2 NPs for nutritional quality (Gui et al., 2023).

Recent studies are accumulating evidence on the beneficial effects of Zn NPs on tolerance against abiotic stresses such as drought and salinity. In sorghum, adding Zinc NPs to soli showed remarkable beneficial effects by increasing the level of drought tolerance, nutrient acquisition (total K, grain K, shoot P, grain Zn) and grain protection (Dimkpa et al., 2019). Interestingly, in the mentioned study (Dimkpa et al., 2019), Zinc NPs were able to reverse and improve the effect of drought at late emergence of flag leaf and grain head. In comparison, with conventional Zn fertiliser, the amendment of Zinc oxide nanoparticles (ZnO NPs) to soil reduced salinity stress in wheat (Adil et al., 2022). Plants treated with ZnO NPs retained

higher chlorophyll contents and yield under salinity stress than conventional fertiliser (Adil et al., 2022).

Most studies have analysed the effect of NPs amendment to soli, and there are few studies on foliar application of NPs. Foliar application of silica NPs alleviated arsenic in rice grain (Ghasemi et al., 2017). Our study is the first study on foliar application of ZnCDs. We found that there is a remarkable difference between the response of nutritional features to ZnCDs treatment between the Zn efficient (IR36) and Zn inefficient varieties (IR26). ZnCDs led to a significant promotion of the contents of Mn, Cu, and Zn in grains as well as Mn in roots.

4.5. Conclusion

The results of the study revealed that application of ZnCD resulted in distinct changes in the Zn content of the Zn efficient rice variety. Further, NP applications did not cause any negative changes to the physiology and the agronomy of the rice plant regardless of the Zn use efficiency status of the cultivar

.

Thus, the outcomes of this chapter highlight the implications of foliar application of ZnCDs in nutrient management and improving grain nutritional contents for human health. The findings of this study suggest considering the foliar application of ZnCDs as an efficient nano fertiliser in improving nutrient quality of rice.

CHAPTER 5: COMPARATIVE TRANSCRIPTOMIC ANALYSIS OF ZINC EFFICIENT RICE VARIETY IR36 AGAINST ZINC INEFFICIENT RICE VARIETY IR26

5.1 Introduction

The mechanisms mediating higher Zn efficiency and the effect of Zn nanoparticles (NPs) have not been fully elucidated. Nevertheless, gene expression after exposure to different metal NPs has been studied in *Arabidopsis*. In *Arabidopsis*, exposure to TiO_2 and CeO_2 NPs altered the regulation of 204 and 142 genes, respectively (Tumburu et al., 2015). In another study, exposure of *Arabidopsis* to AgNPs resulted in the upregulation of 286 genes and the downregulation of 81 genes, including genes involved in plant defence (Kaveh et al., 2013). Tobacco plants treated with Al_2O_3 NPs showed an increased expression of some microRNAs, resulting in reduced growth and development of the seedlings (Burklew et al., 2012). Few studies have been carried out to explain the effect of carbon-based NPs. Application of Multi-walled carbon nanotubes (MWCTs) up-regulated the water-channel LeAqp2 gene and stress-related genes of tomatoes (Khodakovskaya et al., 2011).

Little information exists for rice response to NPs. A study carried out by García-Sánchez et al. (2015) reported transcriptomic changes in *Arabidopsis thaliana* exposed to different NPs such as TiO_2, Ag and MWCNTs (García-Sánchez et al., 2015). This study revealed NP exposure repressed transcriptional responses to microbial pathogen infections and exhibited transcriptional patterns characteristic of phosphate starvation. Few studies have been conducted on NPs in rice. Significant reduction in root elongation, shoot and

root fresh weights, total chlorophyll contents as well as differential transcription of genes related to oxidative stress tolerance has been reported in rice seedlings exposed to AgNPs (Nair et al., 2014).

A recent study demonstrated that Copper oxide nanoparticles (CuONPs) impact yield, nutritional quality, and upregulation of auxin-associated genes in the grains of both weedy and cultivated rice in a dose-dependent manner (Deng et al., 2022). High doses of CuONPs (≥300 mg/kg) prevented grain production. In contrast, CuONPs in the doses of 75 mg/kg and 150 mg/kg led to an increased Fe content, a promising result for the use of CuONPs as a potential nano-fertiliser (Deng et al., 2022).

The above-mentioned studies suggest that exposure to different types and doses of NPs can affect the changes in transcriptome and gene expression profile. To clarify the effect of Zn bound carbon nanodots (ZnCDs) on cereal functional genomics, it is important to carry out gene expression studies and a transcriptomic analysis following NP application to the rice plants. Transcriptome analysis is an important step in understanding the molecular mechanism of response to Zn and its nano carrier (He et al., 2015, Bandyopadhyay et al., 2017, Muvunyi et al., 2022). However, most previous studies have focused on the response of one type of genotype against Zn stress or Zn deficiency (Song et al., 2014, Zeng et al., 2019, Song et al., 2021), rather than transcriptomic comparison of genotypes with different levels of Zn uptake and metabolism.

Having two rice cultivars with different levels of Zn efficiency (IR36 and IR26) provided an opportunity for comparative transcriptomic analysis between Zn efficient variety against inefficient variety, leading to the discovery of genes and associated mechanisms involved in higher Zn efficiency in efficient variety. To best of our knowledge, no studies have profiled the transcriptomic responses of Zn efficient variety against inefficient one.

5.1.1. The goals of this chapter

The goal of this chapter was to discover a transcriptomic signature of response to Zn bounded carbon nanodots (ZnCDs) in Zn efficient variety (IR36), compared to Zn inefficient variety (IR26). Unraveling the underpinning key molecular pathways and mechanisms involved in higher Zn efficiency and response to nanoparticles by computational systems biology analysis was the second goal of this chapter.

5.2 Material and methods

5.2.1 Plant material, sampling, Zn treatment, and RNA extraction

Zn efficient IR36 and Zn inefficient IR26 were grown in low Zn (0.1×10^{-3} mM) sand culture nutrient medium as described in chapter 3. Plants were grown until maturity, and at heading stage were treated with two treatments, namely, ZnCD 500 ppm and control. Treatments were applied using a Paasche sprayer, as described in chapter 3. The experiment was conducted under glasshouse conditions using a randomised complete block design with 3 replicates. Experiments ran from September 2020 to February 2021. The maximum and the minimum temperatures were maintained at 25 °C and 22 °C, respectively.

Three days after spraying, flag leaves were collected from the main tiller of all three replicates at the heading stage. Sampling was done between 9.00 – 11.30 am and samples were placed in storage tubes and were immediately frozen in liquid nitrogen. Samples were then stored at -80 °C until total RNA extraction.

TSP buffer (pH 10) was prepared using EDTA 10mM, KCl 1 M, TRIS-HCl 10mM, and autoclaved. RNase free, sterilised mortars and pestles were stored at -80 °C at least 12 h prior to the extraction. Hundred (100) mg of the flag leaves were ground to a fine powder using liquid N_2 in a pre-chilled mortar and pestle. Total RNA was extracted using Trizol® reagent (Invitrogen by Thermo Fisher Scientific, USA) according to the manufacturer's instructions. Extracted RNA was quantified using a DS-11 Series Spectrophotometer/Fluorometer (DeNovix, USA) and concentration of the RNA samples was adjusted to 1 µg/µL.

Total RNA (1µg) was treated with DNase 1, amplification grade (Invitrogen by Thermo Fisher Scientific, USA) according to the manufacturer's instructions to avoid genomic DNA contaminations. RNA samples were reverse-transcribed using SensiFAST™ cDNA synthesis kit (Catalogue NO-Bio-65054, Bioline, UK) as per the manufacturer's instructions. Twenty (20) µL were introduced into the thermal cycler with the program set at 25 °C for 10 min for primer annealing; 42 °C for 15 min for reverse transcription; and 85 °C for 5 min for inactivation of the process. cDNA was stored at -20 °C until further use.

5.2.2 Plan of experiment

The variables of this study were Zn treatment [in two levels of Zn bound carbon nanodots (ZnCDs) and control] and variety [in two levels of Zn efficient (IR36) and Zn inefficient (IR26). In total, 12 samples were sequenced in RNA-Seq experiments (Two varieties * Two treatments * 3 replications = 12 samples).

5.2.3 High-throughput RNA-sequencing and expression profiling

RNA-seq sequencing was performed using NextSeq machine of Illumina at Genomics Research Platform of La Trobe University (Victoria, Australia) as single read sequencing with an average length of 76bp (after removal of adaptors and indexes). After sequencing, adapters were removed by BaseSpace, a cloud-based Illumina software.

Rice (*Oryza sativa*) reference genome and its gene annotations (FileVersion = IRGSP-1.0, Date = 2022-03-17) were downloaded from Ensembl genome browser (ftp.ensemblgenomes.org/pub/current/plants) and used for mapping

and expression profiling. Quality control, trimming, mapping to reference genome, and differential expression analysis were performed using CLC Genomics Workbench Version 22 (QIAGENE). Trimming was performed using the following parameters: (1) Quality score limit = 0.05; (2) Trim ambiguous nucleotides = Yes;and (3) Maximum number of ambiguities = 2. Mapping was performed using the following parameters: (1) Mismatch cost = 2, (2) Insertion cost = 3, (3) Deletion cost = 3, Length fraction = 0.7, and Similarity fraction = 0.7. Reads per kilobase of exon model per million mapped reads (RPKM) (Mortazavi et al., 2008) was employed for measuring and visualising of gene expression. RPKM is a normalised form of the mapped reads, normalising different depth of sequencing and gene length.Heatmap was used for visualising of differential expression, based on the following parameters: (1) Distance measure = Euclidean distance and (2) Cluster linkage = Average linkage. Also, for creating a heatmap using CLC Genomics Workbench, TMM normalisation was employed to adjust library sizes, and 'log CPM' (Counts per Million) values were calculated for each gene. The CPM calculation used the effective library sizes as calculated by the TMM normalisation. After the above normalisation, the counts for each gene were mean centred, and scaled to unit variance. The generated heatmaps show expression profiles, rather than expression values, by colouring each row relative to the average expression of that row, using the normalisations.

Differential expression analysis was performed using read counts and Generalized Linear Model (GLM), an approach similar to edgeR(Robinson et al., 2010). GLM fits curves to expression values without assuming that the error on the values is normally distributed. The assumption is that the read counts follow a Negative Binomial distribution. GLM fit and dispersion estimate provides the chance to calculate the total likelihood of the model given the data and the uncertainty on each fitted coefficient. Using GLM allows us to fit curves to expression values without assuming that the error on the values is

normally distributed. Here, we assume that the read counts follow a Negative Binomial distribution. GLM fit and dispersion estimate allows us to calculate the total likelihood of the model given the data and the uncertainty on each fitted coefficient. The Negative Binomial distribution can be understood as a `Gamma-Poisson' mixture distribution, the distribution resulting from a mixture of Poisson distributions, where the Poisson parameter is itself Gamma-distributed. In an RNA-Seq context, this Gamma distribution is controlled by the dispersion parameter, such that the Negative Binomial distribution reduces to a Poisson distribution when the dispersion is zero. Then, the tool calculated the TMM (trimmed mean of M) values for every sample and then calculates the TMM-adjusted log CPM counts (Robinson et al., 2010).TMM can be considered as normalisation step for correcting the effect of different sequencing depth between samples. TMM normalisation adjusts library sizes based on the assumption that most genes are not differentially expressed. The p-values were corrected with FDR statistics. Fold changes were calculated from the GLM, which corrects for differences in library size between the samples and the effects of confounding factors. The Wald test was applied to calculate the p-values and FDR p-value for the comparison of all group pairs. Differentially expressed genes in each comparison were filtered based on the following two criteria: (1) FDR p-value < 0.05 and (2) Absolute fold change > 2.

5.2.4 Comparative transcriptomic analysis between Zn inefficient (IR26) and efficient (IR36) varieties in response to ZnCDs

The workflow of comparative transcriptomic analysis is presented in figure 5.1 and includes the following steps:

1- Transcriptomic profiling of ZnCDsresponse in Zn efficient variety (IR36+Zn vs IR36_control)

2- Transcriptomic profiling of ZnCDs response in Zn inefficient variety (IR26+Zn vs IR26_control)

3- Comparative transcriptomic analysis: (IR36+ZnCDs vs IR36_control) vs (IR26+Zn vs IR26_control)]. This important step filters the genes that were solely (specifically) upregulated/downregulated in IR36 in response to ZnCDs and not in IR26.

Specific ZnCDs-responding genes in IR36 were used for enrichment analysis in various classification systems (Gene Ontology, KEGG, Pfam and InterPro), employing a Fisher's exact test followed by a correction for multiple testing.

Figure 5.1: Flowchart of the performed comparative transcriptomic analysis between Zn inefficient (IR26) and efficient (IR36) varieties in response to Zn bounded carbon nanodots (ZnCDs). The arrows highlight the genes that were solely (specifically) upregulated/downregulated in IR36 in response to ZnCDs and not in IR26.

5.2.5 Transcriptomic signature of discovery of ZnCDs efficiency by multivariate analysis

Multivariate analysis was employed to find the genes that can discriminate the ZnCDs-treated IR36 efficient variety from the rest of groups. Analysis was performed using Minitab Statistical Software (www.minitab.com, Product version: 20.2).

Selection of key genes in transcriptomic signature was performed based on the coefficient (weight) each gene received in the separation of groups (IR36+ZnCDs, IR36 Control, IR26+ZnCDs, and IR 26 Control) in PCA analysis. Gene/feature selection based on the coefficients in Discriminant Function Analysis (DFA), and Principle Component/Coordinates Analysis (PCoAAnalysis (PCA/PCoA) is one of the most employed approaches for gene selection and signature discovery (Shih-Yin et al., 2012, Mahdi et al., 2014, Singh et al., 2018, Yip et al., 2021).

5.2.6 Gene Ontology (GO) enrichment analysis

GO enrichment analysis is a computational systems biology tool to extract biological infirmation from a bulk of differentially expressed genes (Fruzangohar et al., 2013, Ebrahimie et al., 2015, Ebrahimie et al., 2017). GO classification classifies genes/proteins based on the controlled universal vocabulary in leading groups of biological process (BP), molecular function (MF), and cellular component (CC), support to achieve a universal functional annotation language and understanding (Consortium, 2004, Consortium, 2019).

5.2.7 The Kyoto Encyclopedia of Genes and Genomes (KEGG) enrichment analysis

The KEGG database (Kanehisa et al., 2000) was used for identification of the significantly enriched pathways by IR36 specific genes (responding to ZnCDs) using the String webtool (https://string-db.org/) (Mering et al., 2003). The statistical significance of each KEGG pathway was determined by Fisher's exact test followed by a correction for multiple testing (Mering et al., 2003, Szklarczyk et al., 2016, Szklarczyk et al., 2021).

5.2.8 Gene interaction network analysis

The String webtool (Szklarczyk et al., 2021)was used for the extraction of possible gene-gene interactions based on a range of relations, such as co-expression, literation mining, and functional annotations. String visualises the interaction network with the help of the integrated Cytoscape tool (Szklarczyk et al., 2016).

5.2.9 Domain enrichment analysis

Protein sequences of IR36, specifically up-regulated genes in response to ZnCDs were extracted. Then, domains of each protein sequence were extracted from the pfam database (http://pfam.sanger.ac.uk/) using the CLC Genomics Workbench. For domain prediction, an E-value = 0.0000001 was used to identify the significant domains.

5.2.10 Signature discovery based on significant pathways

Identifying the ng the key GO groups and selection of genes based on the significant GOs are novel and reliable approaches in gene discovery as the selected genes are central in meaningful biological processes (Ebrahimie et al., 2015). Furthermore, the comparison of GO enrichment of a given sample verses GO distribution of the whole genome (as reference) by Fisher exact test (hyper-geometry approach) illustrates the differential functional groups in a particular sample. Furthermore, recent developments in constructing GO networks provide a unique possibility to investigate the transcriptome in the context of functional interactions between different GO classes.

5.3 Results

5.3.1 Quality and quality of RNA-Seq data

The sequence reads were high quality, according to both per-sequence quality criteria as well as per-base analysis criteria. In the per-sequence category, the following items were measured: uniform length distribution, GC-content, ambiguous base-content, quality distribution (based on average PHRED score). In per-base category, the following criteria were analysed: Coverage, nucleotide contributions, GC-content, quality distribution (based on the PHRED score in each position). Also, over-representation analyses (enriched 5-mers) and sequence duplication levels were considered. The results of the quality of samples are presented in Supplementary (Appendix) files. The samples had a relatively uniform depth of sequencing.

5.3.2 Transcriptomic response of Zn efficient variety (IR36) to ZnCDs treatment

The list of differentially expressed genes in IR36 variety in Zn vs control comparison is provided in the Supplementary (Appendix) files. In total, 681 genes were differentially expressed in response to ZnCDs treatment: 253 were up-regulated by IR36 variety and 428 genes were downregulated. Figure 5.2 represents highly abundant genes (n=43), selected for heatmap, based on: (1) FDR p-value < 0.05, (2) Absolute fold change > 2, and (3) Mean RKPM =>50.
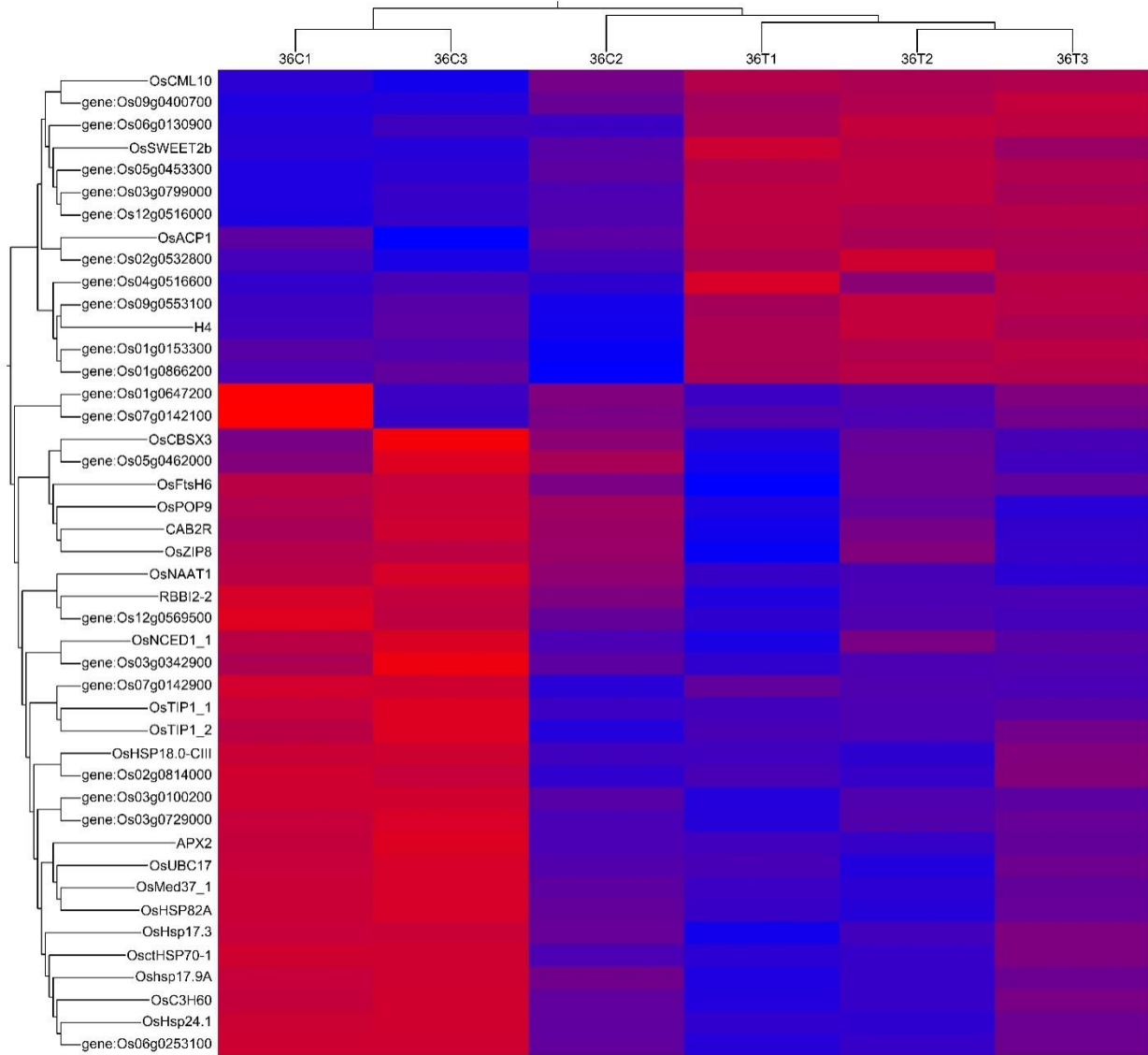
Figure 5.2: Heatmap of expression profiles of highly abundant genes (n=43) genes in Zn efficient variety (IR36) in response to Zn Carbon dots (ZnCDs). Genes were selected for heatmap based on: (1) FDR p-value < 0.05, (2) Absolute fold change > 2, and (3) Mean RKPM =>5. The counts for each gene were mean centered and scaled to unit variance.

5.3.3 Transcriptomic response of Zn inefficient variety (IR26) to ZnCDs treatment

Based on the employed criteria for the selection of differentially expressed genes, 313 genes were up-regulated genes in IR26 in response to Zn, and 41 genes were downregulated (354 differentially expressed genes in total). Highly abundant genes (n=44) are presented in figure 5.3 with FDR p-value < 0.05, Absolute fold change > 2, and (3) Mean RPM =>50.
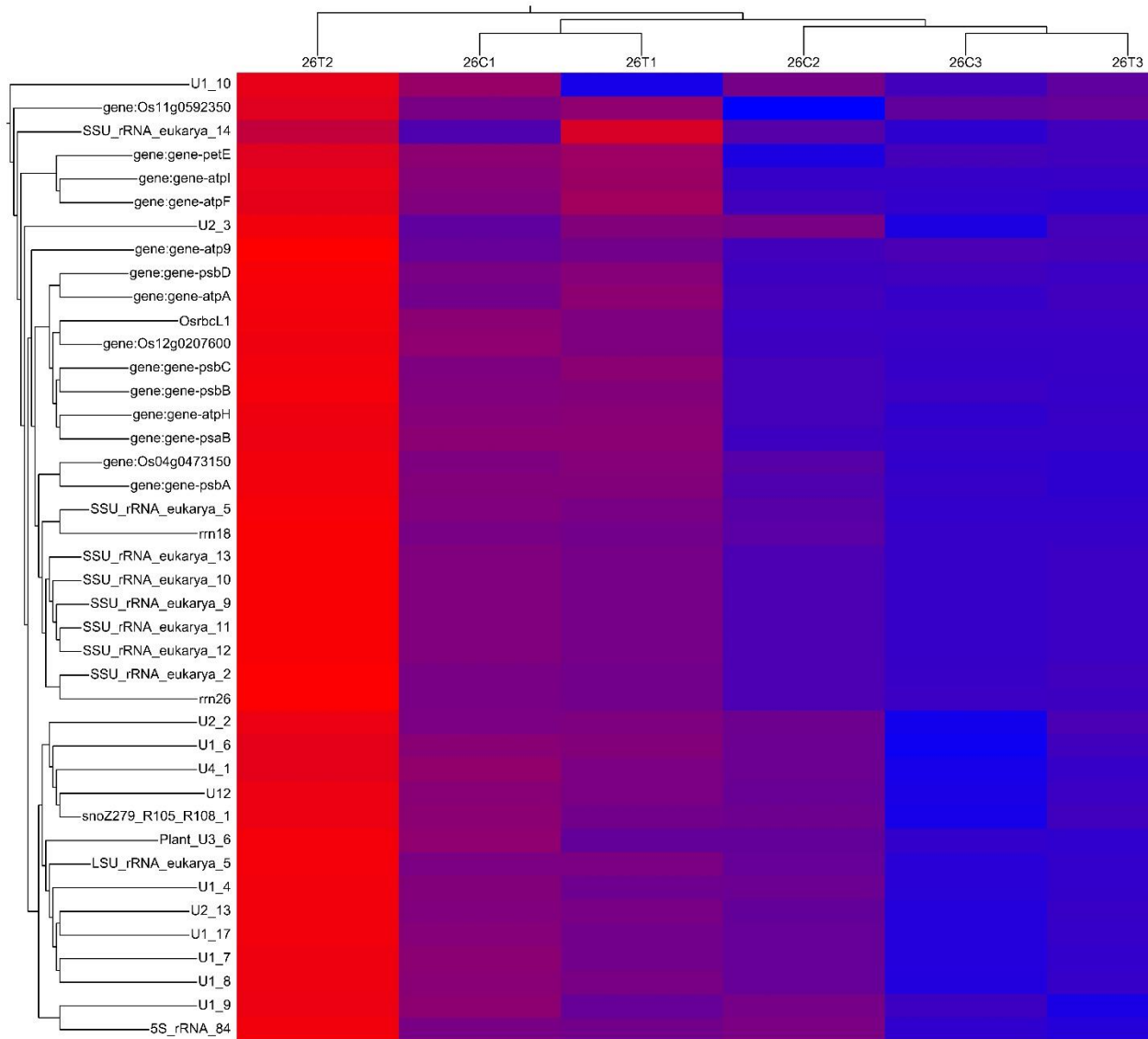
Figure 5.3: Heatmap of expression profiles of highly abundant genes (n=44) genes in Zn inefficient variety (IR26) in response to Zn Carbon dots (ZnCDs). Genes were selected for heatmap based on FDR p-value < 0.05, Absolute fold change > 2, and Mean RKPM =>5. The counts for each gene were mean centered and scaled to unit variance.

5.3.4 Genes that solely upregulated in efficient IR36 variety in response to ZnCDs

Efficient IR36 up-regulated 251 genes in response to ZnCDs that inefficient IR26 variety did not up-regulate (Figure 5.4). Supplementary (Appendix) files provide the list of those genes.
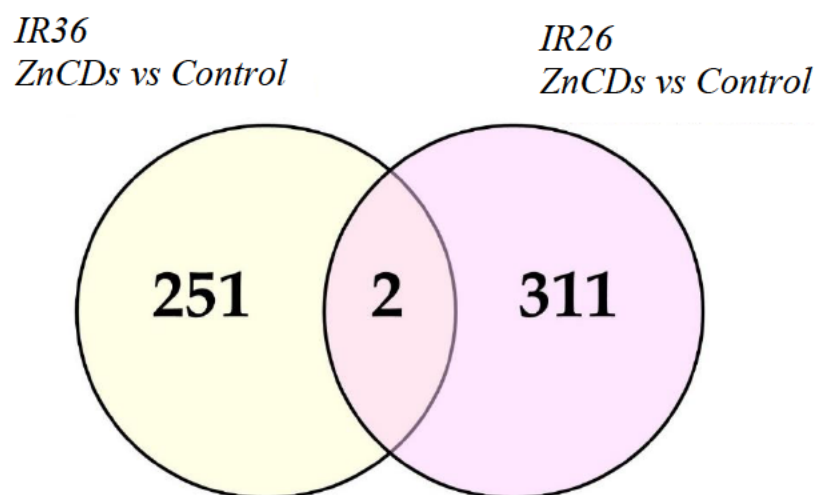
Figure 5.4: Comparative transcriptomics analysis between efficient IR36 variety and the inefficient IR26 variety in response to Zn Carbon dots (ZnCDs). IR36 solely (specifically) up-regulated 251 genes that IR26 variety did not up-regulate.

5.3.5 Genes that solely downregulated in efficient IR36 variety in response to ZnCDs

Efficient variety IR36 down regulated 421 genes in response to ZnCDs that the inefficient variety IR26 did not downregulate (Figure 5.5). The list of genes is provided in the Supplementary (Appendix) files.

IR36
ZnCDs vs Control   IR26
                          ZnCDs vs Control

421   7   34
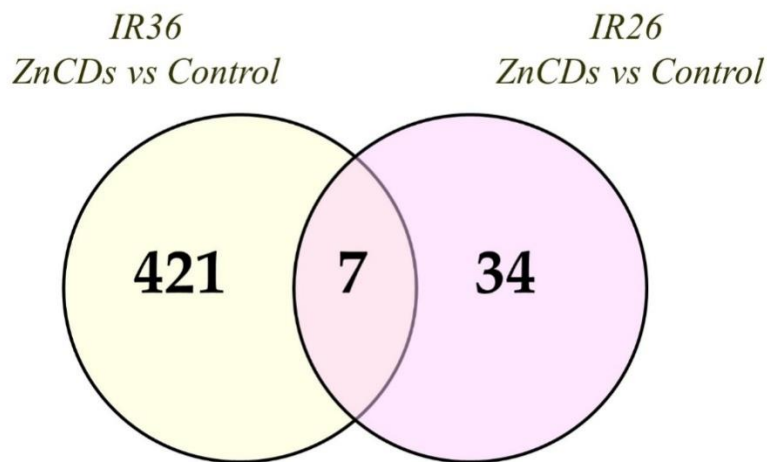
Figure 5.5: Comparative transcriptomics analysis between the efficient IR36 variety and inefficient IR26 variety in response to Zn Carbon dots (ZnCDs). IR36 solely (specifically) downregulated 251 genes that the IR26 variety did not downregulate.

5.3.6 Transcriptomic signature of high Zn efficiency in IR36 in response to ZnCDs

Principle Component Analysis (PCA) of 251 genes that were significantly up-regulated by IR36 (efficient variety) in response to ZnCDs but not in the inefficient variety of IR26, is presented in figure 5.6. PCA analysis highlights the power of the developed signature of ZnCDs efficiency.

The first PCA (PCA1) was able to describe 69.8% of variation in the data, separating IR36+ZnCDs samples from the IR26 Control, IR26+ZnCDs, and IR36 Control samples.
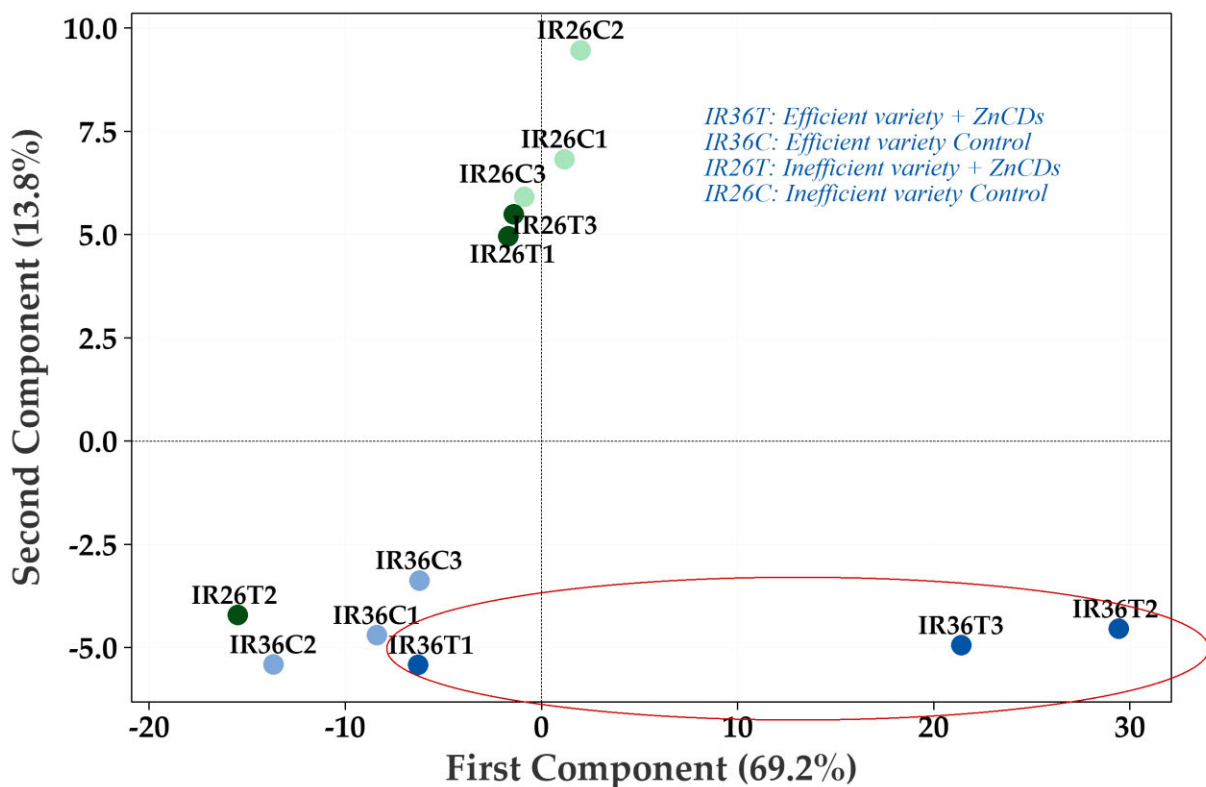
Figure 5.6:PCA plot of 251 genes that were significantly up-regulated inefficient IR36 variety in response to Zn Carbon dots (ZnCDs). PCA analysis approved the power of the developed ZnCDs efficiency signature, discriminating the IR36+ZnCDs from the rest of groups [IR 36 Control, IR26 (inefficient variety)+ZnCDs, and IR26 Control].

The top 25 genes with highest absolute coefficients in PCA1 were selected as top genes in the overall transcriptomic signature of ZnCDs efficiency, discriminating IR36+ZnCDs from the rest of groups (IR26 Control, IR26+ZnCDs, and IR36 Control) (Table 5.1), including *Os01g0723100*, *Os10g0203000*, *OsGT43G*, Os03g0116300, Os04g0523100, Os05g0453300, OsDof2, OsFbox203, OsKANADI1, OsPP2C02, and OsPP2C32.

Table 5.1: The top 25 genes with the highest absolute coefficients in PCA1 were selected as top genes in overall transcriptomic signature of the ZnCDs efficiency, discriminating IR36+ZnCDs from the rest of the groups (IR26 Control, IR26+ZnCDs, and IR36 Control)

Gene	Chr	Region	PCA analysis		IR36: ZincCDs vs Control			IR26: ZincCDs vs Control		
			PC1 coffici ent	Absolu te PCA1 value	Fold chan ge	P-val ue	FDR p-val ue	Fold chan ge	P-val ue	FDR p-val ue
Os01g0723 100	1	30155680..30157642	0.075	0.075	6.62	0.00	0.00	-1.06	0.89	1.00
Os10g0203 000	10	complement(7334820..733 8831)	0.075	0.075	3.02	0.00	0.01	-1.07	0.80	1.00
OsGT43G	10	complement(7499511..750 3453)	0.075	0.075	3.01	0.00	0.01	-1.06	0.80	1.00
Os03g0116 300	3	922684..928190	0.074	0.074	3.02	0.00	0.01	-1.11	0.63	1.00
Os04g0523 100	4	complement(26168660..26 173714)	0.074	0.074	3.93	0.00	0.01	-1.19	0.63	1.00
Os05g0453 300	5	complement(22238995..22 241632)	0.074	0.074	4.98	0.00	0.00	-1.30	0.37	1.00

Gene	Chr	Region	PCA analysis		IR36: ZincCDs vs Control			IR26: ZincCDs vs Control		
			PC1 coffici ent	Absolu te PCA1 value	Fold chan ge	P-val ue	FDR p-val ue	Fold chan ge	P-val ue	FDR p-val ue
OsDof2	2	complement(27435303..27 438545)	0.074	0.074	3.42	0.00	0.05	-1.03	0.92	1.00
OsFbox203	4	complement(18602681..18 609094)	0.074	0.074	3.21	0.00	0.03	-1.08	0.78	1.00
OsKANADI 1	2	28653055..28657883	0.074	0.074	4.12	0.00	0.02	-1.10	0.81	1.00
OsPP2C02	1	complement(10805527..10 808077)	0.074	0.074	2.77	0.00	0.01	-1.06	0.78	1.00
OsPP2C32	3	10163441..10165442	0.074	0.074	3.07	0.00	0.01	1.23	0.39	1.00
ERF3_1	1	33766984..33768044	0.073	0.073	4.41	0.00	0.00	-1.47	0.10	1.00
HSFC2A	2	7464028..7465505	0.073	0.073	3.90	0.00	0.01	-1.02	0.94	1.00
Os01g0687 300	1	28345842..28350882	0.073	0.073	3.01	0.00	0.03	-1.29	0.24	1.00
Os03g0119 900	3	1080801..1081326	0.073	0.073	8.19	0.00	0.00	-1.01	0.99	1.00
Os04g0419 550	4	20734444..20735342	0.073	0.073	4.11	0.00	0.00	-1.19	0.58	1.00

Gene	Chr	Region	PCA analysis		IR36: ZincCDs vs Control			IR26: ZincCDs vs Control		
			PC1 coffici ent	Absolu te PCA1 value	Fold chan ge	P-val ue	FDR p-val ue	Fold chan ge	P-val ue	FDR p-val ue
Os04g0669 475	4	34142529..34143723	0.073	0.073	3.85	0.00	0.00	1.03	0.92	1.00
Os07g0571 300	7	complement(23058800..23 059595)	0.073	0.073	4.93	0.00	0.00	-1.45	0.34	1.00
Os10g0463 600	10	complement(17089205..17 089666)	0.073	0.073	7.51	0.00	0.00	-1.61	0.41	1.00
Os11g0120 300	11	complement(896134..8972 60)	0.073	0.073	3.90	0.00	0.01	-1.06	0.87	1.00
OsEXO70F X1	5	17779880..17781705	0.073	0.073	3.59	0.00	0.01	-1.11	0.78	1.00
OsFbox127	3	942736..944993	0.073	0.073	3.83	0.00	0.01	1.29	0.47	1.00
OsMC8	3	complement(15567899..15 572135)	0.073	0.073	3.10	0.00	0.02	-1.12	0.74	1.00
OsSCR1	11	1119746..1123350	0.073	0.073	2.47	0.00	0.02	-1.21	0.47	1.00
OsSRO1c	3	6895178..6898355	0.073	0.073	5.56	0.00	0.00	-1.12	0.76	1.00

5.3.7 Computational systems biology analysis of genes that specifically expressed in IR36 in response to ZnCDs

Computational systems biology analysis of IR36 ZnCDs specific genes, genes that were differentially expressed in IR36 variety in response to ZnCDs, but were absent in IR26 (the inefficient variety), was performed based on: Gene Ontology (GO) enrichment, KEGG enrichment analysis, protein domain enrichment analysis, and network analysis. A complete list of statistically significant pathways and functions in enrichment analyses are provided in the Supplementary (Appendix) files.

5.3.8 GO enrichment

GO enrichment of specific IR36 differentially expressed genes in response to ZnCDs [(IR36 variety: ZnCDs vs Control) vs (IR26: ZnCDs vs Control)] showed that these genes are significantly ($p<0.05$) involved in key functions such as response to abiotic stimulus, protein folding, and unfolded protein binding.

Table5.2: Gene ontology enrichment of ZnCDs specific genes in the IR36 efficient variety, genes that were differentially expressed in IR36 variety in response to ZnCDs, but were absent in IR26 (the inefficient variety).

Biological Processes					
Term ID	Term description	Observed gene count	Background gene count	Strength	False discovery rate
GO:0009408	Response to heat	22	187	0.97	1.64E-10
GO:0009266	Response to temperature stimulus	25	380	0.72	2.24E-07
GO:0009628	Response to abiotic stimulus	45	1187	0.48	3.21E-07
GO:0006457	Protein folding	17	260	0.71	0.00013
GO:0034605	Cellular response to heat	7	60	0.97	0.0232
GO:0006950	Response to stress	65	3059	0.23	0.0307
GO:0061408	Positive regulation of transcription from RNA polymerase ii promoter in response to heat stress	5	25	1.2	0.0307
GO:0050896	Response to stimulus	96	5169	0.17	0.0445

Molecular Function					
Term ID	Term description	Observed gene count	Background gene count	Strength	False discovery rate
GO:0031072	Heat shock protein binding	11	98	0.95	0.00029
GO:0051879	Hsp90 protein binding	6	19	1.4	0.00059
GO:0051082	Unfolded protein binding	12	164	0.76	0.0018
GO:0051087	Chaperone binding	7	58	0.98	0.0094

5.3.9 KEGG enrichment

KEGG enrichment analysis highlighted that the specific ZnCDs-responding genes in the IR36 variety significantly ($p<0.05$) enriched pathways such as protein processing in the endoplasmic reticulum and Legionellosis (Table 5.3, Figure 5.7, Figure 5.8).

Table 5.3: KEGG enrichment analysis of ZnCDs specific genes in IR36 efficient variety, genes that were differentially expressed in IR36 variety in response to ZnCDs but were absent in IR26 (inefficient variety).

KEEG enrichment analysis					
Term ID	Term description	Observed gene count	Background gene count	Strength	False discovery rate
map04141	Protein processing in endoplasmic reticulum	20	395	0.6	0.0000559
map05134	Legionellosis	5	27	1.17	0.0035
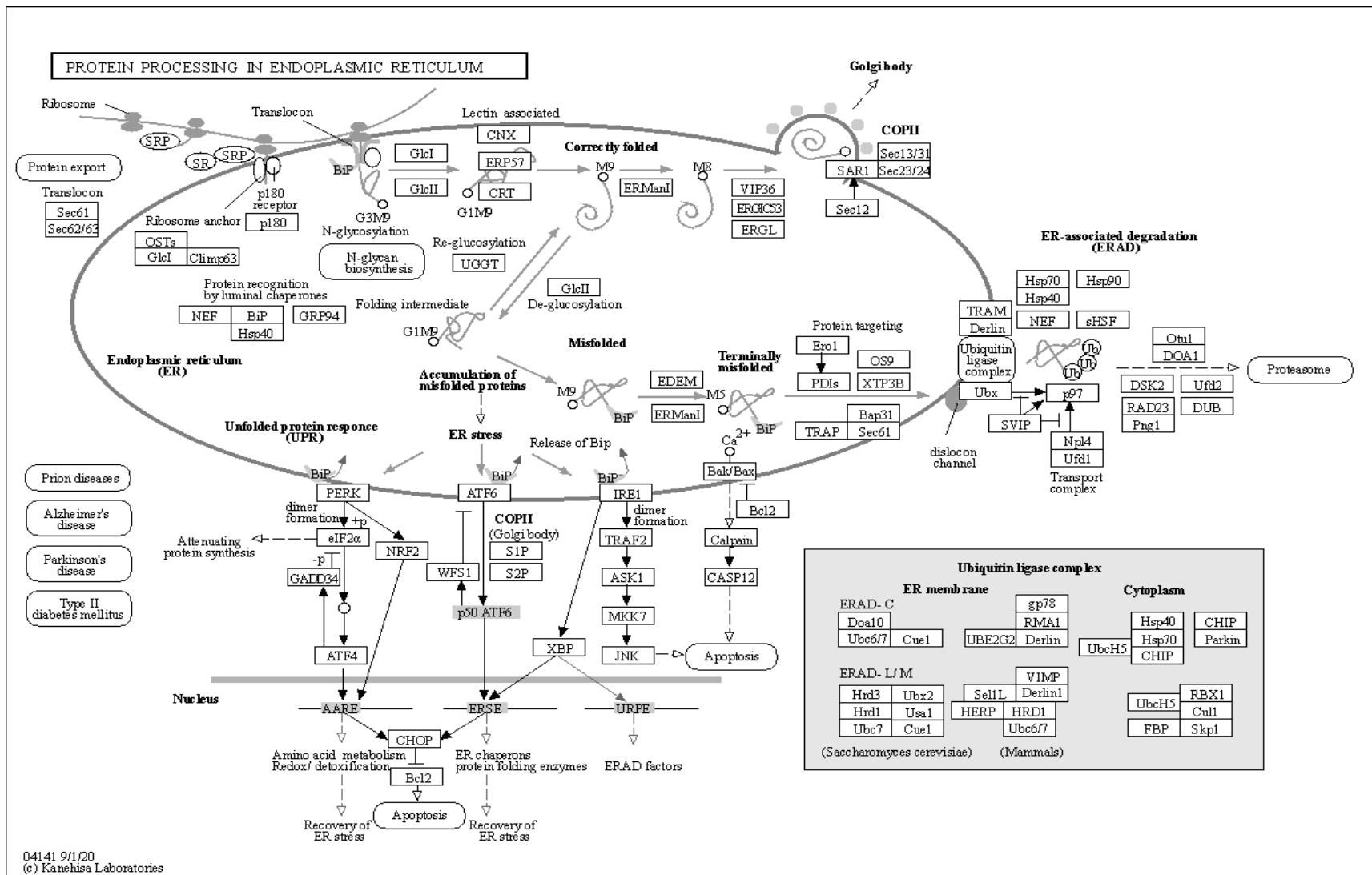
Figure 5.7: "Protein processing in endoplasmic reticulum" pathway is significantly ($p<0.05$) enriched by the specific Zn Carbon dots (ZnCDs) responding genes in IR36 efficient variety.
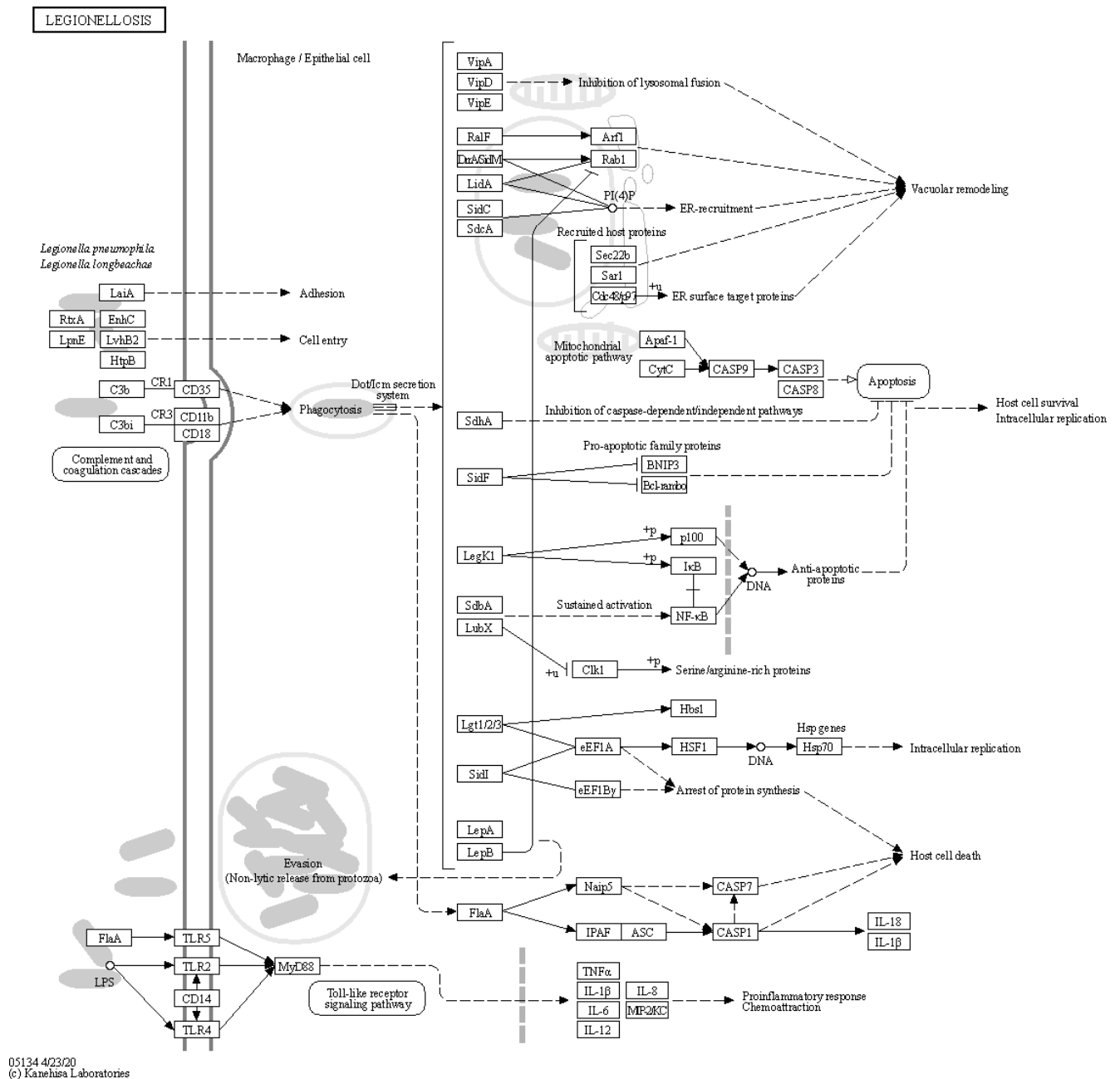
Figure 5.8: "Legionellosis" pathway is significantly (p<0.05) enriched by the specific Zn Carbon dots (ZnCDs) responding genes in IR36 efficient variety.

5.3.10 Protein domain enrichment analysis

Protein domain enrichment analysis of 251 genes that specifically up-regulated in efficient IR36 variety in response to ZnCDs, not in inefficient IR26 variety, demonstrated the significance ($p < 0.05$) enrichment of Histone H2A/H2B/H3 domains in proteomics pool after translation of genes (Table 5.4). The analysis was performed based on the two main databases of protein domains :Pfam and InterPro.

Table 5.4: Protein domain enrichment analysis of 251 genes that specifically up-regulated in efficient IR36 variety in response to ZnCDs. The analysis was performed using both Pfam and InterPro databases.

Pfam Protein domain					
Term ID	**Term description**	**Observed gene count**	**Background gene count**	**Strength**	**False discovery rate**
PF00125	Core histone H2A/H2B/H3/H4	5	47	1.39	8.80E-03
InterPro. Protein domain					
Term ID	**Term description**	**Observed gene count**	**Background gene count**	**Strength**	**False discovery rate**
IPR007125	Histone H2A/H2B/H3	5	38	1.48	0.0065
IPR009072	Histone-fold	6	85	1.21	0.008

5.3.11 *Zn uptake pathway*

Expression of 10 genes involved in the Zn uptake pathway were compared following application of ZnCDs in both IR36 and IR26 varieties (Figure 5.9). *OsZIP7*, *OsZIP2*, *OsDMAS1*, *OsNAAT1*, and *OsZIP8* showed a high level of expression in samples (Figure 5.9). The *OsZIP7*, *OsZIP8*, and *OsNAAT1*showed significant downregulation in IR36 efficient variety providing the ZnCDs.
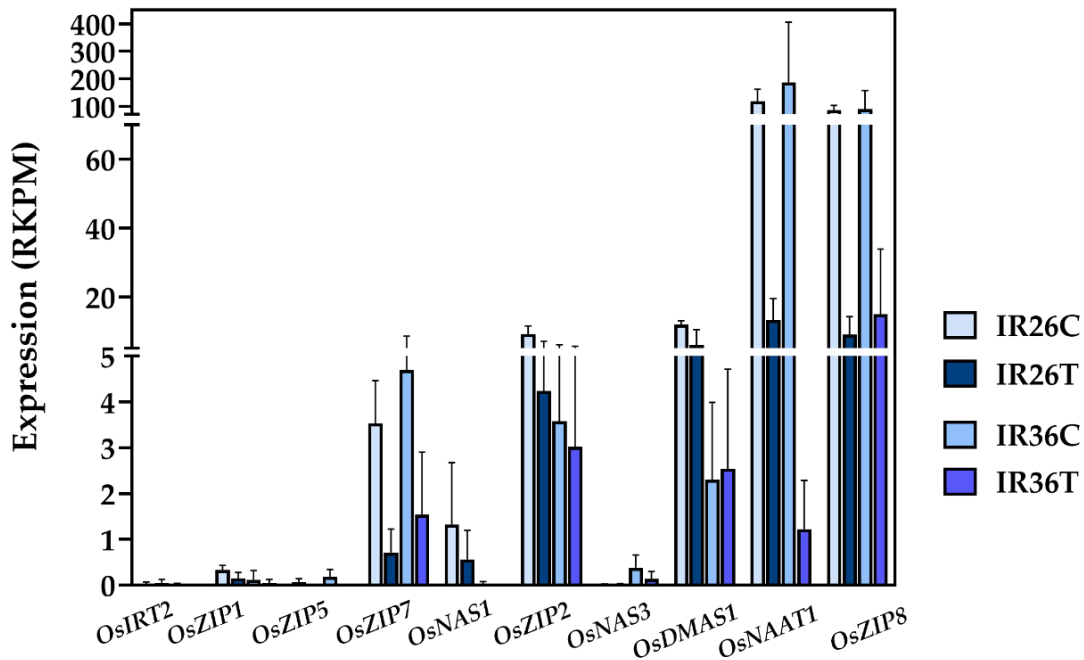
Figure 5.9: Expression of genes involved in Zn update pathway following application of Zn Carbon dots (ZnCDs) in both IR36 and IR26 varieties.IR36T: IR36+ ZnCDs, IR36C: IR36 Control, IR26T: IR26+ ZnCDs, IR26C: IR26 Control.

*OsDMAS1*has overall lower level of expression in the IR36 variety against IR26 (Figure 5.10). After ZnCDs treatment, *OsDMAS1* significantly dropped in IR26. However, its expression remained relatively unchanged in the IR26 variety.
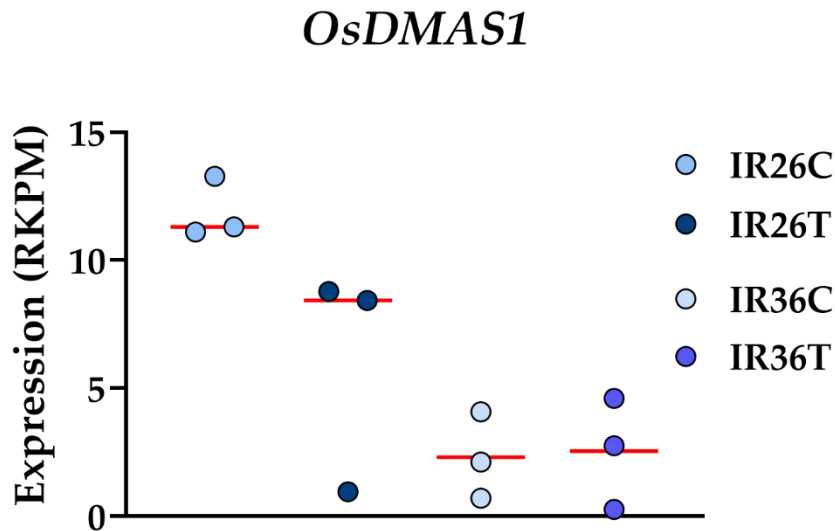
Figure 5.10: Expression profile of *OsDMAS1* in response to Zn Carbon dots (ZnCDs) in both IR36 and IR26 varieties.IR36T: IR36+ ZnCDs, IR36C: IR36 Control, IR26T: IR26+ ZnCDs, IR26C: IR26 Control.

The PCA analysis of 10 genes in Zn uptake pathway is presented in Figure 5.11. PCA analysis of Zn uptake shows the power of the developed signature in separation of IR26 control samples where, PCA1 and PCA2 account for 79.3% of variation in data. PCA1 separates control from ZnCDs treatment. PCA2 separates the IR26 variety from the IR36 variety. PCA2 discriminates most of (5 out of 6) IR26 samples from IR36 samples. It can be concluded

that the Zn uptake pathway is one of the main pathways that discriminates the IR36 efficient variety from the IR26 inefficient variety.

The top gene in PCA2, according to the coefficient, is *OsDMAS*1 which also has a good coefficient in PCA1. *OsZIP8* is important in PCA1, in separation of ZnCDs treatment from control (responding to ZnCDs in both efficient and non-efficient) variety, but not in PCA 2 in separating the IR26 variety from IR36 variety.

In contrast, *OsZIP1*, OsZIP2, OsZIP5, OsZIP7 seem to be important in both PCAs (PCA1 and PCA2).OsZIP2 had high expression in IR26 samples (Figure 5.9); however, its expression decreased in the other groups (IR26T, IR36C, and IR36T).
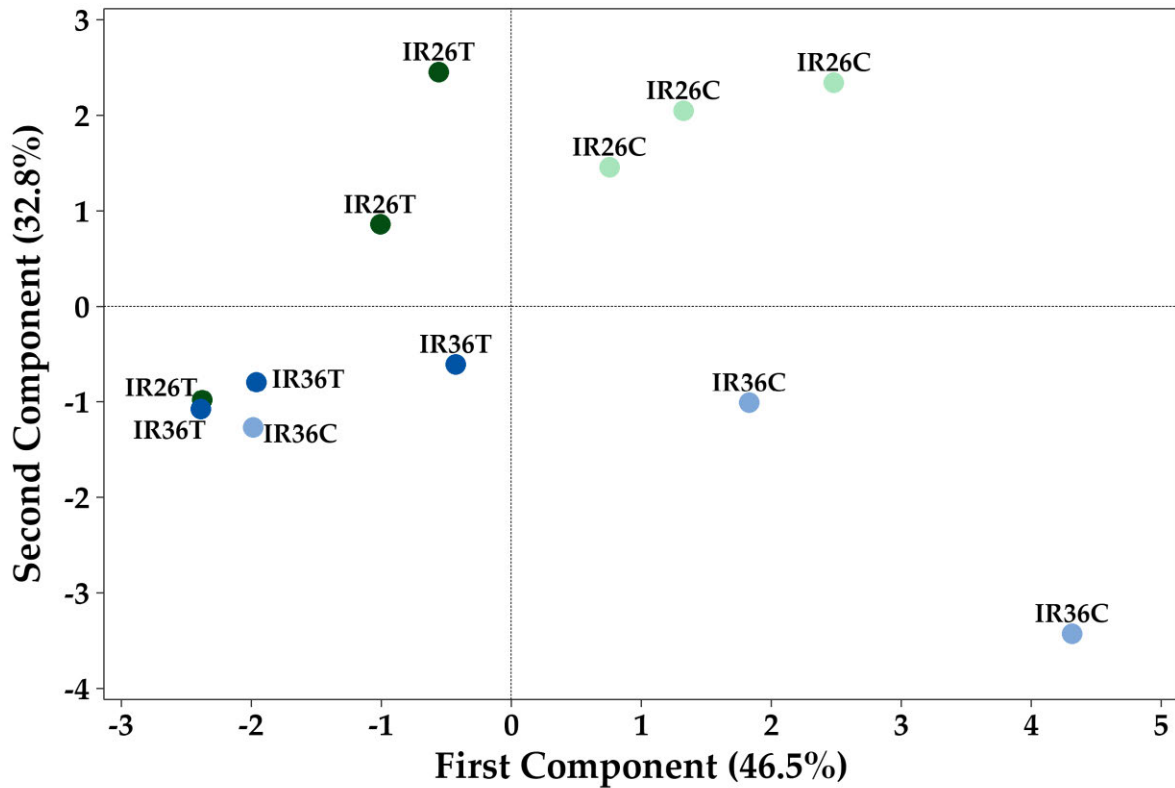
Figure 5.11. PCA plot of 10 genes in the Zn uptake pathway. PCA2 efficiently discriminates most of (5 out of 6) IR26 samples from IR36 samples.IR36T: IR36+ ZnCDs, IR36C: IR36 Control, IR26T: IR26+ ZnCDs, IR26C: IR26 Control.

5.3.12 Grain filling pathway

The expression profile of 5 genes of grain filling pathway following application of ZnCDs in IR36 and IR26 varieties is visualised in Figure 5.12. *OsSUT1* and *OsSUT2 is* significantly up-regulated in IR36 efficient variety in response to ZnCDs.
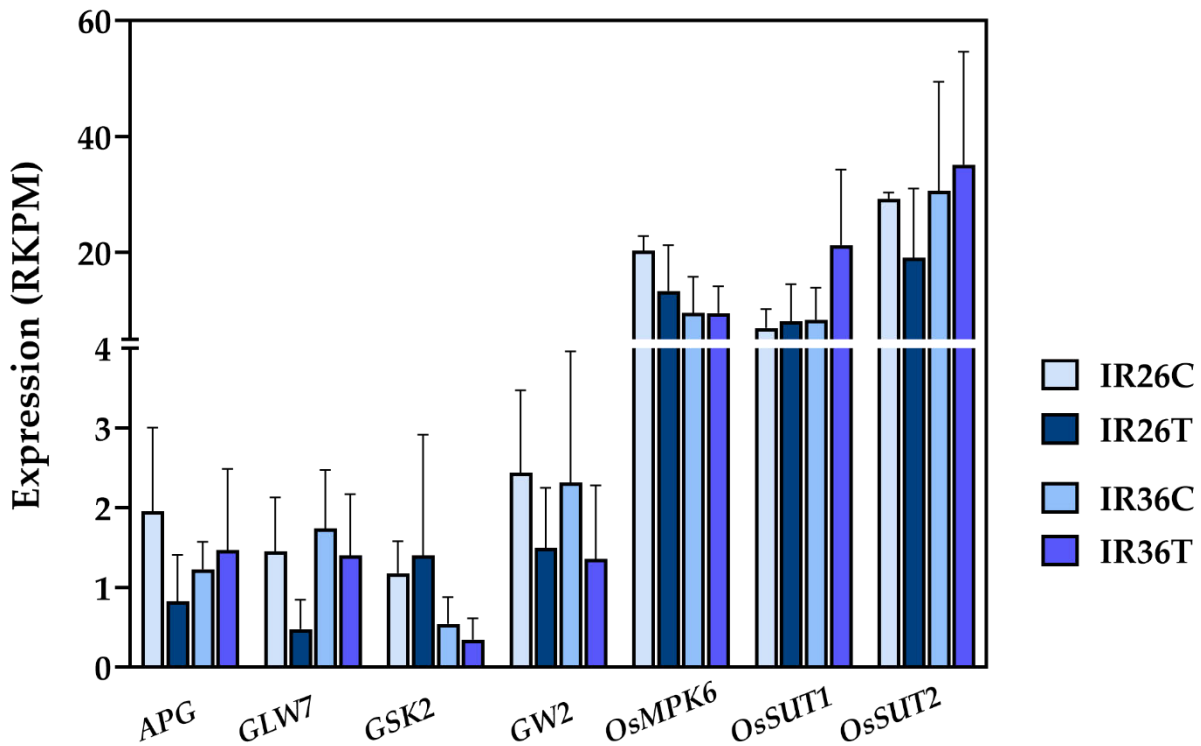
Figure 5.12: Expression of genes in grain filling pathway following application of Zn Carbon dots (ZnCDs) in both IR36 and IR26 varieties.

PCA plot of 7 genes in grain filling pathway is illustrated in Figure 5.13. PCA2 efficiently separates the IR26 genotype from the IR36 genotype. PCA analysis of 7 genes in grain filling shows the power of the developed signature in separation of the IR26 variety from the IR36 where all IR36 samples have negative values of PCA2 and all IR26 samples have positive values. PCA1 and PCA2 describe 79.3% of variation in the data. PCA2 separates the IR26 variety from the IR36 variety.
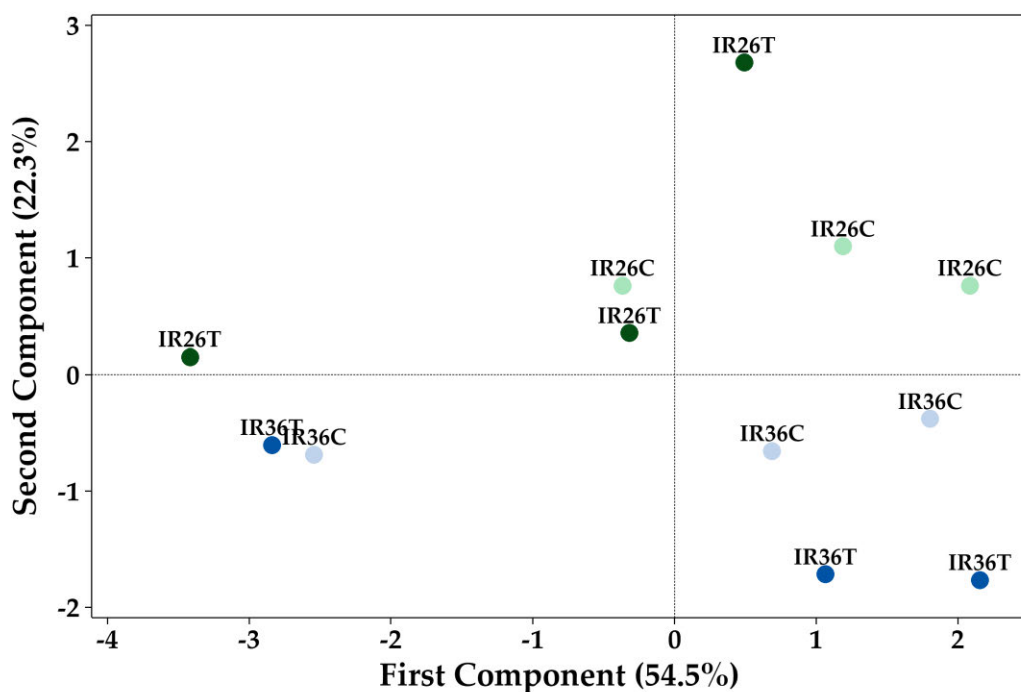
Figure 5.13: PCA plot of 5 genes in the grain filling pathway. PCA2 efficiently separates the IR26 genotype from the IR36 genotype. IR36T: IR36+ ZnCDs, IR36C: IR36 Control, IR26T: IR26+ ZnCDs, IR26C: IR26 Control.

5.3.13 Auxin signaling

Figure 5.14 presents the expression profile of 10 genes in the auxin signaling pathway in response to ZnCDs in IR36 and IR26 varieties. *OsARF16* and *OsARF10_1 are* significantly up-regulated in the IR36 efficient variety in response to ZnCDs (Figure 5.15 and Figure 5.16, respectively). PCA analysis provided in Figure 5.17 differentiates the IR26 genotype from the IR36.

PCA analysis of 10 genes of the Auxin signaling pathway shows the power of the developed signature in overall separation of IR26 from IR36 where PCA2 values of all of 12 samples of IR26 are positive and PCA2 values 5 out of 6 IR36 samples () are negative. PCA1 and PCA2 together describe 84.6% of

variation in data. Altogether, auxin signaling was one of the main pathways differentiating the IR26 variety from IR36. The top genes in PCA2, possibly involved in separation of IR26 from IR36, according to the received coefficients in PCA analysis were *OsARF10_1* and *OsARF16* (Figure 5.15 & Figure 5.16).
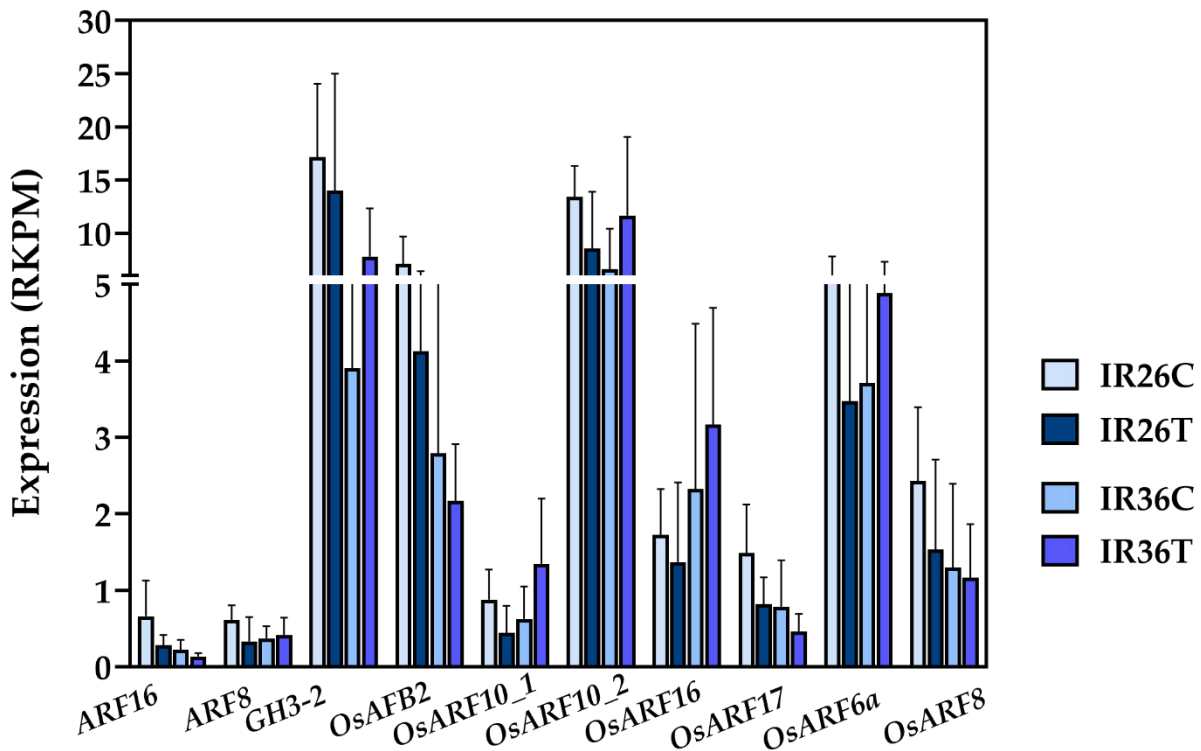
Figure 5.14: Expression of genes in the auxin signaling pathway following application of Zn Carbon dots (ZnCDs) in both IR36 and IR26 varieties. IR36T: IR36+ ZnCDs, IR36C: IR36 Control, IR26T: IR26+ ZnCDs, IR26C: IR26 Control.
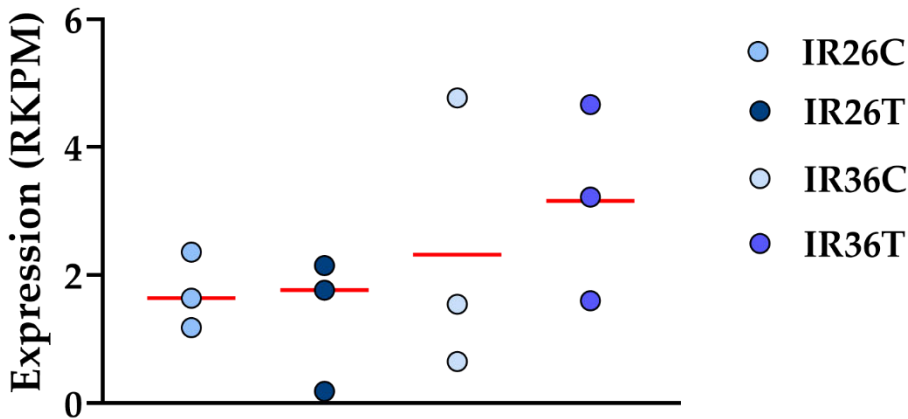
Figure 5.15: Expression profile of *OsARF16* in response to Zn Carbon dots (ZnCDs) in both IR36 and IR26 varieties. IR36T: IR36+ ZnCDs, IR36C: IR36 Control, IR26T: IR26+ ZnCDs, IR26C: IR26 Control.
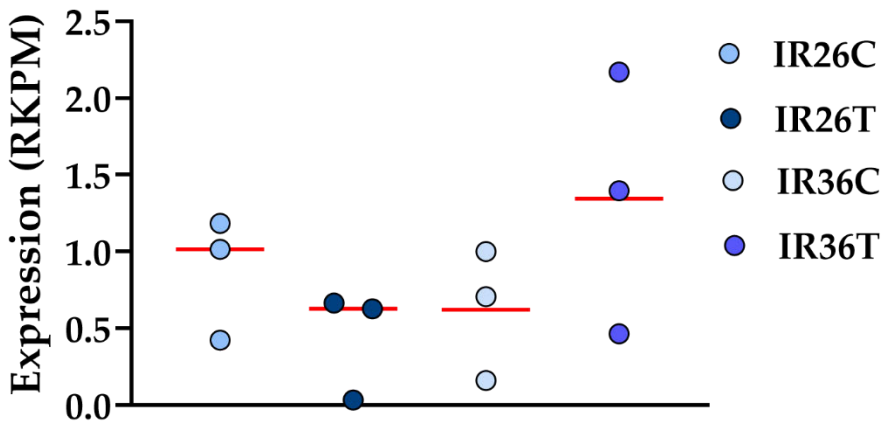
Figure 5.16: Expression profile of *OsARF10_1* in response to Zn Carbon dots (ZnCDs) in both IR36 and IR26 varieties. IR36T: IR36+ ZnCDs, IR36C: IR36 Control, IR26T: IR26+ ZnCDs, IR26C: IR26 Control.
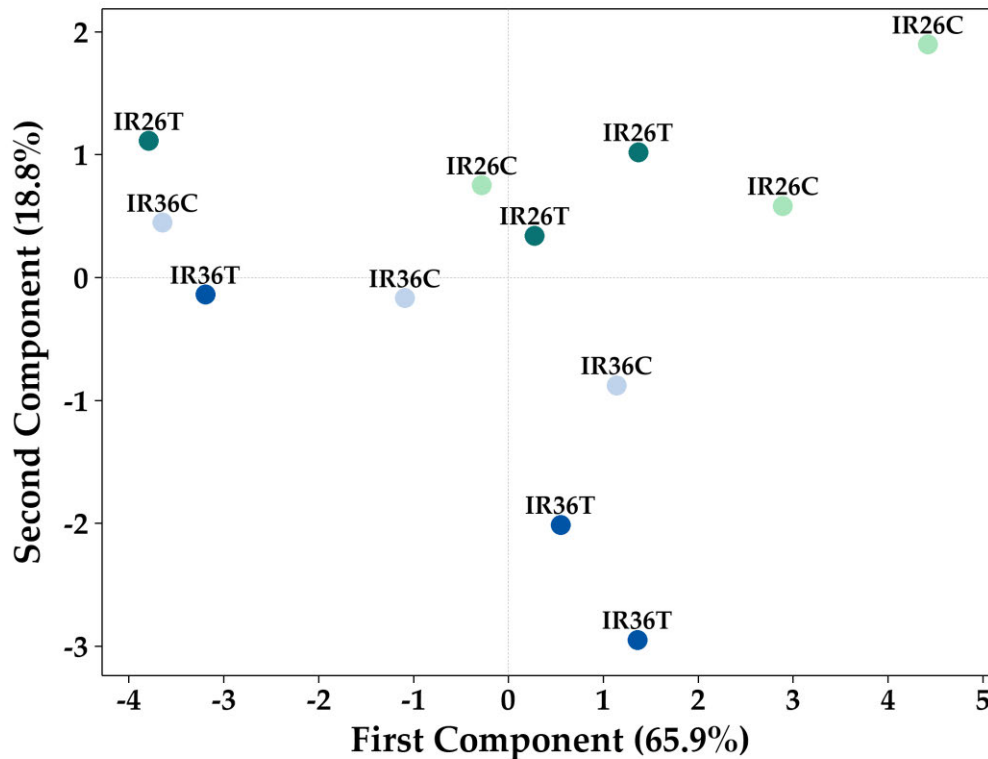
Figure 5.17: PCA plot of Auxin signaling pathway. IR36T: IR36+ ZnCDs, IR36C: IR36 Control, IR26T: IR26+ ZnCDs, IR26C: IR26 Control.

5.3.14 Abiotic stress signaling

PCAplot of the Abiotic stress signaling pathway is presented in Figure 5.18. *OsbZIP72* had upregulation in response to ZnCDs in IR36 which is svisualised in Figure 5.19. PCA analysis of 24 genes in the Abiotic stress signaling pathway showed that PCA1 and PCA2 describe 67.9% of variation in the data. The Abiotic stress signaling pathway data was not successful in separating groups from each other.

OsbZIP72 (Figure 5.19) has different trends in IR26 and IR36. In IR26, its expression decreases after ZnCDs treatment. However, in IR36, its expression increases after ZnCDs treatment.
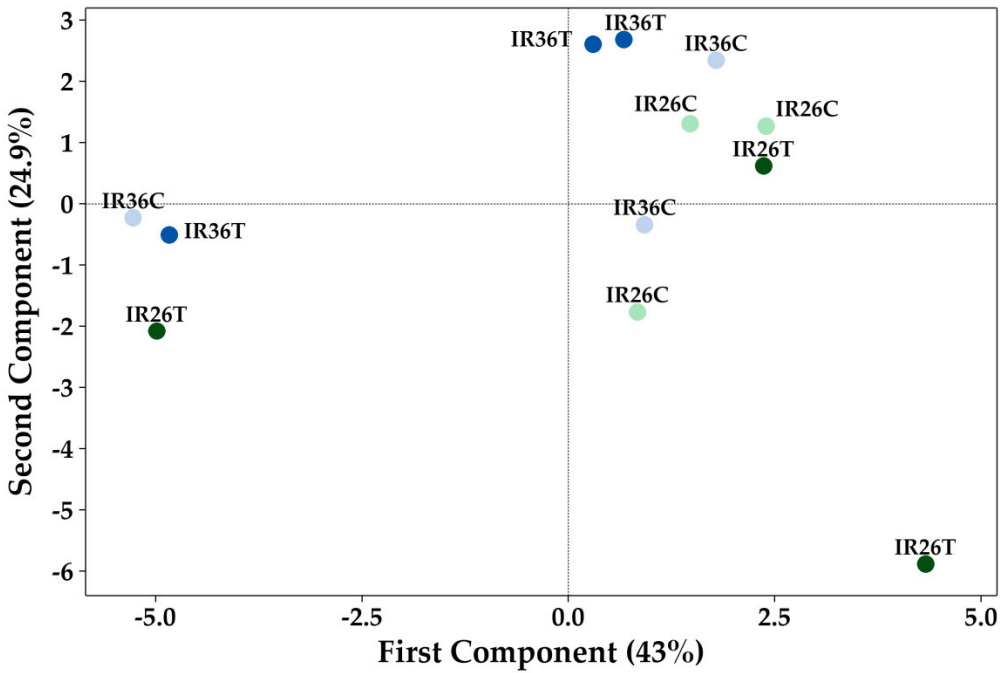
Figure 5.18: PCA plot of Abiotic stress signaling pathway. IR36T: IR36+ ZnCDs, IR36C: IR36 Control, IR26T: IR26+ ZnCDs, IR26C: IR26 Control.

OsbZIP72
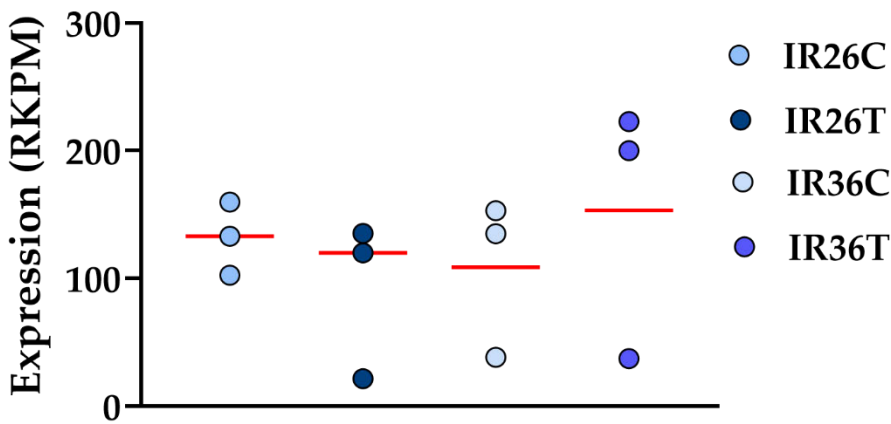
Figure 5.19: Expression profile of *OsbZIP72* in response to Zn Carbon dots (ZnCDs) in both IR36 and IR26 varieties.IR36T: IR36+ ZnCDs, IR36C: IR36 Control, IR26T: IR26+ ZnCDs, IR26C: IR26 Control.

5.3.15 Comparison of discrimination power of selected RNA-seq pathways by PCA

Table 5.5 compares the Eigenvalues of PCA analysis in the studied pathways and their discriminating powers in respect to variety and ZnCDs treatment.

Table 5.5: Comparing Eigenvalues of PCA analysis in the studied pathways.

Pathway	PCA 1 (%)	PCA 2 (%)	PCA1+PCA2 (%)	Best discriminated group
Zn uptake	46.5	32.8	79.3	IR26C
Auxin signaling	65.9	18.8	84.6	IR26 from IR36
Abiotic stress signaling	43	24.9	67.9	Not able to separate either groups, treatments, or varieties
Grain filling	54.5	22.3	76.8	IR26 from IR36
Senescence	65.7	20.4	86.1	IR26 from IR36

5.4 Discussion

NPs has opened a new avenue in increasing nutritional quality of cereals, as potential nano-fertilisers (Deng et al., 2022). Zinc (Zn) deficiency is a major health concern worldwide, and increasing the grain Zn content in cereals, particularly in wheat and rice, is of high importance (Nakandalage et al., 2016, Perera et al., 2019, Kamaral et al., 2022). However, little information is available regarding the impact of Zn nanoparticles in rice, particularly in different genotypes.

Comparative transcriptomic analysis of Zn efficient rice variety (IR36) against inefficient variety (IR26) against ZnCDs was performed to shed light on underpinning reasons of high Zn efficiency in rice and their differential response to ZnCDs. Identifying the significant GOs and pathways groups (based on Fisher Exact test) and selection of genes based on the significant GOs/pathways are robust strategies in transcriptomic analysis and selection of genes that are central in meaningful biological events (Ebrahimie et al., 2015). Furthermore, in this study, multivariate analysis was employed with the power of the transcriptomic signature in efficient discrimination of Zn treated efficient variety. Altogether, Zn-responding specific genes in efficient variety were involved in key functions such as response to abiotic stimulus, and protein processing in endoplasmic reticulum. An interesting finding was the enrichment of genes with histone H2A/H2B/H3 domains by genes that specifically were up-regulated in response to Zn by the IR36 efficient variety.Domain enrichment analysis of differentially expressed genes in RNA-Seq analysis has been recently employed in understanding of wheat leaf rust feature between resistant and susceptible Aegilops accessions to wheat leaf rust(Dorostkar et al., 2022).

Functional genomics tools were employed in this study to examine the underlying molecular mechanisms of better response of IR36 to ZnCDs,

compared to IR26.Identifying the key GO groups and selection of genes based on the significant GOs are novel and reliable approaches in gene discovery as the selected genes are central in meaningful biological processes (Ebrahimie et al., 2015). Additionally, comparing of GO enrichment of a given sample versus GO distribution of whole genome (as reference) using Fisher exact test (hyper-geometry approach) identified the key differential functional groups.

Zn uptake, grain filling, auxin signaling, and abiotic stress signaling were the main pathways that governed higher efficiency of IR36 in utilizing ZnCD, compared to IR26. PCA-based gene selection led us to the genes such as *OsDMAS1* and *OsbZIP72* in the above-mentioned pathways. KEGG enrichment analysis highlighted the significance of protein processing in endoplasmic reticulum and Legionellosis.

The low number of replications in each studied group is a limitation of this study. Increasing the number of replications in future experiments will contribute to higher confidence and a stronger experiment. The transcriptomic analysis was performed at the gene level. Alternative splicing is an important event in transcriptome response (Panahi et al., 2014, Panahi et al., 2015, Ebrahimie et al., 2021). Further analysis of sequencing data at the transcript level (transcript-based mapping and expression analysis) instead of gene-based mapping/expression will provide novel information on the contribution of alternative splicing in response to nano particles. The mentioned analysis can open a new avenue in research and understanding of high Zn efficiency.

The study of activated domains of expressed proteins in addition to traditional gene expression analysis led to better understanding of efficient systems biology in response to inefficient systems. The performed analysis highlighted the role of Histone H2A/H2B/H3 domains in higher ZnCDs efficiency in IR36.

5.5 Conclusion

Using RNA-Seq technology, comparative transcriptomic analysis of Zn efficient rice variety (IR36) against inefficient variety (IR26) in response to ZnCDs was performed to uncover the mechanisms involved in utilising Zn nano particles in cereals. IR36 up-regulated 251 genes in response to ZnCDs that were not up-regulated in IR26. Also, 421 genes were downregulated in response to ZnCDs in IR36 where those genes did not show downregulation in IR26. IR36-specific genes in response to ZnCDs were involved in key functions including Zn uptake, grain filling, auxin signaling, and abiotic stress signaling. This explains the higher performance of IR36 in when treated with Zn nanoparticles.

CHAPTER 6: COMPARATIVE PROTEOMICS ANALYSIS OF ZINC EFFICIENT RICE VARIETY IR36 AGAINST ZINC INEFFICIENT IR26

6.1. Introduction

There are two main challenges in increasing the nutritional contents and quality of grains: (1) efficient uptake of nutrients such as Zn from soil or leaf, and (2) transporting the absorbed Zn into the grain. If the absorbed Zn does not transfer to the grain, the absorbed Zn cannot contribute to increasing the nutritional quality of the grain.

Nanomaterial uptake, translocation and final fate depends on the plant and the properties of the NP. Carbon-based NPs and most of the metal based NPs accumulate inside the plant cells (Rico et al., 2011). The primary use of NPs in agriculture is to reduce the concentration of phytochemicals, optimise fertiliser applications and increase the yield and quality of the plant products by improving the use efficiency of nutrients (Gogos et al., 2012). A high surface area and suitable sorption properties in NPs help reduce runoff and minimize losses due to improved release kinetics (Gogos et al., 2012). Smaller NPs can pass through the pores on the cell wall and membrane while others enter via carrier proteins (transmembrane proteins which allow transportation of molecules), aquaporins (specialized channel proteins for water molecules), and ion channels (transmembrane proteins with pores specialized for ion transportation) or by endocytosis (cell uptake via engulfing and fusing with cell membrane) (Tripathi et al., 2017, Rico et al., 2011). However, Kwak et al. (2019) report that traversing subcellular organelle double lipid bilayers (in the chloroplast) is governed by NP size and surface charge employing a specific method called lipid exchange envelope penetration (LEEP) model (Wong et al., 2016, Kwak et al., 2019). Studies employing water-soluble SWCTs have shown larger NPs mainly

enter plant cells through endocytosis (Rico et al., 2011). However, information on uptake of CDs into plant cells and their fate inside the cells is limited.

The concentration of the NP also plays a critical role in uptake. In soybean, maize and wheat NP solutions such as water-soluble CDs, ZnO of low concentrations, i.e., 200 – 500 ppm, were more effective in absorption (Rico et al., 2011, Tripathi and Sarkar, 2015, Subbaiah et al., 2016). Higher concentrations of NPs tend to agglomerate, increasing their size and making it harder to traverse the membrane via pores (Rico et al., 2011). Once NPs are absorbed by the cells, they either follow a symplastic or apoplastic mechanism. Also, NPs can be transported from one cell to another through the plasmodesmata. Following integration with the apoplast of the endodermis, the vascular system serves as the main pathway for translocating NPs to primary sinks in the leaves or grains.

Uptake and translocation of NPs applied to plants has been widely studied, but the entrapment of NPs on plant surface after the foliar application has not. Using Time of Flight-Secondary Ion Mass Spectroscopy (ToF SIMS) and SEM studies, the entrapment of foliar applied Ag NPs by the cuticle of lettuce leaves has been observed (Larue et al. (2014). However, the entrapment of carbon-based NPs on the leaf cuticle has not been studied.

After the foliar application of zinc incorporated carbon dots (ZnCDs) and penetration of ZnCDs into the flag leaf, activation of transporters can contribute to Zn transport in the grain. As most of studies on nano particles (NPs) have been carried out on soil-amended NPs, knowledge of the events and activated mechanisms of foliar application of CDs and ZnCDs in rice is very limited. The previous studies suggest that exposure to different types and doses of NPs can lead to different types of changes in proteome and protein expression profiles. To clarify the effect of ZnCDs in cereal systems biology, it is important to carry out protein expression studies and a proteomic analysis following NP application to the rice plants are required.

Proteome profiling in response to foliar application of ZnCDs is important to understand the activated mechanism and functional genomics changes after foliar application of ZnCDs. Proteomics profiling can also catalogue the transportation pathways of the absorbed CDs into the plant system. Comparative proteomics profiling of Zn efficient (IR36) and inefficient (IR26) will provide genotype effect on response to ZnCDs.

In this study, we compare the proteomic analysis of the Zn efficient rice variety (IR36) with the Zn inefficient variety (IR26) to determine potential mechanisms involved in high Zn efficiency in rice and their differential response to ZnCDs.

Proteome analysis is an essential step in understanding the molecular mechanism of response to Zn and its nano carrier (Muvunyi et al., 2022, Bandyopadhyay et al., 2017, He et al., 2015). However, most of the previous studies have focused on the response of one type of genotype against Zn stress or Zn deficiency (Song et al., 2014, Zeng et al., 2019, Song et al., 2021), rather than proteomic comparison of genotypes with different levels of Zn uptake and metabolism. Therefore, this study has been carried out to determine the proteomic changes in two different rice varieties with different Zn use efficiencies in response to Zn incorporated carbon dot application.

6.1.1. The goals of this chapter

The goal of this chapter was to discover a proteomic signature of response to Zn-bound carbon nanodots (ZnCDs) in a Zn efficient variety (IR36), compared to a Zn inefficient variety (IR26). Identifying the critical molecular pathways and mechanisms, involved in higher Zn efficiency and response to nano particles, by computational systems biology analysis was the second goal of this chapter.

6.2. Material and methods

6.2.1. Plant material, sampling, zinc treatment, and Protein extraction

Two rice varieties with different Zn use efficiency; IR36 (Zn efficient) and IR26 (Zn inefficient) were used. The experiment was conducted under glasshouse conditions with a randomized complete block design with 3 replicates from September 2020 to February 2021. The maximum and the minimum temperatures were between 25 °C and 22 °C.

Rice plants were grown in low Zn (0.1×10^{-3} mM) sand culture nutrient medium until maturity as described in chapter 3. At the heading stage of rice plants were sprayed with two (02) treatments namely, ZnCD 500 ppm and untreated control. To spray the plants with ZnCD solution and control, a Paasche sprayer was used as described in chapter 3.

Ten days after treatment (Wang et al., 2012) flag leaves were collected from the main tiller of all three replicates. Soon after the sampling they were placed in storage tubes and were frozen in liquid nitrogen. Samples were then stored at -80 °C until total soluble protein extraction.

6.2.2. Total protein extraction

To extract of total proteins from flag leaves of the rice plants, 250 mg of the leaf tissue was ground into a fine powder using liquid nitrogen while maintaining the samples close to frozen. Total soluble proteins were extracted from the ground leaf sample using the "Plant Total Protein Extraction Kit (PE0230-1KT; Sigma-Aldrich)". Quality of the extracted proteins were checked using DS-11 Series Spectrophotometer/Fluorometer (DeNovix, USA).

6.2.3. Rubisco precipitation and protein purification

Total soluble proteins extracted from leaf samples contain a large amount of Rubisco which tends to hamper the detection of other important low abundant proteins in the sample (Gupta and Kim, 2015). As we were focused on all the critical signalling and regulatory proteins in the samples which may be low in abundance, the Rubisco factor was depleted from the sample as suggested by Gupta and Kim (2015). Protamine sulphate solution (1%) was added to the supernatant fraction of the total soluble proteins to a final concentration of 0.1%. The mix was incubated in ice for 30 minutes allowing Rubisco to precipitate. The sample was centrifuged at 12,000 g for 5 min at 4 °C to pellet the precipitated Rubisco. The supernatant was transferred to a clean eppendorf tube. Samples were further purified using Zeba™ Spin Desalting Columns, (7K MWCO; Thermo scientific) as per the manufacturer's instructions.

6.2.4. Protein precipitation

To precipitate proteins, 100 µl of a soluble protein fraction was mixed with 400 µl of methanol and mixed thoroughly. The sample was centrifuged for 10 S at 9000 g. A hundred µl of chloroform was added to 100 µl of protein samples and centrifuged for 10 S at 9000 g. Next, 300 µl of double distilled water was mixed thoroughly to the 100 µl of protein samples. Sample was centrifuged again for 1 min at 9000 g. Following this centrifugation step, 3 clear phases were formed (upper H_2O-Met phase, protein interphase, lower chloroform phase). The upper phase was carefully removed without disturbing or touching the protein interphase and 300 µl of Methanol was added to the remaining phases. The sample was mixed thoroughly and centrifuged for 2 min at 9000 g to pellet the proteins. The supernatant was removed carefully, and the pellet was dried until no chloroform smell was

detected. The pelleted proteins were stored at room temperature until they were used in the mass spectrometry protein analysis.

6.2.5. Leaf proteome analysis

Leaf proteome analysis was carried out at La Trobe University-Comprehensive Proteomics Platform (LTU-CPP), La Trobe Institute for Molecular Science (LIMS), La Trobe University, Melbourne, Australia. The analysis was carried out using liquid chromatography-mass spectrometry (LC252 MS/MS) as described in Lowe et al. (2015).

6.2.6. Sample preparation: Reduction, alkylation, proteolysis and sample clean-up

A hundred µl of urea (8 M urea, 25 mM Tris-HCl, pH=8.0) was used to resuspend each protein sample (50 µg). Next, the disulphide bonds of the samples were reduced for 60 minutes by the addition of TCEP (tris 2-carboxyethyl phosphine) to 2 mM. This step was followed by the alkylation of reduced thiols by adding iodoacetamide (IAA) to 38 mM at 25°C in dark for 45 mins of incubation. Twenty (20) mM of Tris-HCl was used to dilute the sample and to reduce the urea content less than 1 M. Trypsin digestion was carried out by addition of mass-spec grade trypsin/Lys-C mix (Promega, V507A) to a ratio of 1:50 with the original protein amount and incubated at 37°C, overnight. Desalting and concentrating of tryptic peptides were carried out using the StageTips as per the protocol described by Rappsilber et al. (2007).

6.2.7. *Protein identification by LC/MS (nanoLC-ESI-MS/MS Orbitrap Eclipse)*

Protein identification of LC/MS was carried out as per the method supplied by the La Trobe Proteomics and Metabolomics Platform as follows. "A Thermo Ultimate 3000 RSLCnano UHPLC system and a Thermo Orbitrap Eclipse Tribrid mass spectrometer (Thermo-Fisher Scientific, Waltham, MA, USA) was used to perform LC-MS for purified proteins. Peptides were reconstituted in 0.1% (v/v) trifluoroacetic acid (TFA) and 2% (v/v) acetonitrile (ACN), and 500 ng of peptides were loaded onto PepMap C18 5 μm 1 cm trapping cartridge (Thermo-Fisher Scientific, Waltham, MA, USA) at 12 μL/min for 6 min and washed for 6 min before switching the pre-column in line with the analytical column (nanoEase M/Z Peptide BEH C18 Column, 1.7 μm, 130 Å and 75 μm ID × 25 cm, Waters). Throughout the process of analysis, the column compartment was held at 55°C. The separation of peptides was performed at 250 nL/min using a linear ACN gradient of buffer A (0.1% (v/v) formic acid, 2% (v/v) ACN) and buffer B (0.1% (v/v) formic acid, 80% (v/v) ACN), starting at 14% buffer B to 35% over 90 min, then rising to 50% B over 15 min followed by 95% B in 5 min. The column was then cleaned for 5 min at 95% B and afterward a 3 min equilibration step completed at 1% B. Mass-spectra were collected on the Thermo Orbitrap Eclipse in Data Dependent Acquisition (DDA) mode on the orbitrap for MS1 and HCD MS2 spectra in the ion trap. MS1 scan parameters were: cycle time of 3 s, scan range of 375-1650 m/z, 120,000 resolution, injection time 50 ms max, AGC target 4e5, HCD collision energy 30%. Easy-IC internal mass calibration was used. MS2 spectra were collected in the ion trap on rapid mode, with an AGC target of 1e4, and a max IT of 35 ms. The isolation window of the quadrupole for the precursor was 0.8 m/z. Dynamic exclusion parameters were set as follows: exclude isotope on, duration 60 s and using the peptide monoisotopic peak determination mode, charge states of 2-7 were included".

6.2.8. Database search and quantitation

Spectra analysis was performed using the Proteome Discoverer software (version 2.4). Proteins were identified and quantified using the Sequest HT peptide search engine and the *Oryza sativa* proteome downloaded from the UniProt database. Three biological replicates were used for each of the two rice genotypes to determine the proteome response to nanoparticle application.

The protein list with label-free quantitation abundance values for each protein was exported. These values were normalised to total ion chromatogram on a per sample basis so that the distribution of abundances is roughly equivalent.

The DEP R package in Bioconductor was used in the data analysis. The data was filtered, and data imputation was done. Finally differential analysis in DEP was carried out and stored separately.

6.2.9. Plan of experiment

The variables of this study were Zn treatment [in two levels of Zn bound carbon nanodots (ZnCDs) and control] and variety two levels of Zn efficiency, Zn efficient (IR36) and Zn inefficient (IR26). In total, 12 samples were submitted for proteomics analysis (Two varieties * Two treatments * 3 replications).

6.2.10. Comparative proteomic analysis between Zn inefficient (IR26) and Zn efficient (IR36) varieties responding to ZnCDs

The employed workflow for comparative proteomic analysis included the following below steps:

1- Proteomic profiling of ZnCDs response in Zn efficient variety (IR36+ZnCDs vs IR36_control)

2- Proteomic profiling of ZnCDs response in Zn inefficient variety (IR26+ZnCDs vs IR26_control)

3- Comparative proteomic analysis: (IR36+ ZnCDs vs IR36_control) vs (IR26+Zn vs IR26_control)]. This comparison is crucial that filters the proteins that only upregulated/downregulated in IR36 in response to ZnCDs and not in IR26.

ZnCDs-responding proteins in IR36 were used for enrichment analysis, using Fisher's exact test, in the categories of Gene Ontology (GO), KEGG, Pfam and InterPro analysis.

6.2.11. Proteomic signature discovery of ZnCDs response by multivariate analysis

Feature selection (attribute weighting) using Principal Component Analysis (PCA) was used to select the proteins that can separate the ZnCDs-treated IR36 efficient variety from the rest of groups. Analysis carried out by Minitab package (www.minitab.com, Product version: 20.2).

To select the key protein biomarkers proteomic signature, each protein's coefficient (weight) gained in PCA analysis was considered. Feature selection based on the coefficients in Discriminant Function Analysis (DFA)

and Principle Component/Coordinates Analysis (PCoAAnalysis (PCA/PCoA) is extensively used for signature discovery (Mahdi et al., 2014, Yip et al., 2021, Singh et al., 2018, Shih-Yin et al., 2012).

6.2.12. Enrichment (computational systems biology) analysis

GO enrichment analysis using String and ComparativeGO was used to find significant GOs from differentially expressed proteins, as previously described (Ebrahimie et al., 2015, Ebrahimie et al., 2017, Fruzangohar et al., 2013). GO classification was performed in the main categories of biological process (BP), molecular function (MF), and cellular component (CC) (Consortium, 2019, Consortium, 2004).

The Kyoto Encyclopedia of Proteins and Genomes (KEGG) (Kanehisa and Goto, 2000) enrichment was applied to find the significant key pathways in the Zn efficient IR36 proteins in their response to ZnCDs by String web application (Mering et al., 2003). The String application employs Fisher's exact test and multiple testing correction in its analysis (Mering et al., 2003, Szklarczyk et al., 2021, Szklarczyk et al., 2016).

Protein-Protein interaction analysis was conducted using the String tool (Szklarczyk et al., 2021). A range of relations were employed for development of interaction network including phylogeny of proteins, co-expression, literation mining, and functional annotations. String is armed integrated Cytoscape for network visualisation (Szklarczyk et al., 2016).

Domain enrichment analysis of IR36 specifically up-regulated proteins, responding to ZnCDs treatment, was performed based on pfam and Interpro database.

6.2.13. Protein signature discovery using significant pathways and functions

Identifying the significant pathways, functions, and GO groups and then selecting of proteins on the basis of the significant functions/pathways/GOs are strong and robust and reliable approaches in signature discovery as the selected proteins are involved in important biological and molecular functions and processes (Ebrahimie et al., 2015). The mentioned approach was employed in this study.

6.3. Results

6.3.1. Comparative proteomics analysis between Zn efficient variety (IR36) and Zn inefficient variety (IR26) in response to ZnCDs

The list of differentially expressed proteins in IR36 and IR26 varieties in ZnCDs vs control comparison are provided as Supplementary files. In IR36, in total, 163 proteins were differentially expressed in response to ZnCDs treatment where 38 were upregulated in the IR36 variety and 125 proteins were downregulated (Figure 6.1).

As presented in Figure 6.1 the Zn efficient IR36 variety upregulated 36 proteins in response to ZnCDs that the Zn inefficient IR26 variety did not upregulate. Also, 121 proteins solely downregulated in the Zn efficient IR36 variety in response to ZnCD application that were absent in IR26 variety.
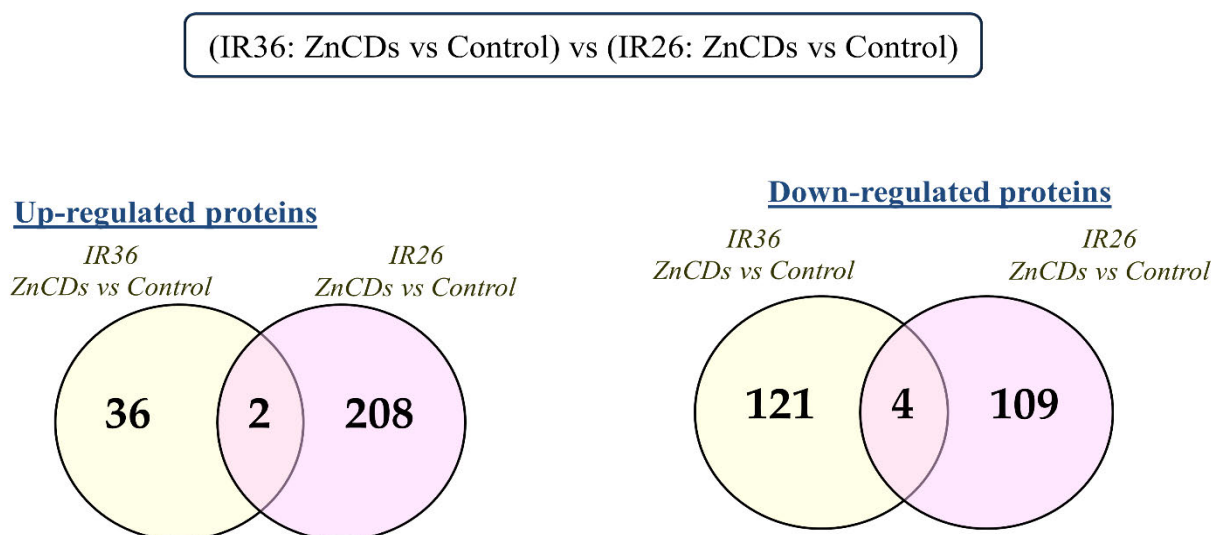
Figure 6.1: Comparative proteomics analysis between Zn efficient IR36 variety and inefficient IR26 variety in response to Zn Carbon dots (ZnCDs). IR36 solely (specifically) upregulated 36 proteins and downregulated 121 proteins that IR26 variety did not alter them.

6.3.2. Proteomic signature of high Zn efficiency in IR36 in response to ZnCDs

PCA analysis of 36 proteins that were significantly upregulated by IR36 (Zn efficient variety) in response to ZnCDs, and not in the Zn inefficient variety of IR26, is presented in Figure 6.2. PCA analysis highlights the power of the developed signature of ZnCDs efficiency. The first PCA (PCA1) was able to describe 76.1% of variation in data, separating IR36+ZnCDs from IR36 Control samples. Great signature was obtained due to efficient discrimination of ZnCDs treatment from the control (Figure 6.2).

Proteins with the highest absolute coefficients in PCA1 were selected as top Proteins in overall proteomic signature of ZnCDs efficiency, discriminating IR36+ZnCDs from the control (data not shown).

Interestingly, rpl33 (peroxidase) was the key upregulated protein in response of Zn efficient variety to ZnCDs, based on the highest absolute coefficient (weight) that this protein has received in PCA1. Figure 6.3 plots the protein expression of rpl33 in response to ZnCDs in efficient and inefficient varieties. IR36 (Zn efficient variety) had the highest expression of peroxidase in response to ZnCDs, compared to the other groups.
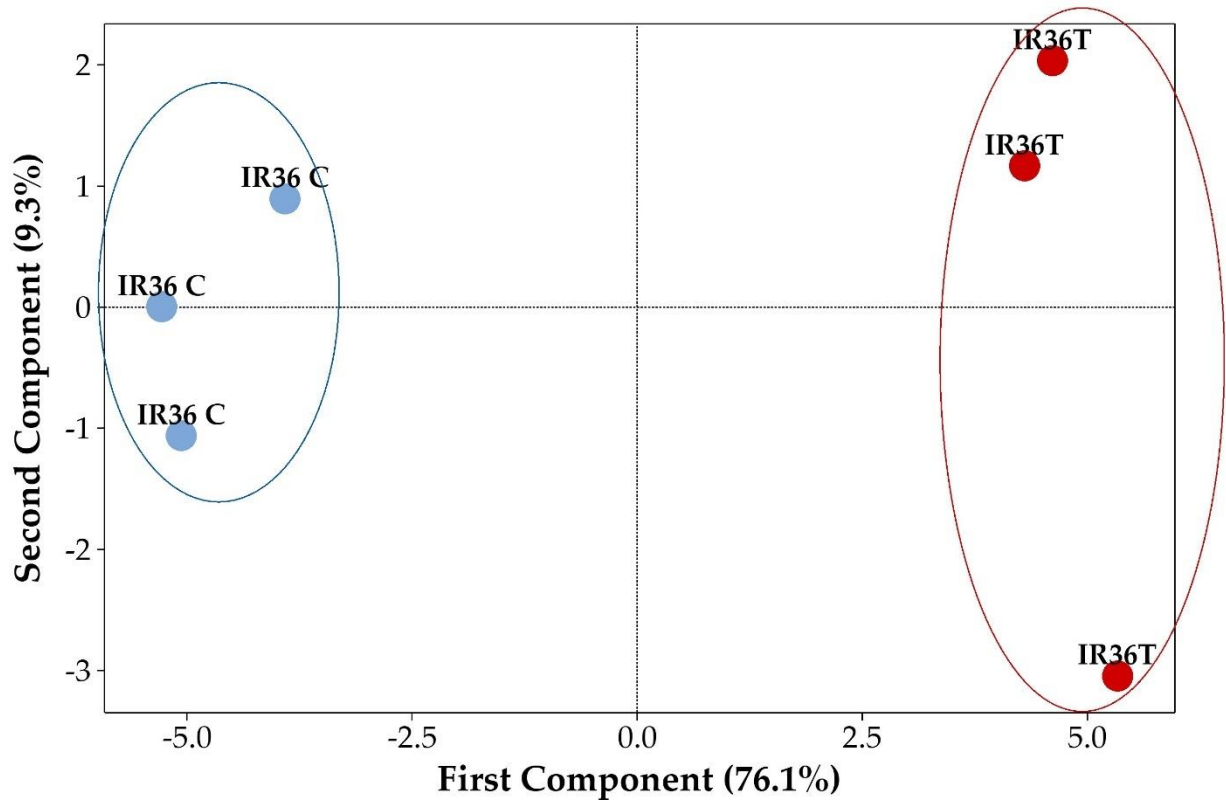
Figure 6.2: PCA plot of 36 proteins that were significantly upregulated in efficient IR36 variety in response to Zn Carbon dots (ZnCDs). PCA analysis approved the power of the developed ZnCDs efficiency signature, discriminating the IR36+ ZnCDs from the control.
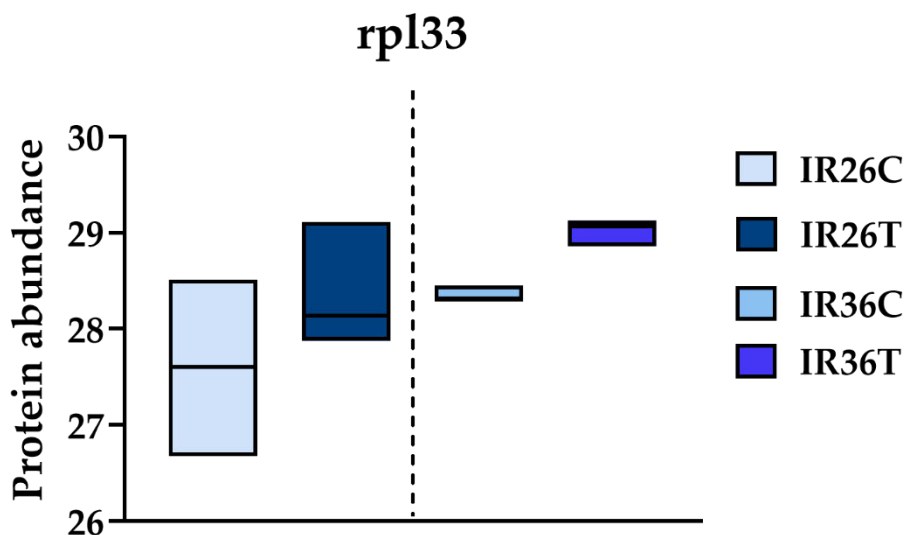
Figure 6.3: Protein expression of rpl33 (Peroxidase) in response to Zn carbon dots (ZnCDs) in efficient and inefficient varieties. IR26C: inefficient variety control, IR26T: inefficient variety + ZnCDs, IR36C: efficient variety control, IR36T: efficient variety + ZnCDs.

146

6.3.3. *Computational systems biology analysis of proteins that were specifically expressed in IR36 in response to ZnCDs*

Computational systems biology analysis of IR36 ZnCDs specific proteins (that were differentially expressed in IR36 variety in response to ZnCDs but were absent in IR26 (inefficient variety)), was conducted based on GO enrichment, KEGG enrichment analysis, protein domain enrichment analysis, and network analysis.

6.3.4. GO enrichment

GO enrichment of specific IR36 differentially expressed proteins in response to ZnCDs [(IR36 variety: ZnCDs vs Control) vs (IR26: ZnCDs vs Control)], showed that these proteins are significantly ($p < 0.05$) involved in key functions such as Hydrogen peroxide catabolic process, Cellular metabolic process, and Oxidation-reduction process (Table 6.1).

Table 6.1: Gene ontology enrichment of ZnCDs specific proteins in IR36 efficient variety, proteins that were differentially expressed in IR36 variety in response to ZnCDs but were absent in IR26 (inefficient variety).

Gene Ontology: Biological Process					
Term ID	Term description	Observed gene count	Background gene count	Strength	False discovery rate
GO:0009987	Cellular process	112	16227	0.29	1.13E-14
GO:0008152	Metabolic process	96	13135	0.31	1.55E-12
GO:0044237	Cellular metabolic process	83	10621	0.34	2.01E-11
GO:0044249	Cellular biosynthetic process	39	3118	0.54	6.57E-09
GO:1901576	Organic substance biosynthetic process	40	3322	0.53	8.35E-09
GO:0055114	Oxidation-reduction process	32	2167	0.62	8.54E-09
GO:1901566	Organonitrogen compound biosynthetic process	27	1537	0.69	8.86E-09
GO:0044271	Cellular nitrogen compound biosynthetic process	25	1431	0.69	4.92E-08
GO:0006518	Peptide metabolic process	18	693	0.86	5.87E-08

Gene Ontology: Biological Process					
Term ID	**Term description**	**Observed gene count**	**Background gene count**	**Strength**	**False discovery rate**
GO:0006412	Translation	16	581	0.89	2.66E-07
GO:0010467	Gene expression	28	1970	0.6	2.66E-07
GO:0034641	Cellular nitrogen compound metabolic process	39	3881	0.45	9.50E-07
GO:0044281	Small molecule metabolic process	26	1831	0.6	9.50E-07
GO:0071704	Organic substance metabolic process	71	11363	0.24	4.05E-05
GO:0006091	Generation of precursor metabolites and energy	12	501	0.83	0.00011
GO:0042744	Hydrogen peroxide catabolic process	7	146	1.13	0.00039
GO:0019725	Cellular homeostasis	8	240	0.97	0.00086
GO:0071840	Cellular component organization or biogenesis	29	3207	0.4	0.00088
GO:0006979	Response to oxidative stress	9	334	0.88	0.00098
GO:0044238	Primary metabolic process	62	10297	0.23	0.0012
GO:0034645	Cellular macromolecule biosynthetic process	18	1518	0.52	0.0021

Gene Ontology: Biological Process					
Term ID	Term description	Observed gene count	Background gene count	Strength	False discovery rate
GO:0045454	Cell redox homeostasis	5	79	1.25	0.0027
GO:0009206	Purine ribonucleoside triphosphate biosynthetic process	4	38	1.47	0.0031
GO:0006108	Malate metabolic process	3	12	1.85	0.0033
GO:0044283	Small molecule biosynthetic process	12	765	0.64	0.004
GO:0006807	Nitrogen compound metabolic process	52	8709	0.22	0.0093
GO:1901564	Organonitrogen compound metabolic process	41	6319	0.26	0.0121
GO:0045333	Cellular respiration	5	121	1.06	0.0128
GO:0006082	Organic acid metabolic process	14	1197	0.52	0.0159
GO:0016043	Cellular component organization	23	2840	0.36	0.0247
GO:0019752	Carboxylic acid metabolic process	13	1115	0.51	0.0247
GO:1901362	Organic cyclic compound biosynthetic process	13	1112	0.51	0.0247
GO:0006563	L-serine metabolic process	3	30	1.45	0.0249
GO:0009060	Aerobic respiration	4	81	1.14	0.0267
GO:0022900	Electron transport chain	6	241	0.84	0.0276

Gene Ontology: Biological Process					
Term ID	Term description	Observed gene count	Background gene count	Strength	False discovery rate
GO:0046034	ATP metabolic process	5	171	0.91	0.0421
GO:1902884	Positive regulation of response to oxidative stress	2	7	1.9	0.0423
GO:0022613	Ribonucleoprotein complex biogenesis	8	496	0.65	0.0444
GO:0044085	Cellular component biogenesis	14	1387	0.45	0.0471

Gene Ontology: Cellular Component					
Term ID	Term description	Observed gene count	Background gene count	Strength	False discovery rate
GO:0005737	Cytoplasm	104	10706	0.43	1.96E-25
GO:0005622	Intracellular	119	15886	0.32	2.10E-21
GO:0009536	Plastid	42	1887	0.79	2.68E-19
GO:0110165	Cellular anatomical entity	135	21835	0.24	2.68E-19
GO:0009507	Chloroplast	40	1752	0.81	1.01E-18

Gene Ontology: Biological Process					
Term ID	Term description	Observed gene count	Background gene count	Strength	False discovery rate
GO:0043229	Intracellular organelle	99	13056	0.33	9.81E-16
GO:0043231	Intracellular membrane-bounded organelle	94	12032	0.34	2.36E-15
GO:0005739	Mitochondrion	25	1308	0.73	1.04E-09
GO:0031975	Envelope	21	874	0.83	1.04E-09
GO:0032991	Protein-containing complex	38	3053	0.54	1.04E-09
GO:0005840	Ribosome	15	391	1.03	1.72E-09
GO:0031967	Organelle envelope	20	871	0.81	5.22E-09
GO:1990904	Ribonucleoprotein complex	17	703	0.83	6.64E-08
GO:0044391	Ribosomal subunit	11	246	1.1	1.55E-07
GO:0070013	Intracellular organelle lumen	22	1431	0.63	6.78E-07
GO:0043232	Intracellular non-membrane-bounded organelle	24	1864	0.56	3.20E-06
GO:0098798	Mitochondrial protein complex	8	147	1.18	4.27E-06
GO:0070469	Respirasome	7	99	1.3	4.94E-06
GO:0009534	Chloroplast thylakoid	11	370	0.92	5.78E-06

Gene Ontology: Biological Process					
Term ID	Term description	Observed gene count	Background gene count	Strength	False discovery rate
GO:0005829	Cytosol	26	2271	0.51	6.37E-06
GO:0005759	Mitochondrial matrix	8	160	1.15	6.47E-06
GO:0098796	Membrane protein complex	13	570	0.81	6.96E-06
GO:0005740	Mitochondrial envelope	11	395	0.89	9.01E-06
GO:0009570	Chloroplast stroma	11	424	0.86	1.66E-05
GO:0031966	Mitochondrial membrane	10	375	0.87	4.11E-05
GO:1990204	Oxidoreductase complex	6	101	1.22	7.22E-05
GO:0009535	Chloroplast thylakoid membrane	9	317	0.9	8.08E-05
GO:0005747	Mitochondrial respiratory chain complex i	4	30	1.57	0.00017
GO:0019866	Organelle inner membrane	9	372	0.83	0.00024
GO:0015934	Large ribosomal subunit	6	133	1.1	0.00026
GO:0022626	Cytosolic ribosome	6	177	0.98	0.0012
GO:0015935	Small ribosomal subunit	5	113	1.09	0.0014
GO:0016469	Proton-transporting two-sector ATPase complex	4	56	1.3	0.0014

Gene Ontology: Biological Process					
Term ID	Term description	Observed gene count	Background gene count	Strength	False discovery rate
GO:0005685	U1 snRNP	3	20	1.62	0.0015
GO:0005743	Mitochondrial inner membrane	7	285	0.84	0.0018
GO:0097525	Spliceosomal snRNP complex	4	64	1.24	0.002
GO:1902494	Catalytic complex	13	1034	0.55	0.002
GO:0005730	Nucleolus	8	401	0.75	0.0021
GO:0033178	Proton-transporting two-sector ATPase complex, catalytic domain	3	26	1.51	0.0027
GO:0005758	Mitochondrial intermembrane space	3	27	1.49	0.0029
GO:0048046	Apoplast	7	322	0.78	0.0032
GO:0045259	Proton-transporting ATP synthase complex	3	31	1.43	0.004
GO:0005761	Mitochondrial ribosome	3	35	1.38	0.0054
GO:0071011	Precatalytic spliceosome	3	35	1.38	0.0054
GO:0097526	Spliceosomal tri-snRNP complex	3	36	1.37	0.0056
GO:0009543	Chloroplast thylakoid lumen	3	43	1.29	0.0089
GO:0005643	Nuclear pore	3	49	1.23	0.0123

Gene Ontology: Biological Process					
Term ID	Term description	Observed gene count	Background gene count	Strength	False discovery rate
GO:0031981	Nuclear lumen	12	1167	0.46	0.0154
GO:0005741	Mitochondrial outer membrane	3	59	1.15	0.0197
GO:0045261	Proton-transporting ATP synthase complex, catalytic core f(1)	2	15	1.57	0.0224
GO:0005682	U5 snRNP	2	16	1.54	0.0248
GO:0005762	Mitochondrial large ribosomal subunit	2	18	1.49	0.0303
GO:0022627	Cytosolic small ribosomal subunit	3	72	1.07	0.0322
GO:0009941	Chloroplast envelope	6	388	0.64	0.0383
GO:0005686	U2 snRNP	2	23	1.39	0.0443

Gene Ontology: Molecular Function

Term ID	Term description	Observed gene count	Background gene count	Strength	False discovery rate
#term ID	term description	observed gene count	background gene count	strength	false discovery rate
GO:0005198	Structural molecule activity	16	458	0.99	4.07E-08
GO:0016491	Oxidoreductase activity	30	1992	0.62	4.07E-08
GO:0003735	Structural constituent of ribosome	14	357	1.04	6.12E-08
GO:0005488	Binding	84	14054	0.22	1.14E-05
GO:0003723	RNA binding	19	1448	0.57	0.00059
GO:0003824	Catalytic activity	65	10778	0.23	0.00094
GO:0019843	rRNA binding	7	161	1.09	0.00094
GO:0016616	Oxidoreductase activity, acting on the CH-OH group of donors, nad or nadp as acceptor	8	250	0.95	0.0012
GO:0008379	Thioredoxin peroxidase activity	3	7	2.08	0.0013
GO:0016615	Malate dehydrogenase activity	3	17	1.69	0.009
GO:0043169	Cation binding	32	4436	0.31	0.0147

Gene Ontology: Molecular Function					
Term ID	Term description	Observed gene count	Background gene count	Strength	False discovery rate
GO:0046933	Proton-transporting ATP synthase activity, rotational mechanism	3	21	1.6	0.0147
GO:0016209	Antioxidant activity	6	203	0.92	0.0154
GO:0016651	Oxidoreductase activity, acting on NAD(P)H	5	131	1.03	0.0174
GO:0051537	2 Iron, 2 Sulphur cluster binding	4	68	1.22	0.0174
GO:0046872	Metal ion binding	31	4402	0.29	0.0225
GO:0004601	Peroxidase activity	5	169	0.92	0.0466
GO:0016765	Transferase activity, transferring alkyl or aryl (other than methyl) groups	5	171	0.91	0.0468

6.3.5.   Network analysis

IR36 specific upregulated genes (IR36: ZnCDs vs Control) vs (IR26: ZnCDs vs Control) interacted according to the network analysis. Rpl33 made a subnetwork and interacted with the important protein, atpF (Figure 6.4).
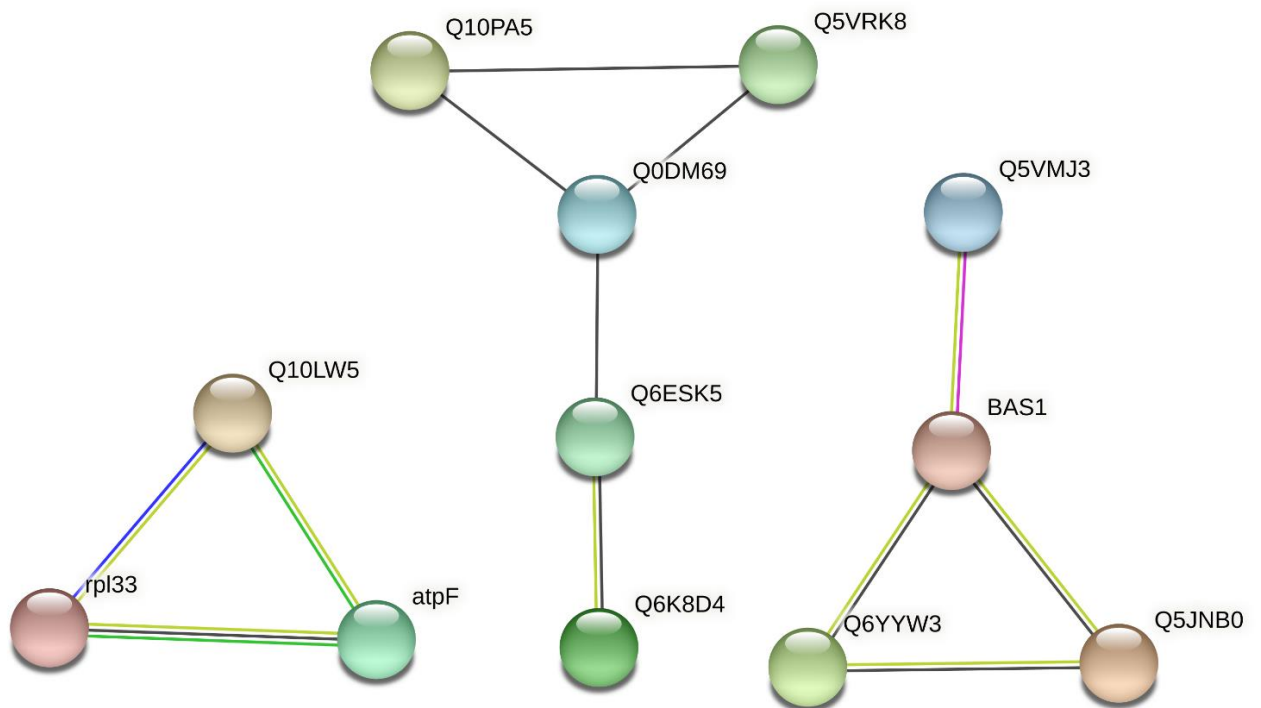
Figure 6.4: Protein-Protein interaction network of IR36 specific upregulated proteins in response to ZnCDs [(IR36: ZnCDs vs Control) vs (IR26: ZnCDs vs Control)]

6.3.4.   KEGG enrichment

KEGG enrichment analysis highlighted that the specific ZnCDs-responding proteins in IR36 variety significantly (p<0.05) enrich pathways such as Carbon fixation in photosynthetic organisms that can contribute to higher yield (Table 6.2).

Table 6.2: KEGG enrichment analysis of ZnCDs specific proteins in IR36 efficient variety, proteins that were differentially expressed in IR36 variety in response to ZnCDs but were absent in IR26 (inefficient variety).

KEEG Pathways					
Term ID	**Term description**	**Observed gene count**	**Background gene count**	**Strength**	**FDR**
dosa03010	Ribosome	14	420	0.97	9.74E-08
dosa01100	Metabolic pathways	43	4581	0.42	1.90E-07
dosa00190	Oxidative phosphorylation	8	204	1.04	5.33E-05
dosa01200	Carbon metabolism	10	365	0.88	5.33E-05
dosa00710	Carbon fixation in photosynthetic organisms	5	105	1.12	0.0015
dosa00270	Cysteine and methionine metabolism	5	169	0.92	0.0107
dosa00195	Photosynthesis	4	99	1.05	0.0115
dosa00620	Pyruvate metabolism	4	114	0.99	0.0168
dosa03040	Spliceosome	6	303	0.74	0.0168
dosa00630	Glyoxylate and dicarboxylate metabolism	4	126	0.95	0.0192
dosa00020	Citrate cycle (TCA cycle)	3	67	1.1	0.0286
dosa00480	Glutathione metabolism	4	149	0.88	0.0286
dosa01110	Biosynthesis of secondary metabolites	18	2359	0.33	0.0286
dosa05132	Salmonella infection	3	79	1.03	0.0353

6.3.5. Protein domain enrichment analysis

Protein domain enrichment analysis of 36 proteins that were specifically upregulated in the efficient IR36 variety in response to ZnCDs but not in the inefficient IR26 variety, demonstrated the significant ($p<0.05$) enrichment of domains of Peroxidase, Antioxidant, Amino-acid biosynthesis, Mitochondrion, and the Respiratory chain (Table 6.3).

Table 6.3: Domain enrichment analysis of upregulated genes in Zn efficient variety in response to ZnCDs [(IR36: ZnCDs vs Control) vs (IR26: ZnCDs vs Control)].

Term ID	Term description	Observed gene count	Background gene count	Strength	False discovery rate
Protein domain: Unipro-Up regulated protein					
KW-0198	Cysteine biosynthesis	2	5	2.69	0.0031
KW-0446	Lipid-binding	3	43	1.93	0.0031
KW-1015	Disulfide bond	5	519	1.07	0.009
Protein domain: Unipro-Down regulated protein					
KW-0687	Ribonucleoprotein	12	277	1.2	1.22E-08
KW-0689	Ribosomal protein	9	229	1.16	4.43E-06
KW-0150	Chloroplast	7	369	0.84	0.0113
KW-0809	Transit peptide	7	371	0.84	0.0113
KW-0560	Oxidoreductase	10	906	0.6	0.015
KW-0249	Electron transport	4	110	1.12	0.0163
KW-0520	NAD	4	116	1.1	0.0173

Protein domain: Unipro-Down regulated protein					
Term ID	Term description	Observed gene count	Background gene count	Strength	False discovery rate
KW-0508	mRNA splicing	3	51	1.33	0.0201
KW-0049	Antioxidant	2	11	1.82	0.0229
KW-0963	Cytoplasm	7	529	0.68	0.0262
KW-0521	NADP	4	147	1	0.0267
KW-0575	Peroxidase	4	146	1	0.0267
KW-0028	Amino-acid biosynthesis	3	75	1.16	0.0364
KW-0747	Spliceosome	2	18	1.61	0.0364
KW-0676	Redox-active center	3	81	1.13	0.0385
KW-0496	Mitochondrion	4	181	0.91	0.0386
KW-0679	Respiratory chain	2	22	1.52	0.0418

6.3.6. Selected Pathways Proteomics

Based on computational systems biology analysis, the following pathways were selected as significant pathways in response to ZnCDs: Cellular response to Oxygen radicals, Glucose metabolism, Photosynthesis and Response to abiotic stimulus.

6.3.7. Cellular response to Oxygen radicals

Figure 6.5 represents the signature power of 3 proteins of Cellular response to Oxygen radicals by multivariate analysis in the separation of the efficient variety of IR36 from the Zn inefficient variety of IR26 in response to ZnCDs. PCA1 describe 88.2% of the variation in data. PCA1 separates the control from ZnCDs treatment.

Figure 6.6 visualises the protein expressions of 3 proteins of Cellular response to Oxygen radicals in response to ZnCDs. The Zn inefficient variety IR26 shows higher oxidative stress in response to ZnCDs in comparison with the Zn efficient variety, IR36.
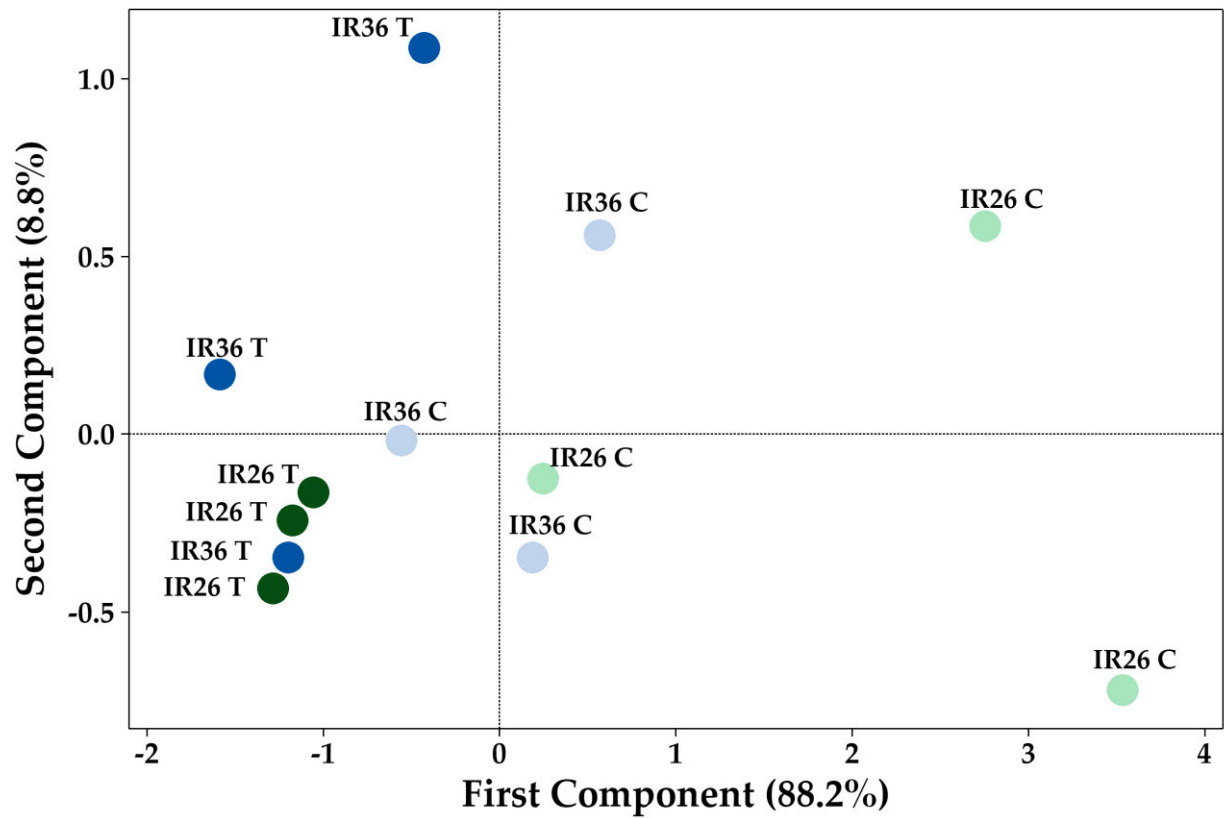
Figure 6.5: PCA analysis of 3 proteins of Cellular response to Oxygen radicals in separation of ZnCDs groups. IR26C: inefficient variety control, IR26T: inefficient variety + ZnCDs, IR36C: efficient variety control, IR36T: efficient variety + ZnCDs.
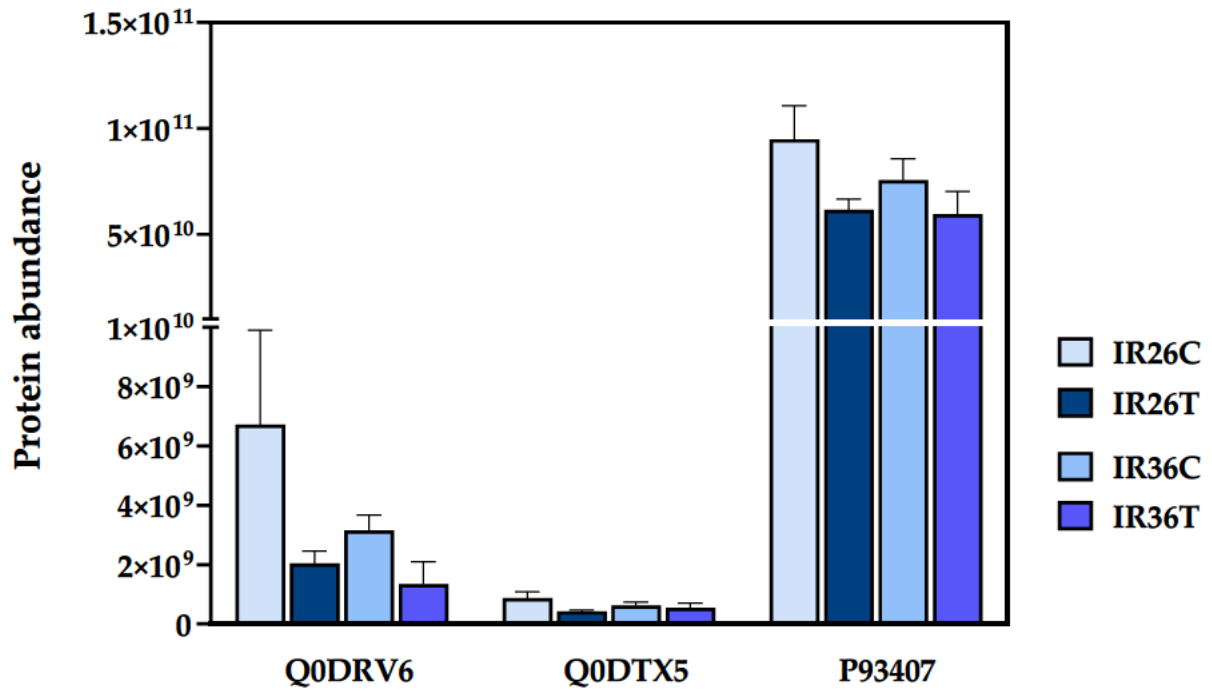
Figure 6.6: Protein Expressions of 3 proteins of Cellular response to Oxygen radicals in response to ZnCDs. IR26C: inefficient variety control, IR26T: inefficient variety + ZnCDs, IR36C: efficient variety control, IR36T: efficient variety + ZnCDs.

6.3.8. Glucose metabolism

PCA analysis of 7 proteins of Glucose metabolism in separation of ZnCDs groups is presented in Figure 6.7. High signature (discrimination) power was observed where PCA1 describe 90.4% of variation in data. PCA1 efficiently separates IR26 treatment from IR36 control. Figure 6.8 and figure 6.9 present the expression of proteins in the Glucose metabolism pathway in response to ZnCDs.
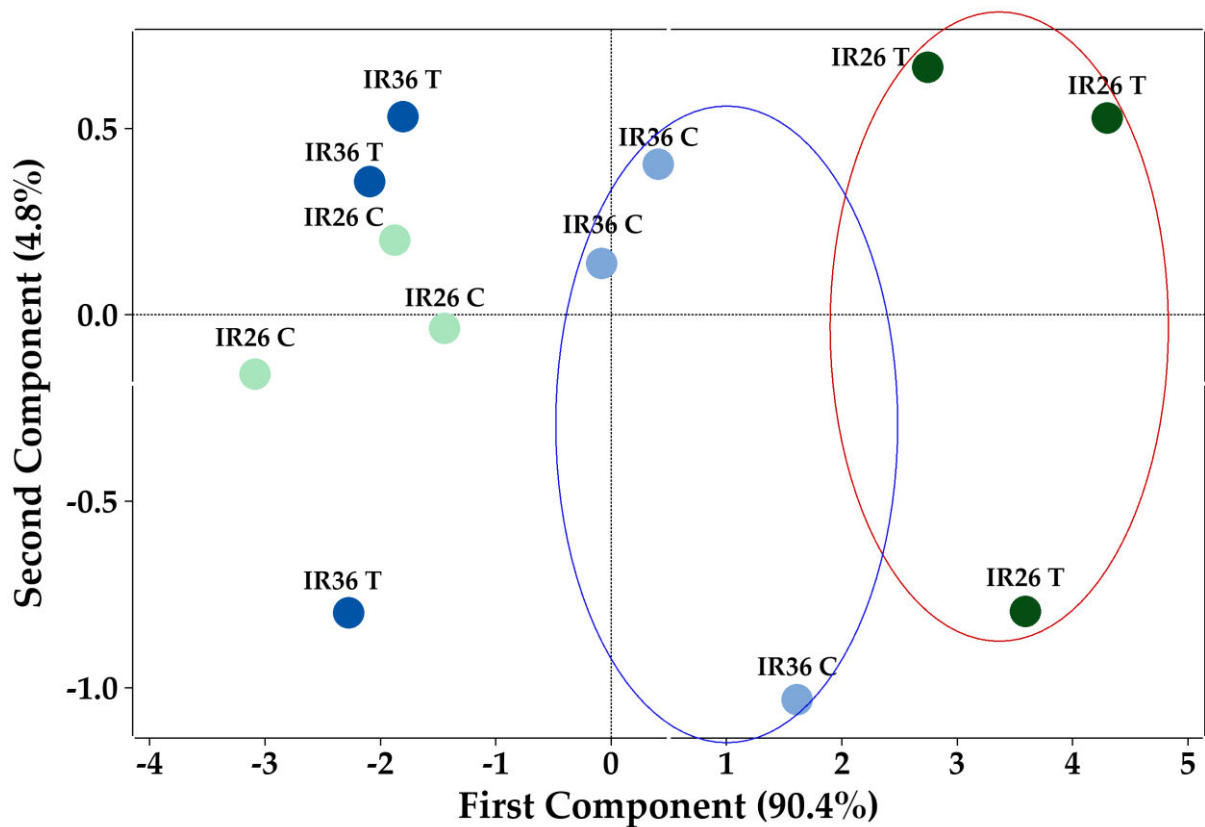
Figure 6.7: PCA analysis of 7 proteins of Glucose metabolism in separation of ZnCDs groups. IR26C: inefficient variety control, IR26T: inefficient variety + ZnCDs, IR36C: efficient variety control, IR36T: efficient variety + ZnCDs.
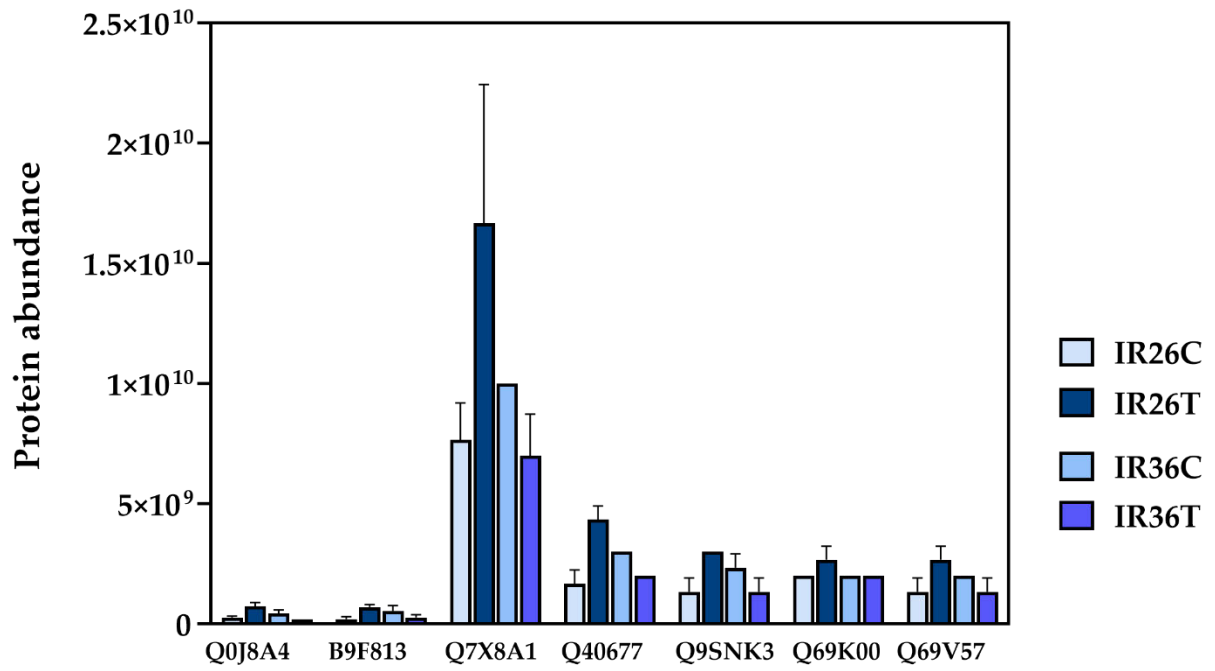
Figure 6.8: Protein Expressions of 7 proteins of Glucose metabolism pathway in response to ZnCDs. IR26C: inefficient variety control, IR26T: inefficient variety + ZnCDs, IR36C: efficient variety control, IR36T: efficient variety + ZnCDs.
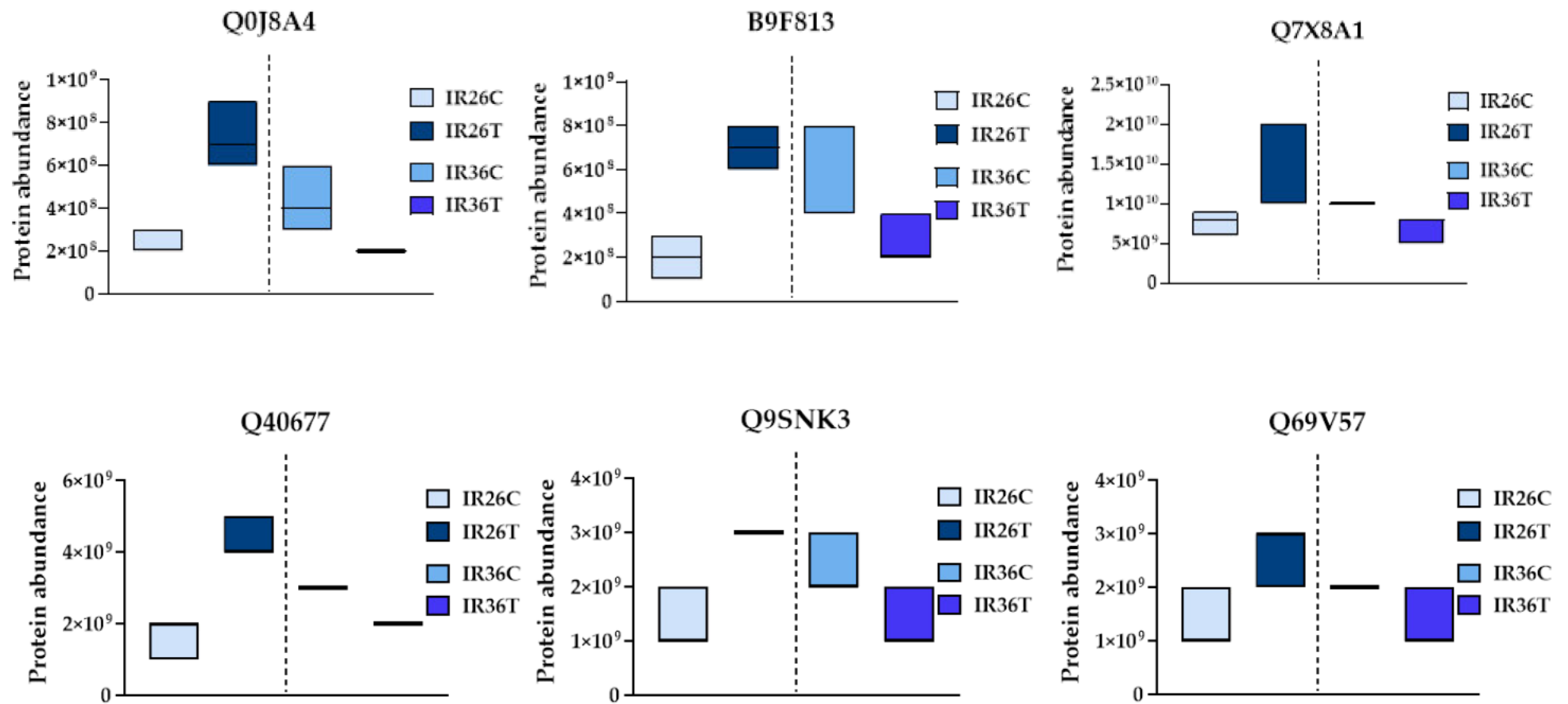
Figure 6.9: Expression of proteins in Glucose metabolism pathway. IR26C: inefficient variety control, IR26T: inefficient variety + ZnCDs, IR36C: efficient variety control, IR36T: efficient variety + ZnCDs.

6.3.9. Photosynthesis

Figure 6.10 presents the PCA analysis of 3 proteins of the Photosynthesis pathway. The expression of proteins in the Photosynthesis pathway is presented in Figure 6.11. PCA1 described 97.4% of variation in data, demonstrating high discriminative power and strong signature. PCA1 separates the IR26 control from the IR26 treatment (IR26+ZnCDs).
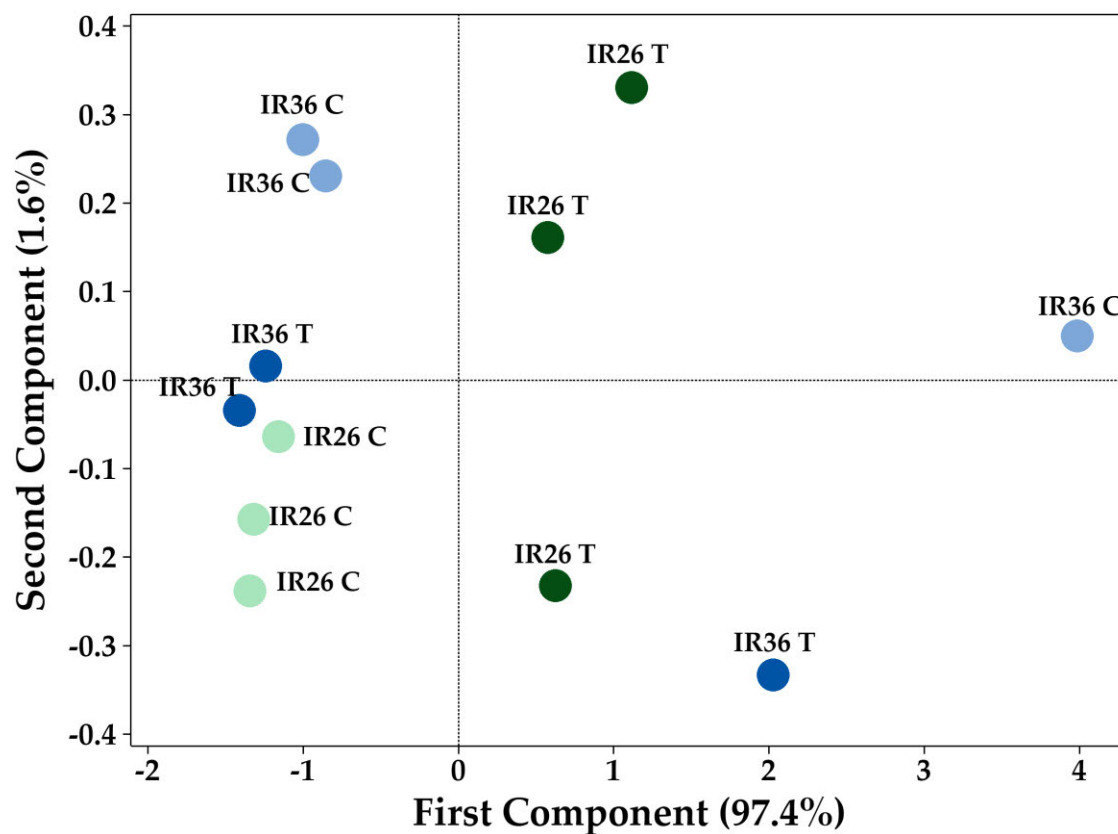
Figure 6.10: PCA analysis of 3 proteins of Photosynthesis pathway. IR26C: inefficient variety control, IR26T: inefficient variety + ZnCDs, IR36C: efficient variety control, IR36T: efficient variety + ZnCDs.
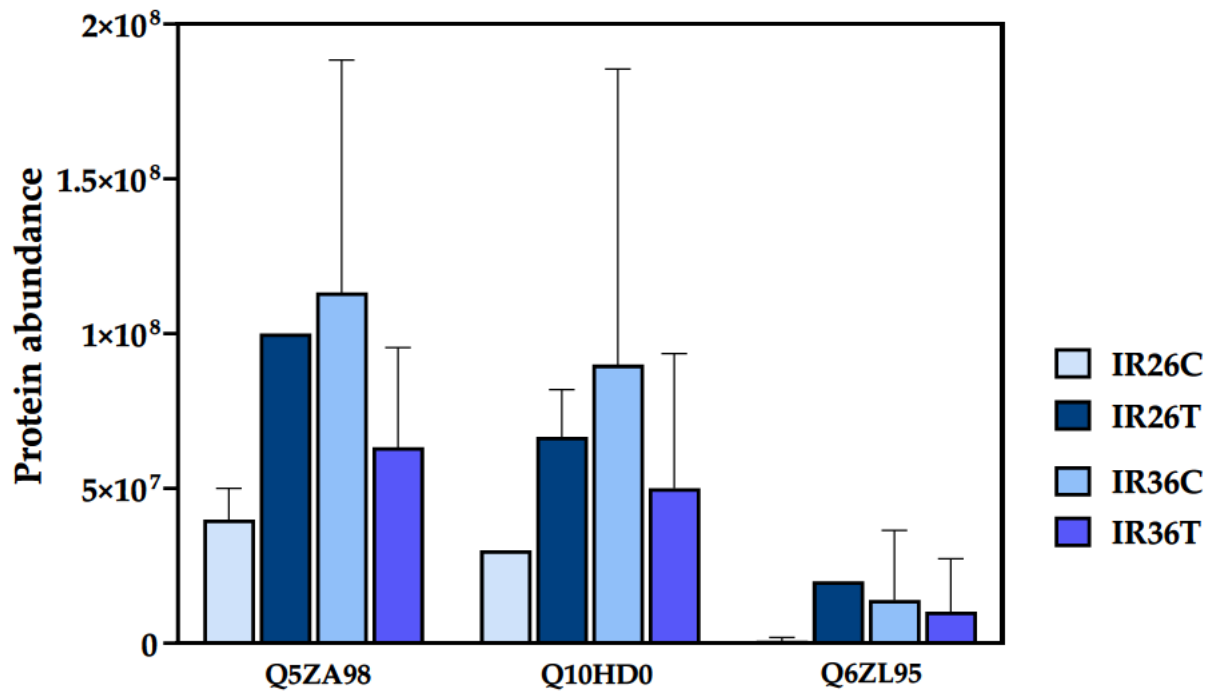
Figure 6.11: Expression of proteins in 3 proteins of Photosynthesis pathway. IR26C: inefficient variety control, IR26T: inefficient variety + ZnCDs, IR36C: efficient variety control, IR36T: efficient variety + ZnCDs.

6.3.10. Response to abiotic stimulus

Figure 6.12 presents the PCA analysis of genes in response to the abiotic stimulus pathway. PCA1 described 54% of variation in the data, demonstrating moderate discriminative power and signature. PCA1 separates the IR26 control from the IR26 treatment (IR26+ZnCDs) whereas IR36 does not show clear separation.

The expression of three proteins is provided in Figure 6.13. The abundance of protein Q6ZL95 in the abiotic stimulus responding pathway is provided in Figure 6.14. Protein Q6ZL95 in IR36 show higher expression in compared to the IR26 control and treatment.
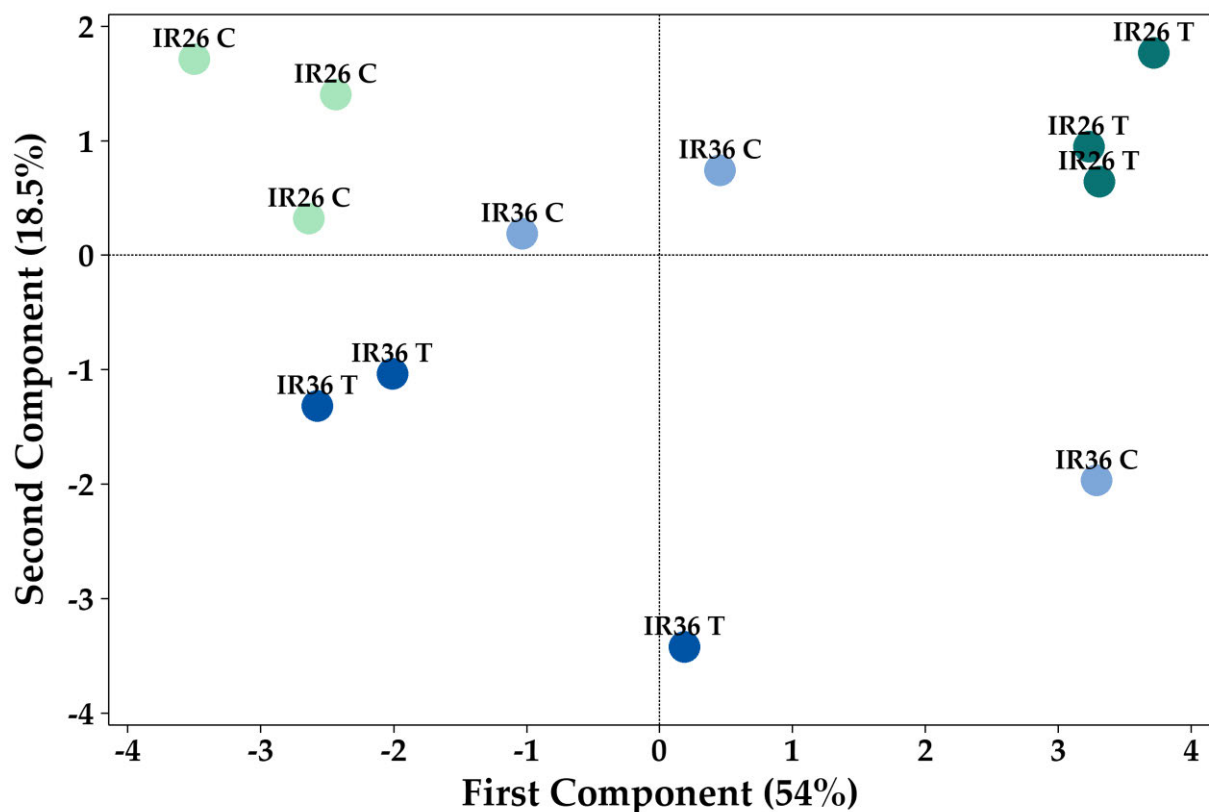
Figure 6.12: PCA analysis of genes in Response to abiotic stimulus pathway. IR26C: inefficient variety control, IR26T: inefficient variety + ZnCDs, IR36C: efficient variety control, IR36T: efficient variety + ZnCDs.
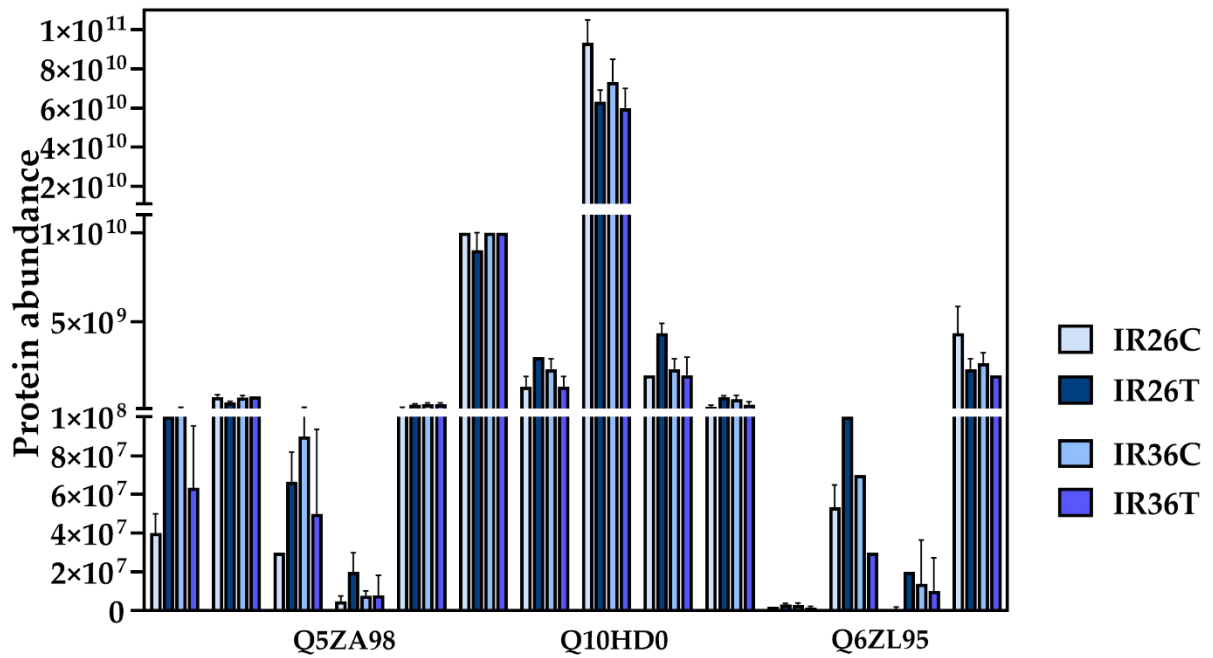
Figure 6.13: The expression of proteins involved in Response to abiotic stimulus pathway. IR26C: inefficient variety control, IR26T: inefficient variety + ZnCDs, IR36C: efficient variety control, IR36T: efficient variety + ZnCDs.
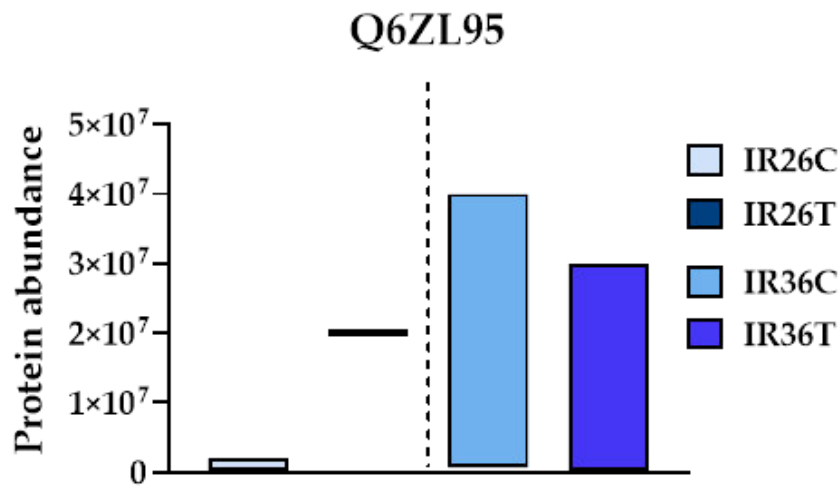
Figure 6.14: Expression of protein Q6ZL95 in abiotic stimulus pathway. IR26C: inefficient variety control, IR26T: inefficient variety + ZnCDs, IR36C: efficient variety control, IR36T: efficient variety + ZnCDs.

6.4. Discussion

The mechanisms mediating higher Zn efficiency and the effect of Zn nanoparticles (NPs), particularly foliar application, are unknown. Proteome analysis is a promising strategy for understanding the molecular mechanism of response to Zn and its nano carrier. However, most of the previous studies have focused on the response of one type of genotype against Zn stress or Zn deficiency (Song et al., 2014, Zeng et al., 2019, Song et al., 2021), rather than a proteomic comparison of genotypes with different levels of Zn uptake and metabolism. Another challenge in increasing the nutritional contents of grains is whether the applied ZnCDs transport to the grain or not.

In this investigation, a comparative proteomic analysis of the Zn efficient rice variety (IR36) with Zn inefficient variety (IR26), both treated with foliar application of ZnCDs, was conducted to determine the pathways and proteins that are involved in high Zn efficiency in rice and their differential response to ZnCDs. Shortlisting the significant GOs and functions and supervised selection of proteins based on the significant GOs/pathways are robust approaches in proteomic analysis and selection of key proteins in systems biology (Ebrahimie et al., 2015, Ebrahimie et al., 2017, Fruzangohar et al., 2013). Additionally, PCA-based protein selection (multivariate analysis) was applied to document the robustness of the developed proteomic signature in distinguishing ZnCDs treatment and variety efficiency.

Multivariate-based signature discovery identified the role of rpl33 (peroxidase) as the key upregulated protein in response to ZnCDs in IR36 (efficient variety). The expression of this gene was higher in IR36+ZnCDs compared to the other groups. Upregulation of peroxidase may help IR36 to cope with the oxidative stress, caused by nano particles.

In conclusion, ZnCDs-responding specific proteins in IR36 (Zn efficient genotype) were involved in critical functions, such as Hydrogen peroxide catabolic process, Cellular metabolic process, Carbon fixation in photosynthetic organisms, and Oxidation-reduction process. The key enriched proteomics pathways were: Cellular response to Oxygen radicals, Glucose metabolism, Photosynthesis, Response to abiotic stimulus, Ribonucleotide metabolism, and Zinc finger proteins.

Domain enrichment analysis reposted the high abundance of domains of Peroxidase, Antioxidant, Amino-acid biosynthesis, Mitochondrion, and Respiratory chain in the structure of proteins that specifically upregulate in response to ZnCDs in the IR36 Zn efficient variety. Analysis of enriched domains in the structure of proteins in addition to conventional protein expression analysis provided valuable clues regarding the functional domain in proteomics pool.

The low number of replications (n=3) in each treatment group, which was also recognized in the previous chapter on RNA-seq analysis, is a limitation of this investigation. A higher number of replicates per group is proposed for future studies to increase the confidence and power of the experiment.

6.5. Conclusion

The two rice varieties with documented different levels of Zn efficiency (IR36 and IR26) provided an excellent opportunity for comparative proteomic analysis between a Zn efficient variety against an inefficient variety, leading to discovery of Proteins and associated mechanisms that solely involved in higher Zn efficiency in the efficient variety. To best of our knowledge, no studies have compared the proteomic responses of a Zn efficient variety against an inefficient variety.

CHAPTER 7: DISCUSSION AND CONCLUSIONS

7.1. General discussion

Zinc (Zn) deficiency is a major health concern worldwide. More than 70 percent of human Zn intake is derived from cereals and pulses, and its concentration has decreased substantially due to breeding for yield and pest and disease resistance. In addition, global warming and climate change contribute to decreasing micronutrients in cereals (Seneweera, 2011). Increasing grain Zn content through the application of Zn nanoparticles (NPs) as a potential nano-fertiliser opens a new avenue to address this challenge. However, our knowledge of the impact of Zn nanoparticles (Zn NPs) in cereals is limited.

Detection of carbon based NPs in plant material has been done using many techniques. Lin et al. (2009) used bright field microscopy to detect MWNT and fullerene 70 in the seed, roots and leaves of rice plants. Fluorescence and confocal 3D mapping has been used with fluorescent SWCTs in spinach chloroplasts (Giraldo et al., 2014). Fluorescence has also been used to determine root uptake of water soluble CDs in wheat seedlings (Tripathi et al., 2015). Uptake and translocation of fluorescent CDs in mung plant seedlings has been successfully studied using laser scanning confocal microscopy images (Li et al., 2016, Wang et al., 2018). Additionally, TEM and SEM has been used to detect carbon-based NPs in plant cells (Chen et al., 2010, Tripathi et al., 2015, Li et al., 2016, Wang et al., 2018).

Several positive impacts of CD and other CNP applications in agriculture, including enhancing seed germination, promoting growth, and water absorption of cereals, have been recorded (Tripathi et al., 2011, Nair et al., 2012, Anita et al., 2014, Tiwari et al., 2014, Lahiani et al., 2015, Joshi et al., 2018, Wang et al., 2018). However, use of CDs as a micronutrient

carrier to cereal plant has not been recorded. Additionally, there was little evidence of a thorough investigation into the development, agronomy, physiological, and nutrient uptake of rice plants treated with CDs.

Therefore, to fill the knowledge gap, the effect of CDs bound with Zn on rice plants with respect to their growth, physiology, agronomy and micronutrient uptake was evaluated. Additionally, to unravel the molecular basis of the CNP application, a high throughput transcriptomic and proteomics analysis was coupled to the study. The critical assumption of the study was that there would be different responses in cultivars that have high or low Zn uptake efficiencies. The study hypothesis that there is a considerable effect of CNP application on both molecular and physiological level responses of the rice plants with different Zn efficiencies.

7.1.1. Major Findings

Effect of CNP's on physiological, agronomical, and nutritional level rice plants:

The evaluations of rice plant growth, physiology, and Zn uptake in response to CD and ZnCD applications showed that ZnCDs have a potential of being a biofortification agent to enhance the Zn status of the plant. Both CDs and ZnCDs did not have any negative impact on plant growth and/or gas exchange. In contrast, compared to other treatments, ZnCD had the highest Zn uptake and retention of Zn content in the plants for at least one month. The most effective dose of the CD and ZnCD was 500 ppm. However, other studies have shown that the optimum concentration could change depending on the physical properties of NP, such as size and surface functionalisation.

Results obtained over one month period for range of physiological and growth parameters of rice plants following teeatment applications (CD,

ZnCD, ZnAC and control) demonstrated the possibility of using nanoparticles as a nutrient supplier for extended period of time. Further this explained the success of a nano particle based foliar spray as a micro nutrient supplier. These findings directly help in the bofortificaion of rice grains for its micronutrient content.

We found a remarkable difference in plant nutrient uptake after treatment of Zn efficient (IR36) and Zn inefficient varieties (IR26) by ZnCDs. ZnCDs led to a significant improvement in the contents of Mn, Cu, and Zn in grains and Mn in roots. Findings of the study carried out with Zn efficient and Zn inefficient varieties demonstared the correlation between the genetic diversity of rice varieties with Zn uptake and Zn utilization efficiency. This leads to the fine tuning of Zn biofortication of rice varieties which is highly dependent on its genetic diversity.

Effect of CNP's on molecular level adjustment in rice plants:

We investigated the response of the Zn efficient rice variety (IR36) to Zn carbon dots (ZnCDs) against the Zn inefficient variety (IR26). Transcriptomic and proteomic analyses were performed on the flag leaf at the last fully expanded growth stage since it is the most essential and efficient functional leaf at the grain filling stage.

Computational systems biology analysis in transcriptomic analysis revealed that Zn uptake, grain filling, auxin signalling, and abiotic stress signalling were the major pathways contributing to better response of the Zn efficient IR36 variety to ZnCDs, compared to the Zn inefficient IR26 variety. Multivariate analysis identified that *OsDMAS1* and *OsbZIP72* genes play a major role in the above-mentioned pathways. Proteomics and transcriptomics analysis shared the same intercellular organelle activity.

Proteomics analysis based on computational system biology revealed that the ZnCD treatments cause significant changes to the protein expression level of cellular response to oxygen radicals, glucose metabolism, photosynthesis and response to abiotic stimulus of IR36 compared to IR26 variety. Of the pathways considered, proteins in the glucose metabolism pathway separates with a high discrimination in PCA analysis the ZnCD treated IR26 plants from the untreated IR36 plants.

Protein rpl33 (a peroxidase) was identified as the key upregulatory protein in ZnCD treated IR36 variety from a multivariate based signature discovery analysis. This suggested that the upregulated peroxidases could support the IR36 Zn efficient variety to cope with oxidative stresses caused by the application of nanoparticles to the plants.

The findings of these studies support establishing a new technique for using carbon nanodots to fertilise plants and deliver micronutrients (using CDs). The genomic studies have provided valuable knowledge in explaining little studied molecular mechanism behind the nanoparticle uptake in plants. Studies on transportation of nanoparticles and accumulation of Zn in plant systems help fill gaps in the scientific literature in Zn uptake, translocation and bio-fortification.

In general, the results of the study associates between the utilization of the ZnCDs and their effect on the growth, physiology and the nutritional uptake of the rice plants. They provide positive insights of developind nanomaterial based micronutrient suppliers in fune tuning the biofortification pathways of rice varieties. Despite the trational methods employed in enhancing the micronutrient contents, specially Zn, in cereals, this study provides a new avenue in increasing Zn content and nutritional quality in rice and other cereals. The outcomes of the research can be effectively employed in Zn biofortification programs of cereals.

7.2. Suggestions for future research

The results obtained from the physiology, agronomy and the micronutrient uptake experiments need to be validated through a series of field experiments using varieties of different Zn use efficiencies. Further, key genes and the pathways identified from the molecular studies of the research could be employed in hastening the genetic biofortification programs of cereals. Additionally, development of biofortified crops could be achieved through the CRISPR-Cas system which allows rapid, site-specific genome modification in a crop plants. The identified key genes in the Zn use efficiency would facilitate the above novel genome editing programs.

Transcriptomic experiment:

Due to limitations in budget and sample preparation, RNA-Seq experiments were performed with only 3 replications in each group. Increasing the number of replications in future experiments will contribute to higher confidence and improved experiment power. The transcriptomic analysis was performed at the gene level. Further analysis of sequencing data at the transcript level (transcript-based mapping and expression analysis) instead of gene-based mapping/expression should provide novel knowledge on the contribution of alternative splicing in response to nano particles. The mentioned analysis can open a new avenue in research and understanding of high Zn efficiency.

Functional validation:

This study shortlisted genes such as *OsDMAS1* and *OsbZIP72*, as key differences between IR36 and IR26 in response to ZnCd. The future laboratory-based validation of those genes by knocking down/downregulation or upregulation/over-expression can provide valuable insight on the functional importance of those selected genes.

Study of foliar application of ZnCDs on improving drought tolerance and grain production under drought stress and ROS generation:

Zn NPs have high potential to help the plant under drought stress by improving drought tolerance and grain quality. The interaction effect of drought and ZnCDs needs to be investigated in future studies.

Application of CNP may lead to some other omics level changes as well. Alternative transcript splicing is one such example which could be a reason for changes in the responses of rice plants for CNP treatments. CNP applications could enhance reactive oxygen species (ROS) and they may affect different patterns of Alternative splicing such as exon inclusion or skipping, alternative splice-site selection, mutually exclusive exons, and intron retention (Srivastava et al., 2009, Van Ruyskensvelde et al., 2018). Therefore another analysis could be done in determining alternative splicing possibilities using generation of ROS in CNP treated rice plants.

REFERENCES

References of Chapter 1:

Akmal, M., Younus, A., Wakeel, A., Jamil, Y. & Rashid, M. A. 2022. Synthesis and application of optimized ZnO nanoparticles for improving yield and Zn content of rice (Oryza sativa L.) grain. *Journal of Plant Nutrition*, 1-14.

Alloway, B. J. 2008. *Zinc in soils and crop nutrition*, International Zinc Association Brussels, Belgium.

Anita, S. & Rao, D. 2014. Enhancement of seed germination and plant growth of wheat, maize, peanut and garlic using multiwalled carbon nanotubes. *European Chemical Bulletin,* 3, 502-504.

Boonchuay, P., Cakmak, I., Rerkasem, B. & Prom-U-Thai, C. 2013. Effect of different foliar zinc application at different growth stages on seed zinc concentration and its impact on seedling vigor in rice. *Soil Science and Plant Nutrition,* 59, 180-188.

Cakmak, I. 2008. Enrichment of cereal grains with zinc: agronomic or genetic biofortification? *Plant and soil,* 302, 1-17.

Corbo, M. D. & Lam, J. 2013. Zinc deficiency and its management in the pediatric population: A literature review and proposed etiologic classification. *Journal of the American Academy of Dermatology,* 69, 616-624. e1.

Deshpande, J. D., Joshi, M. M. & Giri, P. A. 2013. Zinc: The trace element of major importance in human nutrition and health. *Int J Med Sci Public Health,* 2, 1-6.

Deshpande, P., Dapkekar, A., Oak, M. D., Paknikar, K. M. & Rajwade, J. M. 2017. Zinc complexed chitosan/TPP nanoparticles: a promising

micronutrient nanocarrier suited for foliar application. *Carbohydrate polymers,* 165**,** 394-401.

Ghasemi, M., Ghorban, N., Madani, H., Mobasser, H.-R. & Nouri, M.-Z. 2017. Effect of foliar application of zinc nano oxide on agronomic traits of two varieties of rice (Oryza sativa L.). *Crop Research,* 52**,** 195-201.

Giraldo, J. P., Landry, M. P., Faltermeier, S. M., Mcnicholas, T. P., Iverson, N. M., Boghossian, A. A., Reuel, N. F., Hilmer, A. J., Sen, F. & Brew, J. A. 2014. Plant nanobionics approach to augment photosynthesis and biochemical sensing. *Nature materials,* 13**,** 400.

Habib, M. 2009. Effect of foliar application of Zn and Fe on wheat yield and quality. *African Journal of Biotechnology,* 8.

Hussain, A., Rizwan, M., Ali, S., Ur Rehman, M. Z., Qayyum, M. F., Nawaz, R., Ahmad, A., Asrar, M., Ahmad, S. R. & Alsahli, A. A. 2021. Combined use of different nanoparticles effectively decreased cadmium (Cd) concentration in grains of wheat grown in a field contaminated with Cd. *Ecotoxicology and Environmental Safety,* 215**,** 112139.

Itroutwar, P. D., Govindaraju, K., Tamilselvan, S., Kannan, M., Raja, K. & Subramanian, K. S. 2020. Seaweed-based biogenic ZnO nanoparticles for improving agro-morphological characteristics of rice (Oryza sativa L.). *Journal of plant growth regulation,* 39**,** 717-728.

Jalali, M., Ghanati, F., Modarres-Sanavi, A. & Khoshgoftarmanesh, A. 2017. Physiological effects of repeated foliar application of magnetite nanoparticles on maize plants. *Journal of agronomy and crop science,* 203**,** 593-602.

Joshi, A., Kaur, S., Dharamvir, K., Nayyar, H. & Verma, G. 2018. Multi-walled carbon nanotubes applied through seed-priming influence early germination, root hair, growth and yield of bread wheat (Triticum

aestivum L.). *Journal of the Science of Food and Agriculture,* 98**,** 3148-3160.

Kaveh, R., Li, Y.-S., Ranjbar, S., Tehrani, R., Brueck, C. L. & Van Aken, B. 2013. Changes in Arabidopsis thaliana gene expression in response to silver nanoparticles and silver ions. *Environmental science & technology,* 47**,** 10637-10644.

Kim, T. H., Ho, H. W., Brown, C. L., Cresswell, S. L. & Li, Q. 2015. Amine-rich carbon nanodots as a fluorescence probe for methamphetamine precursors. *Analytical Methods,* 7**,** 6869-6876.

Koelmel, J., Leland, T., Wang, H., Amarasiriwardena, D. & Xing, B. 2013. Investigation of gold nanoparticles uptake and their tissue level distribution in rice plants by laser ablation-inductively coupled-mass spectrometry. *Environmental pollution,* 174**,** 222-228.

Kwak, S.-Y., Lew, T. T. S., Sweeney, C. J., Koman, V. B., Wong, M. H., Bohmert-Tatarev, K., Snell, K. D., Seo, J. S., Chua, N.-H. & Strano, M. S. 2019. Chloroplast-selective gene delivery and expression in planta using chitosan-complexed single-walled carbon nanotube carriers. *Nature nanotechnology***,** 1.

Lahiani, M. H., Chen, J., Irin, F., Puretzky, A. A., Green, M. J. & Khodakovskaya, M. V. 2015. Interaction of carbon nanohorns with plants: uptake and biological effects. *Carbon,* 81**,** 607-619.

Landa, P., Vankova, R., Andrlova, J., Hodek, J., Marsik, P., Storchova, H., White, J. C. & Vanek, T. 2012. Nanoparticle-specific changes in Arabidopsis thaliana gene expression after exposure to ZnO, TiO2, and fullerene soot. *Journal of hazardous materials,* 241**,** 55-62.

Li, H., Huang, J., Lu, F., Liu, Y., Song, Y., Sun, Y., Zhong, J., Huang, H., Wang, Y. & Li, S. 2018. Impacts of carbon dots on rice plants: boosting

the growth and improving the disease resistance. *ACS Applied Bio Materials,* 1**,** 663-672.

Li, H., Ye, X., Guo, X., Geng, Z. & Wang, G. 2016. Effects of surface ligands on the uptake and transport of gold nanoparticles in rice and tomato. *Journal of hazardous materials,* 314**,** 188-196.

Lin, S., Reppert, J., Hu, Q., Hudson, J. S., Reid, M. L., Ratnikova, T. A., Rao, A. M., Luo, H. & Ke, P. C. 2009. Uptake, translocation, and transmission of carbon nanomaterials in rice plants. *Small,* 5**,** 1128-1132.

Mondal, A., Basu, R., Das, S. & Nandy, P. 2011. Beneficial role of carbon nanotubes on mustard plant growth: an agricultural prospect. *Journal of Nanoparticle Research,* 13**,** 4519-4528.

Myers, S. S., Zanobetti, A., Kloog, I., Huybers, P., Leakey, A. D., Bloom, A. J., Carlisle, E., Dietterich, L. H., Fitzgerald, G. & Hasegawa, T. 2014. Increasing CO 2 threatens human nutrition. *Nature,* 510**,** 139-142.

Nair, R., Mohamed, M. S., Gao, W., Maekawa, T., Yoshida, Y., Ajayan, P. M. & Kumar, D. S. 2012. Effect of carbon nanomaterials on the germination and growth of rice plants. *Journal of nanoscience and nanotechnology,* 12**,** 2212-2220.

Qian, H., Peng, X., Han, X., Ren, J., Sun, L. & Fu, Z. 2013. Comparison of the toxicity of silver nanoparticles and silver ions on the growth of terrestrial plant model Arabidopsis thaliana. *Journal of environmental sciences,* 25**,** 1947-1956.

Sahoo, S. K., Dwivedi, G. K., Dey, P. & Praharaj, S. 2021. Green synthesised ZnO nanoparticles for sustainable production and nutritional biofortification of green gram. *Environmental Technology & Innovation***,** 101957.

Sawati, L., Ferrari, E., Stierhof, Y.-D. & Kemmerling, B. 2022. Molecular Effects of Biogenic Zinc Nanoparticles on the Growth and Development of Brassica napus L. Revealed by Proteomics and Transcriptomics. *Frontiers in Plant Science,* 13.

Singh, B., Natesan, S. K. A., Singh, B. & Usha, K. 2005. Improving zinc efficiency of cereals under zinc deficiency. *Current Science*, 36-44.

Swift, T. A., Fagan, D., Benito-Alifonso, D., Hill, S. A., Yallop, M. L., Oliver, T. A., Lawson, T., Galan, M. C. & Whitney, H. M. 2021. Photosynthesis and crop productivity are enhanced by glucose-functionalised carbon dots. *New Phytologist,* 229, 783-790.

Syu, Y.-Y., Hung, J.-H., Chen, J.-C. & Chuang, H.-W. 2014. Impacts of size and shape of silver nanoparticles on Arabidopsis plant growth and gene expression. *Plant Physiology and Biochemistry,* 83, 57-64.

Tiwari, D., Dasgupta-Schubert, N., Cendejas, L. V., Villegas, J., Montoya, L. C. & García, S. B. 2014. Interfacing carbon nanotubes (CNT) with plants: enhancement of growth, water and ionic nutrient uptake in maize (Zea mays) and implications for nanoagriculture. *Applied Nanoscience,* 4, 577-591.

Tripathi, S. & Sarkar, S. 2015. Influence of water soluble carbon dots on the growth of wheat plant. *Applied Nanoscience,* 5, 609-616.

Tripathi, S., Sonkar, S. K. & Sarkar, S. 2011. Growth stimulation of gram (Cicer arietinum) plant by water soluble carbon nanotubes. *Nanoscale,* 3, 1176-1181.

Wang, H., Zhang, M., Song, Y., Li, H., Huang, H., Shao, M., Liu, Y. & Kang, Z. 2018. Carbon dots promote the growth and photosynthesis of mung bean sprouts. *Carbon,* 136, 94-102.

Wang, Y., Chen, R., Hao, Y., Liu, H., Song, S. & Sun, G. 2017. Transcriptome analysis reveals differentially expressed genes (DEGs) related to lettuce (Lactuca sativa) treated by TiO2/ZnO nanoparticles. *Plant Growth Regulation,* 83**,** 13-25.

Xiao, L., Guo, H., Wang, S., Li, J., Wang, Y. & Xing, B. 2019. Carbon dots alleviate the toxicity of cadmium ions (Cd 2+) toward wheat seedlings. *Environmental Science: Nano,* 6**,** 1493-1506.

Xun, H., Ma, X., Chen, J., Yang, Z., Liu, B., Gao, X., Li, G., Yu, J., Wang, L. & Pang, J. 2017. Zinc oxide nanoparticle exposure triggers different gene expression patterns in maize shoots and roots. *Environmental Pollution,* 229**,** 479-488.

Zhang, C. L., Jiang, H. S., Gu, S. P., Zhou, X. H., Lu, Z. W., Kang, X. H., Yin, L. & Huang, J. 2019. Combination analysis of the physiology and transcriptome provides insights into the mechanism of silver nanoparticles phytotoxicity. *Environmental pollution,* 252**,** 1539-1549.

Zhang, H., Yue, M., Zheng, X., Xie, C., Zhou, H. & Li, L. 2017. Physiological effects of single-and multi-walled carbon nanotubes on rice seedlings. *IEEE Transactions on Nanobioscience,* 16**,** 563-570.

Zhao, A. Q., Tian, X. H., Cao, Y. X., Lu, X. C. & Liu, T. 2014. Comparison of soil and foliar zinc application for enhancing grain zinc content of wheat when grown on potentially zinc-deficient calcareous soils. *Journal of the Science of Food and Agriculture,* 94**,** 2016-2022.

References of Chapter 2:

Akmal, M., Younus, A., Wakeel, A., Jamil, Y. & Rashid, M. A. 2022. Synthesis and application of optimized ZnO nanoparticles for improving yield and Zn content of rice (Oryza sativa L.) grain. *Journal of Plant Nutrition*, 1-14.

Alloway, B. J. 2008. *Zinc in soils and crop nutrition*, International Zinc Association Brussels, Belgium.

Ashfaq, M., Verma, N. & Khan, S. 2017. Carbon nanofibers as a micronutrient carrier in plants: efficient translocation and controlled release of Cu nanoparticles. *Environmental Science: Nano, 4*, 138-148.

Baker, S. N. & Baker, G. A. 2010. Luminescent carbon nanodots: emergent nanolights. *Angewandte Chemie International Edition, 49*, 6726-6744.

Bala, R., Kalia, A. & Dhaliwal, S. S. 2019. Evaluation of efficacy of ZnO nanoparticles as remedial zinc nanofertilizer for rice. *Journal of Soil Science and Plant Nutrition, 19*, 379-389.

Baldoni, E., Frugis, G., Martinelli, F., Benny, J., Paffetti, D. & Buti, M. 2021. A comparative transcriptomic meta-analysis revealed conserved key genes and regulatory networks involved in drought tolerance in cereal crops. *International Journal of Molecular Sciences, 22*, 13062.

Bao, G., Ashraf, U., Wan, X., Zhou, Q., Li, S., Wang, C., He, L. & Tang, X. 2021. Transcriptomic analysis provides insights into foliar zinc application induced upregulation in 2-acetyl-1-pyrroline and related transcriptional regulatory mechanism in fragrant rice. *Journal of Agricultural and Food Chemistry, 69*, 11350-11360.

Bashir, K., Ishimaru, Y. & Nishizawa, N. K. 2012. Molecular mechanisms of zinc uptake and translocation in rice. *Plant and Soil, 361*, 189-201.

Begum, P., Ikhtiari, R. & Fugetsu, B. 2014. Potential impact of multi-walled carbon nanotubes exposure to the seedling stage of selected plant species. *Nanomaterials,* 4**,** 203-221.

Boonchuay, P., Cakmak, I., Rerkasem, B. & Prom-U-Thai, C. 2013. Effect of different foliar zinc application at different growth stages on seed zinc concentration and its impact on seedling vigor in rice. *Soil Science and Plant Nutrition,* 59**,** 180-188.

Boonyanitipong, P., Kositsup, B., Kumar, P., Baruah, S. & Dutta, J. 2011. Toxicity of ZnO and TiO2 nanoparticles on germinating rice seed Oryza sativa L. *International Journal of Bioscience, Biochemistry and Bioinformatics,* 1**,** 282.

Burklew, C. E., Ashlock, J., Winfrey, W. B. & Zhang, B. 2012. Effects of aluminum oxide nanoparticles on the growth, development, and microRNA expression of tobacco (Nicotiana tabacum). *PloS one,* 7**,** e34783.

Cakmak, I. 2008. Enrichment of cereal grains with zinc: agronomic or genetic biofortification? *Plant and soil,* 302**,** 1-17.

Cakmak, I., Pfeiffer, W. H. & Mcclafferty, B. 2010. Biofortification of durum wheat with zinc and iron. *Cereal Chemistry,* 87**,** 10-20.

Chandra, S., Pradhan, S., Mitra, S., Patra, P., Bhattacharya, A., Pramanik, P. & Goswami, A. 2014. High throughput electron transfer from carbon dots to chloroplast: a rationale of enhanced photosynthesis. *Nanoscale,* 6**,** 3647-3655.

Chen, J., Dou, R., Yang, Z., You, T., Gao, X. & Wang, L. 2018. Phytotoxicity and bioaccumulation of zinc oxide nanoparticles in rice (Oryza sativa L.). *Plant Physiology and Biochemistry,* 130**,** 604-612.

Chen, L., Wang, C., Li, H., Qu, X., Yang, S.-T. & Chang, X.-L. 2017. Bioaccumulation and toxicity of 13C-skeleton labeled graphene oxide in wheat. *Environmental science & technology,* 51**,** 10146-10153.

Chen, R., Ratnikova, T. A., Stone, M. B., Lin, S., Lard, M., Huang, G., Hudson, J. S. & Ke, P. C. 2010. Differential uptake of carbon nanoparticles by plant and mammalian cells. *Small,* 6**,** 612-617.

Clemens, S., Deinlein, U., Ahmadi, H., Höreth, S. & Uraguchi, S. 2013. Nicotianamine is a major player in plant Zn homeostasis. *Biometals,* 26**,** 623-632.

Coleman, J. E. 1992. Zinc proteins: enzymes, storage proteins, transcription factors, and replication proteins. *Annual review of biochemistry,* 61**,** 897-946.

Cui, S., Huang, F., Wang, J., Ma, X., Cheng, Y. & Liu, J. 2005. A proteomic analysis of cold stress responses in rice seedlings. *Proteomics,* 5**,** 3162-3172.

Cultivacegrowth.Com. 2019. *ZnACE* [Online]. CultivAce & KWS Distributing. Available: https://cultivacegrowth.com/blends-2/zn-ace-8-zinc-foliar-spray/ [Accessed 2019 - 09 - 13 2019].

Custom Agronomics. 2019. *Acetate-Based Nutrients* [Online]. Custom Agronomics, Inc,,. Available: http://www.customagronomics.com/ag/acetate/ [Accessed 10-09-2019].

Deng, C., Wang, Y., Navarro, G., Sun, Y., Cota-Ruiz, K., Hernandez-Viezcas, J. A., Niu, G., Li, C., White, J. C. & Gardea-Torresdey, J. 2022. Copper oxide (CuO) nanoparticles affect yield, nutritional quality, and auxin associated gene expression in weedy and cultivated rice (Oryza sativa L.) grains. *Science of the Total Environment,* 810**,** 152260.

Deshpande, P., Dapkekar, A., Oak, M., Paknikar, K. & Rajwade, J. 2018. Nanocarrier-mediated foliar zinc fertilization influences expression of metal homeostasis related genes in flag leaves and enhances gluten content in durum wheat. *PloS one,* 13**,** e0191035.

Deshpande, P., Dapkekar, A., Oak, M. D., Paknikar, K. M. & Rajwade, J. M. 2017. Zinc complexed chitosan/TPP nanoparticles: a promising micronutrient nanocarrier suited for foliar application. *Carbohydrate polymers,* 165**,** 394-401.

Du, W., Yang, J., Peng, Q., Liang, X. & Mao, H. 2019. Comparison study of zinc nanoparticles and zinc sulphate on wheat growth: From toxicity and zinc biofortification. *Chemosphere,* 227**,** 109-116.

Feng, Z.-M., Peng, G., Zhao, J.-H., Wang, G.-D., Zhang, H.-M., Cao, W.-L., Xiang, X., Zhang, Y.-F., Rong, H. & Chen, Z.-X. 2022. iTRAQ-based quantitative proteomics analysis of defense responses triggered by the pathogen Rhizoctonia solani infection in rice. *Journal of Integrative Agriculture,* 21**,** 139-152.

García-Sánchez, S., Bernales, I. & Cristobal, S. 2015. Early response to nanoparticles in the Arabidopsis transcriptome compromises plant defence and root-hair development through salicylic acid signalling. *BMC genomics,* 16**,** 341.

Ghasemi, M., Ghorban, N., Madani, H., Mobasser, H.-R. & Nouri, M.-Z. 2017. Effect of foliar application of zinc nano oxide on agronomic traits of two varieties of rice (Oryza sativa L.). *Crop Research,* 52**,** 195-201.

Ghoneim, A. M. 2016. Effect of different methods of Zn application on rice growth, yield and nutrients dynamics in plant and soil. *J. Agric. Ecol. Res. Int,* 6**,** 1-9.

Giraldo, J. P., Landry, M. P., Faltermeier, S. M., Mcnicholas, T. P., Iverson, N. M., Boghossian, A. A., Reuel, N. F., Hilmer, A. J., Sen, F. & Brew, J. A. 2014. Plant nanobionics approach to augment photosynthesis and biochemical sensing. *Nature materials,* 13**,** 400.

Gogos, A., Knauer, K. & Bucheli, T. D. 2012. Nanomaterials in plant protection and fertilization: current state, foreseen applications, and research priorities. *Journal of agricultural and food chemistry,* 60**,** 9781-9792.

Grotz, N. & Guerinot, M. L. 2006. Molecular aspects of Cu, Fe and Zn homeostasis in plants. *Biochimica et Biophysica Acta (BBA)-Molecular Cell Research,* 1763**,** 595-608.

Guo, K., Fu, D., Adeel, M., Shen, Y., Wang, K., Hao, Y., Bai, T., Wang, Y. & Rui, Y. 2022. Toxicities of nanomaterials and metals to rice under low atmospheric pressure. *Acta Physiologiae Plantarum,* 44**,** 58.

Habib, M. 2009. Effect of foliar application of Zn and Fe on wheat yield and quality. *African Journal of Biotechnology,* 8.

Hong, J., Wang, L., Sun, Y., Zhao, L., Niu, G., Tan, W., Rico, C. M., Peralta-Videa, J. R. & Gardea-Torresdey, J. L. 2016. Foliar applied nanoscale and microscale CeO2 and CuO alter cucumber (Cucumis sativus) fruit quality. *Science of The Total Environment,* 563**,** 904-911.

Hu, J., Jia, W., Wu, X., Zhang, H., Wang, Y., Liu, J., Yang, Y., Tao, S. & Wang, X. 2022. Carbon dots can strongly promote photosynthesis in lettuce (Lactuca sativa L.). *Environmental Science: Nano,* 9**,** 1530-1540.

Hussain, A., Ali, S., Rizwan, M., Ur Rehman, M. Z., Javed, M. R., Imran, M., Chatha, S. a. S. & Nazir, R. 2018. Zinc oxide nanoparticles alter the

wheat physiological response and reduce the cadmium uptake by plants. *Environmental Pollution,* 242**,** 1518-1526.

Ikhajiagbe, B., Igiebor, F. & Ogwu, M. 2021. Growth and yield performances of rice (Oryza sativa var. nerica) after exposure to biosynthesized nanoparticles. *Bulletin of the National Research Centre,* 45**,** 1-13.

Ishimaru, Y., Bashir, K. & Nishizawa, N. K. 2011. Zn uptake and translocation in rice plants. *Rice,* 4**,** 21-27.

Itroutwar, P. D., Govindaraju, K., Tamilselvan, S., Kannan, M., Raja, K. & Subramanian, K. S. 2020. Seaweed-based biogenic ZnO nanoparticles for improving agro-morphological characteristics of rice (Oryza sativa L.). *Journal of plant growth regulation,* 39**,** 717-728.

Jiang, W., Struik, P., Van Keulen, H., Zhao, M., Jin, L. & Stomph, T. 2008. Does increased zinc uptake enhance grain zinc mass concentration in rice? *Annals of Applied Biology,* 153**,** 135-147.

Kashyap, P. L., Xiang, X. & Heiden, P. 2015. Chitosan nanoparticle based delivery systems for sustainable agriculture. *International journal of biological macromolecules,* 77**,** 36-51.

Kaveh, R., Li, Y.-S., Ranjbar, S., Tehrani, R., Brueck, C. L. & Van Aken, B. 2013. Changes in Arabidopsis thaliana gene expression in response to silver nanoparticles and silver ions. *Environmental science & technology,* 47**,** 10637-10644.

Khatri, K. & Rathore, M. S. 2018. Plant Nanobionics and Its Applications for Developing Plants with Improved Photosynthetic Capacity. *Photosynthesis-From Its Evolution to Future Improvements in Photosynthetic Efficiency Using Nanomaterials.* IntechOpen.

Kim, T. H. 2015. *synthesis and applications of carbon nanodots.* Doctor of Philosophy, Griffith University.

Kim, T. H., Sirdaarta, J. P., Zhang, Q., Eftekhari, E., John, J. S., Kennedy, D., Cock, I. E. & Li, Q. 2018. Selective toxicity of hydroxyl-rich carbon nanodots for cancer research. *Nano Research,* 11**,** 2204-2216.

Kwak, S.-Y., Giraldo, J. P., Wong, M. H., Koman, V. B., Lew, T. T. S., Ell, J., Weidman, M. C., Sinclair, R. M., Landry, M. P. & Tisdale, W. A. 2017. A nanobionic light-emitting plant. *Nano letters,* 17**,** 7951-7961.

Kwak, S.-Y., Lew, T. T. S., Sweeney, C. J., Koman, V. B., Wong, M. H., Bohmert-Tatarev, K., Snell, K. D., Seo, J. S., Chua, N.-H. & Strano, M. S. 2019. Chloroplast-selective gene delivery and expression in planta using chitosan-complexed single-walled carbon nanotube carriers. *Nature nanotechnology***,** 1.

Lahiani, M. H., Chen, J., Irin, F., Puretzky, A. A., Green, M. J. & Khodakovskaya, M. V. 2015. Interaction of carbon nanohorns with plants: uptake and biological effects. *Carbon,* 81**,** 607-619.

Li, C. & Yan, B. 2020a. Opportunities and challenges of phyto-nanotechnology. *Environmental Science: Nano,* 7**,** 2863-2874.

Li, H., Huang, J., Lu, F., Liu, Y., Song, Y., Sun, Y., Zhong, J., Huang, H., Wang, Y. & Li, S. 2018a. Impacts of carbon dots on rice plants: boosting the growth and improving the disease resistance. *ACS Applied Bio Materials,* 1**,** 663-672.

Li, H., Ye, X., Guo, X., Geng, Z. & Wang, G. 2016a. Effects of surface ligands on the uptake and transport of gold nanoparticles in rice and tomato. *Journal of hazardous materials,* 314**,** 188-196.

Li, W., Wu, S., Zhang, H., Zhang, X., Zhuang, J., Hu, C., Liu, Y., Lei, B., Ma, L. & Wang, X. 2018b. Enhanced biological photosynthetic efficiency using light-harvesting engineering with dual-emissive carbon dots. *Advanced Functional Materials,* 28**,** 1804004.

Li, W., Zheng, Y., Zhang, H., Liu, Z., Su, W., Chen, S., Liu, Y., Zhuang, J. & Lei, B. 2016b. Phytotoxicity, uptake, and translocation of fluorescent carbon dots in mung bean plants. *ACS applied materials & interfaces,* 8**,** 19939-19945.

Li, X., Mu, L. & Hu, X. 2018c. Integrating proteomics, metabolomics and typical analysis to investigate the uptake and oxidative stress of graphene oxide and polycyclic aromatic hydrocarbons. *Environmental Science: Nano,* 5**,** 115-129.

Li, Y., Gao, J., Xu, X., Wu, Y., Zhuang, J., Zhang, X., Zhang, H., Lei, B., Zheng, M. & Liu, Y. 2020b. Carbon dots as a protective agent alleviating abiotic stress on rice (Oryza sativa L.) through promoting nutrition assimilation and the defense system. *ACS applied materials & interfaces,* 12**,** 33575-33585.

Li, Y., Pan, X., Xu, X., Wu, Y., Zhuang, J., Zhang, X., Zhang, H., Lei, B., Hu, C. & Liu, Y. 2021a. Carbon dots as light converter for plant photosynthesis: augmenting light coverage and quantum yield effect. *Journal of Hazardous Materials,* 410**,** 124534.

Li, Y., Xu, X., Lei, B., Zhuang, J., Zhang, X., Hu, C., Cui, J. & Liu, Y. 2021b. Magnesium-nitrogen co-doped carbon dots enhance plant growth through multifunctional regulation in photosynthesis. *Chemical Engineering Journal,* 422**,** 130114.

Lin, D. & Xing, B. 2007. Phytotoxicity of nanoparticles: inhibition of seed germination and root growth. *Environmental pollution,* 150**,** 243-250.

Lin, S., Reppert, J., Hu, Q., Hudson, J. S., Reid, M. L., Ratnikova, T. A., Rao, A. M., Luo, H. & Ke, P. C. 2009. Uptake, translocation, and transmission of carbon nanomaterials in rice plants. *Small,* 5**,** 1128-1132.

Liu, Q., Chen, B., Wang, Q., Shi, X., Xiao, Z., Lin, J. & Fang, X. 2009. Carbon nanotubes as molecular transporters for walled plant cells. *Nano letters,* 9**,** 1007-1010.

Liu, R. & Lal, R. 2014. Synthetic apatite nanoparticles as a phosphorus fertilizer for soybean (Glycine max). *Scientific reports,* 4**,** 5686.

Liu, R. & Lal, R. 2015. Potentials of engineered nanoparticles as fertilizers for increasing agronomic productions. *Science of the Total Environment,* 514**,** 131-139.

López-Moreno, M. L., De La Rosa, G., Hernández-Viezcas, J. Á., Castillo-Michel, H., Botez, C. E., Peralta-Videa, J. R. & Gardea-Torresdey, J. L. 2010a. Evidence of the differential biotransformation and genotoxicity of ZnO and CeO2 nanoparticles on soybean (Glycine max) plants. *Environmental science & technology,* 44**,** 7315-7320.

López-Moreno, M. L., De La Rosa, G., Hernández-Viezcas, J. A., Peralta-Videa, J. R. & Gardea-Torresdey, J. L. 2010b. XAS corroboration of the uptake and storage of CeO2 nanoparticles and assessment of their differential toxicity in four edible plant species. *Journal of agricultural and food chemistry,* 58**,** 3689.

Lu, L., Tian, S., Liao, H., Zhang, J., Yang, X., Labavitch, J. M. & Chen, W. 2013. Analysis of metal element distributions in rice (Oryza sativa L.) seeds and relocation during germination based on X-ray fluorescence imaging of Zn, Fe, K, Ca, and Mn. *PLoS One,* 8**,** e57360.

Mabesa, R., Impa, S., Grewal, D. & Johnson-Beebout, S. 2013. Contrasting grain-Zn response of biofortification rice (Oryza sativa L.) breeding lines to foliar Zn application. *Field crops research,* 149**,** 223-233.

Milenković, I., BorišEv, M., Zhou, Y., Spasić, S. Z., Leblanc, R. M. & Radotić, K. 2021. Photosynthesis enhancement in maize via nontoxic orange

carbon dots. *Journal of agricultural and food chemistry,* 69**,** 5446-5451.

Mohammadi-Dehcheshmeh, M., Niazi, A., Ebrahimi, M., Tahsili, M., Nurollah, Z., Ebrahimi Khaksefid, R., Ebrahimi, M. & Ebrahimie, E. 2018. Unified transcriptomic signature of arbuscular mycorrhiza colonization in roots of Medicago truncatula by integration of machine learning, promoter analysis, and direct merging meta-analysis. *Frontiers in Plant Science,* 9**,** 1550.

Muthayya, S., Sugimoto, J. D., Montgomery, S. & Maberly, G. F. 2014. An overview of global rice production, supply, trade, and consumption. *Annals of the new york Academy of Sciences,* 1324**,** 7-14.

Nair, P. M. G. & Chung, I. M. 2014. Physiological and molecular level effects of silver nanoparticles exposure in rice (Oryza sativa L.) seedlings. *Chemosphere,* 112**,** 105-113.

Nair, R., Mohamed, M. S., Gao, W., Maekawa, T., Yoshida, Y., Ajayan, P. M. & Kumar, D. S. 2012. Effect of carbon nanomaterials on the germination and growth of rice plants. *Journal of nanoscience and nanotechnology,* 12**,** 2212-2220.

Nakandalage, N., Nicolas, M., Norton, R. M., Hirotsu, N., Milham, P. J. & Seneweera, S. 2016. Improving rice zinc biofortification success rates through genetic and crop management approaches in a changing environment. *Frontiers in plant science,* 7**,** 764.

National Institutes of Health, Office of Dietary Supplements,. 2019. *Zinc; Fact Sheet for Health Professionals* [Online]. USA: USA.gov. Available: https://ods.od.nih.gov/factsheets/Zinc-HealthProfessional/ [Accessed 2019 - 09 - 13 2019].

Neilson, K. A., Mariani, M. & Haynes, P. A. 2011. Quantitative proteomic analysis of cold-responsive proteins in rice. *Proteomics,* 11**,** 1696-1706.

Nezamivand-Chegini, M., Metzger, S., Moghadam, A., Tahmasebi, A., Koprivova, A., Eshghi, S., Mohammadi-Dehchesmeh, M., Kopriva, S., Niazi, A. & Ebrahimie, E. 2023. Integration of transcriptomic and metabolomic analyses provides insights into response mechanisms to nitrogen and phosphorus deficiencies in soybean. *Plant Science,* 326**,** 111498.

Nguyen, V. Q., Sreewongchai, T., Siangliw, M., Roytrakul, S. & Yokthongwattana, C. 2022. Comparative proteomic analysis of chromosome segment substitution lines of Thai jasmine rice KDML105 under short-term salinity stress. *Planta,* 256**,** 12.

Panda, S. 2017. Physiological impact of Zinc nanoparticle on germination of rice (Oryza sativa L) seed. *J Plant Sci Phytopathol,* 1**,** 062-070.

Peng, C., Xia, Y., Zhang, W., Wu, Y. & Shi, J. 2022. Proteomic Analysis Unravels Response and Antioxidation Defense Mechanism of Rice Plants to Copper Oxide Nanoparticles: Comparison with Bulk Particles and Dissolved Cu Ions. *ACS Agricultural Science & Technology,* 2**,** 671-683.

Qian, H., Peng, X., Han, X., Ren, J., Sun, L. & Fu, Z. 2013. Comparison of the toxicity of silver nanoparticles and silver ions on the growth of terrestrial plant model Arabidopsis thaliana. *Journal of environmental sciences,* 25**,** 1947-1956.

Rico, C. M., Majumdar, S., Duarte-Gardea, M., Peralta-Videa, J. R. & Gardea-Torresdey, J. L. 2011. Interaction of nanoparticles with edible plants and their possible implications in the food chain. *Journal of agricultural and food chemistry,* 59**,** 3485-3498.

Satoh-Nagasawa, N., Mori, M., Nakazawa, N., Kawamoto, T., Nagato, Y., Sakurai, K., Takahashi, H., Watanabe, A. & Akagi, H. 2011. Mutations in rice (Oryza sativa) heavy metal ATPase 2 (OsHMA2) restrict the translocation of zinc and cadmium. *Plant and Cell Physiology,* 53**,** 213-224.

Sawati, L., Ferrari, E., Stierhof, Y.-D. & Kemmerling, B. 2022. Molecular Effects of Biogenic Zinc Nanoparticles on the Growth and Development of Brassica napus L. Revealed by Proteomics and Transcriptomics. *Frontiers in Plant Science,* 13.

Seck, P. A., Diagne, A., Mohanty, S. & Wopereis, M. C. 2012. Crops that feed the world 7: Rice. *Food security,* 4**,** 7-24.

Shahzad, R., Jamil, S., Ahmad, S., Nisar, A., Khan, S., Amina, Z., Kanwal, S., Aslam, H. M. U., Gill, R. A. & Zhou, W. 2021. Biofortification of cereals and pulses using new breeding techniques: current and future perspectives. *Frontiers in nutrition***,** 665.

Shen, C. X., Zhang, Q. F., Li, J., Bi, F. C. & Yao, N. 2010. Induction of programmed cell death in Arabidopsis and rice by single-wall carbon nanotubes. *American Journal of Botany,* 97**,** 1602-1609.

Shiri, Y., Solouki, M., Ebrahimie, E., Emamjomeh, A. & Zahiri, J. 2018. Unraveling the transcriptional complexity of compactness in sistan grape cluster. *Plant Science,* 270**,** 198-208.

Sinclair, S. A. & Krämer, U. 2012. The zinc homeostasis network of land plants. *Biochimica et Biophysica Acta (BBA)-Molecular Cell Research,* 1823**,** 1553-1567.

Singh, A., Sengar, R. S., Rajput, V. D., Minkina, T. & Singh, R. K. 2022. Zinc Oxide Nanoparticles Improve Salt Tolerance in Rice Seedlings by

Improving Physiological and Biochemical Indices. *Agriculture,* 12**,** 1014.

Song, U., Jun, H., Waldman, B., Roh, J., Kim, Y., Yi, J. & Lee, E. J. 2013. Functional analyses of nanoparticle toxicity: a comparative study of the effects of TiO2 and Ag on tomatoes (Lycopersicon esculentum). *Ecotoxicology and environmental safety,* 93**,** 60-67.

Song, Y., Jiang, M., Zhang, H. & Li, R. 2021. Zinc oxide nanoparticles alleviate chilling stress in rice (Oryza Sativa L.) by regulating antioxidative system and chilling response transcription factors. *Molecules,* 26**,** 2196.

Sperotto, R. A. 2013. Zn/Fe remobilization from vegetative tissues to rice seeds: should I stay or should I go? Ask Zn/Fe supply! *Frontiers in plant science,* 4**,** 464.

Štefanić, P. P., Cvjetko, P., Biba, R., Domijan, A.-M., Letofsky-Papst, I., Tkalec, M., Šikić, S., Cindrić, M. & Balen, B. 2018. Physiological, ultrastructural and proteomic responses of tobacco seedlings exposed to silver nanoparticles and silver nitrate. *Chemosphere,* 209**,** 640-653.

Subbaiah, L. V., Prasad, T. N. V. K. V., Krishna, T. G., Sudhakar, P., Reddy, B. R. & Pradeep, T. 2016. Novel effects of nanoparticulate delivery of zinc on growth, productivity, and zinc biofortification in maize (Zea mays L.). *Journal of agricultural and food chemistry,* 64**,** 3778-3788.

Suzuki, M., Tsukamoto, T., Inoue, H., Watanabe, S., Matsuhashi, S., Takahashi, M., Nakanishi, H., Mori, S. & Nishizawa, N. K. 2008. Deoxymugineic acid increases Zn translocation in Zn-deficient rice plants. *Plant molecular biology,* 66**,** 609-617.

Swift, T. A., Fagan, D., Benito-Alifonso, D., Hill, S. A., Yallop, M. L., Oliver, T. A., Lawson, T., Galan, M. C. & Whitney, H. M. 2021. Photosynthesis

and crop productivity are enhanced by glucose-functionalised carbon dots. *New Phytologist,* 229**,** 783-790.

Takahashi, R., Bashir, K., Ishimaru, Y., Nishizawa, N. K. & Nakanishi, H. 2012. The role of heavy-metal ATPases, HMAs, in zinc and cadmium transport in rice. *Plant signaling & behavior,* 7**,** 1605-1607.

Takatsuji, H. 1998. Zinc-finger transcription factors in plants. *Cellular and Molecular Life Sciences CMLS,* 54**,** 582-596.

Tan, X.-M., Lin, C. & Fugetsu, B. 2009. Studies on toxicity of multi-walled carbon nanotubes on suspension rice cells. *Carbon,* 47**,** 3479-3487.

The Andersons. 2019. *MicroSolutions* [Online]. The Andersons, Inc. . Available: https://andersonsplantnutrient.com/agriculture/products/microsolutions [Accessed 2019 - 09 - 13 2019].

The International Rice Commission. 2002. *Nutritional Contribution of Rice: Impact of biotechnology and Biodiversity in Rice-consuming Countries* [Online]. Food and Agriculture Organization of the United Nations. Available: http://www.fao.org/3/Y6618E/Y6618E00.htm [Accessed 2019 - 11 - 30 2019].

Torney, F., Trewyn, B. G., Lin, V. S.-Y. & Wang, K. 2007. Mesoporous silica nanoparticles deliver DNA and chemicals into plants. *Nature nanotechnology,* 2**,** 295.

Tripathi, D. K., Singh, S., Singh, S., Pandey, R., Singh, V. P., Sharma, N. C., Prasad, S. M., Dubey, N. K. & Chauhan, D. K. 2017. An overview on manufactured nanoparticles in plants: uptake, translocation, accumulation and phytotoxicity. *Plant Physiology and Biochemistry,* 110**,** 2-12.

Tripathi, S. & Sarkar, S. 2015. Influence of water soluble carbon dots on the growth of wheat plant. *Applied Nanoscience,* 5**,** 609-616.

Tuerhong, M., Yang, X. & Xue-Bo, Y. 2017. Review on carbon dots and their applications. *Chinese Journal of Analytical Chemistry,* 45**,** 139-150.

Tumburu, L., Andersen, C. P., Rygiewicz, P. T. & Reichman, J. R. 2015. Phenotypic and genomic responses to titanium dioxide and cerium oxide nanoparticles in Arabidopsis germinants. *Environmental toxicology and chemistry,* 34**,** 70-83.

Vannini, C., Domingo, G., Onelli, E., De Mattia, F., Bruni, I., Marsoni, M. & Bracale, M. 2014. Phytotoxic and genotoxic effects of silver nanoparticles exposure on germinating wheat seedlings. *Journal of plant physiology,* 171**,** 1142-1148.

Vasconcelos, M., Datta, K., Oliva, N., Khalekuzzaman, M., Torrizo, L., Krishnan, S., Oliveira, M., Goto, F. & Datta, S. K. 2003. Enhanced iron and zinc accumulation in transgenic rice with the ferritin gene. *Plant Science,* 164**,** 371-378.

Wang, H., Zhang, M., Song, Y., Li, H., Huang, H., Shao, M., Liu, Y. & Kang, Z. 2018. Carbon dots promote the growth and photosynthesis of mung bean sprouts. *Carbon,* 136**,** 94-102.

Wang, P., Lombi, E., Sun, S., Scheckel, K. G., Malysheva, A., Mckenna, B. A., Menzies, N. W., Zhao, F.-J. & Kopittke, P. M. 2017a. Characterizing the uptake, accumulation and toxicity of silver sulfide nanoparticles in plants. *Environmental Science: Nano,* 4**,** 448-460.

Wang, S., Liu, H., Zhang, Y. & Xin, H. 2015. The effect of CuO NPs on reactive oxygen species and cell cycle gene expression in roots of rice. *Environmental Toxicology and Chemistry,* 34**,** 554-561.

Wang, Y., Chen, R., Hao, Y., Liu, H., Song, S. & Sun, G. 2017b. Transcriptome analysis reveals differentially expressed genes (DEGs) related to lettuce (Lactuca sativa) treated by TiO2/ZnO nanoparticles. *Plant Growth Regulation,* 83**,** 13-25.

Welch, R. M. & Graham, R. D. 2002. Breeding crops for enhanced micronutrient content. *Food Security in Nutrient-Stressed Environments: Exploiting Plants' Genetic Capabilities.* Springer.

Wong, M. H., P Misra, R., Giraldo, J., Kwak, S.-Y., Son, Y., Landry, M., Swan, J., Blankschtein, D. & S Strano, M. 2016. *Lipid Exchange Envelope Penetration (LEEP) of Nanoparticles for Plant Engineering: A Universal Localization Mechanism*.

Wu, B., Zhu, L. & Le, X. C. 2017. Metabolomics analysis of TiO2 nanoparticles induced toxicological effects on rice (Oryza sativa L.). *Environmental Pollution,* 230**,** 302-310.

Xun, H., Ma, X., Chen, J., Yang, Z., Liu, B., Gao, X., Li, G., Yu, J., Wang, L. & Pang, J. 2017. Zinc oxide nanoparticle exposure triggers different gene expression patterns in maize shoots and roots. *Environmental Pollution,* 229**,** 479-488.

Yan, S., Zhang, H., Huang, Y., Tan, J., Wang, P., Wang, Y., Hou, H., Huang, J. & Li, L. 2016. Single-wall and multi-wall carbon nanotubes promote rice root growth by eliciting the similar molecular pathways and epigenetic regulation. *IET nanobiotechnology,* 10**,** 222-229.

Yang, G., Yuan, H., Ji, H., Liu, H., Zhang, Y., Wang, G., Chen, L. & Guo, Z. 2021. Effect of ZnO nanoparticles on the productivity, Zn biofortification, and nutritional quality of rice in a life cycle study. *Plant Physiology and Biochemistry,* 163**,** 87-94.

Yang, H., Wang, C., Chen, F., Yue, L., Cao, X., Li, J., Zhao, X., Wu, F., Wang, Z. & Xing, B. 2022. Foliar carbon dot amendment modulates carbohydrate metabolism, rhizospheric properties and drought tolerance in maize seedling. *Science of the total environment,* 809**,** 151105.

Yang, Y., Chen, H., Zhao, B. & Bao, X. 2004. Size control of ZnO nanoparticles via thermal decomposition of zinc acetate coated on organic additives. *Journal of crystal growth,* 263**,** 447-453.

Yasmeen, F., Raja, N. I., Mustafa, G., Sakata, K. & Komatsu, S. 2016. Quantitative proteomic analysis of post-flooding recovery in soybean root exposed to aluminum oxide nanoparticles. *Journal of proteomics,* 143**,** 136-150.

Zhang, C. L., Jiang, H. S., Gu, S. P., Zhou, X. H., Lu, Z. W., Kang, X. H., Yin, L. & Huang, J. 2019. Combination analysis of the physiology and transcriptome provides insights into the mechanism of silver nanoparticles phytotoxicity. *Environmental pollution,* 252**,** 1539-1549.

Zhang, H., Yue, M., Zheng, X., Xie, C., Zhou, H. & Li, L. 2017. Physiological effects of single-and multi-walled carbon nanotubes on rice seedlings. *IEEE Transactions on Nanobioscience,* 16**,** 563-570.

Zhang, P., Guo, Z., Luo, W., Monikh, F. A., Xie, C., Valsami-Jones, E., Lynch, I. & Zhang, Z. 2020. Graphene oxide-induced pH alteration, iron overload, and subsequent oxidative damage in rice (Oryza sativa L.): A new mechanism of nanomaterial phytotoxicity. *Environmental science & technology,* 54**,** 3181-3190.

Zhao, A. Q., Tian, X. H., Cao, Y. X., Lu, X. C. & Liu, T. 2014. Comparison of soil and foliar zinc application for enhancing grain zinc content of wheat when grown on potentially zinc-deficient calcareous soils. *Journal of the Science of Food and Agriculture,* 94**,** 2016-2022.

References of Chapter 3:

Akmal, M., Younus, A., Wakeel, A., Jamil, Y. & Rashid, M. A. 2022. Synthesis and application of optimized ZnO nanoparticles for improving yield and Zn content of rice (Oryza sativa L.) grain. Journal of Plant Nutrition, 1-14.

Alloway, B. J. 2008. Zinc in soils and crop nutrition, International Zinc Association Brussels, Belgium.

Bala, R., Kalia, A. & Dhaliwal, S. S. 2019. Evaluation of efficacy of ZnO nanoparticles as remedial zinc nanofertilizer for rice. Journal of Soil Science and Plant Nutrition, 19, 379-389.

Begum, M. C., Islam, M., Sarkar, M. R., Azad, M. a. S., Huda, A. N. & Kabir, A. H. 2016. Auxin signaling is closely associated with Zn-efficiency in rice (Oryza sativa L.). Journal of Plant Interactions, 11, 124-129.

Begum, P., Ikhtiari, R. & Fugetsu, B. 2014. Potential impact of multi-walled carbon nanotubes exposure to the seedling stage of selected plant species. Nanomaterials, 4, 203-221.

Begum, P., Ikhtiari, R., Fugetsu, B., Matsuoka, M., Akasaka, T. & Watari, F. 2012. Phytotoxicity of multi-walled carbon nanotubes assessed by selected plant species in the seedling stage. Applied Surface Science, 262, 120-124.

Castillo-González, J., Ojeda-Barrios, D., Hernández-Rodríguez, A., González-Franco, A. C., Robles-Hernández, L. & López-Ochoa, G. R. 2018. Zinc Metalloenzymes in Plants. Interciencia, 43, 242-248.

Deshpande, P., Dapkekar, A., Oak, M. D., Paknikar, K. M. & Rajwade, J. M. 2017. Zinc complexed chitosan/TPP nanoparticles: a promising micronutrient nanocarrier suited for foliar application. Carbohydrate polymers, 165, 394-401.

Dimkpa, C. O., White, J. C., Elmer, W. H. & Gardea-Torresdey, J. 2017. Nanoparticle and ionic Zn promote nutrient loading of sorghum grain under low NPK fertilization. Journal of agricultural and food chemistry, 65, 8552-8559.

Ding, Y., Di, X., Norton, G. J., Beesley, L., Yin, X., Zhang, Z. & Zhi, S. 2020. Selenite Foliar Application Alleviates Arsenic Uptake, Accumulation, Migration and Increases Photosynthesis of Different Upland Rice Varieties. International Journal of Environmental Research and Public Health, 17, 3621.

Elmer, P. 1996. Analytical methods for atomic absorption spectroscopy. 1996. The Perkin-Elmer Corporation. Branford, Connecticut (USA).

Evans, J. R. & Santiago, L. S. 2014. PrometheusWiki gold leaf protocol: gas exchange using LI-COR 6400. Functional Plant Biology, 41, 223-226.

Ghasemi, M., Ghorban, N., Madani, H., Mobasser, H.-R. & Nouri, M.-Z. 2017. Effect of foliar application of zinc nano oxide on agronomic traits of two varieties of rice (Oryza sativa L.). Crop Research, 52, 195-201.

Hao, Y., Ma, C., Zhang, Z., Song, Y., Cao, W., Guo, J., Zhou, G., Rui, Y., Liu, L. & Xing, B. 2018. Carbon nanomaterials alter plant physiology and soil bacterial community composition in a rice-soil-bacterial ecosystem. Environmental pollution, 232, 123-136.

Hao, Y., Yu, F., Lv, R., Ma, C., Zhang, Z., Rui, Y., Liu, L., Cao, W. & Xing, B. 2016. Carbon nanotubes filled with different ferromagnetic alloys affect the growth and development of rice seedlings by changing the C: N ratio and plant hormones concentrations. PLoS One, 11, e0157264.

Hussain, A., Ali, S., Rizwan, M., Ur Rehman, M. Z., Javed, M. R., Imran, M., Chatha, S. a. S. & Nazir, R. 2018. Zinc oxide nanoparticles alter the

wheat physiological response and reduce the cadmium uptake by plants. Environmental Pollution, 242, 1518-1526.

Hussain, A., Ali, S., Rizwan, M., Ur Rehman, M. Z., Qayyum, M. F., Wang, H. & Rinklebe, J. 2019. Responses of wheat (Triticum aestivum) plants grown in a Cd contaminated soil to the application of iron oxide nanoparticles. Ecotoxicology and environmental safety, 173, 156-164.

Itroutwar, P. D., Govindaraju, K., Tamilselvan, S., Kannan, M., Raja, K. & Subramanian, K. S. 2020. Seaweed-based biogenic ZnO nanoparticles for improving agro-morphological characteristics of rice (Oryza sativa L.). Journal of plant growth regulation, 39, 717-728.

Kabir, A. H., Hossain, M. M., Khatun, M. A., Sarkar, M. R. & Haider, S. A. 2017. Biochemical and molecular mechanisms associated with Zn deficiency tolerance and signaling in rice (Oryza sativa L.). Journal of Plant Interactions, 12, 447-456.

Khush, G. S. 2005. IR varieties and their impact, Int. Rice Res. Inst.

Kim, T. H., Ho, H. W., Brown, C. L., Cresswell, S. L. & Li, Q. 2015. Amine-rich carbon nanodots as a fluorescence probe for methamphetamine precursors. Analytical Methods, 7, 6869-6876.

Koelmel, J., Leland, T., Wang, H., Amarasiriwardena, D. & Xing, B. 2013. Investigation of gold nanoparticles uptake and their tissue level distribution in rice plants by laser ablation-inductively coupled-mass spectrometry. Environmental pollution, 174, 222-228.

Lee, S. M., Raja, P. M., Esquenazi, G. L. & Barron, A. R. 2018. Effect of raw and purified carbon nanotubes and iron oxide nanoparticles on the growth of wheatgrass prepared from the cotyledons of common wheat (triticum aestivum). Environmental Science: Nano, 5, 103-114.

Li, H., Huang, J., Lu, F., Liu, Y., Song, Y., Sun, Y., Zhong, J., Huang, H., Wang, Y. & Li, S. 2018. Impacts of carbon dots on rice plants: boosting the growth and improving the disease resistance. ACS Applied Bio Materials, 1, 663-672.

Li, H., Ye, X., Guo, X., Geng, Z. & Wang, G. 2016. Effects of surface ligands on the uptake and transport of gold nanoparticles in rice and tomato. Journal of hazardous materials, 314, 188-196.

Liu, J., Hou, H., Zhao, L., Sun, Z. & Li, H. 2020. Protective Effect of foliar application of sulfur on photosynthesis and antioxidative defense system of rice under the stress of Cd. Science of The Total Environment, 710, 136230.

Luo, H., He, L., Du, B., Wang, Z., Zheng, A., Lai, R. & Tang, X. 2019. Foliar application of selenium (Se) at heading stage induces regulation of photosynthesis, yield formation, and quality characteristics in fragrant rice. PHOTOSYNTHETICA, 57, 1007-1014.

Ma, Q., Yue, L.-J., Zhang, J.-L., Wu, G.-Q., Bao, A.-K. & Wang, S.-M. 2012. Sodium chloride improves photosynthesis and water status in the succulent xerophyte Zygophyllum xanthoxylum. Tree Physiology, 32, 4-13.

Mae, T. & Ohira, K. 1981. The remobilization of nitrogen related to leaf growth and senescence in rice plants (Oryza sativa L.). Plant and cell physiology, 22, 1067-1074.

Moss, D. N. & Rawlins, S. L. 1963. Concentration of carbon dioxide inside leaves. Nature, 197, 1320-1321.

Naher, T., Sarkar, M., Kabir, A., Haider, S. & Paul, N. 2014. Screening of Zn-efficient rice through hydroponic culture. Plant Environ Dev, 3, 14-18.

Nair, P. M. G. & Chung, I. M. 2014. Physiological and molecular level effects of silver nanoparticles exposure in rice (Oryza sativa L.) seedlings. Chemosphere, 112, 105-113.

Nair, R., Mohamed, M. S., Gao, W., Maekawa, T., Yoshida, Y., Ajayan, P. M. & Kumar, D. S. 2012. Effect of carbon nanomaterials on the germination and growth of rice plants. Journal of nanoscience and nanotechnology, 12, 2212-2220.

Panda, S. 2017. Physiological impact of Zinc nanoparticle on germination of rice (Oryza sativa L) seed. J Plant Sci Phytopathol, 1, 062-070.

Sahoo, S. K., Dwivedi, G. K., Dey, P. & Praharaj, S. 2021. Green synthesised ZnO nanoparticles for sustainable production and nutritional biofortification of green gram. Environmental Technology & Innovation, 101957.

Saxena, M., Maity, S. & Sarkar, S. 2014. Carbon nanoparticles in 'biochar'boost wheat (Triticum aestivum) plant growth. Rsc Advances, 4, 39948-39954.

Singh, A., Sengar, R. S., Rajput, V. D., Minkina, T. & Singh, R. K. 2022. Zinc Oxide Nanoparticles Improve Salt Tolerance in Rice Seedlings by Improving Physiological and Biochemical Indices. Agriculture, 12, 1014.

Subbaiah, L. V., Prasad, T. N. V. K. V., Krishna, T. G., Sudhakar, P., Reddy, B. R. & Pradeep, T. 2016. Novel effects of nanoparticulate delivery of zinc on growth, productivity, and zinc biofortification in maize (Zea mays L.). Journal of agricultural and food chemistry, 64, 3778-3788.

Swift, T. A., Fagan, D., Benito-Alifonso, D., Hill, S. A., Yallop, M. L., Oliver, T. A., Lawson, T., Galan, M. C. & Whitney, H. M. 2021. Photosynthesis

and crop productivity are enhanced by glucose-functionalised carbon dots. New Phytologist, 229, 783-790.

Thuesombat, P., Hannongbua, S., Akasit, S. & Chadchawan, S. 2014. Effect of silver nanoparticles on rice (Oryza sativa L. cv. KDML 105) seed germination and seedling growth. Ecotoxicology and environmental safety, 104, 302-309.

Tripathi, S. & Sarkar, S. 2015. Influence of water soluble carbon dots on the growth of wheat plant. Applied Nanoscience, 5, 609-616.

Tripathi, S., Sonkar, S. K. & Sarkar, S. 2011. Growth stimulation of gram (Cicer arietinum) plant by water soluble carbon nanotubes. Nanoscale, 3, 1176-1181.

Wang, H., Zhang, M., Song, Y., Li, H., Huang, H., Shao, M., Liu, Y. & Kang, Z. 2018. Carbon dots promote the growth and photosynthesis of mung bean sprouts. Carbon, 136, 94-102.

Yang, G., Yuan, H., Ji, H., Liu, H., Zhang, Y., Wang, G., Chen, L. & Guo, Z. 2021. Effect of ZnO nanoparticles on the productivity, Zn biofortification, and nutritional quality of rice in a life cycle study. Plant Physiology and Biochemistry, 163, 87-94.

Zhang, H., Yue, M., Zheng, X., Xie, C., Zhou, H. & Li, L. 2017. Physiological effects of single-and multi-walled carbon nanotubes on rice seedlings. IEEE Transactions on Nanobioscience, 16, 563-570.

References of Chapter 4:

Adil, M., Bashir, S., Bashir, S., Aslam, Z., Ahmad, N., Younas, T., Asghar, R. M. A., Alkahtani, J., Dwiningsih, Y. & Elshikh, M. S. 2022. Zinc oxide nanoparticles improved chlorophyll contents, physical parameters, and wheat yield under salt stress. Frontiers in Plant Science, 13.

Akmal, M., Younus, A., Wakeel, A., Jamil, Y. & Rashid, M. A. 2022. Synthesis and application of optimized ZnO nanoparticles for improving yield and Zn content of rice (Oryza sativa L.) grain. Journal of Plant Nutrition, 1-14.

Amini, M. M., Alizadeh, M., Padasht, F., Elahinia, S. & Khodaparast, S. 2016. Rice grain discoloration effect on physical properties and head rice yield in three rice cultivars. Quality Assurance and Safety of Crops & Foods, 8, 283-288.

Bala, R., Kalia, A. & Dhaliwal, S. S. 2019. Evaluation of efficacy of ZnO nanoparticles as remedial zinc nanofertilizer for rice. Journal of Soil Science and Plant Nutrition, 19, 379-389.

Deng, C., Wang, Y., Navarro, G., Sun, Y., Cota-Ruiz, K., Hernandez-Viezcas, J. A., Niu, G., Li, C., White, J. C. & Gardea-Torresdey, J. 2022. Copper oxide (CuO) nanoparticles affect yield, nutritional quality, and auxin associated gene expression in weedy and cultivated rice (Oryza sativa L.) grains. Science of the Total Environment, 810, 152260.

Dimkpa, C. O., Mclean, J. E., Latta, D. E., Manangón, E., Britt, D. W., Johnson, W. P., Boyanov, M. I. & Anderson, A. J. 2012. CuO and ZnO nanoparticles: phytotoxicity, metal speciation, and induction of oxidative stress in sand-grown wheat. Journal of Nanoparticle Research, 14, 1-15.

Dimkpa, C. O., Singh, U., Bindraban, P. S., Elmer, W. H., Gardea-Torresdey, J. L. & White, J. C. 2019. Zinc oxide nanoparticles alleviate drought-induced alterations in sorghum performance, nutrient acquisition, and grain fortification. Science of the Total Environment, 688, 926-934.

Ding, H., Du, F., Liu, P., Chen, Z. & Shen, J. 2015. DNA–carbon dots function as fluorescent vehicles for drug delivery. ACS applied materials & interfaces, 7, 6889-6897.

Ebrahimie, E., Ebrahimi, F., Ebrahimi, M., Tomlinson, S. & Petrovski, K. R. 2018. A large-scale study of indicators of sub-clinical mastitis in dairy cattle by attribute weighting analysis of milk composition features: highlighting the predictive power of lactose and electrical conductivity. Journal of dairy research, 85, 193-200.

Ghasemi, M., Ghorban, N., Madani, H., Mobasser, H.-R. & Nouri, M.-Z. 2017. Effect of foliar application of zinc nano oxide on agronomic traits of two varieties of rice (Oryza sativa L.). Crop Research, 52, 195-201.

Gui, X., Dong, C., Fan, S., Jiao, C., Song, Z., Shen, J., Zhao, Y., Li, X., Zhang, F. & Ma, Y. 2023. Effects of CeO2 Nanoparticles on Nutritional Quality of Two Crop Plants, Corn (Zea mays L.) and Soybean (Glycine max L.). Molecules, 28, 1798.

Hajiboland, R. & Römheld, V. 2006. Zn Re-translocation during Early Vegetative Growth Stage in Rice Plants: Mechanism for a High Internal Zn Use Efficiency?

Hajiboland, R., Singh, B. & Römheld, V. 2001. Retranslocation of Zn from leaves as important factor for zinc efficiency of rice genotypes. Plant Nutrition: Food security and sustainability of agro-ecosystems through basic and applied research, 226-227.

Hajiboland, R., Yang, X. & Römheld, V. 2003. Effects of bicarbonate and high pH on growth of Zn-efficient and Zn-inefficient genotypes of rice, wheat and rye. Plant and soil, 250, 349-357.

Hajiboland, R., Yang, X., Römheld, V. & Neumann, G. 2005. Effect of bicarbonate on elongation and distribution of organic acids in root and root zone of Zn-efficient and Zn-inefficient rice (Oryza sativa L.) genotypes. Environmental and Experimental Botany, 54, 163-173.

Khush, G. S. 2005. IR varieties and their impact, Int. Rice Res. Inst.

Li, H., Huang, J., Lu, F., Liu, Y., Song, Y., Sun, Y., Zhong, J., Huang, H., Wang, Y. & Li, S. 2018. Impacts of carbon dots on rice plants: boosting the growth and improving the disease resistance. ACS Applied Bio Materials, 1, 663-672.

Mae, T. & Ohira, K. 1981. The remobilization of nitrogen related to leaf growth and senescence in rice plants (Oryza sativa L.). Plant and cell physiology, 22, 1067-1074.

Malhi, A. & Gao, R. X. 2004. PCA-based feature selection scheme for machine defect classification. IEEE transactions on instrumentation and measurement, 53, 1517-1525.

Meng, F., Liu, D., Yang, X., Shohag, M., Yang, J., Li, T., Lu, L. & Feng, Y. 2014. Zinc uptake kinetics in the low and high-affinity systems of two contrasting rice genotypes. Journal of Plant Nutrition and Soil Science, 177, 412-420.

Nair, R., Mohamed, M. S., Gao, W., Maekawa, T., Yoshida, Y., Ajayan, P. M. & Kumar, D. S. 2012. Effect of carbon nanomaterials on the germination and growth of rice plants. Journal of nanoscience and nanotechnology, 12, 2212-2220.

Nakandalage, N., Milham, P. J., Holford, P. & Seneweera, S. 2023. Luxury Zinc Supply Prevents the Depression of Grain Nitrogen Concentrations in Rice (Oryza sativa L.) Typically Induced by Elevated CO2. Plants, 12, 839.

Navarro, E. & Kirschey, K. 1980. ZnO application to soil and its residual effect on rice. Journal of Crop Science, 5, 100-104.

O'brien, R. G. & Kaiser, M. K. 1985. MANOVA method for analyzing repeated measures designs: an extensive primer. Psychological bulletin, 97, 316.

Rehmani, M. I. A., Wei, G., Hussain, N., Ding, C., Li, G., Liu, Z., Wang, S. & Ding, Y. 2014. Yield and quality responses of two indica rice hybrids to post-anthesis asymmetric day and night open-field warming in lower reaches of Yangtze River delta. Field Crops Research, 156, 231-241.

Rico, C. M., Lee, S. C., Rubenecia, R., Mukherjee, A., Hong, J., Peralta-Videa, J. R. & Gardea-Torresdey, J. L. 2014. Cerium oxide nanoparticles impact yield and modify nutritional parameters in wheat (Triticum aestivum L.). Journal of agricultural and food chemistry, 62, 9669-9675.

Rico, C. M., Morales, M. I., Barrios, A. C., Mccreary, R., Hong, J., Lee, W.-Y., Nunez, J., Peralta-Videa, J. R. & Gardea-Torresdey, J. L. 2013. Effect of cerium oxide nanoparticles on the quality of rice (Oryza sativa L.) grains. Journal of agricultural and food chemistry, 61, 11278-11285.

Song, F., Guo, Z. & Mei, D. Feature selection using principal component analysis. 2010 international conference on system science, engineering design and manufacturing informatization, 2010. IEEE, 27-30.

Subbaiah, L. V., Prasad, T. N. V. K. V., Krishna, T. G., Sudhakar, P., Reddy, B. R. & Pradeep, T. 2016. Novel effects of nanoparticulate delivery of zinc on growth, productivity, and zinc biofortification in maize (Zea mays L.). Journal of agricultural and food chemistry, 64, 3778-3788.

Wang, P., Zhou, G., Yu, H. & Yu, S. 2011. Fine mapping a major QTL for flag leaf size and yield-related traits in rice. Theoretical and applied genetics, 123, 1319-1330.

Wang, Q., Huang, X., Long, Y., Wang, X., Zhang, H., Zhu, R., Liang, L., Teng, P. & Zheng, H. 2013. Hollow luminescent carbon dots for drug delivery. Carbon, 59, 192-199.

Wang, W., Cheng, L. & Liu, W. 2014. Biological applications of carbon dots. Science China Chemistry, 57, 522-539.

Welfare, K., Flowers, T., Taylor, G. & Yeo, A. 1996. Additive and antagonistic effects of ozone and salinity on the growth, ion contents and gas exchange of five varieties of rice (Oryza sativa L.). Environmental Pollution, 92, 257-266.

Yan, S., Zhang, H., Huang, Y., Tan, J., Wang, P., Wang, Y., Hou, H., Huang, J. & Li, L. 2016. Single-wall and multi-wall carbon nanotubes promote rice root growth by eliciting the similar molecular pathways and epigenetic regulation. IET nanobiotechnology, 10, 222-229.

Yan, X., Pan, Z., Chen, S., Shi, N., Bai, T., Dong, L., Zhou, D., White, J. C. & Zhao, L. 2022. Rice exposure to silver nanoparticles in a life cycle study: effect of dose responses on grain metabolomic profile, yield, and soil bacteria. Environmental Science: Nano, 9, 2195-2206.

Yang, G., Yuan, H., Ji, H., Liu, H., Zhang, Y., Wang, G., Chen, L. & Guo, Z. 2021. Effect of ZnO nanoparticles on the productivity, Zn

biofortification, and nutritional quality of rice in a life cycle study. Plant Physiology and Biochemistry, 163, 87-94.

Zhang, B., Ye, W., Ren, D., Tian, P., Peng, Y., Gao, Y., Ruan, B., Wang, L., Zhang, G. & Guo, L. 2015. Genetic analysis of flag leaf size and candidate genes determination of a major QTL for flag leaf width in rice. Rice, 8, 2.

References of Chapter 5:

Bandyopadhyay, T., Mehra, P., Hairat, S. & Giri, J. 2017. Morpho-physiological and transcriptome profiling reveal novel zinc deficiency-responsive genes in rice. *Functional & integrative genomics,* 17**,** 565-581.

Burklew, C. E., Ashlock, J., Winfrey, W. B. & Zhang, B. 2012. Effects of aluminum oxide nanoparticles on the growth, development, and microRNA expression of tobacco (Nicotiana tabacum). *PloS one,* 7**,** e34783.

Consortium, G. O. 2004. The Gene Ontology (GO) database and informatics resource. *Nucleic acids research,* 32**,** D258-D261.

Consortium, G. O. 2019. The gene ontology resource: 20 years and still GOing strong. *Nucleic acids research,* 47**,** D330-D338.

Deng, C., Wang, Y., Navarro, G., Sun, Y., Cota-Ruiz, K., Hernandez-Viezcas, J. A., Niu, G., Li, C., White, J. C. & Gardea-Torresdey, J. 2022. Copper oxide (CuO) nanoparticles affect yield, nutritional quality, and auxin associated gene expression in weedy and cultivated rice (Oryza sativa L.) grains. *Science of the Total Environment,* 810**,** 152260.

Dorostkar, S., Dadkhodaie, A., Ebrahimie, E., Heidari, B. & Ahmadi-Kordshooli, M. 2022. Comparative transcriptome analysis of two contrasting resistant and susceptible Aegilops tauschii accessions to wheat leaf rust (Puccinia triticina) using RNA-sequencing. *Scientific Reports,* 12**,** 821.

Ebrahimie, E., Fruzangohar, M., Moussavi Nik, S. H. & Newman, M. 2017. Gene ontology-based analysis of zebrafish omics data using the web tool comparative gene ontology. *Zebrafish,* 14**,** 492-494.

Ebrahimie, E., Nurollah, Z., Ebrahimi, M., Hemmatzadeh, F. & Ignjatovic, J. 2015. Unique ability of pandemic influenza to downregulate the genes involved in neuronal disorders. *Molecular biology reports,* 42**,** 1377-1390.

Ebrahimie, E., Rahimirad, S., Tahsili, M. & Mohammadi-Dehcheshmeh, M. 2021. Alternative RNA splicing in stem cells and cancer stem cells: importance of transcript-based expression analysis. *World Journal of Stem Cells,* 13**,** 1394.

Fruzangohar, M., Ebrahimie, E., Ogunniyi, A. D., Mahdi, L. K., Paton, J. C. & Adelson, D. L. 2013. Comparative GO: a web application for comparative gene ontology and gene ontology-based gene selection in bacteria. *PloS one,* 8**,** e58759.

García-Sánchez, S., Bernales, I. & Cristobal, S. 2015. Early response to nanoparticles in the Arabidopsis transcriptome compromises plant defence and root-hair development through salicylic acid signalling. *BMC genomics,* 16**,** 341.

He, F., Liu, Q., Zheng, L., Cui, Y., Shen, Z. & Zheng, L. 2015. RNA-Seq analysis of rice roots reveals the involvement of post-transcriptional regulation in response to cadmium stress. *Frontiers in plant science,* 6**,** 1136.

Kamaral, C., Neate, S. M., Gunasinghe, N., Milham, P. J., Paterson, D. J., Kopittke, P. M. & Seneweera, S. 2022. Genetic biofortification of wheat with zinc: Opportunities to fine-tune zinc uptake, transport and grain loading. *Physiologia Plantarum,* 174**,** e13612.

Kanehisa, M. & Goto, S. 2000. KEGG: kyoto encyclopedia of genes and genomes. *Nucleic acids research,* 28**,** 27-30.

Kaveh, R., Li, Y.-S., Ranjbar, S., Tehrani, R., Brueck, C. L. & Van Aken, B. 2013. Changes in Arabidopsis thaliana gene expression in response to silver nanoparticles and silver ions. *Environmental science & technology,* 47**,** 10637-10644.

Khodakovskaya, M. V., De Silva, K., Nedosekin, D. A., Dervishi, E., Biris, A. S., Shashkov, E. V., Galanzha, E. I. & Zharov, V. P. 2011. Complex genetic, photothermal, and photoacoustic analysis of nanoparticle-plant interactions. *Proceedings of the National Academy of Sciences,* 108**,** 1028-1033.

Mahdi, L. K., Deihimi, T., Zamansani, F., Fruzangohar, M., Adelson, D. L., Paton, J. C., Ogunniyi, A. D. & Ebrahimie, E. 2014. A functional genomics catalogue of activated transcription factors during pathogenesis of pneumococcal disease. *BMC genomics,* 15**,** 1-15.

Mering, C. V., Huynen, M., Jaeggi, D., Schmidt, S., Bork, P. & Snel, B. 2003. STRING: a database of predicted functional associations between proteins. *Nucleic acids research,* 31**,** 258-261.

Mortazavi, A., Williams, B. A., Mccue, K., Schaeffer, L. & Wold, B. 2008. Mapping and quantifying mammalian transcriptomes by RNA-Seq. *Nature methods,* 5**,** 621-628.

Muvunyi, B. P., Xiang, L., Junhui, Z., Sang, H. & Guoyou, Y. 2022. Identification of Potential Zinc Deficiency Responsive Genes and Regulatory Pathways in Rice by Weighted Gene Co-expression Network Analysis. *Rice Science,* 29**,** 545-558.

Nair, P. M. G. & Chung, I. M. 2014. Physiological and molecular level effects of silver nanoparticles exposure in rice (Oryza sativa L.) seedlings. *Chemosphere,* 112**,** 105-113.

Nakandalage, N., Nicolas, M., Norton, R. M., Hirotsu, N., Milham, P. J. & Seneweera, S. 2016. Improving rice zinc biofortification success rates through genetic and crop management approaches in a changing environment. *Frontiers in plant science,* 7**,** 764.

Panahi, B., Abbaszadeh, B., Taghizadeghan, M. & Ebrahimie, E. 2014. Genome-wide survey of alternative splicing in Sorghum bicolor. *Physiology and Molecular Biology of Plants,* 20**,** 323-329.

Panahi, B., Mohammadi, S. A., Khaksefidi, R. E., Mehrabadi, J. F. & Ebrahimie, E. 2015. Genome-wide analysis of alternative splicing events in Hordeum vulgare: Highlighting retention of intron-based splicing and its possible function through network analysis. *FEBS letters,* 589**,** 3564-3575.

Perera, I., Fukushima, A., Arai, M., Yamada, K., Nagasaka, S., Seneweera, S. & Hirotsu, N. 2019. Identification of low phytic acid and high Zn bioavailable rice (Oryza sativa L.) from 69 accessions of the world rice core collection. *Journal of Cereal Science,* 85**,** 206-213.

Robinson, M. D. & Oshlack, A. 2010. A scaling normalization method for differential expression analysis of RNA-seq data. *Genome biology,* 11**,** 1-9.

Shih-Yin, O., Wilkin, T. & Bee-Yan, H. 2012. Camera-Based Signature Verification System through Discrete Radon Transform (DRT) and Principle Component Analysis (PCA). *Journal of Information Assurance & Security,* 7.

Singh, V., Bhattacharyya, S. & Jain, P. Through the wall human signature detection using principle component analysis (PCA). 2018 IEEE International Symposium on Antennas and Propagation & USNC/URSI National Radio Science Meeting, 2018. IEEE, 1975-1976.

Song, A., Li, P., Fan, F., Li, Z. & Liang, Y. 2014. The effect of silicon on photosynthesis and expression of its relevant genes in rice (Oryza sativa L.) under high-zinc stress. *PLoS One,* 9**,** e113782.

Song, Y., Jiang, M., Zhang, H. & Li, R. 2021. Zinc oxide nanoparticles alleviate chilling stress in rice (Oryza Sativa L.) by regulating antioxidative system and chilling response transcription factors. *Molecules,* 26**,** 2196.

Szklarczyk, D., Gable, A. L., Nastou, K. C., Lyon, D., Kirsch, R., Pyysalo, S., Doncheva, N. T., Legeay, M., Fang, T. & Bork, P. 2021. The STRING database in 2021: customizable protein–protein networks, and functional characterization of user-uploaded gene/measurement sets. *Nucleic acids research,* 49**,** D605-D612.

Szklarczyk, D., Morris, J. H., Cook, H., Kuhn, M., Wyder, S., Simonovic, M., Santos, A., Doncheva, N. T., Roth, A. & Bork, P. 2016. The STRING database in 2017: quality-controlled protein–protein association networks, made broadly accessible. *Nucleic acids research***,** gkw937.

Tumburu, L., Andersen, C. P., Rygiewicz, P. T. & Reichman, J. R. 2015. Phenotypic and genomic responses to titanium dioxide and cerium oxide nanoparticles in Arabidopsis germinants. *Environmental toxicology and chemistry,* 34**,** 70-83.

Yip, S., Dehcheshmeh, M. M., Mclelland, D. J., Boardman, W. S., Saputra, S., Ebrahimie, E., Weyrich, L. S., Bird, P. S. & Trott, D. J. 2021. Porphyromonas spp., Fusobacterium spp., and Bacteroides spp. dominate microbiota in the course of macropod progressive periodontal disease. *Scientific reports,* 11**,** 17775.

Zeng, H., Zhang, X., Ding, M. & Zhu, Y. 2019. Integrated analyses of miRNAome and transcriptome reveal zinc deficiency responses in rice seedlings. *BMC Plant Biology,* 19**,** 1-18.

References of Chapter 6:

Bandyopadhyay, T., Mehra, P., Hairat, S. & Giri, J. 2017. Morpho-physiological and transcriptome profiling reveal novel zinc deficiency-responsive genes in rice. Functional & integrative genomics, 17, 565-581.

Consortium, G. O. 2004. The Gene Ontology (GO) database and informatics resource. Nucleic acids research, 32, D258-D261.

Consortium, G. O. 2019. The gene ontology resource: 20 years and still GOing strong. Nucleic acids research, 47, D330-D338.

Ebrahimie, E., Fruzangohar, M., Moussavi Nik, S. H. & Newman, M. 2017. Gene ontology-based analysis of zebrafish omics data using the web tool comparative gene ontology. Zebrafish, 14, 492-494.

Ebrahimie, E., Nurollah, Z., Ebrahimi, M., Hemmatzadeh, F. & Ignjatovic, J. 2015. Unique ability of pandemic influenza to downregulate the genes involved in neuronal disorders. Molecular biology reports, 42, 1377-1390.

Fruzangohar, M., Ebrahimie, E., Ogunniyi, A. D., Mahdi, L. K., Paton, J. C. & Adelson, D. L. 2013. Comparative GO: a web application for comparative gene ontology and gene ontology-based gene selection in bacteria. PloS one, 8, e58759.

Gogos, A., Knauer, K. & Bucheli, T. D. 2012. Nanomaterials in plant protection and fertilization: current state, foreseen applications, and research priorities. Journal of agricultural and food chemistry, 60, 9781-9792.

Gupta, R. & Kim, S. T. 2015. Depletion of RuBisCO protein using the protamine sulfate precipitation method. Proteomic Profiling. Springer.

He, F., Liu, Q., Zheng, L., Cui, Y., Shen, Z. & Zheng, L. 2015. RNA-Seq analysis of rice roots reveals the involvement of post-transcriptional regulation in response to cadmium stress. Frontiers in plant science, 6, 1136.

Kanehisa, M. & Goto, S. 2000. KEGG: kyoto encyclopedia of genes and genomes. Nucleic acids research, 28, 27-30.

Kwak, S.-Y., Lew, T. T. S., Sweeney, C. J., Koman, V. B., Wong, M. H., Bohmert-Tatarev, K., Snell, K. D., Seo, J. S., Chua, N.-H. & Strano, M. S. 2019. Chloroplast-selective gene delivery and expression in planta using chitosan-complexed single-walled carbon nanotube carriers. Nature nanotechnology, 1.

Larue, C., Castillo-Michel, H., Sobanska, S., Cécillon, L., Bureau, S., Barthès, V., Ouerdane, L., Carrière, M. & Sarret, G. 2014. Foliar exposure of the crop Lactuca sativa to silver nanoparticles: evidence for internalization and changes in Ag speciation. Journal of hazardous materials, 264, 98-106.

Lowe, R. G., Mccorkelle, O., Bleackley, M., Collins, C., Faou, P., Mathivanan, S. & Anderson, M. 2015. Extracellular peptidases of the cereal pathogen Fusarium graminearum. Frontiers in Plant Science, 6, 962.

Mahdi, L. K., Deihimi, T., Zamansani, F., Fruzangohar, M., Adelson, D. L., Paton, J. C., Ogunniyi, A. D. & Ebrahimie, E. 2014. A functional genomics catalogue of activated transcription factors during pathogenesis of pneumococcal disease. BMC genomics, 15, 1-15.

Mering, C. V., Huynen, M., Jaeggi, D., Schmidt, S., Bork, P. & Snel, B. 2003. STRING: a database of predicted functional associations between proteins. Nucleic acids research, 31, 258-261.

Muvunyi, B. P., Xiang, L., Junhui, Z., Sang, H. & Guoyou, Y. 2022. Identification of Potential Zinc Deficiency Responsive Genes and Regulatory Pathways in Rice by Weighted Gene Co-expression Network Analysis. Rice Science, 29, 545-558.

Rappsilber, J., Mann, M. & Ishihama, Y. 2007. Protocol for micro-purification, enrichment, pre-fractionation and storage of peptides for proteomics using StageTips. Nature protocols, 2, 1896-1906.

Rico, C. M., Majumdar, S., Duarte-Gardea, M., Peralta-Videa, J. R. & Gardea-Torresdey, J. L. 2011. Interaction of nanoparticles with edible plants and their possible implications in the food chain. Journal of agricultural and food chemistry, 59, 3485-3498.

Shih-Yin, O., Wilkin, T. & Bee-Yan, H. 2012. Camera-Based Signature Verification System through Discrete Radon Transform (DRT) and Principle Component Analysis (PCA). Journal of Information Assurance & Security, 7.

Singh, V., Bhattacharyya, S. & Jain, P. Through the wall human signature detection using principle component analysis (PCA). 2018 IEEE International Symposium on Antennas and Propagation & USNC/URSI National Radio Science Meeting, 2018. IEEE, 1975-1976.

Song, A., Li, P., Fan, F., Li, Z. & Liang, Y. 2014. The effect of silicon on photosynthesis and expression of its relevant genes in rice (Oryza sativa L.) under high-zinc stress. PLoS One, 9, e113782.

Song, Y., Jiang, M., Zhang, H. & Li, R. 2021. Zinc oxide nanoparticles alleviate chilling stress in rice (Oryza Sativa L.) by regulating antioxidative system and chilling response transcription factors. Molecules, 26, 2196.

Subbaiah, L. V., Prasad, T. N. V. K. V., Krishna, T. G., Sudhakar, P., Reddy, B. R. & Pradeep, T. 2016. Novel effects of nanoparticulate delivery of zinc on growth, productivity, and zinc biofortification in maize (Zea mays L.). Journal of agricultural and food chemistry, 64, 3778-3788.

Szklarczyk, D., Gable, A. L., Nastou, K. C., Lyon, D., Kirsch, R., Pyysalo, S., Doncheva, N. T., Legeay, M., Fang, T. & Bork, P. 2021. The STRING database in 2021: customizable protein–protein networks, and functional characterization of user-uploaded gene/measurement sets. Nucleic acids research, 49, D605-D612.

Szklarczyk, D., Morris, J. H., Cook, H., Kuhn, M., Wyder, S., Simonovic, M., Santos, A., Doncheva, N. T., Roth, A. & Bork, P. 2016. The STRING database in 2017: quality-controlled protein–protein association networks, made broadly accessible. Nucleic acids research, gkw937.

Tripathi, D. K., Singh, S., Singh, S., Pandey, R., Singh, V. P., Sharma, N. C., Prasad, S. M., Dubey, N. K. & Chauhan, D. K. 2017. An overview on manufactured nanoparticles in plants: uptake, translocation, accumulation and phytotoxicity. Plant Physiology and Biochemistry, 110, 2-12.

Tripathi, S. & Sarkar, S. 2015. Influence of water soluble carbon dots on the growth of wheat plant. Applied Nanoscience, 5, 609-616.

Wang, Y.-D., Wang, X. & Wong, Y.-S. 2012. Proteomics analysis reveals multiple regulatory mechanisms in response to selenium in rice. Journal of proteomics, 75, 1849-1866.

Wong, M. H., P Misra, R., Giraldo, J., Kwak, S.-Y., Son, Y., Landry, M., Swan, J., Blankschtein, D. & S Strano, M. 2016. Lipid Exchange Envelope Penetration (LEEP) of Nanoparticles for Plant Engineering: A Universal Localization Mechanism.

Yip, S., Dehcheshmeh, M. M., Mclelland, D. J., Boardman, W. S., Saputra, S., Ebrahimie, E., Weyrich, L. S., Bird, P. S. & Trott, D. J. 2021. Porphyromonas spp., Fusobacterium spp., and Bacteroides spp. dominate microbiota in the course of macropod progressive periodontal disease. Scientific reports, 11, 17775.

Zeng, H., Zhang, X., Ding, M. & Zhu, Y. 2019. Integrated analyses of miRNAome and transcriptome reveal zinc deficiency responses in rice seedlings. BMC Plant Biology, 19, 1-18.

References of Chapter 7:

Anita, S. & Rao, D. 2014. Enhancement of seed germination and plant growth of wheat, maize, peanut and garlic using multiwalled carbon nanotubes. *European Chemical Bulletin,* 3**,** 502-504.

Chen, R., Ratnikova, T. A., Stone, M. B., Lin, S., Lard, M., Huang, G., Hudson, J. S. & Ke, P. C. 2010. Differential uptake of carbon nanoparticles by plant and mammalian cells. *Small,* 6**,** 612-617.

Giraldo, J. P., Landry, M. P., Faltermeier, S. M., Mcnicholas, T. P., Iverson, N. M., Boghossian, A. A., Reuel, N. F., Hilmer, A. J., Sen, F. & Brew, J. A. 2014. Plant nanobionics approach to augment photosynthesis and biochemical sensing. *Nature materials,* 13**,** 400.

Joshi, A., Kaur, S., Dharamvir, K., Nayyar, H. & Verma, G. 2018. Multi-walled carbon nanotubes applied through seed-priming influence early germination, root hair, growth and yield of bread wheat (Triticum aestivum L.). *Journal of the Science of Food and Agriculture,* 98**,** 3148-3160.

Lahiani, M. H., Chen, J., Irin, F., Puretzky, A. A., Green, M. J. & Khodakovskaya, M. V. 2015. Interaction of carbon nanohorns with plants: uptake and biological effects. *Carbon,* 81**,** 607-619.

Li, W., Zheng, Y., Zhang, H., Liu, Z., Su, W., Chen, S., Liu, Y., Zhuang, J. & Lei, B. 2016. Phytotoxicity, uptake, and translocation of fluorescent carbon dots in mung bean plants. *ACS applied materials & interfaces,* 8**,** 19939-19945.

Lin, S., Reppert, J., Hu, Q., Hudson, J. S., Reid, M. L., Ratnikova, T. A., Rao, A. M., Luo, H. & Ke, P. C. 2009. Uptake, translocation, and transmission of carbon nanomaterials in rice plants. *Small,* 5**,** 1128-1132.

Nair, R., Mohamed, M. S., Gao, W., Maekawa, T., Yoshida, Y., Ajayan, P. M. & Kumar, D. S. 2012. Effect of carbon nanomaterials on the

germination and growth of rice plants. *Journal of nanoscience and nanotechnology,* 12**,** 2212-2220.

Seneweera, S. 2011. Effects of elevated CO2 on plant growth and nutrient partitioning of rice (Oryza sativa L.) at rapid tillering and physiological maturity. *Journal of Plant Interactions,* 6**,** 35-42.

Srivastava, V., Srivastava, M. K., Chibani, K., Nilsson, R., Rouhier, N., Melzer, M. & Wingsle, G. 2009. Alternative splicing studies of the reactive oxygen species gene network in Populus reveal two isoforms of high-isoelectric-point superoxide dismutase. *Plant physiology,* 149**,** 1848-1859.

Tiwari, D., Dasgupta-Schubert, N., Cendejas, L. V., Villegas, J., Montoya, L. C. & García, S. B. 2014. Interfacing carbon nanotubes (CNT) with plants: enhancement of growth, water and ionic nutrient uptake in maize (Zea mays) and implications for nanoagriculture. *Applied Nanoscience,* 4**,** 577-591.

Tripathi, S. & Sarkar, S. 2015. Influence of water soluble carbon dots on the growth of wheat plant. *Applied Nanoscience,* 5**,** 609-616.

Tripathi, S., Sonkar, S. K. & Sarkar, S. 2011. Growth stimulation of gram (Cicer arietinum) plant by water soluble carbon nanotubes. *Nanoscale,* 3**,** 1176-1181.

Van Ruyskensvelde, V., Van Breusegem, F. & Van Der Kelen, K. 2018. Post-transcriptional regulation of the oxidative stress response in plants. *Free Radical Biology and Medicine,* 122**,** 181-192.

Wang, H., Zhang, M., Song, Y., Li, H., Huang, H., Shao, M., Liu, Y. & Kang, Z. 2018. Carbon dots promote the growth and photosynthesis of mung bean sprouts. *Carbon,* 136**,** 94-102.

APPENDIX

Supplementary files

The supplementary files of Chapter 5 are available at following address:

https://www.dropbox.com/sh/315wj7lxyjy819k/AABC2NWdbALOQmmV-lizMsMZa?dl=0

Supplementary files of Chapter 6 is shared at the and is available at following address:

https://www.dropbox.com/sh/315wj7lxyjy819k/AABC2NWdbALOQmmV-lizMsMZa?dl=0